NASA TECHNICAL MEMORANDUM

NASA TM-75771

ATOMIZATION OF A LIQUID BY A SPRAY NOZZLE

Edited by

S. S. Kutateladze

Translation of "Raspylivaniye zhidkosti forsunkami," Gosudarstvennoye energeticheskoye izdatel'stvo, Moscow-Leningrad, 1962, 265 pages.

NATIONAL AERONAUTICS AND SPACE ADMINISTRATION
WASHINGTON, D. C. 20546 FEBRUARY 1980

STANDARD TITLE PAGE

1. Report No. NASA TM-75771	2. Government Accession No.	3. Recipient's Catalog No.
4. Title and Subtitle Atomization of a Liquid by a Spray Nozzle		5. Report Date FEBRUARY 1980 6. Performing Organization Code
7. Author(s) Edited by S. S. Kutateladze		8. Performing Organization Report No. 10. Work Unit No. 11. Contract or Grant No. NASw-3198
9. Performing Organization Name and Address SCITRAN Box 5456 Santa Barbara, CA 93108		13. Type of Report and Period Covered Translation
12. Sponsoring Agency Name and Address NASA-LEWIS RESEARCH CENTER CLEVELAND, OHIO 44135		14. Sponsoring Agency Code

15. Supplementary Notes

Translation of "Raspylivaniye zhidkosti forsunkami", Gosudarstvennoye energeticheskoye Izdatel'stvo,Moscow-Leningrad, 1962, 265 pages.

16. Abstract

This monograph is devoted to the atomization of a liquid by different types of spray nozzles which is very important for present day technology. This monograph is important both for researchers and for designers and users of these devices due to the great amount of research carried out, the detailed analysis of several relationships in well-selected generalized coordinates, and the attempt to reduce the results obtained to a form which is suitable for direct engineering use.

17. Key Words (Selected by Author(s))	18. Distribution Statement
	Unclassified - Unlimited

19. Security Classif. (of this report)	20. Security Classif. (of this page)	21. No. of Pages	22. Price
Unclassified	Unclassified	279	

CONTENTS

ATOMIZATION OF A LIQUID BY A SPRAY NOZZLE

Edited by

S. S. Kutateladze

Introduction from the Editor

This monograph is devoted to the atomization of a liquid by different types of spray nozzles, which is very important for present-day technology. This monograph is important both for researchers and for designers and users of these devices due to the great amount of research carried out, the detailed analysis of several relationships in well-selected generalized coordinates, and the attempt to reduce the results obtained to a form which is suitable for direct engineering use.

The extensive material describing the operational principles and the structural formulation of different types of spray nozzles increases the practical value of the book. Although the design methods in this field, generally speaking, are still far from complete, such a large section of the book as the hydrodynamic calculation of atomization under "cold" conditions, has employed complete engineering methods and is illustrated with clear examples.

With respect to the calculations of the combustion of single drops and, in addition, the atomized flame, these are basically qualitative in nature. However, these materials are necessary for a correct qualitative representation of the combustion process of liquid fuel and may, to a certain extent, serve for valuable quantitative calculations.

S. S. Kutateladze

Introduction from the Authors

/4*

The atomization ("breaking up") of a liquid is widely used in present-day technology. In particular, it is used in the chemical and food industries during the extraction of solid substances from liquids, during drying, during different types of interactions between liquids and gases, and also in several other technological processes (breaking up pulp in the aluminum industry, cooling of gases by an atomized liquid in different types of equipment, etc.). Such a wide use of atomization is explained by the fact that in all these processes the decrease in the drop dimensions greatly increases the heat transfer coefficient. Consequently, this decreases the time of the process, which greatly decreases the expenditures for equipment. In addition, the atomization provides very uniform distribution of the liquid and its close interaction with the reacting medium.

The uniform distribution of the liquid and the economic advantages of the dispersing material have led to the success of the fine atomization of dies in the construction and other industries. Atomizers have been widely used for spraying plants in agriculture. The leaves of plants over hundreds of thousands of hectares are yearly covered with fine drops, special chemical compounds designed to combat agricultural diseases. In all these cases, spray nozzles are used for fine and as uniform a distribution as possible of the liquid over the spray cross-section.

The atomization principle is widely used in the combustion of liquid fuel. The liquid fuel is burned in the furnaces of steam boilers, the combustion chambers of gas turbines, industrial furnaces, internal combustion engines, and other devices. The type of liquid fuel which is used depends on the purpose and structure of the equipment: benzine, ligroin, kerosene, /5
solar oil and mazut. All of these fuels are obtained from petroleum. The increase in the extraction of petroleum in the USSR may be seen from the numbers given below:

---

*Numbers in the margin indicate pagination of original foreign text.

Year	Petroleum extraction in USSR, millions of tons	Year	Petroleum extraction in USSR, millions of tons
1913 (present boundaries)	10.3	1958	113.2
		1959	129.6
		1960	148.0
1928	11.6	1961	166.0
1935	25.2	1965 (control figures for development of USSR economy)	230 - 240
1940	31.1		
1945	19.4		
1950	37.9		
1955	70.8		

The great increase in the petroleum extraction in the USSR has changed the fuel balance of the country and has led to the introduction of liquid fuel for energy requirements in the country.

Mazut, which is obtained from reprocessing the extracted petroleum, is basically used in the furnaces of steam boilers, and also in industrial furnaces. In the case of high power, the highly economical combustion of mazut is extremely important, providing enormous savings of fuel and decreasing the weight and size of the combustion equipment.

There are very different methods for the combustion of liquid fuel, since they depend on the equipment productivity, its purpose, and several other factors. For all of these methods, the present techniques used in the combustion of liquid fuel represent a necessary stage in atomization because, intensifying the heat exchange between the pulverized fuel with the gas medium and improving the mixing of the fuel particles with the oxidizer, they contribute to intensification of the combustion process.

It must be noted that liquid fuel was almost never used for combustion before the application of atomization. During this time, petroleum was used, as a rule, only for producing oil and certain other chemical products. Kerosene was used only for illumination. Benzine and mazut were unreliable products of petroleum distillation and frequently were discarded as the residues of industry.

The first attempt to "fractionate" petroleum led to the development of very primitive equipment in the form of pipes which produced comparatively large drops which underwent combustion in the furnace. Only the appearance of /6
spray nozzles led to the industrial use of petroleum and several of its components as a fuel.

To a great extent, the economic advantages of mazut combustion are greatly determined by the quality of its atomization. As will be seen later, as fine a spray as possible is not always necessary for the effective combustion and stable ignition. A fractional composition which would provide the optimal conditions for the process development is necessary.

The enormous importance of liquid atomization for solving several technical problems has led to the development of a great number of constructions for spray nozzles. Numerous studies of spray nozzles have appeared. Most of these studies have had a limited nature, only dealing with a given specific type of spray nozzle. Along with this, research has been carried out on searching for the general principles which would be able to be applied not only to a tested type of spray nozzle when its productivity and operational conditions were changed, but also other spray nozzles operating on the same principle.

This book discusses the theory of atomization by mechanical and pneumatic (or vapor) spray nozzles, and gives the basic design recommendations following from generalization of the material and confirmed by experiments. Sprayers are examined which are widely used in the furnaces of stationary steam boilers, the combustion chambers of gas turbines and industrial furnaces. The material is presented in such a way that it may be used in industries using sprayers for other purposes.

The wide range in the capacities of industrial furnaces, high-power furnaces and combustion chambers has made it necessary to examine the spray nozzles with both small and large productivity.

In recent years, boiler equipment has appeared with a productivity of 50 tons of vapor per hour and above, and there has been a great increase in the specific capacity of boiler equipment, which has made it necessary to produce spray nozzles with a very high hourly consumption of fuel. Unfortunately, furnace technology has very limited knowledge regarding the operation of spray nozzles with this capacity. This book presents data which we hope will assist in the design of sprayers with great productivity.

A single chapter deals with the problems related to the development of highly efficient equipment (spray nozzles with preliminary gasification) for preparing the fuel for combustion with very high volume and cross-section. /7
The structural diagrams of this equipment are given.

Along with the discussion of problems related to the atomization of liquid fuel and the structure of spray nozzles, the book deals with the materials on the combustion of a single drop and flame of liquid fuel. It also considers certain principles for the design of furnaces of steam boilers and the combustion chambers of gas turbines, which is necessary for determining the necessary atomization accuracy and the distribution of liquid fuel drops over the flame cross-section.

The chapters 2, 3, 4 and 5 were written by L. A. Vitman; Sections 6-1 - 6-4 and Chapter 7 -- B. D. Katsnel'son; Chapter 1, Section 6-5 and Chapter 10 -- together by both authors; Chapters 8 and 9 -- I. I. Paleyev.

The material in the book was discussed by all the authors together, and reflects their general viewpoint on all the problems raised. The authors are indebted to the reviewer of the section on science and technology, Prof. G. F. Knorr, for his very valuable advice and comments, which were taken into account in the final editing of the book.

Comments and opinions on the book may be sent to the following address: Leningrad, D-41, Marsovo Pole, D. L., Leningradskoye otdeleniye Gosenergoizdata.

Authors

List of Notation /8

A - geometric characteristic of spray nozzle; experimental coefficients

c_{pn} - vapor heat capacity

$c_{ж}$ - liquid heat capacity

c_{pr} - gas heat capacity

$c_{к}$ - oxygen concentration

$c_{т}$ - fuel concentration

D - diffusion coefficient

d,D - diameter

E - energy

G - consumption of liquid, air; amount of vapor evaporated per unit time

g - weight; acceleration of gravity

H - hydrodynamic head

M - portion of liquid phase in fractions of initial value

p,P - pressure

Q - quantity of heat

$q_{исп}$ - evaporation heat

$q_{гор}$ - combustion heat

q - oscillation increment

R - gas constant

R_i - fraction of drops with dimensions greater than d_i

R,r - radius

S - amount of flue gases

T, t, τ - time

T,t - temperature

U,u,v,w - velocity

V - volume

x,y,z - point coordinates

$\bar{x},\bar{y}$ - relative drop dimension (in Ch. 9)

z_{O_2}, z_T - dimensionless concentration of oxygen and fuel

α - air excess coefficient; angle; oscillation amplitude; heat emission coefficient

β - amount of oxygen required for combustion of 1 kg fuel; volumetric expansion coefficient

γ - volumetric weight

δ - thickness of boundary layer; liquid films; dimensionless parameter

ε - eccentricity; clear opening coefficient

ϑ - dimensionless temperature

θ - angle

λ - oscillation wavelength; heat conductivity coefficient

μ - dynamic viscosity coefficient; flame emission coefficient

ν - kinematic viscosity coefficient

ξ - spray nozzle discharge coefficient; displacement of stream surface

ρ - density

τ - time; tangential stress

σ - surface tension coefficient; evaporation constant

ϕ, θ - point angular coordinates

ϕ - stream angle of taper

CHAPTER ONE /9

GENERAL INFORMATION ON SPRAY NOZZLES, PRINCIPLE OF ACTION AND FIELD OF APPLICATION

The first spray nozzle for the combustion of liquid fuel was developed by A. I. Shpakov in 1864. A spray nozzle developed in 1880 by the engineer, V. G. Shukov, played an important role later on. Due to its technological efficiency, simplicity of construction, and ease of manufacture, it became widely used. Although the Shukov spray nozzle was inferior to certain present-day spray nozzles with respect to specific vapor consumption, it is still extensively employed.

After the first sprayers appeared, an enormous amount of spray nozzles were produced with varying productivities and different operational principles. They differed from each other in structural characteristics, control methods, number of atomization stages, movement of the mixture of fuel and medium being atomized (air, vapor), and many others. It is most convenient to classify all these spray nozzles by their principle of liquid atomization.

Two basic methods are known for liquid atomization: mechanical and pneumatic (or vapor). In agreement with this, spray nozzles may be divided into two large groups: mechanical and pneumatic (or vapor). In recent years, spray nozzles of a combined type have been used, the so-called air-(vapor)-mechanical, and also spray nozzles with preliminary gasification. Mechanical spray nozzles, in their turn, may be arbitrarily divided into centrifugal and direct action.

In a centrifugal spray nozzle, the fuel which is supplied at great pressure is passed along the channels or a special vortical chamber, from which it is passed through a contraction nozzle into a volume filled with gas. Spray nozzles of this type are basically produced for a pressure from 6 to 60 atm, depending on the required degree of dispersion, the given productivity, and the /10
required hitting range of the stream. The requirement for spray nozzles of

great unit productivity and the increased requirement on the control limit have led to different structural devices when the centrifugal atomization principle is used. Thus, spray nozzles have appeared with inverse dumping of liquid fuel, with a controlled area of slow openings, multi-nozzle, rotating, etc.

The use of high velocities in mechanical spray nozzles has led to a decrease in the output nozzle opening and tangential opening of the vortex chambers. Based on this principle, spray nozzles with mechanical atomization require very careful liquid purification. In addition, the use of high velocities has limited the lower consumption limit of the liquid, since the opening dimensions cannot be extremely small -- this changes the normal operation of the spray nozzle. With respect to the upper limit, several technical procedures and the change to increased pressures have made it possible to raise it considerably: spray nozzles have been produced with a unit capacity of several tons of fuel per hour.

In direct action spray nozzles, the fuel, as a rule, is supplied at much higher pressure than in centrifugal spray nozzles. Sometimes it even exceeds 1,000 kG/cm^2. These spray nozzles are primarily used in internal combustion engines, and are not considered in this book.

Pneumatic (or vapor) spray nozzles, where dispersion is basically carried out by a gas stream, require more complex control and more cumbersome communication than mechanical spray nozzles. However, they are more suitable than mechanical spray nozzles due to the fact that they require less processing of the components and gas purification.

This is explained by the fact that, since the volume of gas passing through the nozzle as a rule exceeds by hundreds of times the volume of liquid fuel which is subjected to combustion, the diameter of the output opening must be many times larger and less sensitive to stoppage than mechanical spray nozzles. With respect to the opening for mazut, it has larger dimensions, since as a rule the liquid fuel passes at low velocities (1 - 3 m/sec).

Spray nozzles with air atomization may be arbitrarily divided into two basic groups -- low and high pressure. The first group includes spray nozzles with an atomization agent pressure up to 1,000 mm water; the second group -- a pressure from 1 atm and above. There are spray nozzles with average pressure operating in a pressure range from 1,000 mm water, to 1 atm. However, these spray nozzles have not been widely used in industry. /11

As has already been mentioned, spray nozzles with mechanical atomization are usually prepared with high liquid velocities in the vortex chamber or in the vortex component, and even higher in the output nozzle. In order to overcome resistance along the channel and to produce larger velocities, a high head is required in the liquid supply line.

The situation is different in pneumatic spray nozzles. Here the spray fractionization depends basically on the movement of the gas medium. Therefore, larger velocities are given to the gas movement. At the same time, the liquid velocity is extremely low. The head in the main supply line for the liquid is only necessary for transporting the required amount of liquid to the nozzle opening. Therefore, in certain devices where the ejection principle is used, the gas stream plays the role of the suction factor, and the liquid head does not exceed, as a rule, several tens of fractions of an atm. In other constructions of pneumatic spray nozzles, the head in the liquid supply line may be 2 atm and even higher.

The gas stream velocity in pneumatic spray nozzles with a high head amounts to hundreds of meters per second. In accordance with this, the gas pressure, as a rule, is 3 - 7 atm, and sometimes higher. In these spray nozzles, instead of air, steam with a pressure of 3 - 12 atm is frequently used. Sometimes steam with a higher pressure is used -- up to 25 atm.

The air consumption for the fuel atomization in high head spray nozzles is 7 - 10% of that required theoretically for combustion. The remaining air which is necessary for the fuel combustion is, as a rule, supplied through special devices -- registers.

Studies have shown that good dispersion is provided if 1 kg of atomized air or 0.5 - 0.7 kg atomized steam are used per 1 kg of fuel.

High head pneumatic spray nozzles may be direct flow or centrifugal. The direct flow spray nozzles include a group of so-called ejection spray nozzles which are widely used in power engineering and industrial furnaces. The ejection is done either by a Laval nozzle (in circular spray nozzles), or by a special arrangement of slits (in spray nozzles of the plane type). Centrifugal spray nozzles, in which air (or steam) flows are passed in special channels or in a chamber, are rarely used in power engineering,but recently they have been used in the combustion of liquid fuel in the combustion chambers of gas turbines. /12

For low fuel consumption, spray nozzles with a high head do not provide satisfactory atomization. Therefore, they usually operate with a consumption no lower than 100 kg/hr. One exception is the Chukhov spray nozzle, the first examples of which were used at very low flow rates. With respect to the maximum productivity of high pressure spray nozzles, it depends on their construction. Power engineering basically uses a spray nozzle with a consumption up to 2, and industrial furnaces — up to 3 tons of mazut per hour.

Low head spray nozzles are used basically in furnace technology. As a rule, they only operate with an air blast, but in some constructions designed for the combustion of highly viscous mazut, the air is supplied along with a small amount of steam. The latter plays the role of a fuel heater within the limits of the spray nozzle itself. The air consumption in these spray nozzles is approximately 50 - 100% of the amount necessary for the fuel combustion. The air velocity at the atomization location is about 50 - 70 m/sec, and sometimes 100 m/sec. The air in a low head spray nozzle is supplied in a non-vortex form. However, devices are used in which the flow has a vortex form. In many structures, the principle of two-stage atomization is used.

Low head spray nozzles have been developed to operate with low productivity. Some of them give satisfactory atomization, for an extremely low flow rate, which is about 1.5 kg/hr. in all. A relatively large diameter of the output

nozzle corresponds to this. Usually, the low head spray nozzles are used with a fuel consumption of up to 150 kg/hr. In some types of spray nozzles, the consumption may amount to 200 and even 300 kg/hr.

A tendency has recently appeared toward the production of air-mechanical spray nozzles. This is explained by the attempts to use the advantages of both /13
methods of liquid atomization. These combined spray nozzles differ in a certain complexity of construction, but the air consumption in them is very low, and the pressure in the air channel does not exceed 2 atm. This combined construction provides wide limits of changing the flow rate without a deterioration in the atomization quality, which is very important for combustion chambers of gas turbines. A low productivity compressor may provide for good operation of the air-mechanical spray nozzles with large fuel consumption. These sprayers will undoubtedly find their place in power engineering.

The passage of the liquid fuel along several stages until it was burned led researcher to produce spray nozzles with preliminary gasification. The requirements imposed on atomization equipment of this type are very low, since the liquid fuel which is heated and superheated to a high temperature is evaporated and gasified in a special chamber in the case of very coarse atomization. This organization of the process produces the best movement of the oxygen with the fuel, which provides combustion with a very low air excess and control of the fuel consumption within wide limits. The short flame gives high voltages of the volume and cross-section of the furnace chamber.

In order to design (or adjust) a spray nozzle, it is necessary to use the following initial data and basic technical requirements:

a) spray nozzle productivity (liquid consumption), G, kg/hr.;

b) required atomization fineness, determined by the average drop diameter in the stream and the drop distribution in terms of dimension;

c) stream angle of taper;

d) spray density, i.e., the amount of liquid passing per unit time through a unit surface of the stream clear opening;

e) stream hitting range.

The determination of the drop average diameter plays an important role in designing spray nozzles, for which there are the following formulas:

1) Arithmetic mean diameter:

$$d_{ap} = \frac{\sum n_i d_i}{N}, \tag{1-1}$$

where n_i is the number of drops with the diameter d_i; $N = \Sigma n_i$ -- the sum of all drops. With this method of averaging, the specific content of drops is determined by their relative amount. In addition, a large number of small drops comprises only a small portion of the total mass of the atomized liquid. This means that such averaging does not consider the distribution of the liquid mass in terms of drops; /14

2) The mean mass diameter:

$$d = \frac{\sum g_i d_i}{G} = \frac{\sum n_i d_i^4}{\sum n_i d_i^3}, \tag{1-2}$$

where g_i is the amount of drops with the dimension d_i;

3) In certain cases the dimension of the drop whose ratio of its volume to its surface equals the ratio of the total volume of all the drops to their surface (average diameter according to Zauter) is used as the average value:

$$d_s = \frac{\sum n_i d_i^3}{\sum n_i d_i^2}; \tag{1-3}$$

4) The average diameter follows from the condition that the ratio of the drop diameter with an average dimension to its volume equals the ratio of the sum of all drop diameters to the volume of all drops:

$$d_P = \sqrt{\frac{1}{\sum \frac{V_i}{d_i^2}}}; \tag{1-4}$$

5) The average value is assumed to be the diameter of the drop whose volume equals the arithmetic mean volume of all the drops:

$$d_V = \sqrt[3]{\frac{\sum n_i d_i^3}{\sum n_i}}; \qquad (1\text{-}5)$$

6) The average is also the diameter of a drop whose surface equals the arithmetic mean surface of all the drops:

$$d_F = \sqrt{\frac{\sum n_i d_i^2}{\sum n_i}}; \qquad (1\text{-}6)$$

7) The arithmetic mean diameter:

$$\lg d_l = \frac{\sum g_i \lg d_i}{G}; \qquad (1\text{-}7)$$

8) The median diameter d_m is determined as the diameter of a drop which divides the volume of the atomized stream into two equal parts, i.e., into the total volume of the drops /15

$$\sum_{i=1}^{m} n_i d_i^3 = \sum_{i=m+1}^{n} n_i d_i^3, \qquad (1\text{-}8)$$

whose dimensions are greater than or less than d_m.

The selection of a certain method for determining the average drop diameter depends on the purposes for which the liquid atomization is performed.

The average drop diameter characterizes the dispersion which is far from complete, since for one and the same average diameter different drop distributions by dimension are possible. Therefore, it is necessary to know this distribution determined by means of different empirical formulas.

The following formula is very widely used:

$$\ln R_i = -\left(\frac{d_i}{d_0}\right)^m = -bd_i^m. \qquad (1\text{-}9)$$

where m and b are empirical constants;

d_o - drop dimension corresponding to $R_i = 0.376$;

R_i - the portion of the liquid consisting of drops whose dimensions are greater than d_i.

Instead of the quantity d_o, we may introduce the average drop diameter, and also any drop diameter which is arbitrarily assumed as the largest. Thus, if the average diameter is determined according to formula (1-2), then:

$$\ln R_i = -\left[\Gamma\left(1+\frac{1}{m}\right)\frac{d_i}{d}\right]^m. \qquad \text{(1-10a)}$$

where $\Gamma\left(1+\frac{1}{m}\right)$ is the gamma function.

If the average diameter is determined from the condition (1-8), then:

$$\ln R_i = -0{,}69\left(\frac{d_i}{d_m}\right)^m. \qquad \text{(1-10b)}$$

In determining the average diameter using the formula (1-3), we have

$$\ln R_i = -\left(\frac{d_i}{\Gamma\left(1-\frac{1}{m}\right)d_s}\right)^m. \qquad \text{(1-10c)}$$

With the introduction of a certain largest diameter d_1, corresponding to the determined small value of R_1, formula (1-9) is transformed to the form: /16

$$\ln R_i = -n\left(\frac{d_i}{d_1}\right)^m = -ny^m, \qquad \text{(1-10d)}$$

where $y = d_i/d_1$.

Knowing the distribution of the drops in terms of dimensions, we may find the relationship between the diameters of the drops, obtained by different methods of averaging, and we may thus compare the experimental data of different researchers.

Thus:

$$d = d_s\Gamma\left(1+\frac{1}{m}\right)\Gamma\left(1-\frac{1}{m}\right), \qquad \text{(1-11)}$$

or

$$d = d_m\frac{\Gamma\left(1+\frac{1}{m}\right)}{\sqrt[m]{0{,}69}}, \qquad \text{(1-12)}$$

or

$$d = d_p \sqrt{\Gamma\left(1-\frac{2}{m}\right) \cdot \Gamma\left(1+\frac{1}{m}\right)} \qquad (1\text{-}13)$$

etc.

The basic parameters determining the spray nozzle operational regime are:

a) The liquid head before the spray nozzle; knowing the productivity of the spray nozzle and the head, we may calculate the pump equipment;

b) The velocity of the atomizing gas (or steam) for pneumatic spray nozzles. The calculation of the head losses in the spray nozzle in the gas (steam) channel makes it possible to select a heater for supplying the air or to determine the steam pressure supplied to the spray nozzle;

c) The relationship between the flow rates of liquid and gas in pneumatic spray nozzles;

d) The anti-pressure in the chamber.

Knowing the productivity and assigning the velocity, we may determine the diameter of the spray nozzle liquid nozzles, and in pneumatic spray nozzles we may also determine the slit dimensions for the gas (or steam).

CHAPTER TWO

/17

EQUATIONS FOR LIQUID STREAM MOTION IN GAS FLOW

Section 2-1. Basic equations of hydrodynamics

The motion of a liquid stream in a gas may be described by the equation of motion and the continuity of each phase and the conditions at the phase boundary. In vector form, these equations may be written in the following form [2-2, 3, 4]: equations of motion (gas or liquid)

$$\varrho\bar{F} - \operatorname{grad} p + \mu\left(\nabla^2\bar{v} + \frac{1}{3}\operatorname{grad}\operatorname{div}\bar{v}\right) = \varrho\left[\frac{\partial\bar{v}}{\partial t} + (\bar{v}, \operatorname{grad})\,\bar{v}\right]; \tag{2-1}$$

Continuity equation

$$\frac{\partial\varrho}{\partial t} + \operatorname{div}(\varrho\bar{v}) = 0. \tag{2-2}$$

Here $\bar{F}$ -- volumetric forces, influencing a unit mass (when the volumetric force is the weight, then $\bar{F} = \bar{g}\cdot 1$,
where $\bar{g}$ -- acceleration of gravity);

ϱ -- medium density;

μ -- medium viscosity;

p -- pressure;

$\bar{v}$ -- velocity;

t -- time

In the case of an incompressible medium, the density is constant(ϱ = const), and equations (2-1) and (2-2) may be simplified and assume the form

$$\varrho\bar{g} - \operatorname{grad} p + \mu\nabla^2\bar{v} = \varrho\left[\frac{\partial\bar{v}}{\partial t} + (\bar{v}, \operatorname{grad})\,\bar{v}\right]; \tag{2-3}$$

$$\operatorname{div}\bar{v} = 0. \tag{2-4}$$

We may omit terms corresponding to local nonstationarity for the established process. However, in terms of the operational mode, a spray nozzle with a stationary mode is not obtained. A basic factor in the operation of the spray nozzle is the nonstationarity of the process, and the production of waves which /18
lead to decomposition of the liquid into drops. This process will be examined in greater detail below.

In order to solve the system of equations described separately for each of the media, we must know the initial and boundary conditions which establish the relationship between the velocities and pressures in the plane of the stream flow, and also the conditions for the interactions of the phases at the boundary. In addition, we must have an idea of the form of the boundary surface in the plane of the stream flow.

Section 2-2. Conditions for mechanical interaction on the liquid-gas boundary surface

In terms of its properties, a surface layer differs greatly from the remaining volume of the liquid due to the fact that the molecules of this layer are influenced by the force fields of molecules in different media. As a result, the molecule of the surface layer is influenced by a force directed perpendicular to the surface within the liquid -- molecular pressure. The thickness of the surface layer is very small and is on the order of magnitude of molecular dimensions. Due to the action of the molecular pressure, the liquid surface layer is similar to an extended film which strives to be compressed. Forces tangent to the liquid surface oppose this compression. These forces are called the forces of surface tension.

An increase in the boundary surface by the quantity dS_{rp} is connected with the force of surface tension and leads to an increase in the internal energy of the liquid surface film $dE = \sigma dS_{rp}$.

The energy E represents the portion of internal energy which may be converted into work in the case of isothermic compression and is called the free

energy; σ -- surface tension coefficient which numerically equals the change in the free energy E of the film with an increase in the boundary surface by unity:

$$\sigma = \frac{dE}{dS_{\text{гр}}}. \tag{2-5}$$

The numerical value of the surface tension coefficient depends upon the physical property of the boundary media.

In a state of equilibrium, the value of the free energy must be minimal. /19
Therefore, a liquid stream in the case of equilibrium strives to obtain a form with the smallest surface.

The occurrence of surface tension forces in the case of a curvilinear boundary surface leads to the fact that the pressures in the liquid and the gas are not equal. This difference in the pressures is determined by the Laplace formula:

$$p_{ж} - p_{г} = \sigma\left(\frac{1}{R_1} + \frac{1}{R_2}\right) = p_{\sigma}. \tag{2-6}$$

where R_1 and R_2 -- main radii of curvature of the phase boundary surface.

In general, for the liquid-gas boundaries, the following conditions may be written:

a) The tangential velocity component on the phase boundary surface must become continuous when the phases do not slip with respect to each other:

$$v_{\tau ж} = v_{\tau г}; \tag{2-7}$$

b) When there is no phase conversion, the normal velocity components equal zero:

$$v_{n ж} = v_{n г} = 0; \tag{2-8}$$

c) The tangential stresses equal each other:

$$\tau_{ж} = \tau_{г}; \tag{2-9}$$

d) The normal stresses equal each other:

$$p_{г} + p_{\sigma} = p_{ж}. \tag{2-10}$$

Let us select a rectilinear coordinate system so that the y-axis is directed along the normal to the boundary surface of the phases. Then the boundary conditions are transformed as follows:

$$(v_{xz})_{ж} = (v_{xz})_{г}; \tag{2-11}$$

$$v_{y\,ж} = v_{y\,г} = 0; \tag{2-11'}$$

$$\tau_{xy} = \mu_{ж}\left(\frac{\partial v_{x\,ж}}{\partial y} + \frac{\partial v_{y\,ж}}{\partial x}\right) = \mu_{г}\left(\frac{\partial v_{x\,г}}{\partial y} + \frac{\partial v_{y\,г}}{\partial x}\right); \tag{2-12}$$

$$\tau_{yz} = \mu_{ж}\left(\frac{\partial v_{y\,ж}}{\partial z} + \frac{\partial v_{z\,ж}}{\partial y}\right) = \mu_{г}\left(\frac{\partial v_{y\,г}}{\partial z} + \frac{\partial v_{z\,г}}{\partial y}\right); \tag{2-12'}$$

$$p_{ж} + 2\mu_{ж}\frac{\partial v_{y\,ж}}{\partial y} = p_{г} + 2\mu_{г}\frac{\partial v_{y\,г}}{\partial y} + \sigma\left(\frac{1}{R_1} + \frac{1}{R_2}\right). \tag{2-13}$$

Section 2-3. System of similarity criteria

/20

It is extremely difficult to integrate this system of equations and is only possible in certain specific cases. Therefore, when solving actual problems, it is necessary to resort to experiments. In this connection, it is very important to calculate the conditions of generalizing the results of single experiments using the similarity method (ref. [2-1, 5 and 6]).

Phenomena are called similar for which the fields of dimensionless similar quantities are identical. These phenomena are described by the same dimensionless equations.

To reduce the equations to dimensionless form, it is necessary to select the scales of all the quantities characterizing the phenomenon and -- introducing the scales into the equation, to divide all of the terms by the coefficient for one of them. Thus, we obtain the dimensionless complexes -- criteria which must be identical for the entire class of similar phenomena. Thus, any dimensionless quantity is the function of the criteria formulated from the conditions of uniqueness (dimensional arguments of the process).

The following quantities may be used as the scales in the case examined:

a) The characteristic velocities of gas and liquid, for example, the average flow rate at the output of the nozzle $v_{ж0}$ and $v_{г0}$;

b) Acceleration of gravity g;

c) Physical properties of the gas and liquid: $\varrho_ж$, $\varrho_г$ - density; $\mu_ж$, $\mu_г$ -- viscosity; σ -- surface tension;

d) Characteristic dimension, for example, nozzle diameter d_0;

e) Characteristic time interval, for example, the time from the moment of the outflow to the beginning of the stream decomposition T.

The following system of criteria is obtained as the result of these transformations of the equations:

$\frac{\varrho_ж v_{ж0} d_0}{\mu_ж}$ and $\frac{\varrho_г v_{г0} d_0}{\mu_г}$ -- characterize the hydrodynamic flow regimes of the liquid and gas;

$\frac{v_{ж0}}{gd_0}$ characterizes the relationship of the inertial forces and forces of gravity in the stream;

$\frac{\Delta p_ж}{\varrho_ж v_{ж0}^2}$ and $\frac{\Delta p_г}{\varrho_г v_{г0}^2}$ characterize the relationship between the pressure losses in the streams;

$\frac{T v_{ж0}}{d_0}$ -- homochromatic criterion;

$\frac{v_{г0}}{v_{ж0}}$ -- relationship between gas and liquid velocity; /21

$\frac{\mu_г}{\mu_ж}$ -- relationship between gas and liquid viscosity;

$\frac{\mu_ж v_{ж0}}{\sigma}$ -- relationship between forces of surface tension and liquid viscosity.

These individual criteria may be replaced by a combination of them. For example, instead of the first two criteria, we may give one of them and the relationship: $\varrho_ж$ $\varrho_г$.

The criterion $\frac{\mu_ж v_{ж0}}{\sigma}$ may be replaced by the combination:

$$\frac{\mu_ж v_{ж0}}{\sigma} \cdot \frac{v_{ж0} d_0 \varrho_ж}{\mu_ж} = \frac{\varrho_ж v_{ж0}^2 d_0}{\sigma}.$$

Instead of the criteria $\frac{\varrho_ж v_{ж0} d_0}{\mu_ж}$ and $\frac{\mu_ж v_{ж0}}{\sigma}$, we may introduce one of them and their relationship $\frac{\mu_ж^2}{\varrho_ж \sigma d_0}$, etc.

The criteria formulated from the quantities in the uniqueness condition are decisive, i.e., they are dimensionless arguments of the process.

The system of decisive criteria depends on the formulation of the problem and the selection of the corresponding boundary and initial conditions, and may therefore be changed.

The total number of decisive criteria is found by using the following simple rule of the dimensionality theory: The largest necessary number of decisive dimensionless complexes equals the difference between the number of the scale quantity and the number of their dimensionality.

In many cases, the number of decisive quantities is reduced in practice. This occurs if it is known previously or established by experiment, so that

other factors may be included from the equations due to the unimportance of their action upon the quantity desired.

CHAPTER THREE

DECOMPOSITION OF NONVORTEX LIQUID STREAMS

Section 3-1. Physical nature of the phenomenon

Many experimental studies have shown that the liquid streams flowing from an opening into a gas medium pulsate. Under certain conditions, the liquid pulsation increases along the stream and leads to its decomposition into drops. The nature of the pulsation motion depends on the form of the nozzle from which the stream emanates, the scale of the initial liquid turbulence in the stream, the physical properties of the liquid and gas, and their relative velocity.

Figure 3-1 gives the results of one of the experiments by V. I. Blinov and Ye. L. Feynberg [3-1] on determining the form of the stream emanating from an elliptical opening. The distance z from the nozzle opening, from which the flow emanates, is plotted on the abscissa axis, and on the ordinate axis -- the thickness of the stream 2b. It may be seen from the figure that at a certain distance from the opening, unstable oscillations develop with a sharply increasing amplitude, which cause the decomposition of the stream into sections.

Figure 3-2 shows the photographs given in the study by O. Gol'dfel'der [3-9] of a water stream emanating from a cylindrical nozzle with different properties in a medium of a differing intensity. It may be seen that the greater the gas density and the liquid flow velocity, the more intensively does the stream disintegrate.

Showing the form of the motion and the breakdown of the liquid stream in a schematic way, we may discuss the decomposition in the case of symmetric

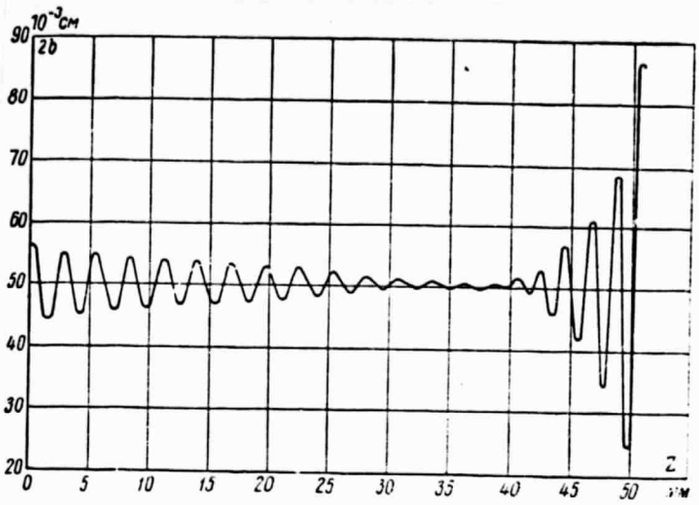

Fig. 3-1. Form of stream flowing from elliptical opening

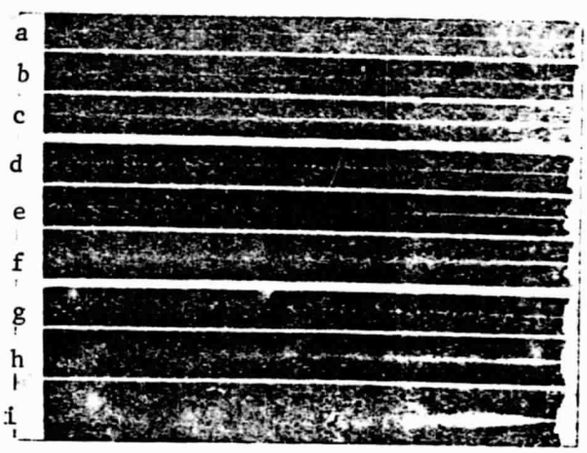

Fig. 3-2. Photograph of water streams from nozzle.

Photographs are arranged in increasing order of velocity and anti-pressure.

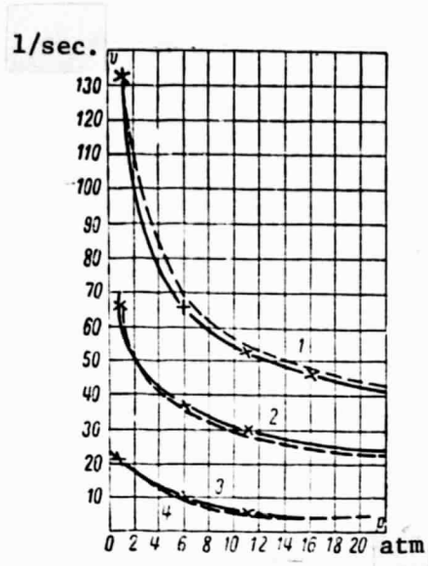

Fig. 3.3. Dependence of limiting flow velocity on antipressure for different forms of decomposition.

Nozzle diameter, 0.5 mm. Sections: 1 - atomization; 2 - wave-like profile with separation; 3 - wave-like profile; 4 - decomposition

/24

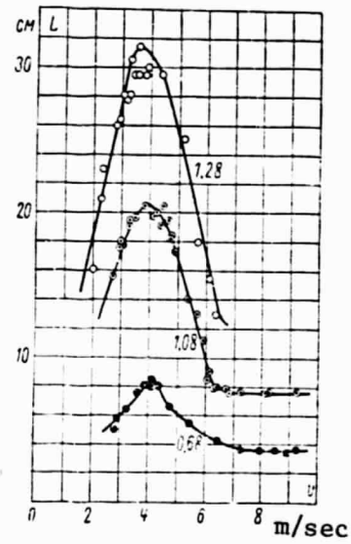

Fig. 3-4. Dependence of length L of solid part of water stream on flow velocity and diameter of nozzle opening.

Numbers on the curves designate diameter of nozzle opening, d_o, mm.

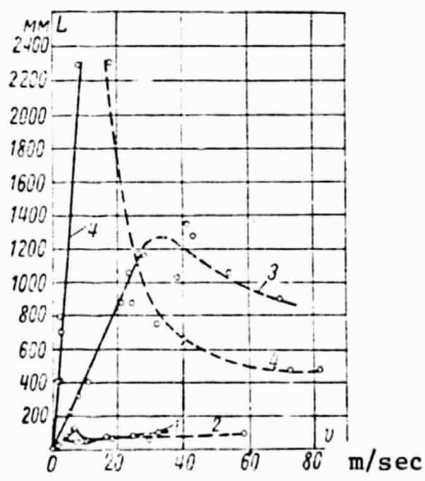

Fig. 3-5. Dependence of length L of solid part of liquid stream with different physical properties on the flow velocity v from the nozzle.

solid lines -- stream decomposition without air influence; dotted lines -- wavelike profile.

oscillations, for which there is no deformation of the stream axis (Fig. 3-2, a-d), the decomposition in the case of wavelike oscillations, for which there is a wavelike curvature of the stream axis (Fig. 3-2, e and f), and atomization (Fig. 3-2, g-i).

Figure 3-3 shows the dependence of the limiting flow velocity on the antipressure or the air density for different forms of decomposition.

The time T, calculated from the time the stream flows up to its decomposition, and the length L of the solid section of the stream are related by the following relationship:

$$L = Tv, \tag{3-1}$$

where v is the average velocity in the section L, which is close to the average velocity of the stream flow.

Figure 3-4 shows the dependence of the length L of the solid section of the air stream on the flow velocity v and the nozzle opening diameter [3-18].

The larger the stream diameter, the longer is its solid section. However, in all cases for certain velocities there is a maximum on the curve L = f(v), after which there is a great decrease in the length of the solid section of the stream.

Comparing formula (3-1) and the curves in Fig. 3-4, we may conclude that /25
at low stream velocities, where the length of the solid section of the stream is proportional to the velocity, the decomposition time T is constant. The right side of the graph in Fig. 3-4 shows the rapid decrease in the time T with an increase in velocity, which points to a reduction in the stability of the stream flow.

Figure 3-5 shows a similar dependence L = f(v) for a stream of water (1), gas oil (2), glycerin (3) and castor oil (4) [3-8]. It may be seen from the

figure that the length of the solid part of the stream and the magnitude of the velocity at which the stream stability begins to sharply decrease, depend on the physical properties of the liquid.

The dependence of the length of the solid part of the stream on the head in the case of decomposition of high velocity streams was obtained by L. F. Vereshchagin, A. A. Semerchan and S. S. Sekoyan [3-3].

Section 3-2. Analytical solutions

The problem of the decomposition of streams may be solved by examining the stability of a given liquid flow. The mathematical study of the motion stability with respect to small perturbations may be found using the equations of motion. For this purpose, a nonstationary small perturbation is applied to a stationary basic flow, so that the resulting motion satisfies the equations of motion. For flow velocities which are of practical interest, we do not consider the influence of gravity on the liquid motion. In this case, the forces of viscosity, surface tension and hydrodynamic pressure influence the liquid stream.

The decomposition conditions of a stream under the influence of capillary forces were first formulated by Raleigh [3-17], who examined the motion of a cylindrical stream of nonviscous liquid under the influence of surface tension when the stream flow velocity was so small that the hydrodynamic interaction of the stream with the surrounding medium could be disregarded.

In cylindrical coordinates (r, z, ϕ), the equation for the perturbed stream surface according to Raleigh may be written in the form:

$$r = a_0 + f(\varphi, z), \tag{3-2}$$

where $f(\phi, z)$ is a small quantity which may be expanded in Fourier series: /26

$$f(\varphi, z) = \sum \alpha_n \cos n\varphi \cos \frac{kz}{r_0}. \tag{3-3}$$

Here n = 0, 1, 2 ...;

k - wave number;

α_n - amplitude of oscillations depending on time.

The value of a_o does not remain constant during the motion, and its value must be determined by the condition that the volume contained in the cylinder is constant. It may be readily shown that

$$\left.\begin{aligned} a_0 &= r_0\left(1 - \frac{1}{8}\cdot\frac{\alpha_n^2}{r_0^2}\right) \quad \text{at n = 1,2,3...} \\ \text{and} \\ a_0 &= r_0\left(1 - \frac{\alpha_n^2}{r_0^2}\right) \quad \text{at n = 0,} \end{aligned}\right\} \tag{3-4}$$

where r_o is the radius of the unperturbed cylinder.

The expression for the potential energy of the system, determined per unit length, shows that the initial position for asymmetric oscillations ($n \geq 1$) is stable [$\alpha_n \sim \cos(pt - \varepsilon)$], and the oscillations do not lead to stream decomposition. In the case of symmetric oscillations (n = 0), the expression for the potential energy has the form

$$E_n = \frac{1}{2}\pi\sigma(k^2 - 1)\frac{\alpha_0^2}{r_0}. \tag{3-5}$$

It may be seen from (3-5) that at $k < 1$, the equilibrium is unstable, i.e., the oscillations with the wavelength λ, which is greater than the length of the unperturbed cylinder circumference, are unstable:

$$\lambda = \frac{2\pi r_0}{k} > 2\pi r_0. \tag{3-6}$$

Thus, the oscillation amplitude may be written in the form:

$$a_0 \sim e^{qt}.$$

The rapidly increasing oscillations having the largest value of the increment q are important for the decomposition.

The kinetic energy of a stream of unit length is determined according to the Green theorem by means of the velocity potential which satisfies the Laplace equation.

For the case n = 0, the kinetic energy /27

$$E_к = \frac{1}{2}\pi\rho r_0^2 \frac{I_0(ik)}{ik\, I_0'(ik)} \left(\frac{\partial \alpha_0}{\partial t}\right)^2. \qquad (3\text{-}7)$$

We have the following from the equations (3-5) and (3-7) for the potential and kinetic energy by the Lagrange method for any values of n:

$$\frac{\partial^2 \alpha_n}{\partial t^2} + \frac{\sigma}{\rho r_0^3} \cdot \frac{ik\, I_n'(ik)}{I_n(ik)} (n^2 + k^2 - 1)\, \alpha_n = 0. \qquad (3\text{-}8)$$

At $n = 0$ $\alpha_0 \sim e^{qt}$, the expression for the oscillation increment has the form:

$$q^2 = \frac{\sigma}{\rho r_0^3} \cdot \frac{ik\, I_0'(ik)}{I_0(ik)} \cdot (1 - k^2). \qquad (3\text{-}9)$$

In this expression $I_0(ik)$ and $I_0'(ik)$ are the Bessel functions. Instability occurs at $k < 1$ (as has already been shown). The analysis of equation (3-9) makes it possible to find the most rapidly increasing oscillation, by determining $d(q^2)/dk = 0$. The wavelength of this oscillation does not depend on the physical properties of the liquid or the surrounding medium, and equals:

$$\lambda = \frac{2\pi r_0}{k} = 9{,}02 r_0. \qquad (3\text{-}10)$$

The dimension of the primary elements into which the stream decomposes is determined by the volume of the liquid in the section of the stream which equals the wavelength of this oscillation, which is approximately nine times greater than the stream radius. Thus, the stream decomposition into drops may occur gradually in the sense that the discrete elements of the liquid

formed pulsate and in certain cases decompose into smaller drops in turn.

The solution of a similar problem for the case when the influence of the hydrodynamic forces for the interaction cannot be disregarded was obtained by G. I. Petrov and T. D. Kalinin [3-12] under the assumption that the liquid and gas are ideal and not compressible. The motion of the liquid stream and the gas surrounding it may be regarded as consisting of basic stationary flow with constant velocities and relative pulsation motion. In this case, the equations for the pulsation motion for each of the media may be reduced to the form /28

$$\frac{\partial v_r}{\partial t} + v_z \frac{\partial v_r}{\partial z} = -\frac{1}{\varrho} \cdot \frac{\partial p}{\partial r} \quad , \text{ etc.} \tag{3-11}$$

The continuity equation for each of the media may be reduced to the Laplace equation for the pressure pulsation:

$$\frac{\partial^2 p}{\partial r^2} + \frac{\partial^2 p}{\partial z^2} + \frac{1}{r^2} \cdot \frac{\partial^2 p}{\partial \varphi^2} + \frac{1}{r} \cdot \frac{\partial p}{\partial r} = 0. \tag{3-12}$$

The pressure pulsation is written in the form:

$$p = \alpha(r)\, e^{i\frac{kz}{n}} e^{in\varphi}, \tag{3-13}$$

where the amplitude $\alpha(r)$ is determined from the Bessel equation when the corresponding boundary conditions are satisfied: finite nature of the solution at $r = 0$ and $r = r_o$ and conditions (2-8) and (2-10).

As a result of several transformations, Petrov and Kalinin obtained the condition for the stream flow instability in the form of the inequality:

$$\delta = \frac{2\varrho_* r_0 (v_* - v_r)^2}{\sigma} > \tag{3-14}$$

$$> \frac{1 - n^2 - k^2}{k^2} \left(\frac{K_n' \varrho_r}{K_n \varrho_*} - \frac{I_n'}{I_n} \right).$$

Here K_n', K_n, I_n', I_n are the Bessel functions.

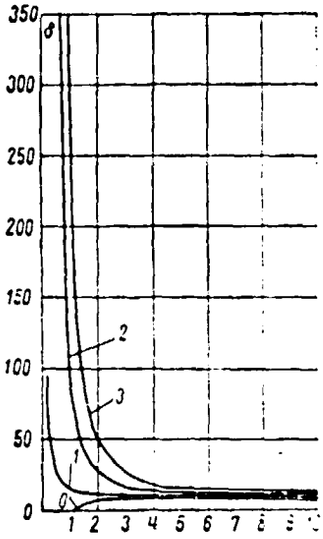

Fig. 3-6. Flow stability boundary of cylindrical stream for different oscillations

Numbers on the curves designate the values of n.

The stream decomposition is possible both for symmetric (n = 0) and asymmetrical oscillations ($n \geq 1$ and $k > 1$) if the condition (3-14) is satisfied.

Figure 3-6 shows the dependence of the parameter δ on the coefficients n and k at the stability boundary of the stream flow. For values of $k < 1$, independently of the value of the parameter δ, oscillations with the parameter n = 0 always increase, and never lead to stream decomposition with the parameter $n > 1$. When $k > 1$, stream decomposition may occur as the result of the development of oscillations with different n. With an increase in parameter δ, the complex oscillations reduce the stream to decomposition.

Consequently, the dimensionless parameter

$$\delta = \frac{2\rho_{ж} r_0 (v_{ж} - v_г)^2}{\sigma}$$

determines the nature of the stream decomposition. The relative dimension of the drops formed during the decomposition is a function of this parameter. /29

The solution obtained is a generalization of the Raleigh condition (3-9) which may be obtained if we assume the following in (3-14)

$$v_{ж} = v_{г} = 0 \text{ and } \varrho_{г} = 0.$$

On the basis of the theory of small oscillations, Weber [3-2] analytically determined the decomposition condition and the length of the solid section of the viscous liquid stream entering the medium of nonviscous gas. The determination was made for two forms of the perturbing motion: symmetric and wavelike oscillations of the liquid in the stream. In particular, Weber obtained the Raleigh solution for the nonviscous liquid.

Assuming that small symmetric perturbations (n = 0) are imposed on the basic flow, Weber wrote the equation with respect to motion of a viscous liquid and the corresponding boundary conditions. Thus, due to the smallness of the surface perturbations and the pressure pulsations, and also their derivatives, Weber disregarded the products and higher orders of these quantities. This made it possible to disregard the convective terms when writing the equation of the relative motion of a viscous liquid for small oscillations. As a result, a partial derivative and a system of linear equations were obtained, instead of the complete derivative of velocity in time. The solution of these equations is obtained from individual particular solutions, for example, using the Fourier series.

The conditions (2-6) - (2-10) may be somewhat simplified due to the fact that 2 . Thus, we omit the condition (2-7), and condition (2-9) is reduced to the form:

$$(\tau_{ж})_{гр} = 0. \qquad (3\text{-}15)$$

$\mu_{г} = 0.$

The influence of the surrounding air medium is taken into account by the condition (2-10) in which the value of the air pressure pulsation is obtained by integration of the linearized Euler equations which describe the motion of an air stream, and the continuity equation. Integration was performed with allowance for the hydrodynamic velocity potential. /30

A conclusion similar to the Raleigh solution, after several simplifications and transformations, leads to the following approximate condition for the case of long waves (k < 1):

$$q^2 + q\frac{3\mu_ж}{\varrho_ж r_0^2}k^2 = \frac{\sigma}{2\varrho_ж r_0^3}(1-k^2)k^2 + \\ + \frac{\varrho_г v_{отн}^2 k^3}{2\varrho_ж r_0^2} f_0(k). \qquad (3\text{-}16)$$

Here $v_{отн}$ is the relative velocity of the medium:

$$f_0(k) = -\frac{i\,H_0'(ik)}{H_1'(ik)} > 0,$$

where $H_0(ik)$, $H_1'(ik)$ -- Hankel function of the zero and first order, respectively.

At $q > 0$, all of the oscillations lead to the stream decomposition. However, the most rapidly increasing oscillation is decisive.

The wavelength of the most rapidly increasing perturbation is determined from the condition:

$$\frac{\partial q}{\partial k} = 0 \qquad \text{and} \qquad \frac{\partial^2 q}{\partial k^2} < 0.$$

For the case of the decomposition of a liquid stream without the influence of the surrounding medium, the value of the parameter $q_{опт}$ is determined from the formula:

$$q_{опт} = \frac{1}{\sqrt{\frac{8\varrho_ж r_0^3}{\sigma} + \frac{6\mu_ж}{\sigma} r_0}}. \qquad (3\text{-}17)$$

Thus, the wavelength

$$\lambda_{опт} = 2\pi r_0 \sqrt{2\left(1 + \sqrt{\frac{9\mu_ж^2}{2\sigma\varrho_ж r_0}}\right)}.$$

The time for the beginning of decomposition, calculated from the moment of the stream flow, is: /31

$$T_0 = \frac{1}{q_{опт}} \ln \frac{r_0}{\xi_0} = \ln \frac{r_0}{\xi_0} \left(\sqrt{\frac{8\varrho_* r_0^3}{\sigma}} + \frac{6\mu_* r_0}{\sigma} \right). \tag{3-18}$$

Here ξ_0 is the perturbation of the stream surface at the time of flow.

In dimensionless form, formula (3-18) may be written:

$$T_0 \frac{\sigma^2 \varrho_*}{27\mu_*^3} = K \left[\left(\frac{2}{9} \cdot \frac{\sigma \varrho_* r_0}{\mu_*^2} \right)^{1/2} + \left(\frac{2}{9} \cdot \frac{\sigma \varrho_* r_0}{\mu_*^2} \right) \right]. \tag{3-18'}$$

A comparison of formula (3-18') with the experimental data [3-8] gives the value K = 10.

It must be noted that the values of the wavelengths which break up the stream, in contrast to the solution for the nonviscous liquid (Raleigh, Petrov and Kalinin), will depend on the value of the liquid viscosity.

The study of A. S. Lyshevskiy [3-14,16] gave the application of the Weber solution to the case of a plane stream decomposition of nonviscous and viscous liquids. The decomposition of a hollow stream was examined in a study by the same author [3-15]. However, these studies are not of practical interest, since a hollow stream without a vortex cannot be achieved for any great length, and one-dimensional oscillations in the plane are very unlikely. Thus, the problem of a hollow stream is not correctly formulated.

The conditions for the decomposition of a nonviscous liquid stream emanating from an elliptical opening were determined by Yu. F. Dityakin [3-11] in the form of the following equation:

$$q \sqrt{\frac{a^3 \varrho_*}{\sigma}} = \frac{1}{A - \frac{\varrho_r}{\varrho_*} B} \times \sqrt{\frac{1 - k^2 k^2}{\varepsilon^3} \left(A - \frac{\varrho_r}{\varrho_*} B \right) - k^2 \delta AB}. \tag{3-19}$$

Here $\varepsilon = a/b$, where a and b are the ellipse semi-axes:

$$\delta = \frac{v^2 \varrho_\infty r_0}{\sigma};$$

$$A = \frac{Ce_m(\xi_0 - p)}{d\,Ce_m(\xi_0 - p)/d\xi_0};$$

$$B = \frac{Fe_m(\xi_0 - p)}{d\,Fe_m(\xi_0 - p)/d\xi_0}, \qquad \underline{/32}$$

where Ce_m and Fe_m are the modified Matye functions of the first and second kind;

$\xi_0 = \operatorname{arc\,th}\,\varepsilon$ -- dimensionless quantity:

$$p = \frac{k^2(1-\varepsilon^2)}{4}.$$

The change from stable oscillations to unstable ones is characterized by the condition:

$$\delta = \frac{1 - \varepsilon^2 k^2 \left(A - \frac{\varrho_r}{\varrho_\infty} B\right)}{\varepsilon^3 k^2 AB}. \qquad (3\text{-}20)$$

For small values of ϱ_r/ϱ_∞, the formula (3-20) is simplified to the form:

$$q \sqrt{\frac{a^3 \varrho_\infty}{\sigma}} = \sqrt{\frac{1 - \varepsilon^2 k^2}{\varepsilon^3 A}}. \qquad (3\text{-}21)$$

Figure 3-7 shows the dependence of the dimensionless increment of the oscillations $q \sqrt{\frac{a^3 \varrho_\infty}{\sigma}}$ on the wave number $k = \frac{2\pi r}{\lambda}$ for different values of ε, calculated using formula (3-21).

It may be seen from the graph that an increase in the ellipticity (decrease of ε) leads to a displacement of the maximum toward small wavelengths (large k) and to an increase in the stream instability. Experiments have confirmed these conclusions qualitatively.

Different conditions for the decomposition of liquid streams have been examined in detail in the study of V. J. Levitch [3-13]. The problems are briefly

examined below which may have a direct relationship to the liquid atomization in spray nozzles. Therefore, we do not consider that portion of the study which examines problems of stability and the decomposition of viscous liquids. In all of the cases examined, equations were obtained for determining the complex frequency. The complex frequencies of unstable oscillations were determined from these equations as a function of the wave number. The wave number and the frequency of the most unstable oscillation were calculated from the condition that this function is at a maximum. In addition, the decomposition time and the length of the solid section were determined. The author of [3-13] did not have the purpose of obtaining the absolute calculated values, and established the relationship between the parameters characterizing the process in each particular case.

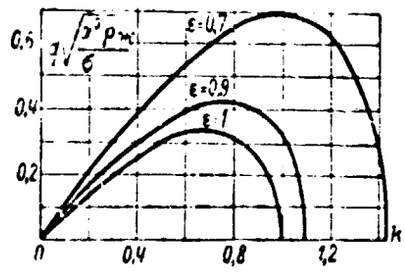

Fig. 3-7. Boundary of flow stability of elliptical stream for different values of the ellipticity coefficient ε.

Numbers on the curves give values of ε.

/33

The influence of the surrounding gas stream may be disregarded in the case of symmetric oscillations of a stream moving at a low velocity. For determining the complex frequency, a very complex equation is obtained which cannot be solved analytically in the general case:

$$q^2 + \frac{2\nu_ж k^2}{r_0^2 I_0(ik)}\left[I_1'(ik) - \frac{2kl}{k^2+l^2}\cdot\frac{I_1(ik)}{I_1(il)}I_1'(il)\right]q = \\ = \frac{-ink}{\rho_ж r_0^3}(1-k^2)\frac{I_1(ik)}{I_0(ik)}\cdot\frac{l^2-k^2}{l^2+k^2}. \qquad (3\text{-}22)$$

where

$$l^2 = k^2 + \frac{qr_0^2}{\nu_ж}; \quad \nu_ж = \frac{\mu_ж}{\rho_ж}.$$

Below, the derivatives of the Bessel functions are taken with respect to the variable r.

In the limiting case of a slightly viscous liquid and long waves ($\lambda \gg r_0$, $k \ll 1$; only these waves lead to decomposition), the inequality $qr_0^2\nu_ж \gg k^2$ holds, and consequently, $l \gg k$. For this case, the condition of the oscillation instability is identical to the result obtained by Raleigh (3-9) and (3-10).

In the time $t = 1/q_{макс} = 8{,}46\sqrt{\varrho_ж r_0^3/\sigma}$, the amplitude of the oscillations increases by a factor of e. Therefore, the decomposition time T is proportional to t, and the length of the nondecomposed part $L \sim vT$.

The formulas are applicable under the condition $\sqrt{r_0\sigma/\varrho_ж\nu_ж^2} \gg 1$ (i.e., $\mu_ж^2/\varrho_ж r_0\sigma \ll 1$).

The solution of the equations of motion for the case of long wave arbitrary deformations may be simplified by the following relationships:

$$\frac{\partial v_z}{\partial z} \approx \frac{\partial v_r}{\partial r} \approx \frac{1}{r}\cdot\frac{\partial v_\theta}{\partial \theta} \quad \text{and} \quad v_z \gg v_r,\ v_\theta.$$

/34

In addition, due to the smallness of the stream radius, we do not consider the change in the component v_z over the radius. In this case, the equation of motion in cylindrical coordinates has the form:

$$\frac{\partial v_z}{\partial t} = \frac{1}{\varrho_ж}\cdot\frac{\partial p_1}{\partial z} + 2\nu_ж\frac{\partial^2 v_z}{\partial z^2}, \tag{3-23}$$

and for the complex frequency, the following equation is obtained:

$$q^2 + 2\nu_ж\frac{k^2 q}{r_0^2} = \frac{\sigma k^2}{2\varrho_ж r_0^3}(1 - n^2 - k^2). \tag{3-24}$$

The real value of q is obtained only at n = 0.

Thus, as was indicated above, at slow velocities of stream motion, decomposition only occurs as the result of symmetrical oscillations (n = 0). Thus,,

$$q = -\frac{\nu_{ж}k^2}{r_0^2} \pm \sqrt{\left(\frac{\nu_{ж}k^2}{r_0^2}\right)^2 + \frac{\sigma k^2}{2\varrho_{ж}r_0^3}(1-k^2)}. \qquad (3\text{-}25)$$

The oscillations with n > 0 are stable.

The value of q reaches its maximum value at

$$k = \frac{1}{r_0\left(\sqrt{\frac{\mu_{ж}^2}{2\varrho_{ж}r_0\sigma}+2}\right)^{1/2}}.$$

The value of $q_{макс}$ coincides with the formula (3-17), obtained by Weber.

However, the wavelength of the most unstable oscillation has a different value equal to:

$$\lambda_{опт} = 2\pi r_0\sqrt{2\left(1+\sqrt{\frac{\mu_{ж}^2}{8\varrho_{ж}r_0\sigma}}\right)}.$$

The problem of a liquid stream decomposition at large velocities, i.e., under conditions when it is necessary to consider the dynamic influence of the gas on the liquid surface, is examined under the assumption that the gas viscosity may be disregarded in the first approximation. It is assumed that the gas moves at the velocity v_r along the z-axis, and the stream does not move. Then, for the velocity potential in the gas, we may write the equation:

$$\Delta\varphi_r = 0. \qquad (3\text{-}26)$$

When writing the boundary conditions, we assume that the tangential stresses equal zero, but we do not consider the fact that not only the normal, but also the tangential velocity components of the gas and liquid are equal. /35

Thus, we obtain the following expression for the velocity potential in the case of symmetric waves:

$$\varphi_r = v_r z + bK_0\left(\frac{kr}{r_0}\right) e^{\frac{ikz}{r_0} + qt}. \tag{3-27}$$

where 1) is the Bessel function of the second kind (McDonald function) which vanishes at infinity.

The velocity distribution and pressure distribution in the gas are found from this equation. We thus obtained the following expression for b:

$$b = \frac{r_0 q + ikv}{k} \cdot \frac{1}{K_0'(k)} \xi_0,$$

where ξ_0 is the initial surface displacement. The surface displacement

$$\xi = \xi_0 e^{\frac{ikz}{r_0} + qt}.$$

The velocity in the gas v_r is related with the stream flow velocity v_0 as follows:

$$v_0 = v_r \ln \frac{r_0}{\xi_0},$$

which is obtained from the condition of the formation of a boundary layer in the gas on the stream surface. To determine the complex frequency q, after several transformations and simplifications (the small terms $\varrho_r q^2$ and $\varrho_r \frac{ikv_r q}{r_0}$ are omitted), we obtain the equation:

$$\begin{aligned} q^2 + \frac{2\nu_* k^2}{r_0^2 I_0(ik)}\left[I_1'(ik) - \frac{2kl}{l^2-k^2}\cdot\frac{I_1(ik)}{I_1(il)} I_1'(il)\right]\eta = \\ = -i\left[\frac{\sigma k}{\varrho_* r_0^3}(1-k^2)\frac{I_1(ik)}{I_0(ik)}\cdot\frac{l^2-k^2}{l^2-k^2} + \right. \\ \left. + \frac{\varrho_r k^2 v_r^2}{\varrho_* r_0^2}\cdot\frac{K_0(k) I_1(ik)}{K_1(k) I_0(ik)}\cdot\frac{l^2-k^2}{l^2-k^2}\right]. \end{aligned} \tag{3-28}$$

In the case of short waves, the arguments of the Bessel functions are large as compared with unity, and after applying the asymptotic solutions /36

$$K_0(x) = -K_0(x) \approx \sqrt{\frac{\pi}{2x}}\, e^{-x}$$

and simplifications, we obtain the solution:

$$q^2 + \frac{2\nu_{ж} k^2 q}{r_0^2}\left(1 - \frac{2kl}{l^2 + k^2}\right) =$$

$$= -\frac{\sigma k^3}{\varrho_{ж} r_0^3}\cdot\frac{l^2 - k^2}{l^2 + k^2} + \frac{\varrho_г k^2 v_г^2}{\varrho_{ж} r_0^2}\cdot\frac{l^2 - k^2}{l^2 + k^2}. \qquad (3\text{-}29)$$

For the case of low viscosity, it was shown that the linear term q is small as compared with the square one, and $l \gg k$.
Therefore:

$$q \approx \sqrt{\frac{r_0 \varrho_г k^2 v_г^2 - \sigma k^3}{r_0^3 \varrho_{ж}}}. \qquad (3\text{-}30)$$

Thus, at large velocities and low viscosity, the oscillations are unstable at

$$k \leqslant \frac{\varrho_г v_г^2 r_0}{\sigma},$$

i.e., for the relative wavelength

$$\frac{\lambda}{r_0} \leqslant \frac{2\pi\sigma}{\varrho_г v_г^2 r_0}.$$

The quantity q has a maximum for the value of

$$k = \frac{2}{3}\cdot\frac{\varrho_г v_г^2 r_0}{\sigma},$$

which equals

$$q_{макс} = 0{,}4\frac{v_г^3}{\sigma}\sqrt{\frac{\varrho_г^3}{\varrho_{ж}}}. \qquad (3\text{-}31)$$

In the time T, which equals:

$$T \approx 2{,}6 \frac{\sigma}{v_r^3} \sqrt{\frac{\varrho_*}{\varrho_r^3}}, \qquad (3\text{-}32)$$

the amplitude increases by a factor of e.

Thus, the dimension of drops obtained from the atomization of a slightly viscous liquid is a function of the criterion $\varrho_r v_r^2 r_0/\sigma$ and decreases with an increase in this criterion. /37

The formulas derived will be applied at

$$\frac{\mu_* v_r}{\sigma} \sqrt{\frac{\varrho_r}{\varrho_*}} \ll 1.$$

The law of energy conservation is used to calculate the atomization time [3-13]. The energy transmitted to the liquid by a gas stream is used for dissipation and the formation of a new surface.

Thus, the atomization time is equal to:

$$T \sim t \frac{r_0}{L_0} \approx \sqrt{\frac{\varrho_*}{\varrho_r}} \cdot \frac{r_0}{v_r}. \qquad (3\text{-}33)$$

and the length of the solid section $L \sim \sqrt{\varrho_* \varrho_r} \cdot r_0$ does not depend on the velocity of motion of the gas flow. However, this formula is only approximate and gives only the order of magnitude.

In the case of arbitrary but rather long waves (k << 1), the solution for the complex frequency has the form:

$$q^2 + \frac{2\nu_* k^2}{r_0^2} q = \frac{\sigma k^2}{2\varrho_* r_0^3}(1 - n^2 - k^2) - \frac{\varrho_r k^4 v_r}{2 r_0^3 \varrho_*} \ln\left(\frac{r_0}{r_0}\right). \qquad (3\text{-}34)$$

For a slightly viscous liquid, disregarding the linear term, we obtain the solution in the form:

$$q = \sqrt{\frac{\varrho_r k^4 v_r^2 \ln\frac{k}{2}}{2\varrho_ж r_0^2} + \frac{\sigma k^2}{2\varrho_ж r_0^3}(1 - n^2 - k^2)}. \qquad (3\text{-}35)$$

The symmetric waves (n = 0) correspond to the largest value of q.

At large velocities, when

$$\varrho_r v_r^2 k^4 \gg \frac{\sigma}{r_0} k^2,$$

$$q = \sqrt{\frac{\varrho_r}{2\varrho_ж}} \cdot \frac{v_r}{r_0} k^2 \left(-\ln\frac{k}{2}\right)^{1/2}, \qquad (3\text{-}36)$$

the maximum value $q_{макс} \approx \sqrt{\frac{\varrho_r}{\varrho_ж}} \cdot \frac{v_r}{r_0}$ occurs at k = 0.75 (i.e., $\lambda \approx 8r_0$).

Thus: /38

$$T \sim \frac{1}{q_{макс}} \approx \sqrt{\frac{\varrho_ж}{\varrho_r}} \cdot \frac{r_0}{v_r} \text{ и } L \sim \sqrt{\frac{\varrho_ж}{\varrho_r}} \cdot r_0. \qquad (3\text{-}37)$$

Under the influence of air, a slightly viscous liquid decomposes into drops due to the development of long and short unstable waves of differing order, and the decomposition time has one and the same order of magnitude.

The dependences obtained may be extended to masses of liquid with arbitrary form.

For a slightly viscous liquid at low velocities

$$T \sim \sqrt{\frac{\varrho_ж r_0^3}{\sigma}}.$$

At large velocities

$$T \sim \frac{r_0}{v_r}\sqrt{\frac{\varrho_ж}{\varrho_r}}.$$

The complete analytical solution for the problem of a stream decomposition, including the determination of the drop dimensions, entails several difficulties at the present time.

The drops produced are the result of a complex process of the breakdown of the larger drops which are first formed. This latter process may be expressed by an equation of pulsation motion and the boundary conditions corresponding to the intermediate state of the drops. However, it is not possible to formulate the boundary conditions for the intermediate stages, since it is impossible to follow all of the changing forms of the stream decomposition. Thus, this scheme excludes the possibility of a complete analytical solution of the problem. Nevertheless, it is advantageous to derive the similarity criteria, which characterize the atomization process, from the equation for the stream instability. If it is considered that when the processes are similar, the same relationships between the length of the oscillation waves and the diameters of the drops produced remain the same, then on the basis of experiments we may obtain the form of the functional relationship between the criteria. This makes it possible to determine the average drop diameter.

Section 3-3. System of criteria characterizing the atomization of a nonvortex stream

/39

The similarity criteria characterizing the atomization of a viscous liquid, flowing from a cylindrical nozzle, may be obtained by analyzing the equation (3-16) or (3-29). It must be considered that the oscillation increment q included in the equation is inversely proportional to the time interval T from the time the stream leaves the spray nozzle until its decomposition begins, and may be replaced in the criteria by the quantity 1/T. The wave number q in the criteria is expressed by the oscillation wavelength $2\pi r_0/\lambda$.

After several transformations, we obtain the following criteria [3-4, 6]:[1)]

[1)] When writing the criteria, instead of the stream radius r_0, we may use the diameter $d_0 = 2r_0$ as the determinant dimension.

$$\Pi_1 = \frac{\mu_*^2}{\varrho_* \sigma d_0}; \qquad (3\text{-}38)$$

$$\Pi_2 = \frac{\varrho_r v^2 d_0}{\sigma}; \quad \Pi_3 = \frac{d_0}{\lambda}; \quad \Pi_4 = \frac{\mu_*}{\varrho_r v^2 T}.$$

The criteria Π_1 and Π_2 are determinant. The criteria Π_3 and Π_4, containing the quantities λ and T are indeterminant.

Assuming that for similar processes $\Pi_3 = \lambda/d$ = idem, where d is the average drop diameter, instead of the criterion $d_0\lambda$, we may introduce the criteria d_0/d or the quantity inverse to it, i.e., d/d_0.

Then the functional relationship (3-38) between the criteria characterizing the average drop dimension is represented in the form:

$$\frac{d}{d_0} = f\left(\frac{\mu_*^2}{\varrho_* \sigma d_0}, \frac{\varrho_r v^2 d_0}{\sigma}\right). \qquad (3\text{-}39)$$

The criteria $\mu_*^2/\varrho_* \sigma d_0$ characterize the relationship between the forces of viscous, inertial and surface tension.

The criteria $\varrho_r v^2 d_0/\sigma$ characterize the relationship between the inertial forces of the air stream and the forces of surface tension, i.e., it considers the interaction of the deformed stream with the external medium.

The criterion d/d_0 gives the ratio of the average drop diameter to the characteristic dimension and determines the flame degree of dispersion. /40

For small values of the liquid viscous forces, as compared with the inertial forces and the surface tension forces, the decomposition process will be determined only by the criterion $\varrho_r v^2 d_0/\sigma$.

Thus, equation (3-39) is simplified and assumes the following form:[1)]

[1)] In the Raleigh solution, where the decomposition of a nonviscous liquid is examined when there is no influence of external forces, the quantity d/d_0 has a constant value.

$$\frac{d}{d_0} = f\left(\frac{\rho_r w^2 d_0}{\sigma}\right). \qquad (3\text{-}40)$$

The numerical values of the coefficients in the functional relationship (3-39) may be changed in view of the difference in the initial stream flow conditions, which in their turn are characterized by the characteristic of different spray nozzle structures.

However, the form of the functional relationship must remain unchanged for different spray nozzles.

It must be noted that the dependence obtained does not consider the braking of the gas flow of a liquid stream occurring in pneumatic spray nozzles, since the initial relative velocity is included in the criterion. The velocity change in the atomization process will be different depending on the magnitude of the criterion $\mu_ж/\rho_r w^2 T$, characterizing the decomposition time, and depending on the relationship between the quantity of gas and liquid. This problem will be considered separately, when analyzing data on the atomization of a liquid by pneumatic spray nozzles.

Section 3-4. Basic characteristics of the atomization stream

As was indicated above, under certain conditions a stream may be unstable and may be decomposed into sections almost at the opening itself, and these sections continue to break apart. As a result, an atomization stream is obtained consisting of drops with different dimensions.

The studies of M. S. Volysnkiy [3-7] showed that drops whose dimensions do not exceed a certain quantity, which is determined by the following condition for a nonviscous liquid: /41

$$\frac{\rho_r w^2 d_{макс}}{\sigma} < 14. \qquad (3\text{-}41)$$

are stable in a gas stream. Here $d_{макс}$ is the initial drop dimension.

A study by Tresch [3-21] was devoted to an investigation of the finite dimensions of drops formed during decomposition. Based on these data, the following equation holds:

$$Z_1 (1 + \alpha_1 Z_2)^{1/\alpha} (1 - \alpha_2 Z_3) = K = \text{const.} \qquad (3\text{-}42)$$

Here

$$Z_1 = \frac{\sigma}{\varrho_{ж} v_{отн}^2 d_{макс}}; \quad Z_2 = \frac{\mu_{ж}^2}{\sigma \varrho_{ж} d_{макс}}; \quad Z_3 = \frac{\varrho_г}{\varrho_{ж}};$$

α_1; α_2; K = constants

Tresch, using the experimental data of Beer, determined the numerical values of the constants:

$$K = 4{,}8 \cdot 10^{-3}; \quad \alpha_1 = 10^6; \quad \alpha_2 \text{ (according to Weber)} = 0.5$$

Formula (3-42) may be used, according to the author of [3-21] under the following conditions:

1. At any point in the atomization, the velocity corresponding to the drop deformation time must be determined.

2. The drops do not interact in the space of atomization.

3. A third medium (for example, plate placed against the nozzle) does not influence the atomization process.

This method for determining the stream dispersion has several disadvantages. The value of the constants given is not universal, and must depend on the atomization construction. There are several difficulties involved in determining the largest drop dimension by experimental methods, because the number of large drops in the stream is small and it is difficult to establish ahead of time the dimension of the reliable sample (based on the number of drops).

The application of the probability theory to an analysis of the drop distribution in terms of dimension does not require determining either their minimum or maximum dimensions. The curves for the drop dimension distribution have clearly expressed maxima, and the probability of finding both very large and very small drops is negligibly small.

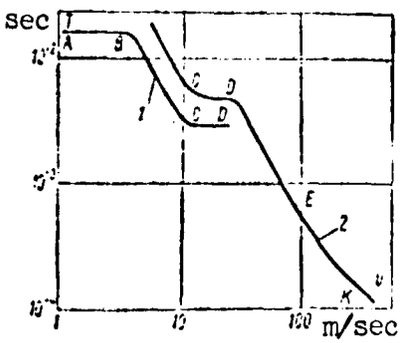

Fig. 3-8. Dependence of time at which water stream begins to decompose on the flow velocity from nozzle. /42

1 - [3-3]; 2 - [3-8].

As has been shown [3-4], it is advantageous to use formula (1-9) transformed to the form (1-10a) for determining the functional composition of drops in a flame:

$$\ln R_i = -\left[\Gamma\left(1+\frac{1}{m}\right)\frac{d_i}{d}\right]^m.$$

Here, R_i -- relative proportion of drops whose dimensions are greater than d_i;

m -- constant determined from experiment, whose value depends on the spray nozzle construction;

d -- average drop diameter using the formula (1-2).

This formula generalizes all the data on the drop distribution for all the modes, i.e., for all values of the average drop diameter d obtained in a given spray nozzle.

Section 3-5. Generalization of experimental material on decomposition of nonvortex streams

The data of [3-3] and [3-8] examined in Sec. 3-1 are compared in Fig. 3-8 in logarithmic coordinates in the form of the dependence of the beginning of water stream decomposition on the flow velocity. In this graph, the region ABC is characterized by symmetric oscillations. Thus, in the section AB the medium has a slight influence upon the increase of perturbations of the stream surface. The increasing influence of the surrounding medium on the stream

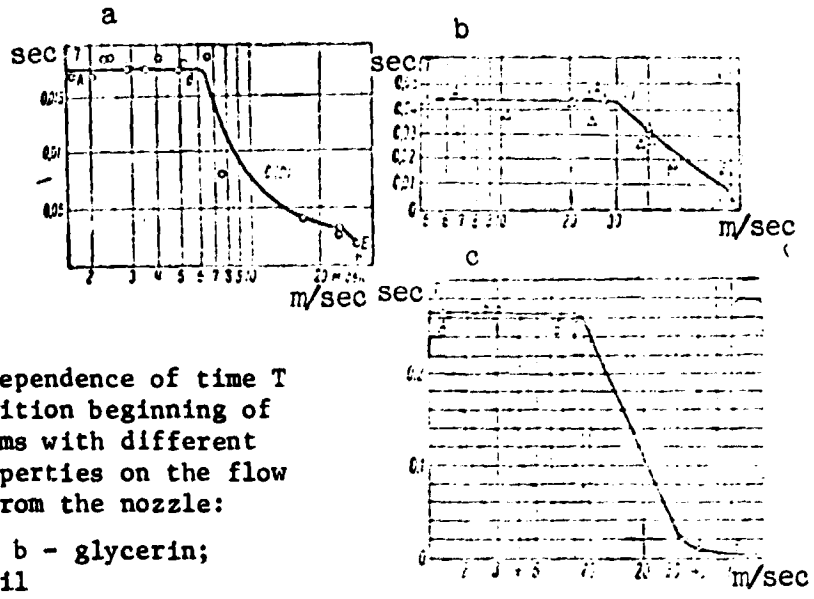

Fig. 3-9. Dependence of time T for decomposition beginning of liquid streams with different physical properties on the flow velocity v from the nozzle:

a - gas oil; b - glycerin; c - castor oil

surface causes a reduction in its stability (section BC) and leads to the development of wavelike oscillations (section CDE). A change in the liquid flow velocity in the section CD has no great influence on the degree of stream stability. With a further increase in the velocity, the interaction of the surface with the surrounding medium again causes a decrease in the decomposition time beginning and, consequently, increases the stream instability. Thus (in the section EK) /43 breakdown and atomization of the liquid begins.

A comparison of the data on the water stream decomposition (Fig. 3-8) and the decomposition of other more viscous liquids (Fig. 3-9) shows that the interaction of a stream of viscous liquid with the surrounding gas causes its wavelike oscillation. Thus, on the curve in Fig. 3-9,a there is no section CD, and on the curves of Fig. 3-9,b and c -- the section BCD.

The system of similarity criteria characterizing the motion of gas-liquid media was examined above in Sec. 2-3. Disregarding the influence of the force of gravity during the flow of liquid in a fixed gas medium, we may confine ourselves to selecting the following similarity criteria:

$$\frac{\rho_\infty \sigma l}{\mu_\infty^2};\ \frac{\rho_\infty}{\rho_r};\ \frac{\mu_\infty v_0}{\sigma};\ \frac{T_0 v_0}{l};\ \frac{\mu_\infty}{\mu_r};\ \frac{\Delta p}{\rho_\infty v_0^2}. \quad (3\text{-}43)$$

Let us use this system when determining the liquid flow velocities v_0(v_{01} and v_{02}) at which there is a sharp decrease in the stability of the stream in the case of symmetric and wavelike oscillation and for the largest decomposition time T_0(T_{01} and T_{02}) for the given modes. For this purpose, we transform the system to the following form:

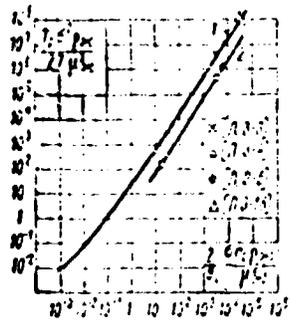

Fig. 3-10. Dependence of the largest times of stream decomposition beginning in the region of symmetric (1) and wavelike (2) oscillations. /44

$$\frac{\rho_\infty}{\rho_r};\ \frac{\mu_\infty}{\mu_r};\ \frac{\mu_\infty v_0}{\sigma};\ \frac{\rho_\infty \sigma l}{\mu_\infty^2};\ \frac{T_0 \sigma^2}{\mu_\infty^3};\ \frac{\Delta p}{\rho_\infty v_0^2}. \quad (3\text{-}44)$$

In this sytem, the criteria $\rho_\infty \sigma l / \mu_\infty^2$, μ_∞ / μ_r and ρ_∞ / ρ_r, are determinant, which contain the physical and geometric parameters.

Thus, the indeterminant criteria in which we are interested may be expressed as a function of these criteria:

$$\frac{\mu_\infty v_0}{\sigma} = f_1\left(\frac{\rho_\infty \sigma l}{\mu_\infty^2};\ \frac{\mu_\infty}{\mu_r};\ \frac{\rho_\infty}{\rho_r}\right); \quad (3\text{-}45)$$

$$\frac{T_0 \sigma^2 \rho_\infty}{\mu_\infty^3} = f_2\left(\frac{\rho_\infty \sigma l}{\mu_\infty^2};\ \frac{\mu_\infty}{\mu_r};\ \frac{\rho_\infty}{\rho_r}\right). \quad (3\text{-}46)$$

In an analysis of the equation which did not consider the force of gravity, it was shown that there are two determinant criteria for the decomposition (Sec. 3-3). However, all of the studies examined did not consider the viscosity during the interaction between the gas flow and the atomized liquid stream. When this fact is taken into account, the number of determinant criteria, as we shall see, increases to three.

As is customary when processing the experimental material, the dependence is found in the form of a power complex of the criteria. The dependence (3-18) represents the particular form of the dependence (3-46) for the case $\mu_r = 0$ or $\mu_r \ll \mu_\infty$.

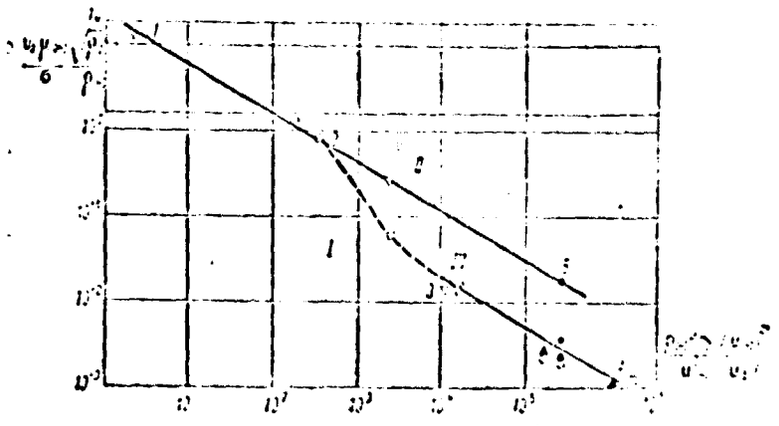

Fig. 3-11. Dependence of critical flow velocity of liquid stream on physical properties of medium and nozzle dimensions.

○, △, ▽, ▲ -- castor oil, glycerin, gas oil, water -- all in air [3-8]; ● -- water in air [3-3]; 0 -- water in air [3-18]; - -- water in air [3-10]; X -- water in kerosene [3-18].

A. Generalization for T_0

Figure 3-10 shows a comparison of the calculated line 1, corresponding to formula (3-18'), with the experimental data [3-3]. There is a good agreement between calculation and experiment. This figure also plots the experimental data corresponding to sections CD of the curve in Fig. 3-8. The line 2, calculated using the formula (3-18), is drawn through these points for a value of K = 1.22. Thus, the influence of the medium on the time for the beginning of the decomposition was taken into account by a different value of the coefficient K in the sections AB and CD. /45

B. Generalization for v_0

When processing the experimental data [3-3, 8, 10 and 18], the relationship was considered [3-9] between the critical velocity and the density of the medium, in which the flow takes place, $v_0 \sim (\rho_1)^{-0.5}$. Thus, the functional relationship between the similarity criteria may be expressed in the following

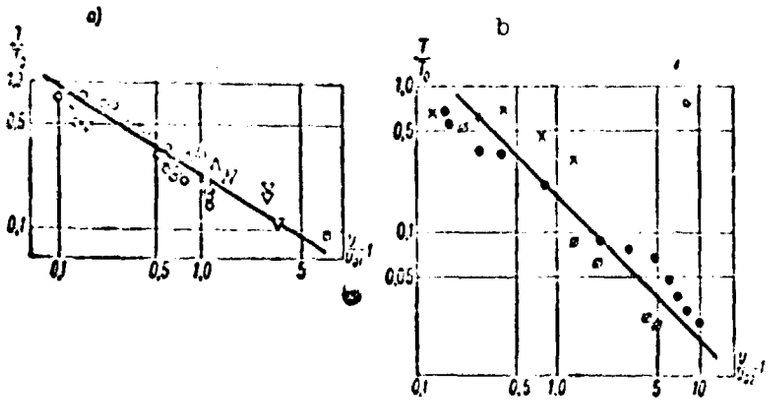

Fig. 3-12. Dependence of dimensionless time for beginning of stream decomposition on dimensionless flow velocity from nozzle for symmetric (a) and wavelike (b) oscillations.

Δ -- water [3-9]; 0 -- water [3-18]; ◇ -- water [3-10]; ▽ -- gas oil [3-8]; Ø -- castor oil [3-8]; X - glycerin [3-8]; ● -- water [3-3].

form:

$$\frac{\rho_0 u_\infty}{\sigma}\sqrt{\frac{\rho_0}{\rho_\infty}} = A\left[\frac{\rho_\infty l_0 \sigma}{\mu_\infty^2}\left(\frac{\mu_\infty}{\mu_0}\right)^m\right]^n. \qquad (3\text{-}47)$$

The initial steam radius r_0 is used as the determinant dimension l from formulas (3-43) - (3-46).

The initial comparison of the experimental data on the decomposition of a stream of the same liquid leaving one and the same nozzle into different media showed that the exponent may equal $m = 0.5$ for the ratio of the viscosity coefficients.

Figure 3-11 shows the result of generalizing the dependence (3-47) in coordinates. The following may be concluded from examining this graph:

Domain 1, located below line 1-2-3-4, characterizes the stream decomposition as the result of the development of symmetrical oscillations without the influence of the surrounding medium. /46

Domain II, which is above line 1-2-5, characterizes the stream decomposition as a result of the development of wavelike oscillations caused by the influence of the external medium.

Domain III is a mixed domain, in which the decomposition is caused by both types of oscillations.

The generalized criterial relationship, determined by formula (3-47), is valid for a value of the coefficients n = -0.58 for all cases of decomposition, with the exception of the section of the curve 2-3. The value of the coefficient A equals 15 on the line 1-2-5 and 4 on the line 3-4.

In each specific case, knowing the flow velocity, the nozzle dimensions, and the physical parameters of the medium, using the graph in Fig. 3-11, we may establish in what domain the decomposition occurs.

C. Generalization for T

The selection of v_o and T_o as the scale of the characteristic quantities makes it possible to generalize the research results on the decomposition of a liquid stream with different physical properties. In Fig. 3-12, in the coordinates

$$\frac{T}{T_0} = f\left(\frac{v}{v_0}\right) \tag{3-48}$$

for the regions for symmetric and wavelike oscillations, the experimental data given in the primary coordinates T = f(v) in Figs. 3-8 and 3-9 are plotted. It can be observed that there is a certain degree of generalization of the experimental data, which makes it possible to give calculation recommendations. /47

The data on the decomposition of liquid streams in air in the region of symmetric oscillations may be generalized by the formulas:

$$T = T_{01} \quad \text{at} \quad v \leqslant v_{01}, \tag{3-49}$$

$$T = 0{,}23T_{01}\left(\frac{v}{v_{01}} - 1\right)^{-0{,}6} \quad \text{at} \quad v > 1{,}1v_{01}. \tag{3.49'}$$

In the region of wavelike oscillations:

$$T = T_{02} \quad \text{at} \quad v < v_{02}; \qquad (3\text{-}50)$$

$$T = \frac{0{,}17T_{02}}{\frac{v}{v_{02}} - 1} \quad \text{at} \quad v > 1{,}1v_{02}. \qquad (3\text{-}50')$$

For large stream flow velocities, when $v/v_{02} \gg 1$, the time for the beginning of the stream decomposition is inversely proportional to the velocity ($T \sim 1/v$), and the length of the solid section of the stream does not depend on the flow velocity, which coincides with the theoretical results [3-13].

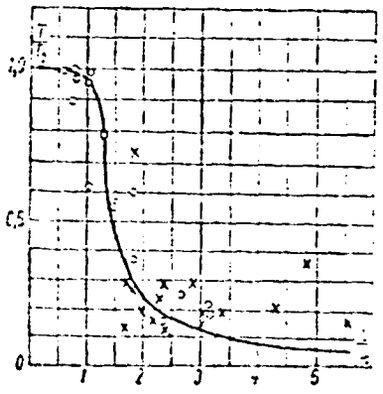

Fig. 3-13. Dependence of time of water stream decomposition (X) and liquid nitrogen (0) on relative flow velocity from nozzle.

This generalization was used to process the data in [3-19] on the decomposition of the stream of water and liquid nitrogen in air [3-5]. /48

Table 3-1 gives the calculated velocities v_o and the value of T_o, either calculated directly using experimental data or determined by calculation using the formula (3-18'). The calculation shows that the decomposition of these streams takes place in the region of wavelike oscillations. In the coordinates of the formula (3-48), Fig. 3-13 shows a comparison of the experimental data with the calculated dependence (3-50). There is agreement between experiment and calculations. The problems presented in Sec. 3-5 are discussed in greater detail in the study of L. A. Vitman [3-5].

Calculation example.

Determine at what distance and in what time period a stream of kerosene leaving a nozzle into the atmosphere is decomposed. We have: nozzle diameter $d_o = 10^{-3}$ m, flow velocity v = 2 m/sec., 5 m/sec., 20 m/sec. and 100 m/sec,

TABLE 3-1

stream diameter d, mm	water		nitrogen	
	m/sec	sec	m/sec	sec
2,53	19.5	0,018	10.2	0,0175
2,38	20.6	0,0154	10,6	0,0486
1,98	23.0	0,009	11.7	0,0333
1,56	—	—	14.3	0,0198
1,42	28,0	0,007	—	—
1,07	32.7	0,0056	—	—
1,03	—	—	17,8	0,0131
0,714	41,0	0,003	21,2	0,00715

$\sigma = 2.8 \cdot 10^{-3}$ kg/m, $\gamma_{ж} = 800$ kG/m^3, $\mu_{ж} = 3 \cdot 10^{-4}$ kG $\cdot$ sec/m^2. Let us calculate the velocities v_{o1} and v_{o2} according to the formula (3-47):

$$v_{c1} = 3.32 \text{ m/sec and } v_{o2} = 12.5 \text{ m/sec.}$$

Let us calculate the corresponding extremal values of the time T_{o1} and T_{o2} using the formula (3-18'):

$$T_{o1} = 0.0565 \text{ sec and } T_{02} = 0.0069 \text{ sec.}$$

At $v_1 = 2$ m/sec, formula (3-49) holds:

$$T_1 = T_{o2} = 0.0565 \text{ sec and } L_1 = 11 \text{ cm.}$$

At $v_{o1} < v_2 = 5$ m/sec $< v_{o2}$, the formula (3-49') holds:

$$T_2 \approx 0.02 \text{ sec;}$$
$$L_2 \approx 10 \text{ cm.}$$

At $v_3 = 20$ m/sec $> v_{o2}$, formula (3-50') holds:

$$T_3 = 1.9 \cdot 10^{-3} \text{ sec and } L_3 = 3.9 \text{ cm}$$

At $v_4 = 100$ m/sec

$$T_4 \approx 1.770^{-4} \text{ sec, } L_4 \approx 1.7 \cdot 10^{-2} \approx 1.7 \text{ cm.}$$

With a nozzle diameter of $d = 0.2 \cdot 10^{-3}$ and a flow velocity of v = 100 m/sec, the decomposition time is $T \approx 5.9 \cdot 10^{-5}$ sec, and the atomization occurs at a distance of L ≈ 6 mm from the nozzle opening.

CHAPTER FOUR

/49

ATOMIZATION OF A LIQUID BY CENTRIFUGAL SPRAY NOZZLE

Section 4-1. Liquid flow rate through centrifugal spray nozzle and stream angle of taper

Figure 4-1 shows schematically a centrifugal spray nozzle. The liquid enters the chamber tangentially and, while rotating, moves in the direction toward the opposite opening located on the end wall of the spray nozzle. When the liquid flows from the nozzle, due to the fact that the centripetal forces of the walls stop influencing the stream, the liquid particles move along rectilinear paths which are tangential to the cylindrical surface adjacent to the output nozzle of the spray nozzle. The angle ϕ formed by the velocity vector with the nozzle axis is determined by the ratio of the tangential and axial velocities from the equation

$$\varphi = \operatorname{arc\,tg} \frac{v_\tau}{v_z}. \qquad (4\text{-}1)$$

A theory for the motion of an ideal liquid in the chamber of a centrifugal spray nozzle was developed by G. N. Abramovich [4-11] and reduced to the following basic statements.

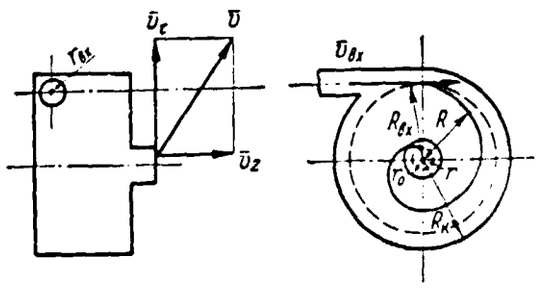

Fig. 4-1. Diagram of centrifugal spray nozzle.

Let us consider the motion of a liquid element in the sprayer

chamber. On the basis of the theorem of the conservation of momentum when there are no resistance forces, the ratio may be determined between the velocity of input and the velocity of rotation at the output from the chamber.

The tangential velocity component of the liquid at the output of the chamber equals: /50

$$v_\tau = \frac{v_{вх} R_{вх}}{r}. \tag{4-2}$$

Here $R_{вх}$ -- radius of rotation for a liquid element at the input cross-section;

r -- radius of rotation for the element being examined at the chamber output.

It follows from formula (4-2) that the tangential velocity component decreases with the distance from the axis to the periphery according to a hyperbolic law. According to the Bernoulli equation, under the condition that we can disregard the difference between the input and output points (with respect to the plane of comparison passing along the stream axis), the total head equals:

$$H = \frac{p}{\gamma} + \frac{v_z^2}{2g} + \frac{v_\tau^2}{2g} = \frac{p_{вх}}{\gamma} + \frac{v_{вх}^2}{2g}. \tag{4-3}$$

Here p, $p_{вх}$ -- excess pressure in the cross-sections examined.

Under the given input conditions $(p_{вх}, v_{вх})$ for all the streams, the head has one and the same value.

It follows from equations (4-1) and (4-2) that the liquid cannot completely fill the output section, since thus the velocity of excess would have to be infinitely large and positive, and the pressure would have to be infinitely large and negative, which is physically impossible. Therefore, an

air vortex arises in the cross-section center with a pressure which equals the pressure in the surrounding medium ($p_m = 0$).

The clear opening coefficient which characterizes the degree with which the liquid fills the output cross-section equals:

$$\varepsilon = 1 - \left(\frac{r_m}{r_0}\right)^2. \tag{4-4}$$

Here r_m -- vortex radius;
r_o -- output opening radius.

The distribution of the axial velocities in the output section is determined according to the Delambre principle which may be applied to a liquid element having the volume dV = 1·dr and as shown in Fig. 4-2. Projecting the forces in the radius direction, we have:

$$dp - dF = 0.$$

Thus: /51

$$dp = dF = dm\,\frac{v_\tau^2}{r} = \frac{\gamma v_\tau^2 dr}{gr} = -\frac{\gamma}{g}\,v_\tau dv_\tau, \tag{4-5}$$

Since according to equation (4-2):

$$dv_\tau = -\frac{v_\tau dr}{r}.$$

As the result of integrating (4-5) and determining the constants from the conditions at the boundary of the air vortex, we may establish the relationship which shows that the pressure depends only on the distribution of tangential velocity components:

$$\frac{p}{\gamma} = \frac{v_{\tau m}^2}{2g} - \frac{v_\tau^2}{2g}. \tag{4-6}$$

A comparison of formulas (4-3) and (4-6) leads to the conclusion that the axial velocity component in the chamber output section is a constant determined from the relationship

$$\frac{v_z}{2g} = H - \frac{v_{\tau m}^2}{2g}. \qquad (4\text{-}7)$$

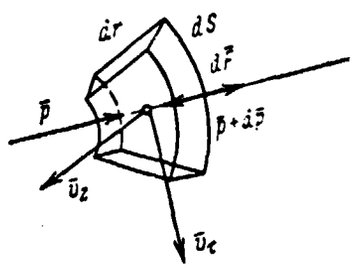

Fig. 4-2. Schematic image of forces acting on rotating liquid element.

In actual calculations, the equivalent velocity is frequently introduced determined by the formula:

$$v_э = \frac{Q}{\pi r_0^2} = v_z \varepsilon, \qquad (4\text{-}8)$$

where $Q = \pi r_{вх}^2 n v_{вх} = \pi r_0^2 v_z \varepsilon$ -- volumetric liquid flow rate;

n -- number of input openings.

The relationship between the equivalent and tangential velocities at the vortex boundary may be expressed as follows as the result of comparing the equations (4-2) and (4-8):

$$v_{\tau m} = \frac{A v_э}{\sqrt{1-\varepsilon}}, \qquad (4\text{-}9)$$

where $A = (R_к - r_{вх})\, r_0 / n r_{вх}^2$ is the geometric characteristic of the spray nozzle giving the relationship of the tangential velocity at the external stream boundary to the equivalent velocity.

Substituting (4-8) and (4-9) into (4-7), we obtain the expression for the equivalent velocity and flow rate of the spray nozzle: /52

$$\left.\begin{aligned} v_э &= \xi \sqrt{2gH}, \\ Q &= \xi \pi r_0^2 \sqrt{2gH}, \end{aligned}\right\} \qquad (4\text{-}10)$$

where $\xi = 1/\sqrt{\frac{1}{\varepsilon^2} + \frac{A^2}{1-\varepsilon}}$ is the flow rate coefficient of the spray nozzle.

The system of equations obtained is not closed (the number of unknowns is greater than the number of equations by one) and therefore assumes an infinitely

large number of solutions. To obtain the required solution, additional conditions are required.

Based on the fact that from all of the possible solutions, we must select the most stable one, G. N. Abramovich assumed a flow rate maximum as the stability condition for a given head. Similar assumptions are applied by other researchers for the same type of problem.

Then:

$$\frac{d\xi}{d\varepsilon} = 0. \tag{4-11}$$

Thus

$$\left.\begin{aligned} A &= \frac{1-\varepsilon}{\sqrt{\varepsilon^{3/2}}} \\ \xi &= \varepsilon\sqrt{\frac{\varepsilon}{2-\varepsilon}}. \end{aligned}\right\} \tag{4-12}$$

and

The average value of the stream angle of taper is obtained by substituting into (4-1) the average value of the tangential component, and is expressed by the following relation:

$$\operatorname{tg}\varphi = \frac{v_{\text{тср}}}{v_z} = \frac{(1-\varepsilon)\sqrt{8}}{(1+\sqrt{1-\varepsilon})\sqrt{\varepsilon}}. \tag{4-13}$$

The dependence of the clear opening coefficient ε, the flow rate coefficient ξ and the stream angle of taper ϕ on the geometric characteristic of the spray nozzle is shown in Fig. 4-3.

As experimental verification has shown, the theory of G. N. Abramovich correctly describes the basic features of the process of liquid motion in centrifugal spray nozzles. However, it does not consider the influence of viscosity, which in certain cases greatly changes the nature of the flow, and consequently, also the spray nozzle parameters, such as the stream angle of

/53

taper and the flow rate coefficient.

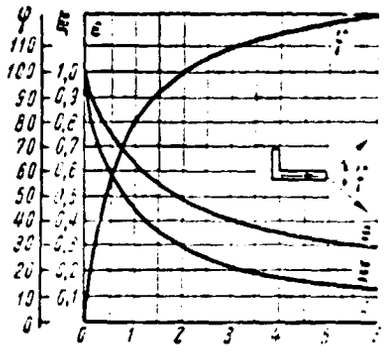

Fig. 4-3. Dependence of clear opening coefficient, flow rate coefficient, and stream angle of taper on the geometric characteristic of the spray nozzle.

Taylor [4-20] examined the problem of the motion of an ideal liquid in a centrifugal spray nozzle and determined the relationship between the dimension of the air kernel in the vortex chamber and the output nozzle, the flow rate coefficient, and the stream angle of taper. In examining this problem, he introduced the following basic parameters:

Ω — moment of velocity at the input to the sprayer with respect to the axis of rotation;

U — flow velocity ($U = \sqrt{2H/\varrho}$, where H is the total head);

u — axial velocity component in the output nozzle, whose radius is r_0;

r_2 — the kernel radius in the nozzle for the axial velocity u;

r_3 — the same at the input to the chamber (when u = 0).

These parameters form the dimensionless complexes

$$x = \frac{u}{U}; \quad y = \frac{\Omega}{U r_0} = \frac{r_3}{r_0} \qquad \text{and} \qquad z = \frac{r_2}{r_0}, \tag{4-14}$$

one of which (for example, y) is a quantity determined by the geometric parameters of the sprayer, and the two others are determined from the flow equation.

In the Taylor scheme, just as was the case for Abramovich, it is assumed the liquid is ideal, and the Bernoulli equation and the law governing the equality of the momentum moments are used. The insufficient condition is derived from the principle of the flow rate maximum. The only difference consists of the fact that Taylor considers the energy expenditure to produce the central gas vortex. However, since the gas density is much less than the liquid density, the Taylor corrections are insignificant.

Figure 4-4 shows the dependence of the flow rate coefficient ξ, the dimensionless radius of the air vortex z in the nozzle and the angle of taper ϕ on /54

the dimensionless radius of the air vortex at the input to the vortex chamber y.

It may be seen from Fig. 4-4 that the quantity z, which characterizes the dimensions of the air kernel in the nozzle, are always greater than the quantity y characterizing the dimensions of the vortex in the chamber cross-section (at u = 0). Consequently, the radius of the air kernel in the nozzle is always less than in the vortex chamber.

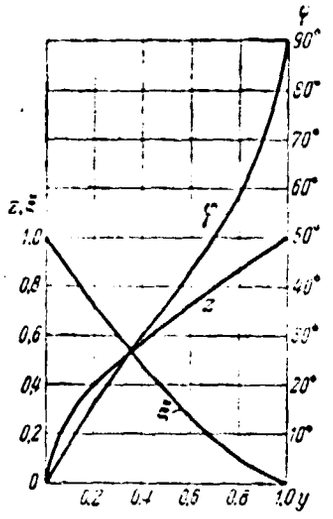

Fig. 4-4. Dependence of parameters z, ξ and ϕ on the parameter y.

However, experiments conducted with a real liquid show that the air vortex radius in the chamber is approximately the same as in the nozzle, which contradicts the result obtained. On the basis of this, Taylor assumed that the theory for the centrifugal spray nozzle, developed for the case of an ideal liquid, is not applicable for calculating the flow of a real liquid. He assumed that at the input of a real liquid to the sprayer, a braked boundary layer is formed at the walls of the vortex chamber. This boundary layer moves within the chamber due to the beginning of a radial pressure gradient. This boundary layer encompasses the boundary layer created at the walls of the output nozzle. The calculations made by Taylor and the experiments he carried out show the presence of an axial flow over the entire surface of the air kernel. The thickness of the boundary layer obtained in the calculation approximately equals the thickness of a film of liquid leaving the nozzle of a centrifugal sprayer. Thus, it may be seen that all the liquid passes in the form of the boundary layer. In this connection, the thickness of the boundary layer is calculated below.

L. A. Klyachko [4-7] examined the same scheme for the motion of a liquid, as did G. N. Abramovich, but considered the change in the liquid momentum in the vortex chamber due to the action of the forces of friction. He thus obtained the dependence $\xi = f(A,)$., just as in the study [4-1], under the condition that the following equivalent geometric characteristic is introduced: /55

$$A_1 = \frac{A}{1 + \frac{\lambda}{2}\left(\frac{R^2}{r_3^2} - A\right)}. \qquad (4\text{-}15)$$

Here

$$r_3 = \sqrt{\frac{f_{вх}}{\pi}}; \quad \lambda = \frac{1{,}05}{\mathrm{Re}^{0{,}3}}; \quad \mathrm{Re} = \frac{v_{вх} d_{вх}}{\nu};$$

$f_{вх}$ -- total area of the input openings;

λ -- friction coefficient.

V.V. Talakvadze [4-11] examined the motion of a liquid in the chamber of a centrifugal spray nozzle, using the assumption of a variable radius of the air vortex. Instead of the condition of the flow rate maximum, he used the theorem of a change in momentum as the additional equation. However, inaccuracies are contained in the solution, which lead to great errors in calculating the flow rate coefficient and the stream angle of taper for small changes in the geometric characteristics of the spray nozzle, which was examined in detail by L. A. Klyachko (Teploenergetika, 1962, No. 3).

Section 4-2: Boundary layer in the converging nozzle of a centrifugal atomizer

Taylor [4-2] solved the problem of calculating the boundary layer in the case of liquid flow in a converging nozzle of a centrifugal sprayer under certain simplifying assumptions. The stream of viscous liquid enters tangentially into a chamber with the radius R_3 and, passing over the converging conical section with the expansion 2α, leaves the nozzle with the radius R_2, which is much less than R_3 (Fig. 4-5).

The examination of these problems is confined to the case when the longi- /56
tudinal velocity component in the basic section of the stream (outside of the boundary layer) is small as compared with the tangential component, which made it possible to consider only the rotational motion, disregarding the translational velocity component. In this case, the basic section of the flow moves along a circle with a common center located on the axis of rotation. The liquid

moves at velocities equal to Ω/r, where Ω is a constant which equals the velocity moment with respect to the axis of rotation, and r -- radius of the circle. Under these conditions, the thickness of the boundary layer formed due to the braking of the flow at the wall by the forces of viscosity was calculated. The coordinate system is shown in Fig. 4-5. Assuming that the boundary layer is thin, we may disregard the pressure change in it. If we omit the series of terms which are small as compared with the remaining ones, and consider that

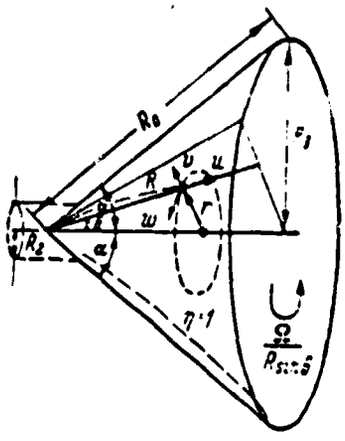

Fig. 4-5. Axes of coordinates and basic notation when calculating the boundary layer.

$$\frac{p}{\varrho} = -\frac{1}{r}\cdot\frac{\Omega^2}{R^2\sin^2\theta} + \text{const},$$

then the equation of motion of a viscous liquid and the continuity equation in the boundary layer, close to the internal cone surface, may be reduced to the form:

$$u\frac{\partial u}{\partial R} + \frac{v}{R}\cdot\frac{\partial u}{\partial\theta} + \frac{\Omega^2}{R^3\sin^2\theta} - \frac{w^2}{R} = \frac{\nu}{R^2}\cdot\frac{\partial^2 u}{\partial\theta^2}; \qquad (4\text{-}16)$$

$$u\frac{\partial w}{\partial R} + \frac{v}{R}\cdot\frac{\partial w}{\partial\theta} + \frac{wu}{R} = \frac{\nu}{R^2}\cdot\frac{\partial^2 w}{\partial\theta^2}; \qquad (4\text{-}17)$$

$$\frac{\partial u}{\partial R} + \frac{2u}{R} + \frac{1}{R}\cdot\frac{\partial v}{\partial\theta} = 0. \qquad (4\text{-}18)$$

Here R -- distance from the point to the pole, located at the apex of the cone;

θ -- angle formed by the radius vector R with the axis of the cone;

u -- radial velocity component;

w -- velocity component perpendicular to the axial planes;

v -- velocity component in the axial planes perpendicular to R;

p -- pressure;

ν -- kinematic viscosity;

ρ -- liquid density.

It is not possible to perform precise integration of the equation. Therefore, Taylor used the approximate Pohlhausen method [4-18] to calculate the thickness of the boundary layer. This method is based on replacing the real velocity distribution in a section of the boundary layer by a single-parametric family of velocity profiles which satisfy the given boundary conditions. Thus, the parameter is determined from the momentum equation. In this case, the momentum equation is obtained by integration of equations (4-16) and (4-17) with allowance for (4-18). Integration is performed over the thickness of the boundary layer δ, i.e., within the limits of a change in the coordinate θ from $\theta = \alpha - \delta/R$ to $\theta = \alpha$, for a constant value of the radius R.

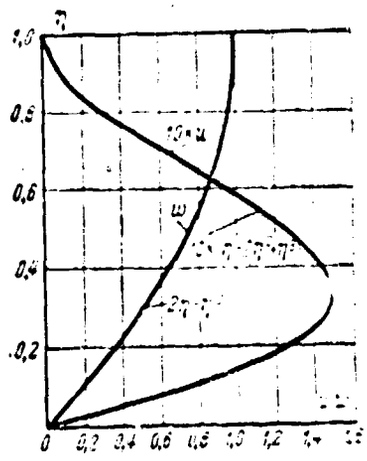

Fig. 4-6. Distribution of velocity component in the boundary layer.

After certain transformations, equations (4-16) and (4-17) assume the form:

$$2\int u\frac{\partial u}{\partial R}\,d\theta + 2\int\frac{u^2}{R}\,d\theta + \int\left(\frac{\Omega^2}{R^2\sin^2\alpha} - \frac{\omega^2}{R}\right)d\theta = -\frac{\nu}{R^2}\left[\frac{\partial u}{\partial\theta}\right]_{\theta=\alpha}; \tag{4-19}$$

$$\frac{\Omega}{R^2\sin\alpha}\int\left(R\frac{\partial u}{\partial R} + 2u\right)d\theta + \int\frac{\partial}{\partial R}(u\omega)\,d\theta + 3\int\frac{u\omega}{R}\,d\theta = -\frac{\nu}{R^2}\left(\frac{\partial\omega}{\partial\theta}\right)_{\theta=\alpha}. \tag{4-20}$$

The simplest distribution of the velocity component over the cross-section, which satisfies the boundary condition $w = u = 0$ at $\theta = \alpha$ and $u = 0$, $\omega = \Omega/R\sin\alpha$, $du/d\theta = 0$, $d\omega/d\theta = 0$ at $0 = \alpha - \delta/R$, is the distribution shown in Fig. 4-6:

$$u = \frac{\Omega E}{R\sin\alpha}f(\eta) = \frac{\Omega E}{R\sin\alpha}(\eta - 2\eta^2 + \eta^3); \tag{4-21}$$

$$w = \frac{\Omega}{R\sin\alpha}\Phi(\eta) = \frac{\Omega}{R\sin\alpha}(2\eta - \eta^2). \tag{4-22}$$

where

$$\eta = \frac{R(a-0)}{\delta}.$$

/58

Thus, the distributions of the velocity component at any point of the boundary layer are determined by the variables E and δ. The variable η is a function of θ and changes over the thickness of the boundary layer from 0 to 1.0, and E and δ are functions only of the radius R and may be determined by means of equations (4-19) and (4-20).

Let us introduce the dimensionless coordinates:

$$R_1 = \frac{R}{R_0} \quad \text{and} \quad \delta_1 = \frac{\delta}{R_0}\sqrt{\frac{\Omega}{\nu \sin a}}.$$

Thus, substituting expressions (4-21) and (4-22) with the corresponding derivatives into the momentum equations (4-19) and (4-20), we transform them as follows:

$$\delta_1^2\left(\frac{dE^2}{dR_1} + \frac{1}{2}\cdot\frac{E^2}{\delta_1^2}\cdot\frac{d\delta_1^2}{dR_1} - \frac{E^2}{R_1}\right)\left[\int_0^1 f^2\,d\eta - \right.$$

$$\left. - \frac{1}{R_1}\left(1 - \int_0^1 \Phi^2\,d\eta\right)\right] = ER_1\left(\frac{\partial f}{\partial \eta}\right)_{\eta=0}; \tag{4-23}$$

$$\frac{1}{2}\delta_1^2\left(\frac{dE^2}{dR_1} + \frac{E^2}{\delta_1^2}\cdot\frac{d\delta_1^2}{dR_1}\right)\left(\int_0^1 f\,d\eta - \int_0^1 f\Phi\,d\eta\right) =$$

$$= -ER_1\left(\frac{d\Phi}{d\eta}\right)_{\eta=0}. \tag{4-24}$$

The transformed boundary conditions may be written in the form:

$$f = \Phi = 0 \text{ at } \eta = 0 \quad \text{and} \quad f = 0, \quad \Phi = 1 \quad \text{at} \quad \eta = 1.$$

The integrals and the derivative of the function f and Φ for the distribution, shown in Fig. 4-6, have the following numerical values in the equations (4-23) and (4-24):

$$\int_0^1 f^2\,d\eta = 0{,}009524; \quad \int_0^1 \Phi^2\,d\eta = 0{,}5333; \quad \int_0^1 f\Phi\,d\eta = 0{,}0500;$$

$$\int_0^1 f\,d\eta = 0{,}08333; \quad \left(\frac{df}{d\eta}\right)_{\eta=0} = 1{,}0; \quad \left(\frac{d\Phi}{d\eta}\right)_{\eta=0} = 2{,}0. \tag{4-25}$$

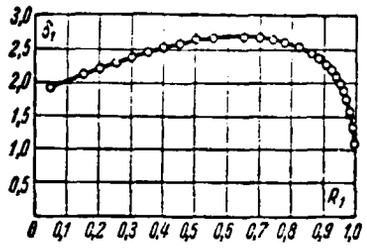

Fig. 4-7. Dependence of dimensionless thickness of boundary layer δ_1 on dimensionless radius of the sprayer R_1.

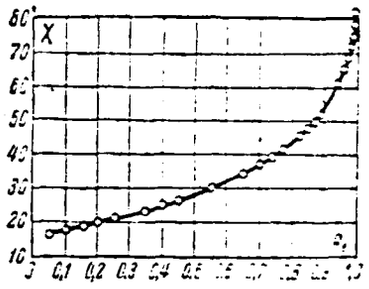

Fig. 4-8. Dependence of the angle χ on the dimensionless radius of the sprayer R_1.

After substituting (4-25) into (4-23) and (4-24), we obtain the following equations for the numerical calculation of δ_1, using the variables E^2 and $E\delta_1^2$: :

$$\frac{dE^2}{dR_1} = -\frac{98}{R_1} + \frac{2E^2}{R_1} - 330\frac{E^2R_1}{E\delta_1^2}; \qquad (4\text{-}26)$$

$$\frac{d}{dR_1}(E\delta_1^2) = \frac{49E\delta_1^2}{E^2R_1} - \frac{E\delta_1^2}{R_1} + 285R_1. \qquad (4\text{-}27)$$

In the calculation, the entire region in which R_1 changes from 1 to 0 is divided into several intervals.

The results of the calculation are given in Fig. 4-7, which shows the dependence of the dimensionless boundary layer thickness δ_1 on the dimensionless radius R_1, and in Fig. 4-8, which shows the dependence of the angle χ on the dimensionless radius R_1 (the angle χ is comprised of the force of friction and the generatrix of the conical surface, along which the liquid particle moves; this angle shows the velocity direction of the particle).

The magnitude of the angle χ is determined by the dependence:

$$\operatorname{ctg}\chi = \left(\frac{\frac{\partial H}{\partial \eta}}{\frac{\partial v}{\partial \eta}}\right)_{\eta=0} = \frac{1}{2}E. \qquad (4\text{-}28)$$

Figure 4-9 shows the path of particles on the cone surface in polar coordinates R_1 and θ. The arrow shows the direction of rotation of the flow kernel. Curve 1 represents the boundary of the cone; curve 2 -- the path of the particle. In the case of a plane disc, curve 2 shows the real path of the liquid particle passing over the tangent to the disc circle and emanating in its center. /60

In contrast to the case examined above, in centrifugal sprayers the velocity outside the boundary layer has the component which is directed parallel to the generatrix. However, in the majority of cases, the magnitude of this component is much less than the tangential component at all points of the flow, with the exception of points at the output nozzle. Therefore, the approximate solution obtained may be used to estimate the thickness of the boundary layer and to explain the problem of whether the liquid flow from the nozzle is in the form of the boundary layer or in the form of the basic flow of rotating liquid.

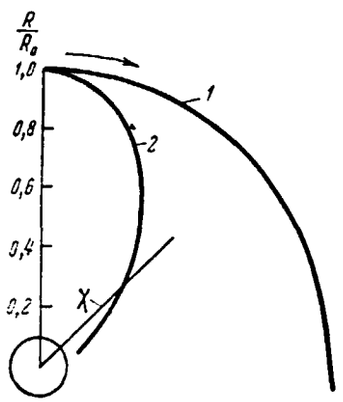

Fig. 4-9. Path of particle on cone surface.

Let us designate the radius of the output nozzle by R_2, and the radius of the chamber by R_3. Then the dimensionless radius at the output $R_1 = R_2/R_3$, and the relative thickness of the boundary layer is

$$\frac{\delta}{R_2} = \frac{\delta_1 R_0}{R_2}\sqrt{\frac{\nu \sin\alpha}{\Omega}} = \frac{\delta_1}{R_1 \sin\alpha^{1/2}}\sqrt{\frac{\nu}{\Omega}}.$$

The quantity $\Omega < R_2 \sqrt{2p/\rho}$, where p is the pressure at which liquid flow occurs. For a spray nozzle having a radius of the output nozzle R_2 = 1 mm, the ratio of the nozzle and chamber radii R_2/R_3 = 0.1 and the angle $\alpha = 45^\circ$, an approximate calculation of the boundary layer thickness gives the value:

$$\frac{\delta}{R_2} \geqslant 23{,}8\sqrt{\frac{\nu}{\Omega R_2^2}}.$$

For water ($\nu = 0{,}01$ cm^2/sec) at a pressure of $p \approx 210$ atm ($u \approx 45$ m/sec) $\delta/R_2 \geqslant 0{,}11$.

It must be considered that the air vortex occupies a large portion of the output cross-section, as was shown above. Thus, we may assume that the basic part of the liquid is located in the boundary layer, whose thickness is inversely proportional to the square root of the Re number, calculated over the radius of the output cross-section. /61

The occurrence of a boundary layer changes the flow rate coefficient of centrifugal sprayers. For large Re numbers, when the boundary layer is very thin, its influence on the flow rate coefficient does not have to be considered. However, as the Re number decreases, the influence of the boundary layer increases and the flow rate coefficient begins to increase due to a slowdown in the liquid rotation in the boundary layer and a corresponding decrease in the stream angle of taper. For small Re numbers, there is an increase in the resistance coefficient and a corresponding increase in the head losses in the spray nozzle, which slows down the flow rate coefficient increase somewhat. The change in the flow rate coefficient depends on the geometric parameters -- the ratio of the radii of the chamber and the nozzle (R_1) and the ratio of the radius and the height of the chamber characterized by the angle α.

An increase in $R_1 = R_2/R_3$ leads to a decrease in the relative thickness of the boundary layer, and, consequently, to a decrease in the flow rate coefficient. An increase in α (which corresponds to a decrease in L/R_3) also decreases the flow rate coefficient. However, the influence of this factor is weaker, since it is expressed by the quantity $\sqrt{\sin \alpha}$. It is possible to establish the form of the dependence and the region in which it is necessary to consider deviations of the flow conditions from ideal conditions on the basis of generalizing experimental material.

Section 4-3: Experimental data on determining the flow rate coefficient and angle of taper

Experimental studies of centrifugal atomizers confirm the statements made above. For large Reynolds numbers, the liquid flow rate changes in proportion to the square root of the head. Then the flow rate coefficient is a function of the geometric characteristic for an ideal spray nozzle, and for real spray nozzles — a function of A and the geometric parameters L/d_0 and $D_к/d_0$, which consider the deviations from the ideal spray nozzle (the square law of resistance). For small Reynolds numbers, the degree of the flow rate dependence on the head changes, which is expressed by the variable nature of the flow rate coefficient which increases as the Re number decreases. The limits of the parameters for which the calculation may be performed using the formulas for the flow from an ideal spray nozzle depend on the structure of the atomizer and the processing of its surface. /62

A. G. Blokh and Y. S. Kichkina [4-2] studied the atomization of liquids with different physical properties (water, aqueous solutions of glycerin, gas oil, kerosene) by a centrifugal spray nozzle, which is shown in Fig. 4-10. The parameters change within the following limits: The dynamic viscosity coefficient $\mu = 10^{-4}-2{,}9\cdot10^{-4}$ kG·sec/m^2; the surface tension coefficient $\sigma = 3\cdot10^{-3}-7{,}5\times10^{-3}$ kG/m; the specific weight $\gamma = 1000-1190$ kg/m^3; the pressure p = 5 - 30 at; $D_к/d_0 = 3{,}22-10$; $A = 1{,}72-9{,}51$; $\mathrm{Re} = v_0 d_0/\nu = 10^3-25\cdot10^3$. For given numbers of $\mathrm{Re} \leqslant 1{,}6\cdot10^4$, the experimental material (Fig. 4-11) may be generalized by the formula:

$$\xi = 12{,}9\xi_0\left(\frac{D_к}{d_0}\right)^{0{,}5}\mathrm{Re}^{-1/3}, \tag{4-29}$$

where ξ_0 — the flow rate coefficient of an ideal spray nozzle.

At $\mathrm{Re} > 1{,}6\cdot10^4$, self-modeling is observed of the flow rate coefficient with respect to the Re number and weakens the dependence of this coefficient on the ratio $D_к/d_0$, which leads to a certain scatter of the points in the /63

coordinates in Fig. 4-11. In the region $1{,}6\cdot10^4 < \mathrm{Re} < 2{,}5\cdot10^4$ the flow rate coefficient may be expressed by the formula:

$$\xi = \xi_0 \left(\frac{D_к}{d_0}\right)^n. \qquad (4\text{-}30)$$

where n is a coefficient determined experimentally.

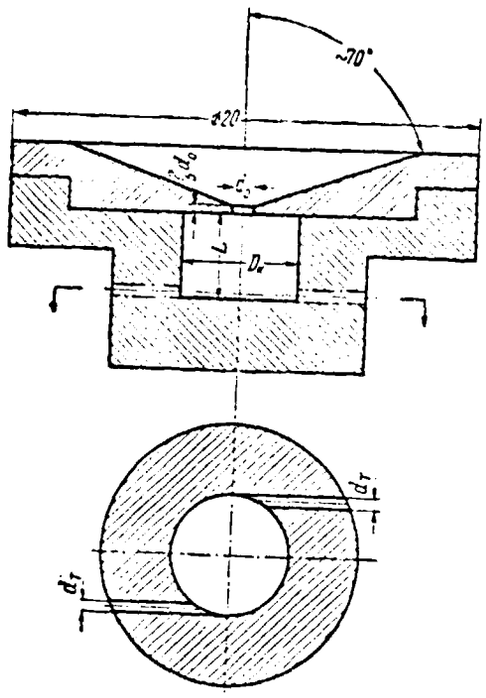

Fig. 4-10. Diagram of spray nozzle [4-3].

The dependence (4-30) is shown in Fig. (4-12), where the curve corresponds to the theoretical calculation using the formula (4-12), and the circles (○) designate the experimental data using formula (4-30) at n = 0.2 [4-3]. There is an agreement between calculations and experiments. In this same figure, the crosses (X) show the experimental data at n = 0.3 [4-15], obtained in the region of the parameter change $\mathrm{Re} = (12\text{-}93)\cdot10^3$, A = 1.02 - 17.7 and $D_к/d_0 = 1{,}23$ -8.4 in a study of the atomization of water by a spray nozzle, which is shown in Fig. 4-13. In the region investigated, there was no dependence of the flow rate coefficient on the Re number. The influence of the parameter L/d_0 was small and within the accuracy limits of the measurements.

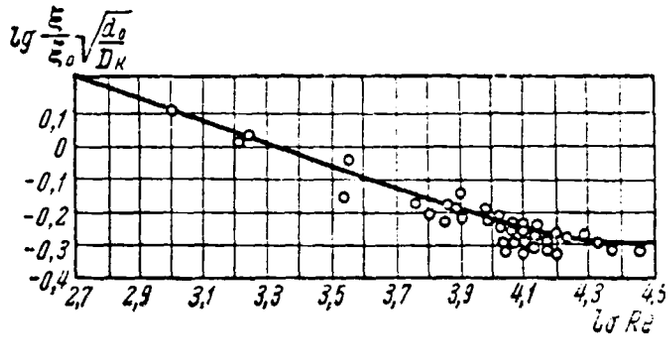

Fig. 4-11. Dependence of spray nozzle flow rate coefficient on Reynolds number.

As follows from Fig. 4-12, the experimental data may be generalized by a power formula (4-30) for a value of the exponent of n = 0.3. Consequently, the flow conditions for a given atomizer in the region studied differ somewhat from ideal conditions, and are weaker than in the study [4-12]. The authors of [4-15] generalize the material by the formulas of Abramovich (4-12) and (4-13), replacing the parameter A by $A' = A\,(d_0/D_к')^{0.5}$. in them without any theoretical justification. However, this method of generalizing the results does not have any particular advantages.

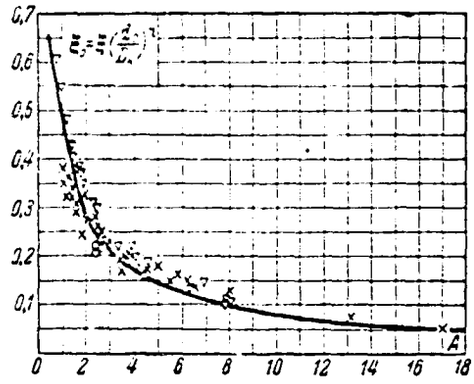

Fig. 4-12. Comparison of flow rate coefficient of real spray nozzle ξ and the ideal spray nozzle ξ_0 based on data from the studies:

0 - n = 0.2 [4-3]; x - n = 0.3 [4-15]; ∇ - n = 0 [4-12].

/64

Studies on the atomization of kerosene (γ = 0.805) by different centrifugal spray nozzles with the change of A ≈ 0.7 - 9.2 showed [4-12] the applicability of the theoretical formula (4-12). In Fig. 4-12, these data are shown for n = 0 by the triangles (∇) which show that $\xi = \xi_0$.

The study [4-19] showed the fact that the flow rate coefficient does not depend on the pressure in centrifugal atomizers. This study investigated the atomization of colored water with a surface tension coefficient of 62.5 dyne/cm in the region of Re = $9 \cdot 10^3$ - $20 \cdot 10^3$ numbers.

A study of atomization by these sprayers of glucose solution with different concentration showed that an increase in the liquid viscosity reduces the air vortex radius, and as a result of this an increase of the flow rate coefficient until the air vortex disappears. The lack of data on the geometric dimensions of sprayers makes it impossible to compare the values obtained for the flow rate coefficients with the data from other researchers.

/65

The results of studying spray nozzles (4-15) showed [4-22] a certain increase in the flow rate coefficient at a Re number less than 10^4. However, an

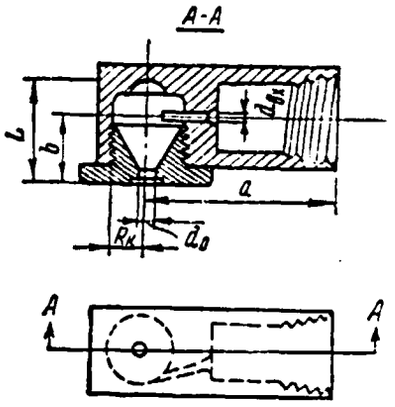

Dimensions, inches

Nozzle	a	b
1/4 1/8 3/8	13/16 5/8 31/32	1/2 3/5 9/16

Fig. 4-13. Atomizer diagram [4-14].

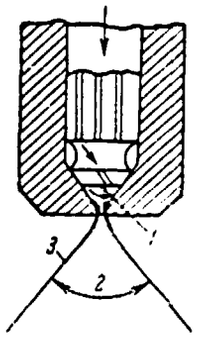

Fig. 4-14. Diagram of atomizer [4-19].

1 - air vortex; 2 - angle of taper; 3 - empty conical stream

increase in the nozzle diameter for a given chamber dimension does not lead to a great change in the flow rate coefficient. The dependence of the flow rate coefficient of β-naphthene and benzoic acid on the Re number for a spray nozzle (4-15,a) is shown in Fig. 4-16. The study [4-22] indicates that the flow rate coefficient increases with an increase in the $D_к/L$ ratio and with a decrease in the L/d_o ratio.

The study of Z. I. Geller and M. Ya. Miroshkin [4-4] gives experimental data for determining the flow rate coefficients for three forms of spray nozzles when the fuel is introduced into the chamber along channels with a circular form tangentially and at an angle to the spray nozzle axis, and along channels with a rectangular cross-section. The results of the experiments are generalized by the formula:

$$\xi = f(A_{зд}), \tag{4-31}$$

which is shown in Fig. 4-17.

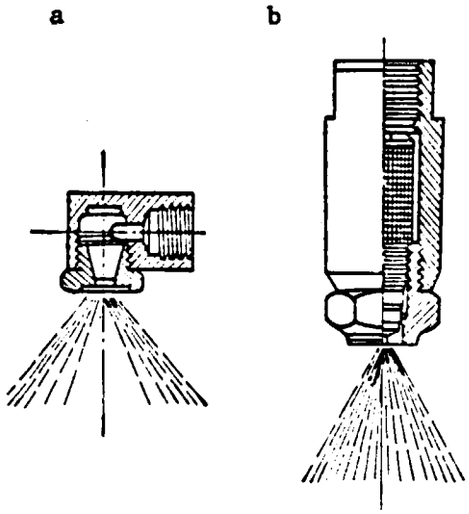

Fig. 4-15. Atomizer diagram [4-22].

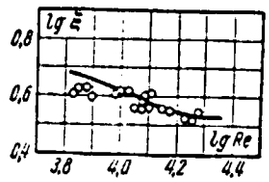

Fig. 4-16. Dependence of flow rate coefficient ξ on Re number

The characteristic $A_{вх}$ which has an equivalent influence takes into account the geometric factors affecting the atomization and the head losses, which are both local and take place over the length, and is expressed by the formula: /66

$$A_{вх} = \frac{A_{пр}}{1 + \frac{\lambda}{2}\left(\frac{A}{\zeta_{вх}}\cos\theta - A_{пр}\right)}.$$

Here

$$A_{пр} = \left(\frac{A}{\zeta_{вх}}\right)^2 + \delta(1-\varepsilon);$$

A $\frac{\pi R r_0}{n l_{вх}} \sin\beta$ - geometric characteristic of the spray nozzle;

θ - angle of input channel deviation from tangential location;

δ - coefficient accounting for head losses in the throat;

$\zeta_{вх} = 0{,}85$ - input resistance coefficient;

λ = 0.065 at $\frac{2G}{\pi r_{вх} \nu \sqrt{n}} \geqslant 1300$;

β - angle of inclination of input channels to the nozzle axis;

G - fuel flow rate;

ε - clear opening coefficient;

n - number of tangential openings.

Figure 4-17,a gives experimental data for spray nozzles with channels of circular cross-sections at an angle to the nozzle axis (point 1), and with channels having a rectangular cross-section located tangentially (point 2), and the curve was calculated using the theoretical formula of [4-1]. An examination of the figure shows that in the experiments with these spray nozzles, for which the geometric characteristic A = 0.82 - 1.81 and the characteristic $A_{э1}$ which has an equivalent influence which differs little from A, the dependence (4-31) was close to the theoretical value.

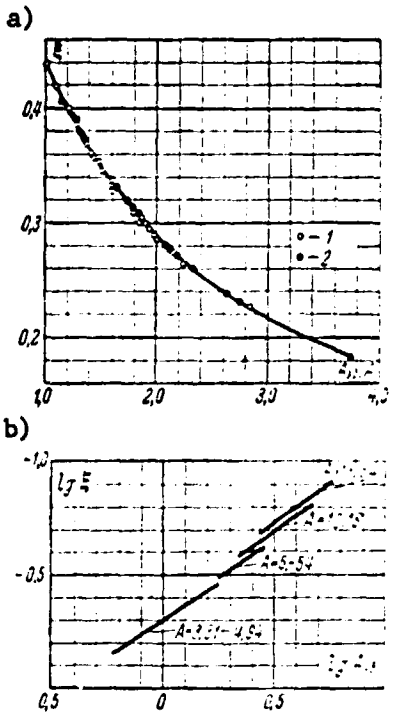

Fig. 4-17. Dependence of flow rate coefficient on the parameter $A_{э1}$ based on data in [4-4].

The results of experiments with spray nozzles having tangential channels with circular cross-sections, at A = 3.31 - 13.54 (Fig. 4-17,b), differ greatly from the results obtained in the studies of Abramovich and Klyachko, and do not give the unique dependence of the flow rate coefficient on $A_{э1}$.

Thus, to calculate the flow rate coefficient of spray nozzles, we may use the following:

a) Formula (4-29) for small Re numbers (when $Re < 10^4$);

b) Formula (4-30) at n = 0 - 0.3, when $Re > 2 \cdot 10^4$. The coefficient n depends on the structural component, the material, and the method of processing the sprayer surface. The smaller is n, the closer is the sprayer to an ideal one.

The problem of the angle of taper of the atomized stream is also of great interest. The study [4-2] showed that, for a slightly viscous liquid ($II_1 = \mu_ж^2/\rho_ж \sigma d_0 < < 4 \cdot 10^{-3}$), the angle of taper does not depend on the flow rate

a) b)

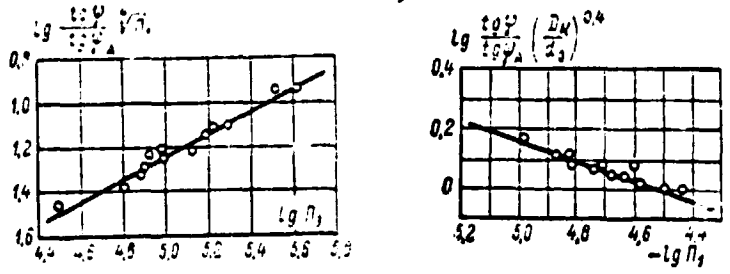

Fig. 4-18. Dependence of angle of taper on physical properties of liquid and atomizer dimensions for a slightly viscous liquid (a) and for a highly viscous liquid (b).

(Fig. 4-18,a) and may be calculated by the formula:

$$\frac{\operatorname{tg}\varphi}{\operatorname{tg}\varphi_0} = 3{,}05\cdot 10^{-2}\left(\frac{D_к}{d_0}\right)^{-0{,}4}\Pi_1^{-1/8}. \qquad (4\text{-}32)$$

For a highly viscous liquid $(\Pi_1 > 3\cdot 10^{-4})$, the angle of taper increases in proportion to the flow rate and decreases slightly with an increase in viscosity for a sprayer with the given dimensions (4-18,b): /68

$$\frac{\operatorname{tg}\varphi}{\operatorname{tg}\varphi_0} = K\Pi_1^{0{,}25}\mathrm{Re}, \qquad (4\text{-}33)$$

where K -- a constant, depending on the geometric dimensions of the sprayer.

In the study [4-15], the dependence of the angle of taper on the sprayer geometric dimensions in the case of water atomization is expressed by the formula (Fig. 4-19):

$$\varphi = 43{,}5 \lg 14A',$$

where

$$A' = A\left(\frac{d_0}{D_к - d_{вх}}\right)^{0{,}5}.$$

The liquid distribution over the stream cross-section depends both on the initial stream flow conditions (velocity components, physical properties of the

liquid, geometric dimensions of the sprayer), and on the conditions for the interaction of the drop and the surrounding gas medium. An analysis of the data shown in Fig. 4-20 [4-3] shows that with a reduction in the velocity, a decrease in the nozzle diameter, and an increase in the viscosity, the sprinkling density maxima approach the center and, under certain conditions, they merge, forming one maximum on the rotation axis. This occurs when vortices are formed in the stream, since the nature of the dependence of the flow rate coefficient on the Re number is the same as previously, i.e., it increases with a decrease in the Re number due to a decrease in the tangential velocity component.

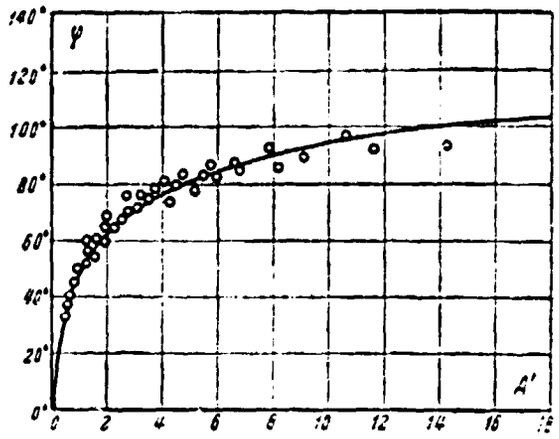

Fig. 4-19. Dependence of angle of taper for a stream of water ϕ on the geometric characteristic A' of a spray nozzle [4-15].

Since the drop dimension (as will be shown below) is a function of the nozzle diameter and the Re, Π_1 and A criteria, these criteria are the main factors in determining the form of the atomized stream during flow into a fixed medium. It follows from an analysis of the data that as the Re and A criteria decrease (decrease of the centrifugal forces of inertia), the maxima of the curves approach the axis. /71

A comparison of Fig. 4-21,a and 4-21,b shows that the nature of the curves is the same. There are small drops in the center of the flame, and the large drops are located along the edges. This result was obtained in [4-14], which investigated the atomization of a stream of water for different pressures in the chamber (p_o = 0.035; 1 and 8 atm).

Trapping of the liquid in measurement vessels at a given distance from the spray nozzle output for different angular distances from the stream axis makes it possible to determine the sprinkling density distribution and the drop velocity in this section as a function of the flow rate (pressure drop)

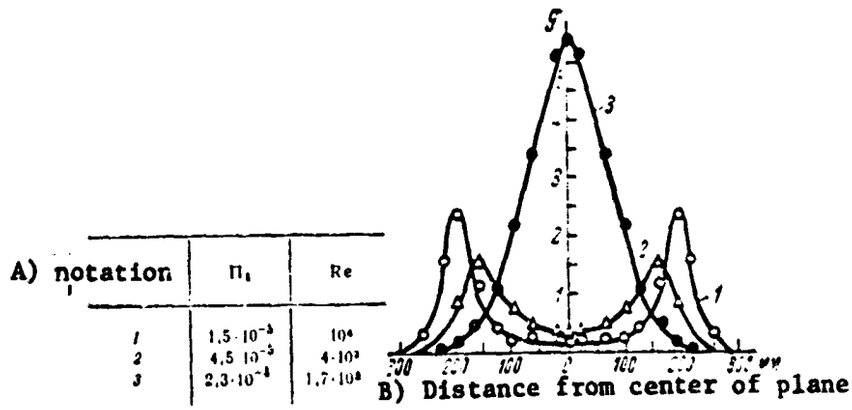

Fig. 4-20. Distribution of dimensionless density of sprinkling g over the flame cross-section.

$d_0 = 0.94$ мм; $D/d_0 = 9.73$; $A = 4.4$; $x/d_0 = 170$.

and the counterpressure in the chamber. The curves in Fig. 4-22 show that as the counterpressure increases, the stream becomes more viscous and the maximum moves toward the center from the periphery.

Section 4-4: Drop dimensions in the case of atomization by centrifugal spray nozzles

A film of liquid leaving a centrifugal sprayer does not have a stable form. Photographs of the film made by many researchers show that it represents several deformations caused both by turbulence and by interaction with the surrounding medium. Figure 4-23 [4-10] shows the characteristic forms of the liquid film decomposition. With an increase in the head, the film decomposition site approaches the spray nozzle opening, and at certain velocities the decomposition occurs directly at the output opening of the sprayer.

There are no theoretical formulas at present for determining the drop dimensions. Numerical studies employ either empirical formulas, used only in the region of the parameters studied and for the sprayers investigated, or generalized empirical formulas obtained by the method of similarity and dimensionality, which somewhat expands the region of their applicability. A system

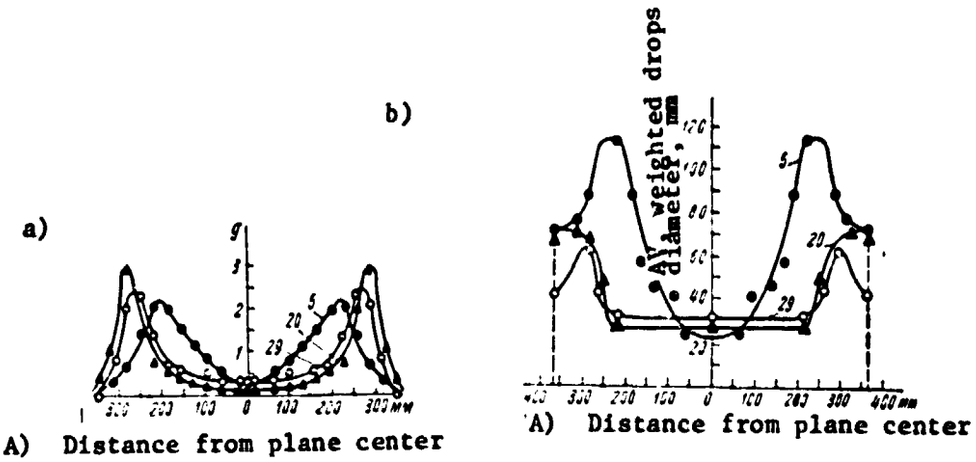

Fig. 4-21. Distribution of dimensionless density g of sprinkling (a) and average weighted diameter (b) over the flame cross-section.

$d_0 = 0{,}94$ мм; $D_к/d_0 = 6{,}38$; $A = 5{,}38$; $z\,d_0 = 165$.

Numbers on the curve of Fig. 4-21, a - pressure p, atm.

of criteria for similarity, suitable for generalizing the experimental data on atomization, was obtained above in Chapter Two.

As the determinant dimension, let us select the diameter of the sprayer output nozzle. We shall consider the case when the atomization occurs in a fixed gas ($v_r = 0$). At flow velocities occurring in centrifugal sprayers, we may disregard the influence of the force of gravity on the decomposition and we do not introduce the criteria v^2/gL in the examination. The geometric parameters characterizing the sprayer in this case will be A, $D_к/d_0$ and h/d_0. /72

Since the atomization is produced as a result of the interaction of the surface tension forces, the viscous forces and the forces caused by the external interaction of the medium, the criteria determining the atomization may be obtained from the ratio between the forces.

The ratio between the forces of surface tension to the forces of viscosity gives the criterion $\sigma/\mu_ж v$ (1). The ratio for the forces of the stream action upon the liquid gives the criterion $\varrho_r v d_0/\mu_ж$ (2). The ratio between the inertial forces of the liquid to the interaction of the gas stream gives $\varrho_ж/\varrho_r$ (3). We may set $\varrho_r v d_0/\mu_ж : \varrho_ж/\varrho_r = \mathrm{Re}$. Combining the criteria 1, 2 and 3, in order /73

to exclude the velocity, we obtain

$$\mu_ж^2 \varrho_ж \sigma d_0.$$

It is natural to select the ratio of the average drop diameter to the diameter of the nozzle opening.

Thus, the general dependence has the form:

$$\frac{d}{d_0} = f\left(A, \frac{D}{d_0}, \frac{h}{d_0}, \mathrm{Re}_ж, \frac{\mu_ж^2}{\varrho_ж \sigma d_0}, \frac{\varrho_ж}{\varrho_г}\right). \quad (4\text{-}34)$$

where d -- average drop dimension.

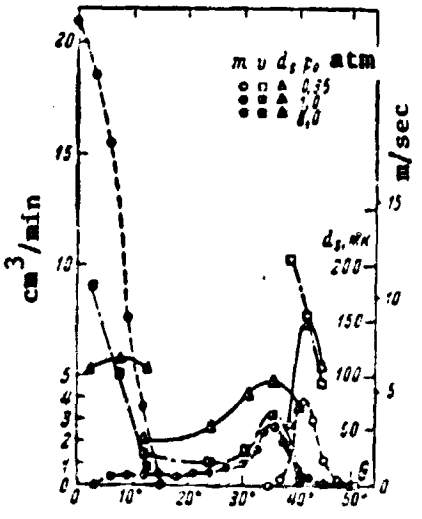

Fig. 4-22. Distribution of sprinkling density m, diameter of drop d_s and their velocity v as a function of the angle θ.

With respect to the form of the dependence and the influence of individual criteria, they may only be established experimentally. It must be noted that the quantity $\varrho_ж/\varrho_г$ changes very little. Under laboratory conditions, it is particularly difficult to formulate experiments so as to change this quantity by several factors.

Experiments show that only the quantity A greatly influences the dispersion. If we write the dependence (4-34) in the form of a power complex, it assumes the form:

$$\frac{d}{d_0} = CA^n \mathrm{Re}_ж^{\cdot} \left(\frac{\mu_ж^2}{\varrho_ж \sigma d_0}\right)^{k}. \quad (4\text{-}35)$$

The study of Blokh and Kichkina [4-2], as was shown above, carried out the atomization of a liquid by a series of sprayers into the atmosphere. Therefore, it was not possible to determine the influence of the physical parameters of the gas medium, in which the liquid was atomized ($\varrho_г$, $\mu_г$). . Experiments were performed for the parameters: $A = 1.72 - 9.51$;

$\mu_ж^2/\varrho_ж \sigma d_0 = 8 \cdot 10^{-6} - 10^{-2}$; $\mathrm{Re}_ж = 500 - 25000$.

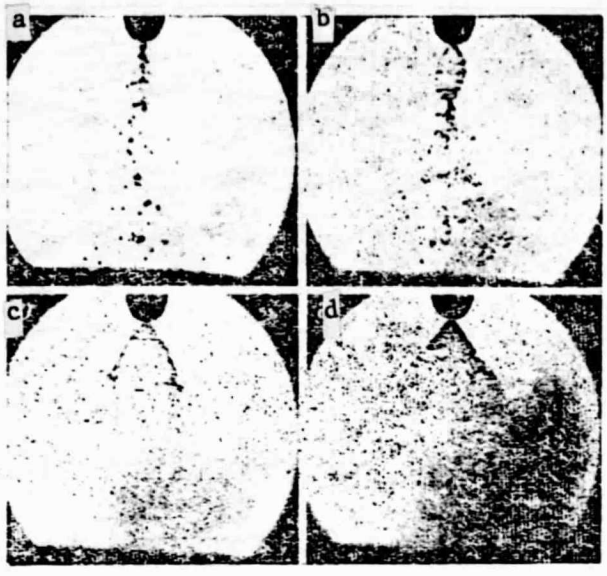

Fig. 4-23. Forms of liquid film decomposition at Δp (atm), which equals approximately: 0.056 (a); 0.14 (b); 0.31 (c) and 2.4 (d).

In the first series of these experiments, spray nozzles were tested with different geometric dimensions with one and two tangential grooves when they were used with water and solutions of glycerin soap in this water. This made it possible to change the liquid surface tension with practically no change in viscosity and density. In the second series of experiments, one spray nozzle was tested when used with water and aqueous solutions of glycerin. This made it possible to change, within wide limits, the liquid viscosity with practically no change in density and surface tension. The studies showed the fact that the relative average drop diameter d/d_o did not depend on the parameters $D_к/d_0$ and h/d_o.

In order to determine the dimensions of the drops, the latter were placed /74
in a mixture of vaseline with transformer oil applied to a glass plate. After this, individual parts of the plate were photographed under a microscope and then the dimensions of the drops were calculated. The average diameter was calculated as the mean weighted diameter according to formula (1-2).

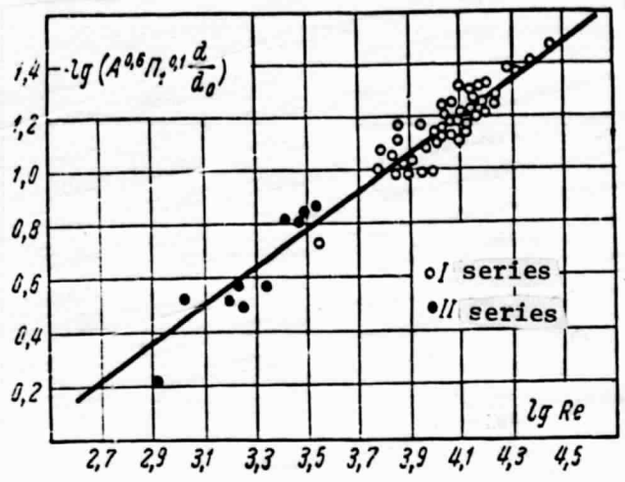

Fig. 4-24. Dependence of average drop diameter on physical properties of the liquid, flow velocity and sprayer dimensions.

The experimental data shown in Fig. 4-24 may be generalized by the formula:

$$\frac{d}{d_0} = 47{,}8A^{-0.6}\left(\frac{\mu_ж^2}{\rho_ж\sigma d_0}\right)^{-0.1}\left(\frac{v_э d_0}{\nu}\right)^{-0.7} = 47{,}8A^{-0.6}\mathrm{Re}^{-0.7}\Pi_1^{-0.1}. \qquad (4\text{-}36)$$

In the study by Watson and Clark [4-12], data are presented on the atomization of kerosene ($\gamma = 0.805$) by a centrifugal sprayer in the form of the dependence:

$$d_s = f(K, \sqrt{p}).$$

Here: $K = \frac{Q}{\sqrt{p}} = C\omega^2\omega$ - flow number;

Q - volumetric liquid flow rate;

p - excess pressure before the sprayer;

ω - area of output nozzle transverse cross-section; /75

C - dimensionality conversion coefficient;

d_s - average diameter according to formula (1-3).

Figure 4-25 shows the dependence of the average weighted diameter of the drop d on $\sqrt{p}$ for a constant lue of K. For the case of the liquid atomiza-

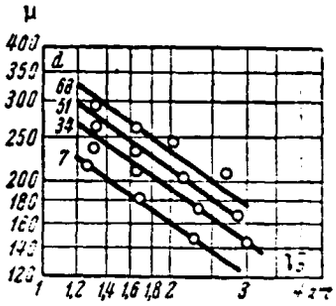

Fig. 4-25. Dependence of average drop diameter on pressure [4-12].

Numbers on the curves — values of K, liters/hr.

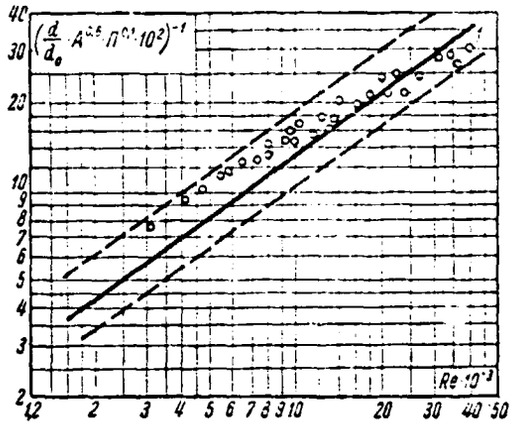

Fig. 4-26. Dependence (4-36) [4-12].

tion by any single sprayer, the lines in Fig. 4-25 show the dependence of the average drop diameter on the flow rate, since in this case the flow rate coefficient remains constant.

Analytically, this dependence may be represented by the following formula:[1)]

$$d \sim (1 - \bar{p})^{-0,7}.$$

Figure 4-26 shows the criterial dependence (4-36).[2)] An examination of Fig. 4-26 leads to the conclusion that the experimental data in [4-12] may be generalized by the formula (4-36) (line 1). Deviations of the points, which do not exceed those observed in [4-2], occur mainly at Re < 10^4 numbers, when the conditions of flow from the spray nozzle, studied by Blokh and Kichkina, greatly differ from the conditions for an ideal spray nozzle, whereas based on data in [4-12] such deviations were not observed in the entire range studied. In addition, the spray nozzle constructions may differ somewhat. /76

[1)] The drop diameters were converted according to formula (1-11). The value of the gamma-function was determined according to the graphs in [4-12] $x = f_1(\sqrt{\bar{p}}, K)$ and $d_s = f_2(\sqrt{\bar{p}}, K)$ and the condition $\Gamma(1 - 1/m) = x/d_s$.

[2)] The calculation was performed with the values of ξ = 0.1; 0.235 and 0.5; A = 1.06; 3.14; 7.85 and Re ≈ $3 \cdot 10^3$ – $35 \cdot 10^3$.

In the experiments of Turner and Moulton [4-22], a study was made of the atomization of benzoic acid and β-naphthene by centrifugal spray nozzles, which are shown in Fig. 4-15, for several values of the output nozzle diameter.

The dispersion was determined by freezing the drops and subsequently calculating the number of drops in groups, and the dimensions of the drops within each group differed from each other by no more than 20 micron. The average drop diameter was determined using the logarithmic formula (1-7). A comparison of the values for the average diameter calculated using the formulas (1-2) and (1-3) shows that they closely coincide[1)] (the deviation for the values for the drop dimension distribution given in the article was about 2-3%). Processing the experimental data of [4-22] in criterial form leads to the following relations for determining the average drop diameter: as applied to a spray nozzle, shown in Fig. 4-15, a:

$$\frac{d_l}{d_0} = 3{,}38A^{-0{,}1}\left(\frac{\mu_ж^2}{\varrho_ж \sigma d_0}\right)^{-0{,}16}\mathrm{Re}^{-0{,}51;\,2} \qquad (4\text{-}37)$$

as applied to the spray nozzle shown in Fig. 4-15, b: /77

$$\frac{d_l}{d_0} = 2{,}23\left(\frac{d_0}{d=1}\right)^{0{,}04}\left(\frac{\mu_ж^2}{\varrho_ж \sigma d_0}\right)^{-0{,}17}\mathrm{Re}^{-0{,}44}, \qquad (4\text{-}38)$$

---

1)
$$\frac{d}{d_l} = \frac{\sum_{i=1}^{n} K_i\left(i-\frac{1}{2}\right)}{\prod_{i=1}^{n}\left(i+\frac{1}{2}\right)^{K_i}},$$

where $K_i = g_i/G$ is the weighted portion of drops within the i-th group. Thus:

$$\sum_{i=1}^{n} K_i = 1.$$

2) The geometric dimensions, with the exception of d_o are necessary for calculating A and were determined from the drawing, and the change in A in each given series was only due to the quantity d_o (for the value of d_o, see [4-22]).

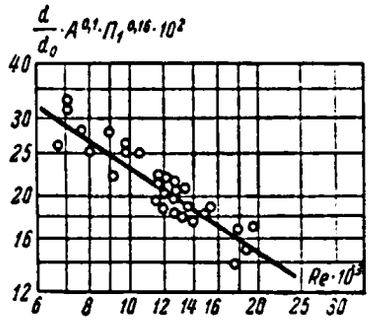

Fig. 4-27. Dependence (4-35) [4-22].

where $\frac{d_0}{d=1}$ is the dimensionless diameter of the output opening.[1)]

Figure 4-27 shows the experimental data on spray nozzle tests (Fig. 4-15,a). To compare the values of the average drop diameter using formulas (4-36) and (4-37), a comparative calculation was made for specific conditions ($\Pi_1 = 10^{-5}$ and A = 2), which showed that in this case the values of the average drop diameters are close to each other (Table 4-1).

The experimental data of several authors may be generalized [4-10] by the formula for a constant value of the coefficient of the surface tension σ = 24 dyne/cm):

$$d_s = 77{,}5p^{0{,}458}G^{0{,}209}\nu^{0{,}215}, \qquad (4\text{-}39)$$

where p -- excess pressure, kG/cm^2;

G -- weighted flow rate, kg/hr;

ν -- kinematic viscosity coefficient, centistokes;

d_s -- average drop diameter, mm.

If we assume that the dependence on the surface tension coefficients

---

[1)] Since there were no data on the spray nozzle dimensions, with the exception of the output nozzle, it was necessary to introduce this parameter. All of the remaining geometric dimensions are included in the constant.

corresponds to the criterial formula (4-36), then the dependence (4-39) may be transformed to the dimensionless form: /78

$$\frac{d_s}{d_0} = 11{,}5\xi^{0{,}91}\mathrm{II}_1^{-0{,}24}\mathrm{Re}^{-0{,}7}, \qquad (4\text{-}39')$$

where $\xi = f(A)$ is the spray nozzle flow rate coefficient.

TABLE 4-1

Re	$\frac{d}{d_0}$ formula (4-36)	$\frac{d_l}{d_0}$ formula (4-37)
5 000	0,257	0,232
10 000	0,158	0,143
20 000	0,098	0,095

Different researchers have proposed several relationships. Thus, for example, N.N. Strulevich (see [4-7]) atomized parafin with a centrifugal sprayer and, using the method of freezing the drops with the subsequent determination of their dimensions, arrived at the formulas:

$$\left.\begin{aligned} \frac{\delta}{r_0} &= \frac{1-\sqrt{1-\xi\cos\frac{\varphi}{2}}}{\cos\frac{\varphi}{2}}, \\ \frac{\delta}{d_0} &= 0{,}11\mathrm{Re}^{0{,}31}, \end{aligned}\right\} \qquad (4\text{-}40)$$

where ϕ - atomization angle;

δ - film thickness;

d_0 - average drop diameter;

$$\mathrm{Re} = \frac{v\delta\rho_{ж}}{\mu_{ж}};$$

v - flow velocity;

r_0 - nozzle radius.

Longwell [4-10] proposed the formula:

$$\frac{d_m}{d_0} = \frac{0{,}135e^{0{,}7\nu}}{\Delta p^{0{,}37}\sin\frac{\varphi}{2}}, \qquad (4\text{-}41)$$

where Δp - pressure drop (changing from 0.5 to 21 atm);

ν - 0.08 - 0.8 cm^2/sec;

ϕ - stream angle of taper;

d_m - median diameter according to mass.

This formula does not consider the influence of the liquid surface tension, and the influence of the structure is determined by the stream angle of taper. Schaffer and Boye [4-10] obtained:

$$\frac{d}{d_0} = f\left(\frac{\varrho v_э^2 d_0}{\sigma}\right).$$

This did not take into account the influence of viscosity on the average drop diameter. /79

Tate and Marschall [4-19] studied water atomization with an admixture of 25% nigrosin so that the drops could be photographed. The authors changed the viscosity of the solution, adding glucose of a different concentration to it. They determined the dispersion, by adding the drops to a vessel filled with a special solution, which was not mixed with water and had the same density as it. Due to this, the drops retained a spherical form and barely touched the floor. The vessel was covered with glass and the drops were subjected to photomicrophotography. The drops were calculated visually and a special electron analyzer was used to determine the drop dimension distribution. The authors determined the dependence of the average drop diameter on the velocity components along the axis at the output from the nozzle and the tangent at the entrance to the spray nozzle chamber, as well as the nozzle diameter. This research used centrifugal spray nozzles with vortex grooves (Fig. 4-14). Processing of the data in the similarity criteria led to the following relation:

$$\frac{d}{d_0} = 2{,}9\left(\frac{v_{\tau_0}}{v_э}\right)^{-0{,}5}\left(\frac{\mu_ж^2}{\varrho_ж \sigma d_0}\right)^{-0{,}24}\mathrm{Re}^{-0{,}7}, \qquad (4\text{-}42)$$

where $v_э$ — equivalent velocity at the nozzle output;

$v_{\tau 0}$ — tangential velocity component at the output from the vortex grooves.

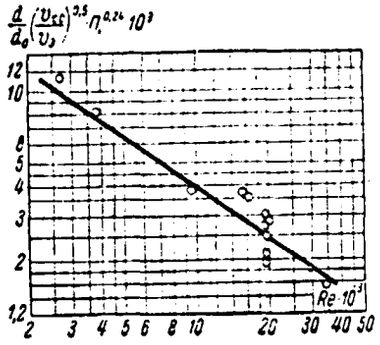

Fig. 4-28. Dependence (4-35) [4-19].

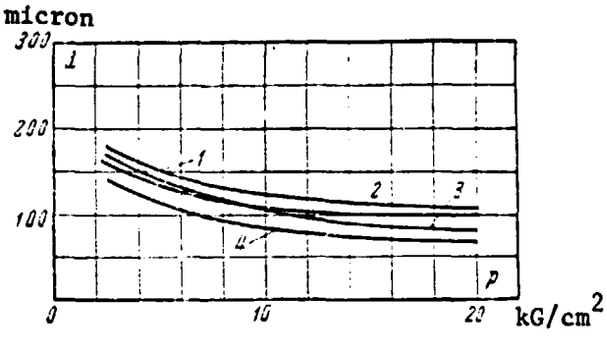

Fig. 4-29. Comparison of dependence of average drop diameter on pressure calculated using different formulas.

1 — (4-36); 2 — (4-37); 3 — (4-39'); 4 — (4-41).

The ratio of these velocities is a certain geometric characteristic of the sprayer, which equals:

$$\frac{v_{\tau 0}}{v_э} = \frac{f_0 \cos\theta}{n f_{вх}},$$

where f_0 is the area of the spray nozzle output;

n - number of vortex grooves;

$f_{вх}$ - area of their transverse cross-section;

θ - angle of their deviation from a tangential location.

Figure 4-28 shows the experimental data in the coordinates of the relation (4-42).

In this case, the average drop diameter changes in proportion to $Re^{-0.7}$.

A comparison of these data showed that the degree to which the individual parameters influence the average diameter of the drops differed in different studies. Thus, with an increase in the velocity (excess pressure), the drop /80
diameter decreases, but the exponent for the velocity differs, changing from 0.34 to -1. In the majority of studies, it is close to -0.7. The dimension of the sprayer output nozzle greatly influences the dispersion. In similar sprayers (constant value of the parameter A), an increase in the output nozzle

diameter worsens the dispersion $d \sim d_0^{0,1-0,64}$.

The physical properties of the liquid have the following influence: increase of viscosity in the majority of cases worsens the atomization, but the degree of influence is different ($d \sim \mu_{ж}^{0,2-0,5}$) depending on the region in which the viscosity changes; for small values of the viscosity, its influence upon the atomization becomes weaker. Thus, in the case of atomization of a highly viscous fuel, the influence of this factor must be considered. Heating the fuel, thus lowering its viscosity, worsens the atomization conditions. With respect to the surface tension, based on data of the majority of authors, it has a slight influence on the degree of dispersion ($d \sim \sigma^{0,1-0,2}$). Another conclusion is given only in the study of Schaffer and Boye, where $d \sim \sigma^{0,5}$. The influence of this factor in several studies was not taken into account due to the fact that its change was small for different types of liquid fuel.

Figure 4-29 compares the dependence of the average drop diameter on the pressure, calculated using different formulas for the specific case of atomization of kerosene by a centrifugal spray nozzle (γ = 815 kg/m^2; $\sigma = 27 \cdot 10^{-3}$ kG/m; $\mu_{ж} = 2 \cdot 10^{-6}$ m^2/sec). An examination of the curves leads to the conclusion that for a pressure greater than 10 atm, lines 1 and 2 give similar results; lines 3 and 4 give somewhat smaller values for the diameter. Thus, it is probable that not all the factors influencing the liquid atomization were considered by the criteria and are included in the experiment constants, which consider individual features of sprayers, particularly a different initial turbulence.

Naturally, spray nozzle structural components, the ratio of the chamber height to the diameter, the number of tangential openings, and even their form, were not the same in different studies. There were structural differences in the transition from the vortex chamber to the nozzle. All this leads to the fact that the dimensionless value of the average drop, determined by the similarity criteria, cannot be one and the same even under equal conditions. However, it is important that for experiments of each author, when the spray nozzle construction is the same, the processing using the criteria /81

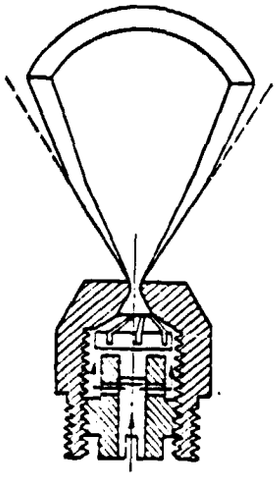

Fig. 4-30. Atomizer diagram [4-14].

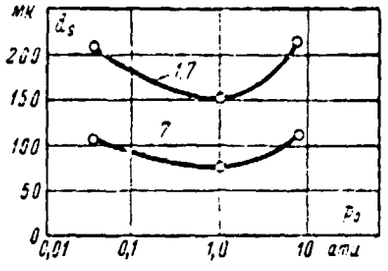

Fig. 4-31. Dependence of average drop diameter on counterpressure.

Numbers on the curves - values of Δp, atm.

$$\frac{d}{d_0} = f\left(A,\ \mathrm{Re},\ \frac{u_*^2}{\varrho_* \sigma d_0}\right)$$

gives a single value dependence. This shows that the criteria selected correctly describe the actual conditions for liquid atomization, but do not consider, and cannot consider, the structural features of individual spray nozzles. For spray nozzles with tangential fuel supplies, the formula (4-36) may be recommended.

All of the studies examined were performed for a liquid flow into an air medium located at atmospheric pressure. As was indicated above, this did not make it possible to clarify the influence of the gas density (counterpressure) on the atomization. Studies on this problem were mainly carried out for the atomization of a liquid by diesel spray nozzles operating at large excess pressures (hundreds of atmospheres). Thus, contradictory results were obtained. Thus, /82
Li [4-8] and Woltjen [4-23] did not detect any great influence of the air density on the stream dispersion, but Zass [4-6] and Giffenen and Lamb [4-17], as well as Lyshevskiy [4-9] noted a decrease in the drop diameter with an increase in the air density.

The study of De Corso [4-14] was devoted to centrifugal sprayers (Fig. 4-30).

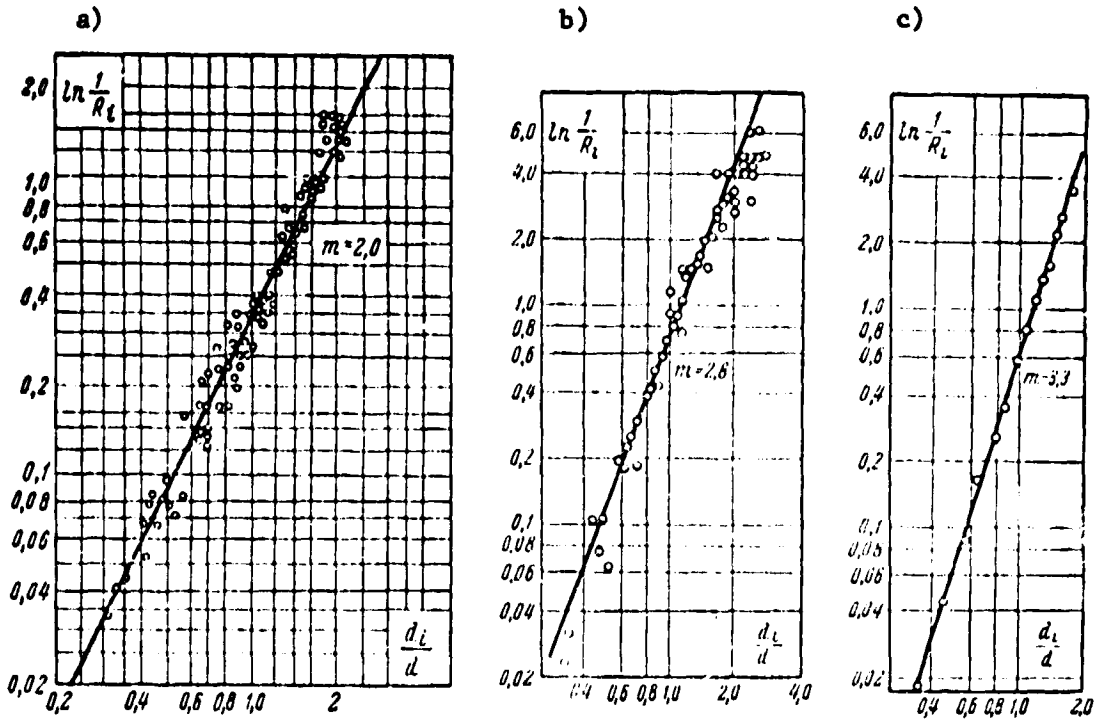

Fig. 4-32. Drop dimension distribution: a - [4-3]; b - [4-19]; c - [4-22].

The drop dimensions were determined by photographing them in flight and, subsequently, calculating the number of drops under a microscope. The average drop diameter was determined using formula (1-3) for different angles formed by the plane in which the photography was performed, and the stream axis at a given distance from the output nozzle.

The drop dimension over the cross-section (see Fig. 4-22) did not remain constant: the smallest drops were located close to the stream axis. With increasing distance from the axis, the drops became larger and then decreased somewhat at the external boundary of the stream. The average drop diameter depends on the counterpressure (Fig. 4-31). As it increases, the average drop diameter first decreases, and then begins to increase. The increase in the drop dimensions is explained by the author by the union of the drops, which occurs for large sprinkling densities occurring in the case of a high pressure in the chamber (the calculations show the possibility of this phenomenon -- see [4-5]).

Dependence of the average drop diameter on the pressure drop in the spray nozzle is expressed by the power formula: /84

$$d_s = K (p)^{-n}, \qquad (4\text{-}43)$$

where K is a constant, depending for a liquid on the geometric sprayer dimensions and the value of the counterpressure, and the exponent n in the studied range of counter pressures approximately equals 0.48, which corresponds to a somewhat stronger dependence on velocity than is the case using formula (4-36).

The drop dimension distribution is an important characteristic of the dispersion which influences the process of the liquid evaporation in the combustion chamber. An analysis of the data from several researchers showed that it may be expressed by the dependence (1-10) for values of m from 2 to 4 (Fig. 4-32).

When designing centrifugal sprayers, it is necessary to keep in mind the dependence of the flow rate and the average drop diameter on the pressure and the sprayer dimensions. Thus, for a given type of spray nozzle (A = const), the flow rate increases for given p in proportion to d^2, and for given d_o -- in proportion to $\sqrt{p}$. At the same time, the average drop diameter increases in proportion to $d_0^{0.5}$ for a given pressure drop, and for a given d_o -- inversely proportional to $p^{0,35}$.

Thus, an increase in the productivity when it is necessary to retain the value of the average drop diameter requires an increase in the pressure in front of the sprayer. In practice, in order to increase the productivity, several sprayers are placed in the chamber. The dependence of the flow rate and the drop diameter on the pressure limits the extent to which the fuel supply can be controlled, since a decrease in the fuel supply in the given sprayer is connected with the necessity of decreasing pressure. This unavoidably worsens the dispersion. Therefore, when it is necessary to control the flow rate within wide limits, either special devices can be created with a recirculation of the fuel within the spray nozzle, or pneumo-mechanical spray nozzles can be used in which the fuel atomization takes not only due to the centrifugal effect, but also due

to the interaction of the fuel with the high velocity stream of air. The use of pneumatic spray nozzles makes it possible to produce flames of a given dispersion for different flow rates, which improves the sprayer operational conditions.

CHAPTER FIVE

/85

BASIC CHARACTERISTICS OF LIQUID ATOMIZATION BY PNEUMATIC SPRAY NOZZLES

Section 5-1. Stream dispersion in the case of liquid atomization by pneumatic spray nozzles

Recently there have been experimental data in the literature which make it possible (in view of the theory given above for a liquid decomposition) to qualify the influence of different physical properties and parameters upon a stream dispersion by an atomized gas (or vapor).

B. D. Katsnel'son and V. A. Shvab [5-6] used the similarity method when studying liquid atomization by pneumatic spray nozzles. They assumed that the atomization is the result of the influence of the air stream upon the liquid stream, and generalized the experimental material by the criterial dependence:

$$\mathrm{Lap} = \frac{r\rho_r v^2}{\sigma} = A\left(\frac{v r_m}{\nu_r}\right)^n. \tag{5-1}$$

where Lap -- Laplace criterion;

r -- average drop radius;

σ -- surface tension coefficient;

ρ_r and ν_r -- density and kinematic viscosity coefficient of the atomized air;

v -- relative velocity of air and liquid at their contact point, which equals the velocity of the air stream;

A and n -- experimental constants depending on the sprayer construction.

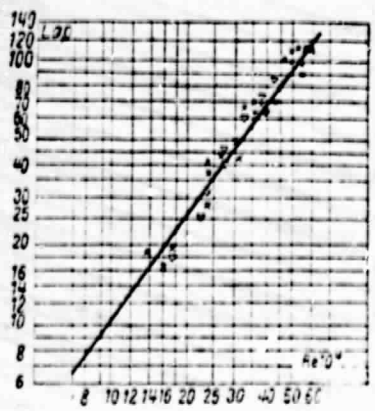

Fig. 5-1. Dependence of $Lap = f(Re)$ for a high pressure spray nozzle of the centrifugal type.

x - Lining from Fig. 6-22,a;

∇ - Lining from Fig. 6-22,b.

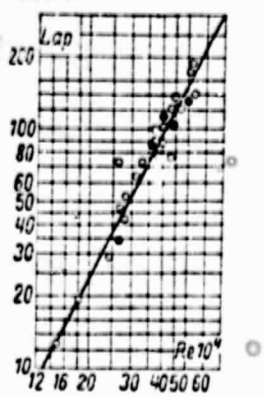

Fig. 5-2. Dependence of $Lap = f(Re)$ for a high pressure spray nozzle of the ejection type.

O - atomization only with primary air;

● - atomization with primary and secondary air.

The atomization of water has been studied by two types of pneumatic spray nozzles with a productivity of 600 kg/r each, one of which is centrifugal (see Fig. 6-21) and the other is ejection (see Fig. 6-25). The head components were changed in the centrifugal spray nozzle; several experiments were performed with three different linings while one of them was standard. At the contact site with air, the second one had a small skirting for deflecting the air stream (see Fig. 6-22,a), and the third was used for producing vortices in the fuel stream (see Fig. 6-22,b).

The experiments were carried out with water flow rates from 200 - 800 kg/r, and the ratio of the primary air flow rate to the water flow rate changed from 0.13 to 1.7 kg/kg. The air pressure before the spray nozzle /86 was 6 atm. Atomization was performed both with the supply of only primary air, and with primary air supplied together with secondary air (the latter was added through a register). A determination was made of the stream dispersion and liquid distribution over the flame cross section. The results of all the experiments for the centrifugal spray nozzle are shown in Fig. 5-1. It may be seen from an examination of the graph that the use of the vortex generator does not improve the atomization conditions, since the fuel velocity is small

as compared with the air velocity, and cannot greatly change the stream turbulence.

The data in Fig. 5-1 may be represented by the approximate relation

$$\frac{\rho Q_r v^2}{\sigma} = A\left(\frac{v d_0}{\nu_r}\right)^{1.4}. \qquad (5\text{-}1')$$

which shows that the average drop dimension changes in proportion to $v^{-0.6}$.

In formula (5-1) the influence of the ratio between the gas and liquid flow rates upon atomization is not considered, although in some experiments the authors noted that this fact has an influence.

The supply of secondary air somewhat improves the stream dispersion produced in a spray nozzle of the centrifugal type, but it does not influence the degree of stream dispersion by an ejection spray nozzle. This may be explained by the fact that in the former case, due to the centrifugal effect caused by the formation of vortices in the stream by the air flow, the largest drops are located on the periphery and they are additionally broken down with the secondary air.

An examination of Fig. 5-2, which shows the dependence (5-1) for an ejection spray nozzle, shows that when the air velocity is greater than the critical value

$$\frac{\rho Q_r v^2}{\sigma} = A\left(\frac{v d_0}{\nu_r}\right)^{1.97}. \qquad (5\text{-}1'')$$

It is possible that the atomization process may be somewhat influenced by the fact that the encounter between the gas and liquid stream is accompanied by a shock wave of differing force, depending on the degree to which the sonic velocity is exceeded. When the air and water flow rates are approximately equal, the air velocity has practically no direct influence on the stream dispersion.

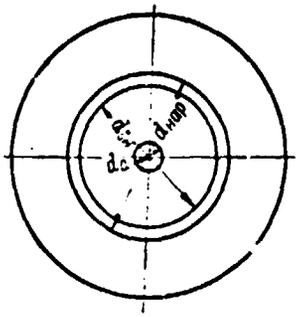

Fig. 5-3. Sprayer diagram.

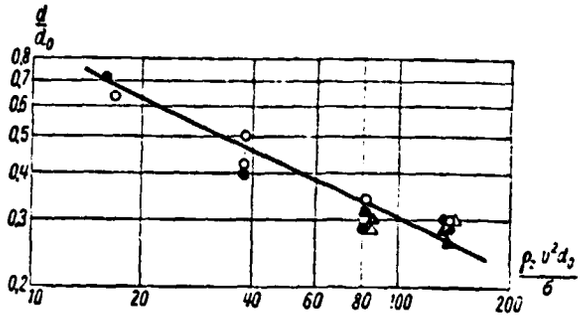

Fig. 5-4. Dependence $d/d_0 = f(\rho_1 v^2 d_0/\sigma)$ at the distance from the nozzle cone:
▲ — 75 мм; ● — 125 мм; ○ — 200 мм;
△ — 275 мм.

In the study mentioned previously, it was assumed that a stream is broken down due to the interaction between the gas and liquid flow. The Re criterion, which is determinant, and the Lap criterion, which is not determinant, were obtained from analyzing the decomposition scheme. Only the air velocity, and to a certain extent its density, were changed in the experiments. The properties of the liquid and the gas viscosity were not changed, so that in essence the influence of the air velocity and the geometric dimensions upon the water atomization was determined.

A study of the atomization of liquids having different physical properties by low pressure pneumatic spray nozzles [5-2,5] clarified the dependence of the average drop diameter on the liquid physical properties, and made it possible to establish the drop dimension distribution, the distribution of the atomized liquid over the stream cross section and the stream angle of taper, as well as the influence of the ratio between the liquid and air flow rates upon the dispersion.

The experiments were performed for three similar spray nozzles shown schematically in Fig. 5-3. The basic dimensions are given in Table 5-1. The liquid was added by air pressure through a central opening; the atomizing air -- through a circular slit. The spray nozzles were arranged vertically /88
to the opening from below, which provided a symmetric form for the stream. The liquid distribution over the stream cross section was determined by measuring glasses placed along the diameter of the atomized stream at different distances

from the nozzle opening, with subsequent weighing of the liquid on analytical scales. The dispersion was determined by trapping the drops on glass at the same location as the measuring glasses, with subsequent calculation of the drops under a microscope. In experiments with spray nozzle No. 1, the measuring glasses and the glasses were placed at four distances over thelength of the stream 75 - 275 mm from the spray nozzle opening. In experiments with spray nozzles Nos. 2 and 3, the liquid was placed at a distance of 125 mm from the spray nozzle opening. The average drop diameter was determined from formula (1-2).

The change in the drop dimensions within each interval was 25 microns. Aqueous solutions of glycerin with differing concentration, kerosene and benzene were subjected to atomization.

TABLE 5-1

BASIC DIMENSIONS OF SPRAY NOZZLES TESTED

Spray nozzle number	Material	Liquid nozzle cross-section diameter, mm	Circular cross-section for air flow	
1	Glass	0,506	3,08	3,63
2	Latun	0,860	5,50	6,46
3	Latun	0,450	2,66	3,18

The basic parameters of the process were changed within the following limits: the ratio between the air and liquid flow rates 0.25 - 3.15; the air velocity in the output cross-section 43 - 121 m/sec; the liquid velocity in the output cross-section 0.5 - 4.4 m/sec; air pressure at the spray nozzle opening 54 - 550 mm/Hg; volumetric weight of the liquid 745 - 1250 kg/m^3; coefficient of dynamic viscosity $(0.0675 - 54.5)\cdot10^{-3}$ $kG.sec/^{m2}$; surface tension $(2.39 - 7.18)\cdot10^{-3}$ kG/m. Experiments with spray nozzle No. 1 clarified the influence of the physical properties of the liquid and the relative velocity upon the stream dispersion. Experiments with spray nozzles Nos. 2 and 3 clarified the

/89

Fig. 5-5. Dependence $d/d_0 = f(\varrho_r v^2 d_0/\sigma)$ for liquid of differing physical properties.

Numbers on the lines are the values of the π_4 criterion.

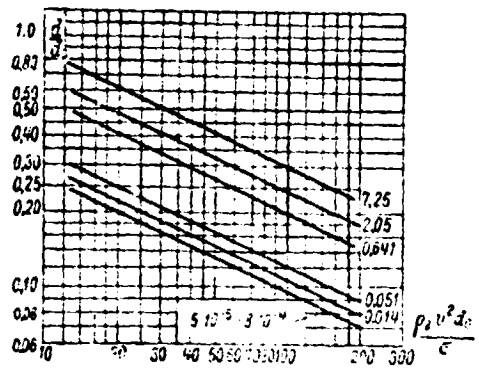

influence of the nozzle geometric dimensions.

In the experiments, it was noted that the nozzle diameter remained constant over the length of the atomized stream. This may be seen from Fig. 5-4, which shows the results of measurements at different distances from the nozzle opening of the average drop diameter obtained in the case of atomization of the same liquid by spray nozzle No. 1 in the coordinates of the relation (3-39) for a constant value of the criterion $\mu_ж^2/\varrho_ж\sigma d_0$. In the first place, this indicated that the breakdown of the stream and the drops apparently takes place in a very small section after the air encounters the liquid; in the second place, it indicates that there is no noticeable coagulation as a result of the drop collision. Dependences similar in form were obtained for other liquids, which corresponds to different values of the criterion $\mu_ж^2/\varrho_ж\sigma d_0$.

The comparative location of the curves pertaining to different series of experiments is shown in Fig. 5-5, where the criterion $\mu_ж^2/\varrho_ж\sigma d_0$ is given by the parameter. All these curves may be described by an equation of the type:

$$\frac{d}{d_0} = A\left(\frac{\varrho_r v^2 d_0}{\sigma}\right)^n, \qquad (5\text{-}2)$$

in which the coefficient A depends on the physical properties of the atomized liquid and the sprayer construction. The exponent n is a constant and equals -0.45 for all the experiments. The form of the dependence of coefficient A on the criterion $\mu_ж^2/\varrho_ж\sigma d_0$ for spray nozzle No. 1 may be determined from the graph in Fig. 5-6, where the experimental data are given in the form of the relationship: /90

Fig. 5-6. Generalized dependence $A = f(\Pi_1)$.

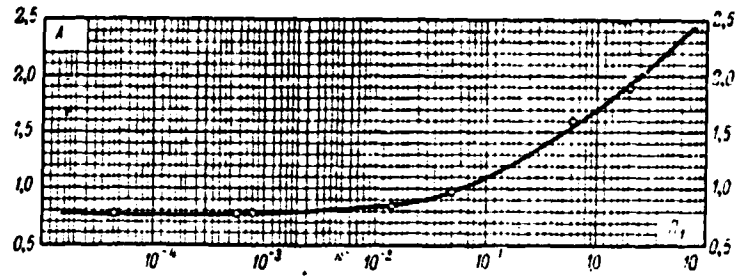

$$A = \frac{d}{d_0}\left(\frac{\varrho_г v^2 d_0}{\sigma}\right)^{0,45} = f\left(\frac{\mu_ж^2}{\varrho_ж \sigma d_0}\right). \qquad (5\text{-}3)$$

The behavior of the curve shows that at $\frac{\mu_ж^2}{\varrho_ж \sigma d_0} > 5 \cdot 10^{-3}$ the criterion containing the liquid viscosity begins to influence the dispersion. The curve in Fig. 5-6 may be approximately expressed by the following formulas:

at $\frac{\mu_ж^2}{\varrho_ж \sigma d_0} < 0{,}005$

$$\frac{d}{d_0} = A_0\left(\frac{\varrho_г v^2 d_0}{\sigma}\right)^{-0,45}; \qquad (5\text{-}3')$$

at $0{,}005 < \frac{\mu_ж^2}{\varrho_ж \sigma d_0} < 0{,}5$

$$\frac{d}{d_0} = \left[A_0 + 1{,}24\left(\frac{\mu_ж^2}{\varrho_ж \sigma d_0}\right)^{0,62}\right]\left(\frac{\varrho_г v^2 d_0}{\sigma}\right)^{-0,45}; \qquad (5\text{-}3'')$$

at $\frac{\mu_ж^2}{\varrho_ж \sigma d_0} > 0{,}5$ /91

$$\frac{d}{d_0} = \left[A_0 + 0{,}94\left(\frac{\mu_ж^2}{\varrho_ж \sigma d_0}\right)^{0,28}\right]\left(\frac{\varrho_г v^2 d_0}{\sigma}\right)^{-0,45}. \qquad (5\text{-}3''')$$

For spray nozzle No. 1 $A_0 = 0.77$.

These formulas are valid for the value of the criterion $\mu_ж^2/\varrho_ж \sigma d_0$ from $4.5 \cdot 10^{-5}$ to 7.25 and a value of $\frac{d}{d_0}\left(\frac{\varrho_г v^2 d_0}{\sigma}\right)^{0,45}$ from 0.77 to 2.4.

To verify the influence of the geometric dimensions on the stream dispersion, experiments were performed on liquid atomization by spray nozzles Nos. 2 and 3

in the region where the criterion $\mu_ж^2/\rho_ж \sigma d_0$ did not influence the dispersion. Figure 5-7 shows the results of these experiments in the form of a dependence corresponding to formula (5-2). As may be seen from the graph, the experiment points for spray nozzles of differing dimensions are located about a straight line for the value of the coefficient $A_0 = 0.64$.

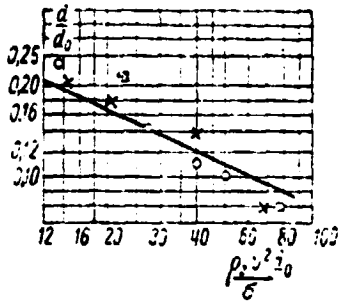

Fig. 5-7. Dependence $d/d_0 = f(\rho_г v^2 d_0/\sigma)$ for a liquid atomized by spray nozzles No. 2 (O) and No. 3 (X).

We may thus conclude that the results of these experiments (performed for different modes with sprayers of different dimensions and liquids of different physical properties in the interval for the parameter $G_ж/G_г$ when the studies did not influence the atomized stream dispersion) may be generalized by the criterial relationship (3-39), which determines the atomization process of a viscous liquid by pneumatic spray nozzles. /92

Two graphs which are shown in Figs. 5-8 and 5-9 were compiled for a graphic representation of the influence of the viscosity and surface tension upon the atomization fineness. Both graphs were based on the formulas given above. Figure 5-8 shows the dependence of the average diameter of the drops formed on the viscosity $d = f(\mu_ж)$ for different velocities under the assumption that all the remaining quantities in the formula -- the coefficient of surface tension, density and geometric dimensions -- are constant. Figure 5-9 shows a graph which gives the dependence of the average drop diameter on the surface tension coefficients for a liquid $d = f(\sigma)$ for different velocities, under the assumption that all the remaining factors -- viscosity, density and geometric dimension -- are constant.

The behavior of curves in Fig. 5-8 shows that in the case of atomization of highly viscous liquids, viscosity is the important factor which influences the stream dispersion. Therefore, one of the practical methods for improving the atomization quality is heating the highly viscous fuel. Therefore, the heating contributes to the stages which follow after the atomization and which precede the combustion -- evaporation and pyrogenetic decomposition.

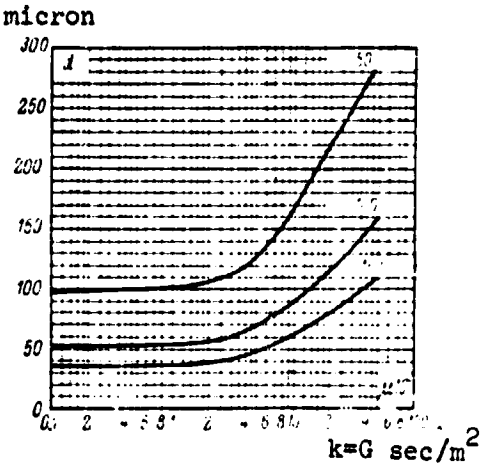

Fig. 5-8. Dependence of average drop diameter on the viscosity coefficient. Numbers on the curves -- values of the relative velocity, m/sec.

An increase in the surface tension leads to an increase in the drop dimensions. However, the limits within which the fuel surface tension changes are small. Therefore, this factor cannot have a great influence upon the atomization quality. Thus, fuel heating also leads to a reduction of the surface tension and a corresponding decrease in the drop dimensions. /93

Let us determine the average drop diameter as a function of the spray nozzle dimension and the relative stream velocity. In the case of the atomization of heated mazut, the viscosity has barely any influence upon the atomization fineness. Therefore, we shall use formula (5-3') which will be somewhat transformed. The surface tension coefficient of mazut approximately equals $3.5 \cdot 10^{-3}$ kG/m. The density of the atomizing air is assumed to equal 0.12 kg.sec^2/m^4. Then:

$$\frac{d}{d_0} = A\left(\frac{0{,}12v^2 d_0}{0{,}5 \cdot 10^{-3}}\right)^{-0{,}45}$$

and

$$d_0 = 0{,}204A\frac{d_0^{0{,}55}}{v^{0{,}9}}. \qquad (5\text{-}4)$$

Sometimes it is of interest to express the average drop diameter in terms of the air flow rate. Since the mazut velocity is much less than the air stream velocity, we may approximately assume

$$v = v_r,$$

and then the air flow rate:

$$L = vF \cdot 3600 \ [м^3/час],$$

where F is the area of the transverse section of the air slit. Thus,

$$d = 258A \frac{d_0^{0.33} F^{0.9}}{L^{0.9}}. \qquad (5\text{-}4')$$

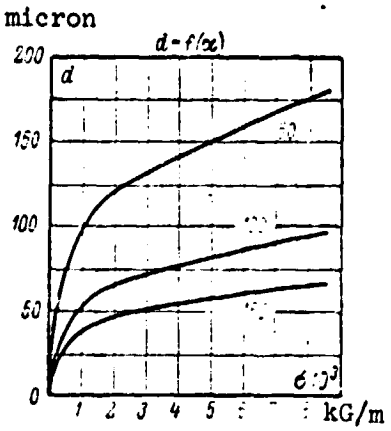

Fig. 5-9. Dependence of average drop diameter on surface tension coefficient.

Numbers on the curves -- values of the relative velocity, m/sec.

The relations given above express the relationship between the average dimensions of the drops and the parameters characterizing the atomization process.

In actuality, as was already indicated above, in the case of atomization of a liquid, the drops produced cannot have the same dimensions; their diameters differ from the average value. In order to have a complete concept regarding the operational quality, it is necessary to know the uniformity of the drop dimensions. In order to determine the granulometric composition of the drops, the relation (1-10) was used. It may be seen from Fig. 5-10 that the experimental points for all the experiments with spray nozzle No. 1 are combined by one curve at m = 2.3. /94

The relations (5-2) and 1-10) were used in processing the results of testing industrial spray nozzles of low pressure [5-5]. The spray nozzles STS-FDB-1 and STS-FOB-2 with a set of experimental linings and nozzles were tested, and the STS-FDM-1, of the Glushakov system, was a two-stage one. A detailed description of these spray nozzles is given in Chapter Six. The testing method and the processing of the experiments were the same as when testing the laboratory spray nozzles.

The relative velocity of the gas-liquid stream for the case of primary and secondary air being supplied to the spray nozzle was calculated according to the formula:

$$v = \sqrt{\frac{v_{1в}^2 G_в' + v_{2в}^2 G_в''}{G_в}}. \qquad (5\text{-}5)$$

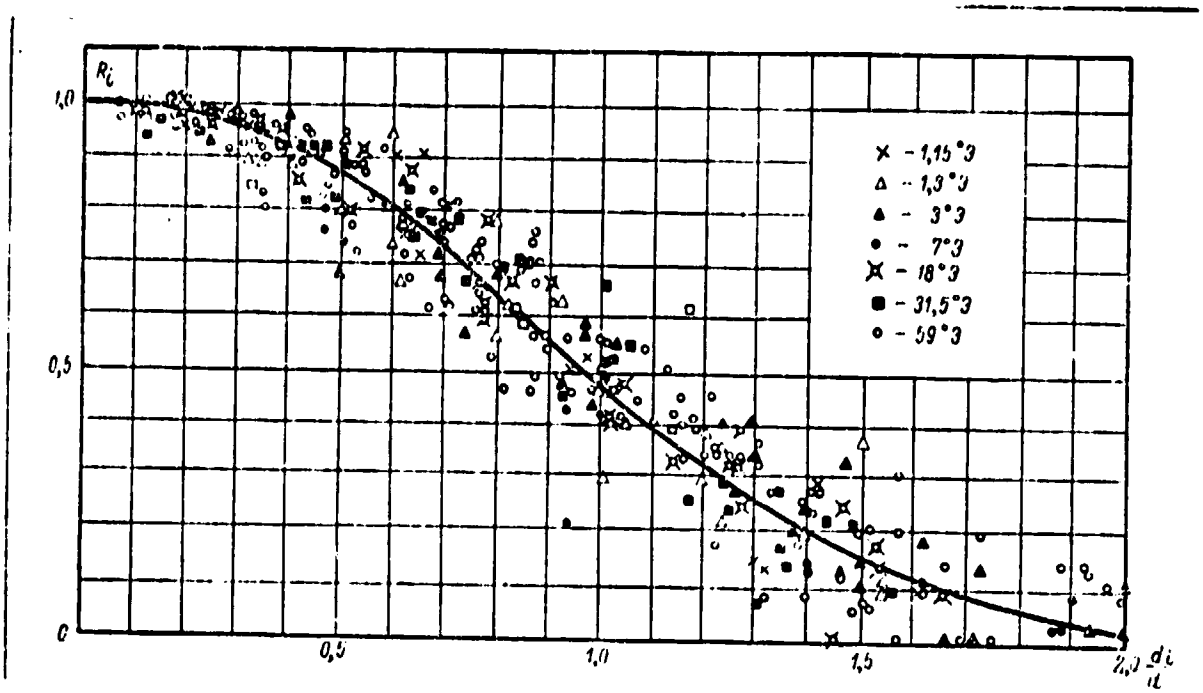

Fig. 5-10. Dependence R = $f(d_i/d)$ for spray nozzle No. 1 [5-3].

where v_{10} -- initial relative velocity between the primary air and the liquid stream;

v_{20} -- relative velocity of the gas-liquid stream when encountering the secondary air;

$G_в'$ -- primary air flow rate;

$G_в''$ -- secondary air flow rate;

$G_в$ -- total air flow rate.

The experiments with all the spray nozzles were basically performed with their design productivity. The amount of air supplied and the ratio between the air and liquid flow rate changed within wide limits. The primary and secondary air flow rates were determined from the ratio of the clear openings. Several experiments with the STS-FDB spray nozzle were performed only with primary air (with complete blockage of the secondary air). Figure 5-11 shows the functional dependence (5-2) for all the spray nozzles tested. It may be seen from Fig. 5-11,a that the points of all the experiments carried out with the spray nozzle STS-FOB-2 with different modifications, i.e., for different combinations of

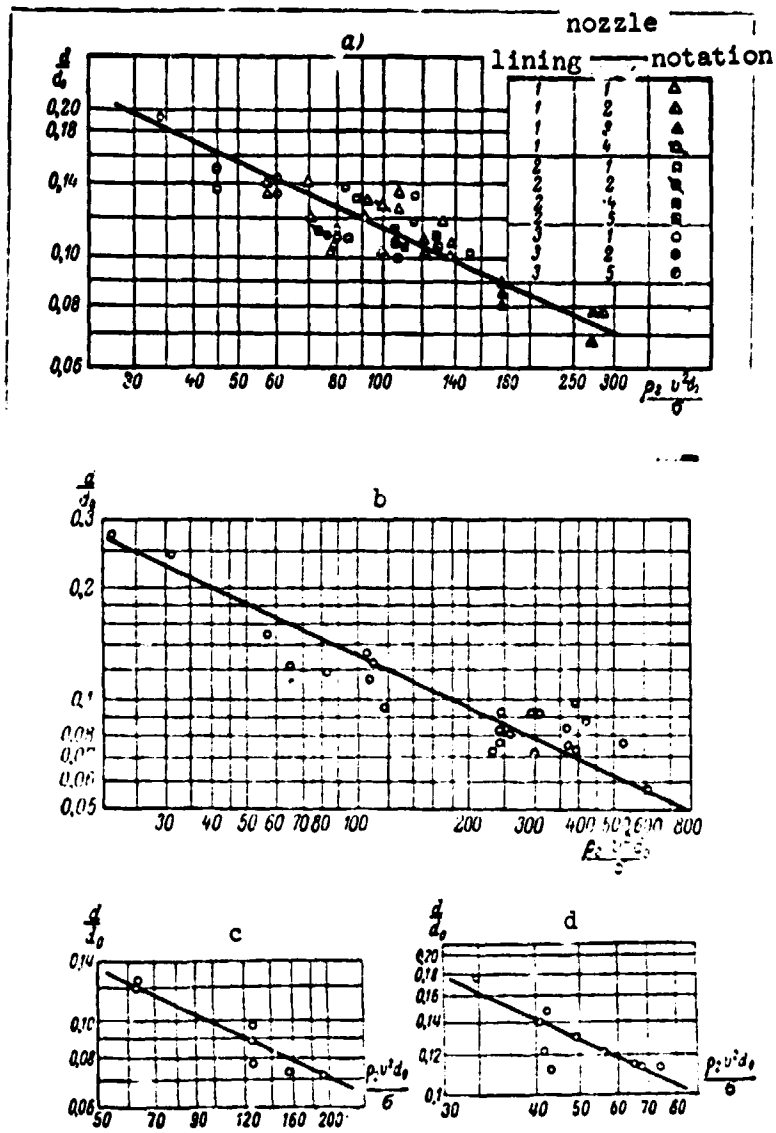

Fig. 5-11. Dependence $d/d_0 = f(\rho_r v^2 d_0/\sigma)$ for different sprayers:
a - STS-FOB-2 spray nozzle: b - STS-FDB-1 spray nozzle;
c - STS-FDM-1 spray nozzle; d - Glushakov spray nozzle.

linings with nozzles, were combined on one line, which may be expressed by the equation (5-3'):

$$\frac{d}{d_0} = A_0 \left(\frac{\rho_r v^2 d_0}{\sigma} \right)^{-0,45}.$$

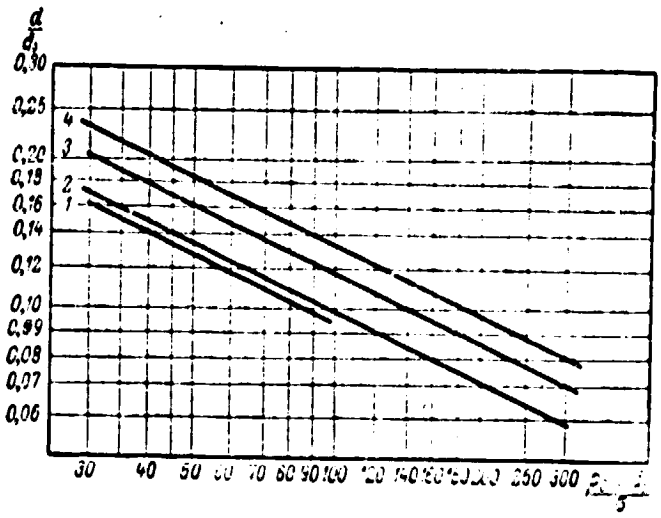

Fig. 5-12. Dependence $d/d_0 = f(Q_r^2 d_0 n)$ for different sprayers.

1 - Glushakov spray nozzle;
2 - STS-FDM-1 spray nozzle;
3 - STS-FOB-2 spray nozzle;
4 - STS-FDB-1 spray nozzle.

/97

TABLE 5-2

VALUE OF THE COEFFICIENTS A AND m FOR LOW PRESSURE SPRAY NOZZLES

Name of Sprayer	A	m
STS-FDB-1	1.20	2.8
STS-FOB-2	0.90	2.6-3.0
STS-FDM-1 (Kel'man)	0.78	2.8
Glushakov	0.75	2.3
Two-stage	0.61	2.8

As would be expected, due to the low velocity of the liquid, the generation of vortices in the liquid stream did not include the liquid atomization. The same type of dependence is obtained for the remaining spray nozzles tested (Fig. 5-11,b,c,d). The comparative locations of the curves for (5-3') shown in Fig. 5-12 for all the spray nozzles tested.

The value of the coefficient A depends on the sprayer construction and is shown in Table 5-2.

An examination of the graph in Fig. 5-12 shows that when a liquid is atomized by spray nozzles STS-FDM-1 and Glushakov, obtaining a certain degree of

dispersion requires smaller velocities of the air stream (consequently smaller heads with respect to the air line) than in the case of atomization by spray nozzles STS-FOB-1 and STS-FDB-1.

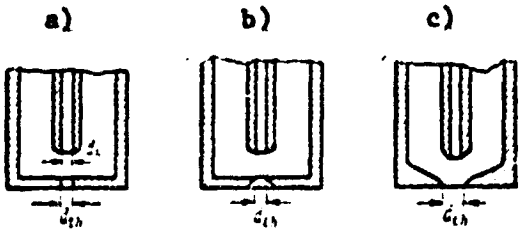

Fig. 5-13. Sprayer diagram [5-16].

The drop dimension distribution satisfies relation (1-10). Table 5-2 gives the values of the coefficient m for these spray nozzles. As may be seen from Table 5-2, the Glushakov spray nozzle has the smallest drop dimension uniformity. All the remaining spray nozzles tested have similar drop dimension distributions.

The study of Nukiyam and Tanasav [5-16, 17, 18] investigated the liquid atomization by pneumatic spray nozzles with a submerged nozzle, which is shown in Fig. 5-13. The hydrodynamic picture of the liquid and air flow in these spray nozzles differs sharply from that in the experiments given above with spray nozzles Nos. 1, 2 and 3 [5-2, 5]. Since the liquid stream encounters the air within the spray nozzle, primary breakdown of the stream occurs. The final breakdown of the stream occurs with the concurrent flow of liquid and air from the second nozzle into the atmosphere.

In the first series of experiments [5-16], the water was atomized by air at subsonic velocities in a spray nozzle which is shown in Fig. 5-13,a.

The nozzle diameters for water $d_ж$ and air d_r changed within the limits $d_ж$ = 0.2--1.0 mm and d_r = 2 - 5 mm. The average drop diameter was calculated using formula (1-3).

The value of the average drop diameter decreased with an increase in the relative velocity, calculated in the cross-sections of the corresponding nozzles, and also with an increase in the ratio between the air and liquid volumes when it was less than 5,000. This value did not depend on the nozzle dimensions d_r and $d_ж$.

In the second series of experiments [5-17], it was shown that the air nozzle configuration (5-13, b and c) has only a slight influence upon the dispersion of the water stream under the condition that the relative velocity is calculated in the contracted section of the air stream. It has a slight influence upon the atomization quality and the position of the water nozzle, if the water is supplied up to the contracted section or within it itself. When the nozzle moves below the contracted section, where the air velocity is smaller, the atomization deteriorates. /99

In the third series of experiments [5-18], a study was made of the influence of the liquid physical properties upon the dispersion of the stream atomized in the spray nozzle shown in Fig. 5-13, c.

As a result of the empirical processing of the experimental material in [5-18], a formula is given for determining the dependence of the average drop diameter on the liquid physical properties and the parameters of the process:

$$d_s = \frac{585\sqrt{\sigma}}{v_0\sqrt{\varrho_\text{ж}}} + 597\left(\frac{\mu_\text{ж}}{\sqrt{\varrho_\text{ж}\sigma}}\right)^{0.45}\cdot\left(\frac{1}{v_0}\cdot\frac{\varrho_\text{г}}{\varrho_\text{ж}}\right)^{1.5}. \qquad (5\text{-}6)$$

Here d_s -- average drop diameter determined as the diameter of a drop having the same ratio of the volume to the surface as the total sum of drops, micron;

v_0 -- relative velocity in the contracted section, m/sec;

$\varrho_\text{ж}$ = 0.7 - 1.2 G/cm^3; v_0 = 100 - 300 m/sec;

σ = 19 - 73 dyne/cm; $\frac{G_\text{ж}\varrho_\text{г}}{G_\text{г}}$ = 600 - 10,000.

Since formula (5-6) is purely empirical, it may only be used for the given type of spray nozzles in the studied range of the process parameter changes. The average drop diameters determined experimentally by Zauter in a study with a pneumatic spray nozzle were compared [5-10] with those calculated using the formula which gives a sharp divergence between the experimental and calculated values.

Ingebo [5-15] investigated the atomization of an isooctane stream when it is injected into an air stream. The experiments were performed for constant pressure and air temperature and velocities v_r = 43 and 55 m/sec. The average drop diameter was determined at different distances from the nozzle cross-section. The average drop diameter at a distance of 2.5 cm from the nozzle cross-section was compared with the data in [5-18] at an air stream velocity of 55 m/sec, but the dependence of the drop dimension on the velocity was found to be somewhat weaker.

Krubetskiy [5-10] studied the atomization by air of water streams supplied /100
in parallel or normally to an air stream. The experiment showed that the best results were obtained when liquid was supplied in parallel to an air stream at the site of the greatest velocity.

The study [5-12] investigated the influence of physical properties of a gas which atomized a liquid in a sprayer of the venturi type. A comparison of the data on the atomization by nitrogen and ethane showed that a decrease in the gas viscosity by 60% led approximately to the same increase in the average drop dimension. A decrease in the gas density by a factor of approximately 7, when the nitrogen was replaced by helium, led to an increase in the average drop diameter by approximately a factor of 2, in spite of a certain increase in velocity.

It was shown above that the stream dispersion under certain conditions depends on the ratio between the liquid and atomizing gas flow rates. This occurs when it is necessary to consider the braking of the air stream during the atomization time as a function of the ratio of the weighted air flow rates and the liquid flow rates $G_в/G$ and other factors. The value of the ratio $G_в/G$ at which a correction for velocity begins to play an important role, depends on the spray nozzle construction and the properties of the atomized liquid. The nature of the correction which considers this phenomenon may be found from the following considerations [5-4].

The average drop dimension was determined by the dependence (3-39):

$$\frac{d}{d_0} = f\left(\frac{\rho_г v^2 d_0}{\sigma},\ \frac{\mu_ж^2}{\rho_ж \sigma d_0}\right),$$

where v is the relative gas velocity in the case of liquid atomization.

If the initial relative velocity v_0 is introduced, then the dependence (3-39) may be transformed as follows:

$$\frac{d}{d_0} = f\left(\frac{\rho_г v^2 d_0}{\sigma},\ \frac{\mu_ж^2}{\rho_ж \sigma d_0},\ \frac{v}{v_0}\right). \qquad (5\text{-}7)$$

The ratio v/v_0 may be expressed by means of the determining parameters. For this purpose, we may write the law of conservation of momentum per second for the liquid-gas system:

$$dK_г = -dK_ж \qquad \text{or} \qquad dv_г = -dv_ж \frac{G}{G_в}. \qquad (5\text{-}8)$$

Taking the fact into account that /101

$$v = v_г - v_ж \qquad \text{and} \qquad dv = dv_г - dv_ж,$$

we have

$$dv = -dv_ж \left(1 + \frac{G}{G_в}\right).$$

After integration:

$$v - v_0 = -\left(1 + \frac{G}{G_в}\right)(v_ж - v_{ж0})$$

and

$$\frac{v}{v_0} = 1 - \left(1 + \frac{G}{G_в}\right)\frac{v_ж - v_{ж0}}{v_0}. \qquad (5\text{-}9)$$

When the initial liquid momentum per second is small with respect to the initial gas momentum, equation (5-9) may be simplified to the form:

$$\frac{v}{v_0} = 1 - \left(1 - \frac{G}{G_в}\right)\frac{v_ж}{v_0}. \qquad (5\text{-}9')$$

Here $v_ж$ is the stream velocity at the time of atomization.

Let us write the equation of motion for an elementary volume of liquid which equals $\pi R^2 dz$, where R is the stream boundary radius, dz -- element of length, $v_ж$ -- liquid velocity, c -- stream resistance coefficient (drop) when it moves in air, and v -- relative velocity of the medium:

$$\varrho_ж \pi R^2 dz \frac{dv_ж}{dt} = c \frac{\varrho_г v^2}{2} \cdot 2\pi R dz. \tag{5-10}$$

Thus:

$$dv_ж = c \frac{\varrho_г}{\varrho_ж} \cdot \frac{v^2}{R} dt. \tag{5-10'}$$

This equation gives the dimensionless complex:

$$\frac{v_ж R}{T v^2} \cdot \frac{\varrho_ж}{\varrho_г}.$$

Excluding the time from it (by combination with the criterion $\Pi_4 = \frac{\mu_ж}{\varrho_г v^2 T}$) and considering that at the converging points R/d_0 = idem, we find that in similar processes at the converging points: /102

$$v_ж \sim \frac{\mu_ж}{d_0 \varrho_ж}.$$

On the other hand, we have the following for similar processes:

$$\frac{\varrho_г v_0^2 d_0}{\sigma} = \text{idem},$$

from which we have

$$v_0 \sim \sqrt{\frac{\sigma}{\varrho_г d_0}}.$$

Thus:

$$\frac{v_ж}{v_0} \sim \frac{\mu_ж}{\varrho_ж} \sqrt{\frac{d_0 \varrho_г}{\sigma}} = \sqrt{\Pi_1} \frac{\varrho_г}{\varrho_ж}. \tag{5-11}$$

Examining the system of criteria (5-7) with allowance for the relationships

(5-9') and (5-11), for determining the flame degree of dispersion we reach the following functional relationship:

$$\frac{d}{d_0} = f\left(\frac{\varrho_г v_0^2 d_0}{\sigma};\ \frac{\mu_ж^2}{\varrho_ж \sigma d_0};\ \frac{G_в}{G};\ \sqrt{\frac{\mu_ж^2}{\varrho_ж \sigma d_0} \cdot \frac{\varrho_г}{\varrho_ж}}\right). \qquad (5\text{-}12)$$

In order to explain the form of the relation (5-12), we carried out several experiments on liquid atomization by a spray nozzle when the ratio $G_в/G$ influenced the stream dispersion. The results of these experiments are shown in Fig. 5-14 in the coordinates $d/d' = f(G_в/G)$ for constant values of the criteria

$\frac{\mu_ж^2}{\varrho_ж \sigma d_0}$; $\frac{\varrho_г v_0^2 d_0}{\sigma}$ and $\frac{\varrho_г}{\varrho_ж}$.

Here d -- average drop diameter for a given ratio $G_в/G$;

d' -- average drop diameter when the ratio $G_в/G$ does not influence the atomization.

Analytically, this dependence may be expressed by the formula:

$$\frac{d}{d_0} = \left[1 + B\left(\frac{G}{G_в}\right)^m\right] \frac{d'}{d}, \qquad (5\text{-}12')$$

where B = 0.011 and m = 2.

The value of d'/d_0 was determined using the formula (5-3). Then finally we have: /103

$$\frac{d}{d_0} = A\left[1 + B\left(\frac{G}{G_в}\right)^m\right]\left(\frac{\varrho_г v_0^2 d_0}{\sigma}\right)^{-0.45}. \qquad (5\text{-}12'')$$

Here the coefficients:

$$A = f\left(\frac{\mu_ж^2}{\varrho_ж \sigma d_0}\right)$$

and

$$B = f\left(\frac{\mu_ж^2 \varrho_г}{\varrho_ж \sigma d_0}\right)$$

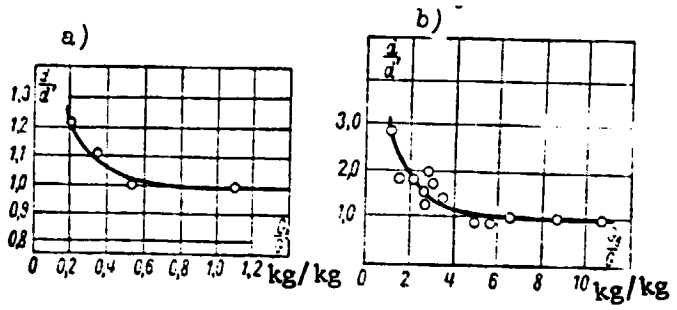

Fig. 5-14. Dependence of d/d' on the parameter $G_в/G$:

a - [5-3] (spray nozzle No. 3);
b - [5-16].

depend only on the sprayer construction. This may be seen by comparing the data in [5-3] and [5-18], shown in Fig. 5-14.

An examination of the data in [5-6] shows that the exponent m also depends on the sprayer construction. Thus, Fig. 5-15 shows the dependence of the average drop dimension using the data of [5-6], for which the value of the coefficient m is somewhat smaller.

The influence of the liquid physical properties on the drop dimension under the conditions when it is necessary to consider the braking of the air stream is confirmed by the data given above [5-18], and also the data in [5-12,13] which will be examined below.

The study [5-12] investigated the atomization of liquid sulphur by air at a temperature of 150° C in a Venturi sprayer (Fig. 5-16) having a nozzle diameter of d_o = 6.3 mm.

At an air velocity less than the speed of sound, the average diameter according to Zauter was determined by the formula: /104

$$d_s = 336 \frac{1{,}5 + \frac{G}{G_в}}{G_в^{0{,}9}} \text{ [microns]} \qquad (5\text{-}13)$$

where G -- sulfur flow rate, kg/hr.

$G_в$ -- air flow rate, kg/hr.

The dependence of the average drop diameter on the air velocity in this case

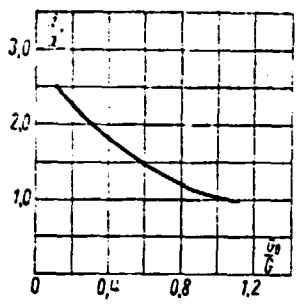

Fig. 5-15. Dependence of d/d' on the parameter $G_в/G$ [5-6].

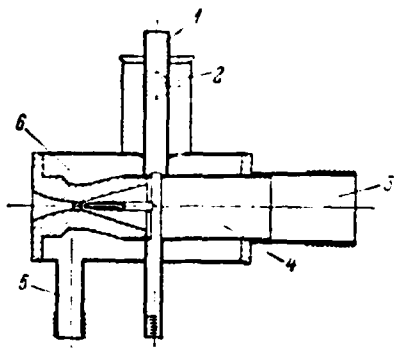

Fig. 5-16. Sprayer [5-12].

1 - connection for sulphur supply;
2 - connection for hot vapor supply;
3 - connection for air supply;
4 - tube for air supply;
5 - hot vapor output;
6 - vapor jacket.

for small $G/G_в$ ratios corresponds to the formula (5-2).

At sonic velocities of air, the dependence of the average drop diameter on the air flow rate is increased and expressed by the formula:

$$d_s = 8100 \frac{1{,}5 + \frac{G}{G_в}}{G_в^{1{,}63}} \text{ [microns]} \qquad (5\text{-}14)$$

It was proposed in [5-12] that formulas (5-13) and (5-14) may be used for sprayers with other values of d_o. It was thus necessary to multiply the air flow rates and the liquid flow rates by the square of the diameter ratios $(6.3/d_o)^2$, since the average drop diameter was determined by the velocity of the air stream in the smallest nozzle cross-section and the ratio of the weighted flow rates of liquid in air.

Air sprayers operating at sonic velocities were also studied in [5-13]. Three converging nozzles of differing dimensions were studied (Fig. 5-17,a) and one diverging nozzle (Fig. 5-17,b). Samples of the drops were placed on a plate covered with oil and smoothed across the atomized stream. The experimental results showed that the average mass diameter for a given ratio of the air and water flow rates does not depend on the air pressure of the spray nozzle and the water flow rate, and increases with an increase in the $G/G_в$ ratio /105

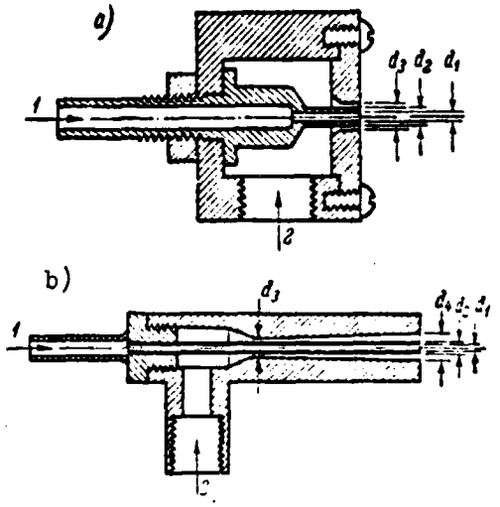

Sprayer	Diameter, mm			
	d_1	d_2	d_3	d_4
According to Fig. 5-17, a:				
Small.	1.62	1.97	3.17	-
Average.	2.64	3.18	5.15	-
Large.	3.83	4.64	7.55	-
According to Fig. 5-17, b . . .	2.64	3.18	5.15	6.14

Fig. 5-17. Sprayer with converging (a) and diverging (b) nozzle [5-13].

1 - water; 2 - air

(Fig. 5-18), which corresponds to the data in [5-6] and diverges from the data in [5-12]. A diverging nozzle had better results than the converging nozzle with the smallest diameter.

An increase in the nozzle diameter leads to an enlargement of the drops. In such nozzles, the average drop diameter increases in proportion to $d_3^{0.4}$ (Fig. 5-19).

A comparison of the experimental results on atomization with a small sprayer of ethylene-glycol ($\varrho_ж = 1{,}12\,g/cm^3$, $\mu_ж = 0{,}199$ poise, $\sigma = 48$ dyne/cm), water and a solution consisting of 85% methyl alcohol and 15% glycerin ($\varrho_ж = 0.88\ g/cm^3$, $\mu_ж = 0.014$ poise and $\sigma = 23$ dyne/cm), showed that at sonic velocities of air an increase in the liquid viscosity leads to an increase in the average drop /106

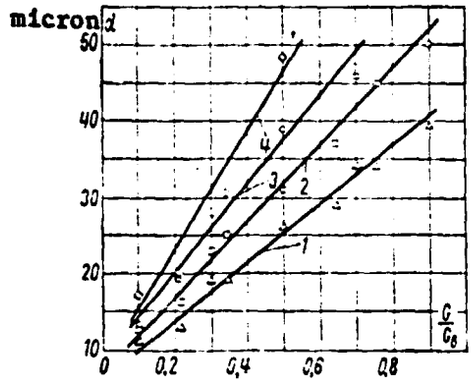

Fig. 5-18. Dependence of average drop diameter on the ratio between water and air flow rates.

1 - small converging nozzle;
2 - average converging nozzle;
3 - large converging nozzle;
4 - diverging nozzle

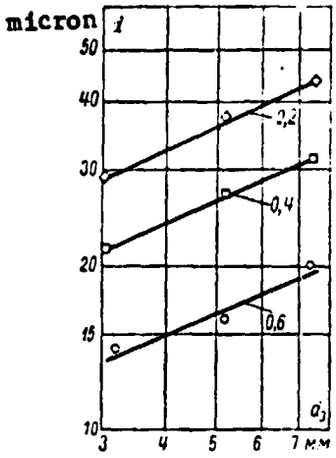

Fig. 5-19. Dependence of average drop diameter on the diameter of the air nozzle d_3 for sprayers with converging nozzles.

Numbers on the line -- the ratio $G/G_в$.

diameter, whereas the influence of the viscosity is much stronger than the influence of the surface tension (Fig. 5-20,a). If we introduce the criteria $\mu_ж^2 \rho_ж \sigma d_3$, then these data may be generalized by the dependence shown in Fig. 5-20,b.

The study [5-14] investigated the sprayer shown in Fig. 5-21,a and used for atomization of a highly viscous fuel with air at high pressure in the combustion chamber of gas turbines. In this spray nozzle the air is supplied along tube 1 into the screw-shaped channel formed by the lining 2, and leaves at a high rotational velocity through nozzle 3. The fuel enters the spray nozzle along tube 4 in a radial direction and through the circular slit 5 is supplied to the nozzle opening. The experiments were performed for two values of the slit width (0.127 and 0.254 mm). The air pressure changed approximately from 1.4 to 7 atm; the fuel pressure -- from 0.7 to 3.5 atm. The ratio of the fuel and air flow rates was from 0.8 to 40.0. The atomization took place in the atmosphere. The drop dimensions were determined by the paraffin method, and the viscosity of the atomized paraffin fluctuated from 10 to 20 centistokes. The air and the paraffin were supplied at the same temperature. The average drop diameter increased with an increase in the dimensions of the slit for supplying the fuel, the fuel flow

/108

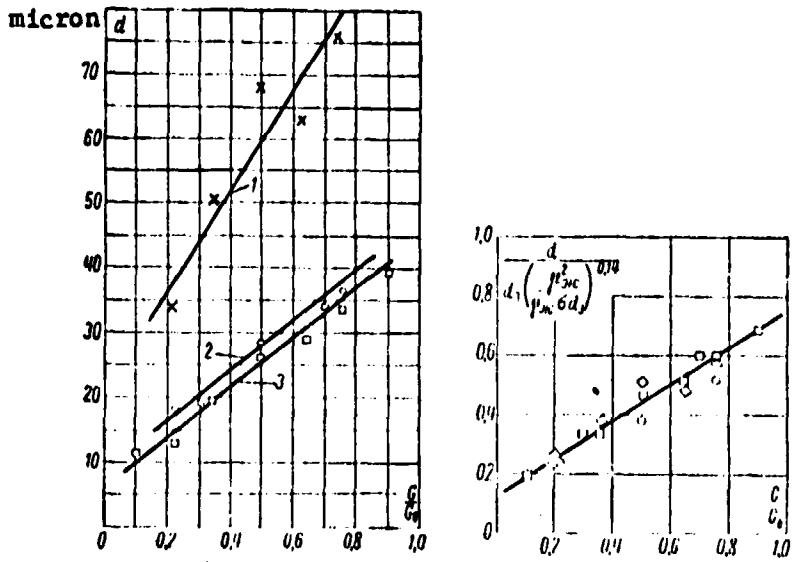

Fig. 5-20. Dependence of average drop diameter on the ratio between the liquid and air flow rates for different physical properties of the atomized liquid.

X -- ethylene-glycol; 0 -- solution consisting of 85% methyl alcohol and 15% glycerin; ◻ — water

rate and its viscosity, and with a decrease in the air flow rate.

The experiments with a similar sprayer, but larger dimensions (Fig. 5-21,b) are described in [5-19]. The fuel viscosity changed from 20 to 40 centistokes, and the fuel and air pressure changed within the same limits as in [5-14]. The average drop diameter calculated with formula (1-3) increased with an increase in the ratio between the air and fuel flow rates and with an increase in the fuel viscosity. For a given ratio $G_в/G$, the increase in the air stream velocity led to a finer breaking up of the liquid. A comparison of the data in [5-14] and [5-19] showed that the average drop diameter increased in proportion /109 to $\sim 1/\bar{d}_{ш}$. The experimental results are given in Fig. 5-22.

Section 5-2. Sprinkling density of an atomized stream by a liquid

This section presents materials dealing with the distribution of a liquid in the cross-section of an atomized stream and an attempt is made to generalize the experimental data in view of the present concepts regarding the motion of an admixture suspended in a stream.

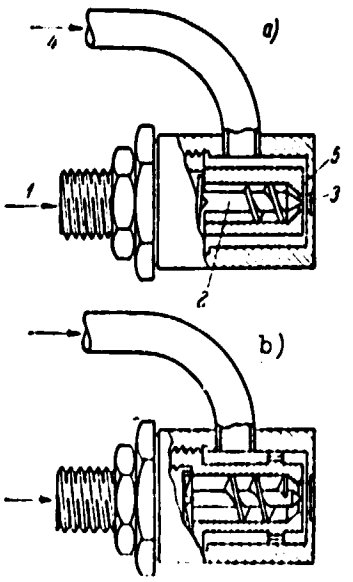

Fig. 5-21. High pressure sprayer with nozzle diameter of 3.18 (a) and 6.36 mm (b).

On the basis of measurements, the study [5-3, 5] determined the sprinkling density by a liquid g (i.e., the amount of liquid falling per unit time on a unit surface perpendicular to the stream axis) at different distances from the stream axis. Figure 5-23 shows the curve for the sprinkling density obtained at different distances from the nozzle opening for one and the same mode. All the curves have a symmetrical form with a maximum on the stream axis. With increasing distance from the nozzle, the stream expands and there is a more uniform distribution of the liquid over the area of the transverse cross-section.

These data are shown in Fig. 5-24 in relative coordinates. The abscissa shows the value of r/x, which represents the relative distance from the stream axis to the point r (x - distance from the cross-section to the spray nozzle opening); the ordinate axis - the relative sprinkling density $g_x g_{ox}$, where g_x is the sprinkling density at a given point of the cross-section; g_{ox} - sprinkling density on the stream axis in a given cross-section. The distribution of the liquid over the stream axis is not a single-valued function of r/x, i.e., the relative expansion of the stream is not constant but decreases with the distance.

Figure 5-25 shows the distribution of the liquid over the stream cross-section at different modes at one and the same distance from the spray nozzle

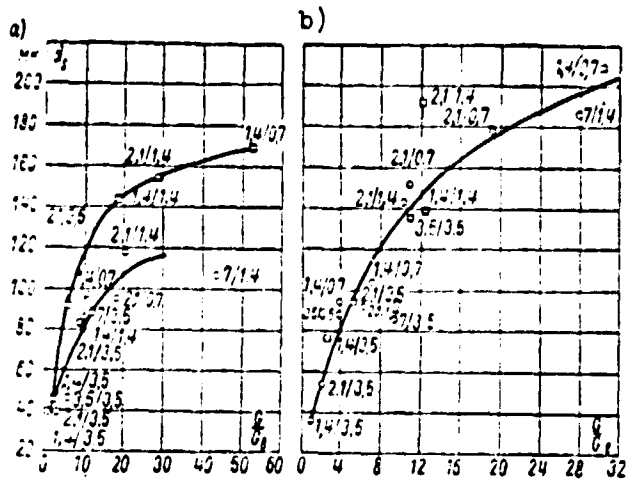

Fig. 5-22. Dependence of average drop diameter d_s on the parameter G/G_B for the fuel viscosity of 20 (a) and 40 centistokes (b).

Numbers on the curves show the fuel pressure (numerator) and the air pressure (denominator) atm. The slit width 5 (Fig. 5-21); 0 -- about 2.5, □ - about 0.5 mm

opening. As the air stream velocity increases, the stream form becomes sharper. /111 Figure 5-26 shows the curves for the liquid distribution over the stream cross-section, obtained at the same distance from the spray nozzle opening for two values of liquid viscosity in the case of identical relative flow velocities. It may be noted that as the viscosity increases, the curve for the relative stream sprinkling density becomes flatter. Figure 5-27 gives the following dimensionless dependence in logarithmic coordinates:

$$\frac{g_{ox}}{g_x} = f\left(\frac{r}{r_{ox}}\right), \qquad (5\text{-}15)$$

where r_{ox} is the distance from the stream axis to the point on the cross-section at which $g_x/g_{ox} = 1/2$.

This coordinate system makes it possible to generalize the data on the sprinkling densities obtained for cross-sections located at different distances from the spray nozzle opening for different modes of the distribution for a liquid having different physical properties. The curve in Fig. 5-27 may be approximately described by the following formula:[1)]

$$\frac{g_x}{g_{ox}} = e^{-0.7\left(\frac{r}{r_{ox}}\right)^{1.6}}. \qquad (5\text{-}15')$$

---

1) The study [5-7] shows the applicability of the formulas (5-15') and (5-18) obtained in [5-3] for describing the distribution of a liquid atomized by a mechanical spray nozzle, which is not of the centrifugal type, over the stream cross section.

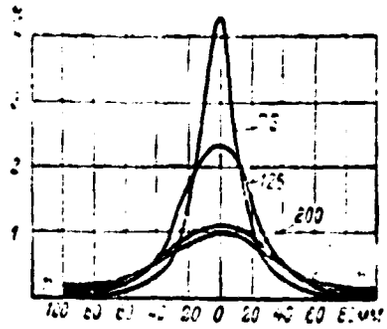

Fig. 5-23. Curves for the sprinkling density by an atomized liquid [5-5].

Numbers on the curves -- distance from the spray nozzle opening, mm.

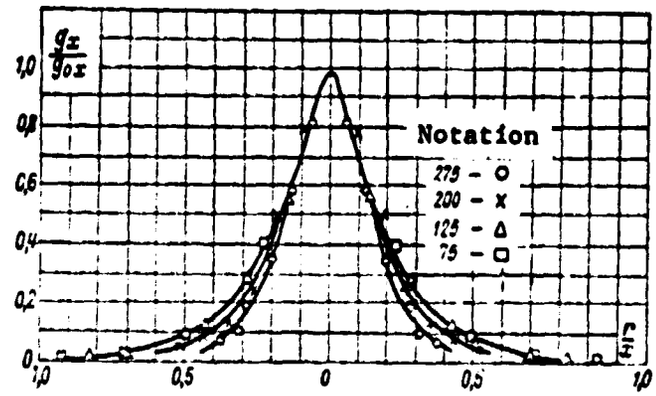

Fig. 5-24. Sprinkling density curves in relative coordinates:

$$\frac{g_x}{g_{ox}} = f\left(\frac{r}{x}\right).$$

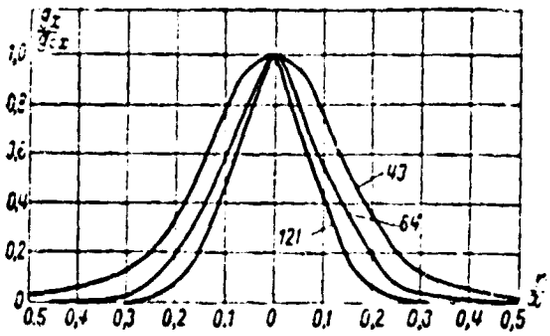

Fig. 5-25. Sprinkling density curves at the same distance from the spray nozzle opening.

Numbers on the curves -- air stream velocity, m/sec.

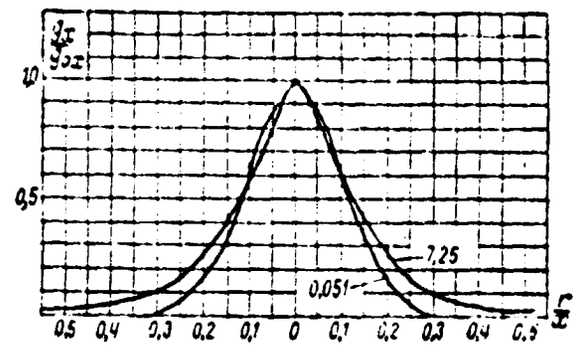

Fig. 5-26. Sprinkling density curves by liquids of differing viscosity.

Numbers on the curves -- values of n_1.

Thus, to calculate the quantity g, it is necessary to know the dependence of g_{ox} and r_{ox} on the process parameters. /112

It may be assumed that the process of liquid atomization by a pneumatic spray nozzle consists of the following stages: a) breakdown of the stream into drops with subsequent breakdown of the large drops obtained into smaller drops; b) acceleration of the drops due to interaction with the air stream and (c) further transport of the drops by the gas stream.

Fig. 5-27. Generalized dependence: $\frac{g_{ax}}{g_x} = f\left(\frac{r}{r_x}\right)$.

● - spray nozzle No. 1; X - spray nozzle No. 2; O - spray nozzle STS-FDM.

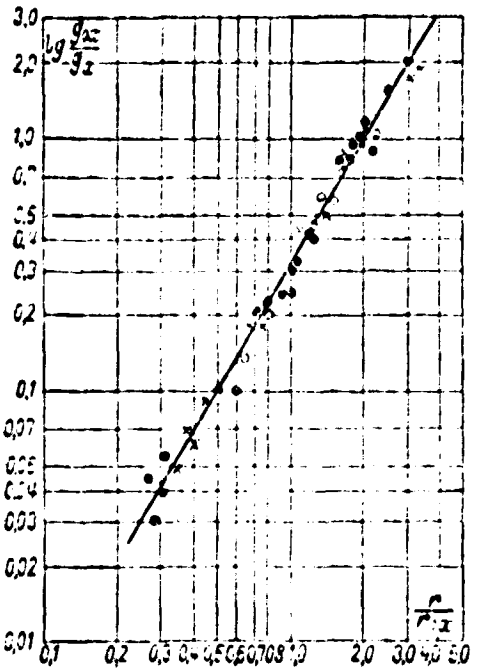

According to this scheme, part of the air stream energy is expended in the interaction of air with the deformed stream and the drops which are formed. When a reduction in the relative velocity during the atomization is small, we may disregard the change in the air stream velocity. Thus, atomization occurs in the immediate vicinity of the spray nozzle. The diagram of the phenomenon is given in the following form. /113

A stream of gas emanating at the velocity v_r from a circular cylindrical lining with an internal radius R_o contains an admixture of liquid particles with a concentration c_o. We may designate the liquid flow rate by G. The admixture of the liquid defuses in the gas, as the result of which the liquid concentration decreases on the axis with an increase along the edges. Based on the law of conservation of matter, we may write the liquid flow rate G through any cross-section perpendicular to the stream axis as follows:

$$G = g_m \pi R_x^2 \int_0^{R_x} 2\pi g_x r\,dr, \qquad (5\text{-}16)$$

where $g_m = G/\pi R_x^2$;

R_x -- largest radius (at g = 0) in the x cross-section.

Let us transform formula (5-16) to the dimensionless form:

$$\int_0^{R_x/R_0} \frac{g_x}{g_0} \cdot \frac{r}{R_0} d\left(\frac{r}{R_0}\right) = \frac{1}{2}. \qquad (5\text{-}16')$$

As a scale of the sprinkling density and the distance from the stream axis, we select the same quantities as used when deriving formula (5-15) and transform formula (5-16'):

$$\frac{g_{ox}}{g_0}\left(\frac{r_{ox}}{R_0}\right)^2 \int_0^{R_x/r_{ox}} \frac{g_x}{g_{ox}} \cdot \frac{r}{r_{ox}} d\left(\frac{r}{r_{ox}}\right) = \frac{1}{2}. \qquad (5\text{-}16'')$$

In accordance with the experimental dimensionless dependence (5-15'), the integral may be transformed to the form:

$$\int_0^{R_x/r_{ox}} f\left(\frac{r}{r_{ox}}\right) d\left(\frac{r}{r_{ox}}\right) = \text{const} \qquad (5\text{-}17)$$

or

$$C = \int_0^{R_x/r_{ox}=0.7\left(\frac{r}{r_{ox}}\right)^{3.5}} e^{\frac{r}{r_{ox}}} d\left(\frac{r}{r_{ox}}\right). \qquad (5\text{-}17')$$

A graphic integration gives the value $C \approx 1$.

Combining expressions (5-16") and (5-17'), we obtain: /114

$$\frac{g_{ox}}{g_0}\left(\frac{r_{ox}}{R}\right)^2 = \frac{1}{2C} = \frac{1}{2}$$

and

$$\frac{r_{ox}}{R_0} = \sqrt{\frac{1}{2} \cdot \frac{g_0}{g_{ox}}}. \qquad (5\text{-}18)$$

Thus, the dimensionless radius r_{ox}/R_o is a function of g_{ox}/g_o, and to determine it it is necessary and sufficient to know the value of g_{ox}/g_o. The latter may be determined by examining the motion of the drops suspended in the gas stream.

Let us write the relationship between the sprinkling density and the volumetric liquid concentration in the gas stream:

$$g = vc\gamma. \tag{5-19}$$

Then for the cross-sections compared, we may write:

$$\frac{g_x}{g_{ox}} = \frac{v_x c_x}{v_0 c_0} = \frac{v_x}{v_0} \cdot \frac{c_x}{c_0}, \tag{5-19'}$$

were c_o and v_o are the concentration and velocity in the initial stream cross-section; c_x and v_x -- the same, at the cross-section point at a distance of x from the nozzle opening.

The dimensionless axial velocity v_x/v_o for free streams is a function of the dimensionless coordinate and may be expressed by the equation:

$$\frac{v_x}{v_0} = \frac{A}{B + \frac{x}{R_0}} = f\left(\frac{x}{R_0}\right). \tag{5-20}$$

The dimensionless concentration c_x/c_o is determined by the transport conditions in the gas stream. The equation of diffusion in the case of isotropic turbulence may be written in the form:

$$\frac{\partial c}{\partial t} + v_x \frac{\partial c}{\partial x} + v_y \frac{\partial c}{\partial y} + v_z \frac{\partial c}{\partial z} =$$
$$= \frac{\partial}{\partial x}\left(k \frac{\partial c}{\partial x}\right) + \frac{\partial}{\partial y}\left(k \frac{\partial c}{\partial y}\right) + \frac{\partial}{\partial z}\left(k \frac{\partial c}{\partial z}\right), \tag{5-21}$$

where k is the turbulent diffusion coefficient.

Several studies [5-1, 8 and 10] for determining the turbulent diffusion coefficient showed that this coefficient may be assumed to be constant over the cross-section, and changes little along the stream axis. It also depends to a great extent on the initial conditions. /115

In accordance with this, we assume in the first approximation that the coefficient k may be completely determined by the initial conditions, i.e., the flow conditions (form of nozzle, roughness of the nozzle walls, etc.) and the atomization process, respectively. When the similarity of the initial conditions is observed, the coefficient k at different points of the stream is a constant which does not depend on the coordinates or velocity. Under these assumptions, for the case of an axisymmetric stationary flow, equation (5-21) written in cylindrical coordinates has the form:

$$v_x \frac{\partial c}{\partial x} + v_r \frac{\partial c}{\partial r} = k \left(\frac{\partial^2 c}{\partial r^2} + \frac{1}{r} \cdot \frac{\partial c}{\partial r} \right). \qquad (5\text{-}21,a)$$

We may obtain the following criteria from equation (5-21,a):

$$\frac{x}{R_0} \quad \text{and} \quad \frac{vR_0}{k}.$$

In its turn, the coefficient k, according to the hypothesis assumed, is a function of the stream decomposition process. As was shown above, the latter is unequivocally determined by the criteria:

$$\frac{\mu_ж^2}{\varrho_ж \sigma d_0} \quad \text{and} \quad \frac{\varrho_г v_0^2 d_0}{\sigma}.$$

Thus, it is possible to write the following relationship:

$$k = k_0 f \left(\frac{\varrho_г v_0^2 d_0}{\sigma}, \frac{\mu_ж^2}{\varrho_ж \sigma d_0} \right). \qquad (5\text{-}22)$$

where k_0 is only determined by the spray nozzle construction.

In accordance with this, the functional relationship for the dimensionless concentration on the axis may be written in the form:

$$\frac{c_{0x}}{c_0} = f \left(\frac{x}{R_0}, \frac{vR_0}{k}, \frac{\mu_ж^2}{\varrho_ж \sigma d_0}, \frac{\varrho_г v_0^2 d_0}{\sigma} \right). \qquad (5\text{-}23)$$

Finally, in accordance with formulas (5-19'), (5-20), (5-22) and (5-23), we shall have: /116

$$\frac{g_{ox}}{g_0} = f\left(\frac{x}{d_0},\ \frac{vd_0}{k_0},\ \frac{\mu_{ж}^2}{\varrho_{ж}\sigma d_0},\ \frac{\varrho_r v_0^2 d_0}{\sigma}\right). \tag{5-24}$$

where $d_o = 2R_o$.

As the result of processing the experimental data on determining the sprinkling density, we obtain the specific form of the criterial dependence under the condition $x/d_0 \gg 1$:

$$\frac{g_x}{g_0} = \frac{d_0 v_э}{k_0 x} \cdot \frac{e^{-0.7\left(\frac{2r}{d_0\sqrt{\frac{d_0^2}{k_0 x}\cdot\frac{v_э}{f(\Pi_1)}}}\right)^{1.6}}}{f(\Pi_1)}. \tag{5-24a}$$

where

$$f(\Pi_1) = 1 + \frac{2.7}{1 + 0.35\left(\frac{\mu_{ж}^2}{\varrho_{ж}\sigma d_0}\right)^{-0.45}};$$

$$v_э = v_r\sqrt{1 - \left(\frac{d_{вн}}{d_{нар}}\right)^2} \qquad [5\text{-}9];$$

$d_{нар}$ and $d_{вн}$ -- internal and external diameters of the air nozzle.

Combining formulas (5-18) and (5-24a), we obtain:

$$\frac{r_{ox}}{d_0} = \sqrt{\frac{kx}{8d_0^2 v_э}}, \tag{5-25}$$

where $k = k_0 f(\Pi_1)$.

It follows from formula (5-15'):

$$\frac{r}{r_{ox}} = \left[\frac{\lg\frac{g_x}{g_{ox}}}{0.7\lg e}\right]^{0.625}. \tag{5-26}$$

The transformation of these formulas makes it possible to determine the lines of equal sprinkling densities as a function of the parameter $kx/v_э$.

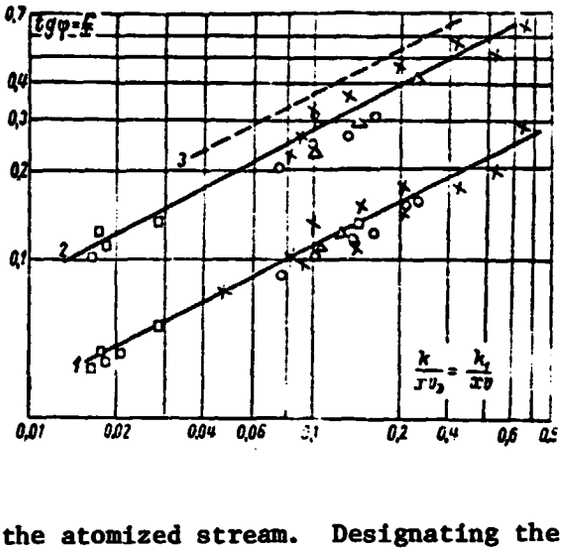

Fig. 5-28. Dependence $\varphi = f(k/xv_э)$ for different ratios of g_x/g_{ox}; 1-0.5; 2-0.05; 3-0.01. X -spray nozzle No. 1; O-spray nozzle No. 2; Δ - spray nozzle No. 3; □ - STS-FDM spray nozzle

and also the angle of taper of the atomized stream. Designating the relative coordinate $r\,x = \operatorname{tg}\varphi$, we have:

$$\operatorname{tg}\varphi = \frac{r}{r_{ox}} \cdot \frac{r_{ox}}{d_0} \cdot \frac{d_0}{x} = \left[\frac{\lg \frac{g_x}{g_{ox}}}{0{,}7 \lg e}\right]^{0{,}625} \cdot \sqrt{\frac{k}{xv_э}}. \qquad (5\text{-}27)$$

On the basis of the formula (5-27), the equations for the lines of equal densities assume the form: /117

For $g_x/g_{ox} = 0.5$

$$\operatorname{tg}\varphi_{0,5} = 0{,}35 \sqrt{\frac{k}{xv_э}}; \qquad (5\text{-}27a)$$

For $g_x/g_{ox} = 0.1$

$$\operatorname{tg}\varphi_{0,1} = 0{,}74 \sqrt{\frac{k}{xv_э}}; \qquad (5\text{-}27b)$$

For $g_x/g_{ox} = 0.05$

$$\operatorname{tg}\varphi_{0,05} = 0{,}87 \sqrt{\frac{k}{xv_э}}. \qquad (5\text{-}27c)$$

Assuming $g_x/g_{ox} = 0.01$ as the stream boundary, we have

$$\operatorname{tg}\varphi_{\text{граш}} = 1{,}14 \sqrt{\frac{k}{xv_э}}. \qquad (5\text{-}27d)$$

Figure 5-28 shows the calculated lines corresponding to formulas (5-27a) and (5-27b) and the experimental points for $g_x/g_{ox} = 0.5$ (1) and 0.05 (2). This graph gives line 3 corresponding to $\varphi_{гран} = 0.01$ in the form of the dot-dashed line. It was not possible to determine accurately the experimental boundary of the stream.

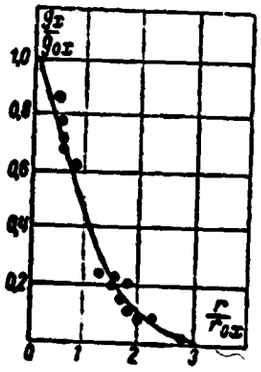

Fig. 5-29. Liquid distribution over cross-section of stream atomized by spray nozzle STS-FDM.

In actual calculations, in some cases it is more advantageous to use the relative velocity and not the equivalent velocity. The relationship between these velocities may be represented by the equation $v_1 = \psi v$, where ψ depends on the construction and method of organizing the air stream in the sprayer. Introducing the coefficient $k_1 = k\psi$ into (5-27), we obtain

$$\operatorname{tg}\varphi = \left[\frac{\lg \frac{g_x}{g_{ox}}}{0.7 \lg e}\right]^{0.625} \cdot \sqrt{\frac{k_1}{g_{ox}}}. \qquad (5\text{-}28)$$

For determining k_1, it is sufficient to measure the distance from the stream axis for a given relative sprinkling density, for example, at $g_x/g_{ox} = 1/2$.

Figure 5-29 shows the liquid distribution over the cross-section obtained in tests with the spray nozzle STS-FDM [5-5]. As may be seen from this figure, the experimental points are only arranged along the line corresponding to formula (5-15'). Consequently, to calculate the angle of taper of the stream atomized by this spray nozzle, we may use formula (5-28). Processing of the experimental data using this formula gives the value $k_1 = 0.85$.

CHAPTER 6

DESIGN DIAGRAMS AND CHARACTERISTICS OF MECHANICAL AND PNEUMATIC ATOMIZATION SPRAY NOZZLES

Since the time when the combustion of liquid fuel began in steam boilers and industrial furnaces, many designs of both mechanical and air (steam) atomization spray nozzles have been created. Only a few of these designs -- the simplest, most economical and easily regulated ones -- have earned a firm place in industrial use. /119

Recently, when the power ratings of steam boilers have sharply increased, the requirements made on the regulation limits of the single spray nozzle have sharply increased, and such a new engine type as the gas turbine has appeared. A number of complicated spray nozzle designs has been created. These are called upon to ensure the reliable operation of aggregates during the combustion of liquid fuel under new conditions.

This chapter examines types of spray nozzles which have become widely used in energy generation and in industrial furnaces, as well as certain original designs which can evidently be the basis for the development of new, effective sprayers in the immediate future.

Section 6-1. Mechanical atomization spray nozzles

The TsKKB spray nozzle. The general view of the spray nozzle is shown in Fig. 6-1. The functional component of the spray nozzle is the sprayer, which consists of the housing 1, the atomizing washer 2, the sprayer 3, the turbulent nozzle 4, and the nuts and counternuts 6. Liquid fuel under pressure proceeds through connection 7 along a tube, through the distributor 3, to the turbulence nozzle 4, and thence through washer 2 is sprayed into the furnace chamber in atomized form.

The spray nozzle is used for a fuel flow rate of from 80 to 2500 kg/hr. In this case, one should bear in mind that regulation during which good

atomization quality is ensured lies within limits of from 70 to 100%. Consequently, in order to regulate productivity within wider limits, one should change the design dimensions. It is sufficient to have two housings for this goal, of which one is for productivity of approximately up to 1,000 kg/hr. and the other -- from 1,000 to 2500 kg/hr. The change in the intermediate fuel flow rates is ensured by changing the atomizing washer and the turbulence nozzle. The recommended working pressure in the spray nozzle is 35 atm, according to the investigations of A. I. Dvoretskiy (VTI). With regulation of up to 70%, pressure drops to 20 atm. Operation based on the spray nozzle is also possible at a somewhat lower pressure, but this strongly worsens the quality of atomization.

/120

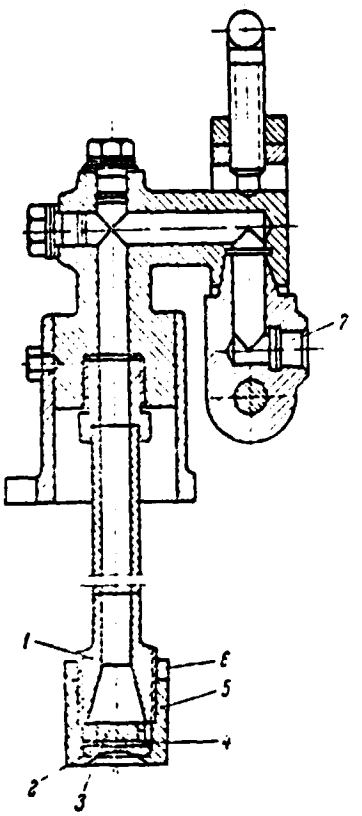

Fig. 6-1. The TsKKB spray nozzle.

The Grigor'yev spray nozzle. This spray nozzle (Fig. 6-2) is also called "Atom," is used for low flow rates, and consists of the nozzle 1 and stem 2. The nozzle is a cylinder with an internal spiral and cone 3, at whose apex outlet aperture 4 is located. The stem has a bushing 5, with slots 6 for passing the fuel. A truncated, tapered head 7, with slant channels 8 from the base of the cone 3 along the tangent to its apex is attached at the end of the stem. The fuel, running along these channels, is turbulized and is discharged into the furnace chamber through the medial aperture in the atomized state.

Industry manufactures 16 sizes of Grigor'yev spray nozzles with outlet aperture diameters ranging from 0.6 to 2.9 mm. These sizes ensure fuel flow rates from 12 to 200 kg/hr at 6 atm pressure. However, one should bear in mind that at low flow rates, the spray nozzle operates unreliably, inasmuch as in this case the outlet aperture and the tangential channels very frequently clog (even with extremely careful filtering of the liquid fuel). Tests consisting in water atomization yielded the results shown in Table 6-1.

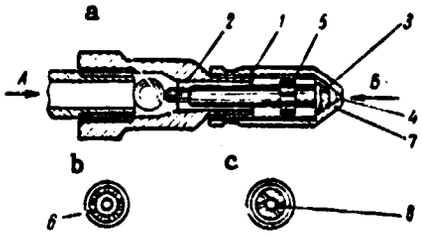

Fig. 6-2. Grigor'yev spray nozzle: a - overall view; b - view along arrow A of detail 5; c - view along arrow B of detail 7.

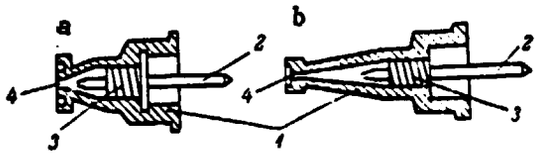

Fig. 6-3. Kerting spray nozzle: a - short flame sprayer (double turn thread); b - long flame sprayer (six turn thread)

TABLE 6-1

FLOW RATE OF LIQUID OF THE GRIGOR'YEV SPRAY NOZZLE, kg/hr.

Diameter of outlet nozzle, mm	Pressure, atm	
	6	8
1.5	97	107
2.5	245	280

When designing a Grigor'yev spray nozzle, one should bear in mind that the cross-sectional area of all tangential channels should be 2 - 2.4 times greater than the area of the outlet nozzle. /121

The Kerting spray nozzle. This spray nozzle (Fig. 6-3), employed for small fuel flow rates, consists of a nozzle 1 and stem 2. The foreward end of the stem has a groove which lies directly adjacent to the inside walls of the nozzle and forms the spiral channel 3. The fuel supplied through these channels acquires a rotational motion and is discharged into the furnace via nozzle 4 in the atomized state. The change in the angle of inclination of the spiral line and in the angle of taper of the nozzle makes it possible to obtain either a shorter or longer fuel spray. The diameter of the outlet nozzle end ranges from 1 to 4 mm. The selection of any particular diameter of this nozzle is determined by the assigned output of the sprayer, which can fluctuate within limits of from 70 to 450 kg/hr. The spray nozzle operates at fuel pressures ranging from 5 to 14 atm.

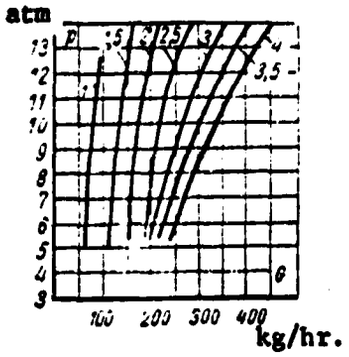

Fig. 6-4. Relationship between fuel oil flow rate G and pressure p in the Kerting spray nozzle.

Numbers next to the curve lines are nozzle diameter, mm.

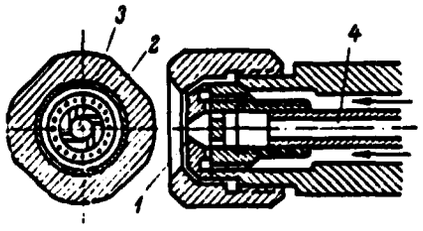

Fig. 6-5. Spray nozzle with back flow.

Figure 6-4 shows the relationship between the flow rate of fuel and pressure with different diameters of the outlet aperture [6-17]. It is evident from the graph that when one has a 1 mm nozzle diameter, the fuel flow rate increases from 70 to 100 kg/hr when pressure increases from 5 to 14 atm, and when the nozzle diameter is 4 mm, the fuel flow rate changes from 250 to 450 kg/hr when pressure increases from 6 to 14 atm.

The reverse discharge spray nozzle. The reverse discharge nozzle (Fig. 6-5) employs the principle of preserving a constant amount of rotating fuel when its flow rate changes. In this spray nozzle, the fuel proceeds to a vortex chamber 1 via tangential apertures 2, and then via a nozzle 3 to the furnace chamber. A tube 4 runs from the vortex chamber, through which part of the fuel can be returned again to the tank. The amount of returned fuel is regulated by a valve. In the opinion of the inventors of this spray nozzle, constancy of the amount of the spiral fuel flow at different flow rates should ensure constancy of the quality of atomization within broad limits of the load change. However, experience shows that the range of change of the fuel flow rate with an unchanged quality of atomization is comparatively narrow: it lies within limits of 50 to 100%. A shortcoming of this spray nozzle is also the fact that it requires an increased consumption of energy with low productivity. /122

The BPK spray nozzle (Kalachev spray nozzle). This spray nozzle has three standard sizes: four flow rates of up to 250, up to 1,000, and up to 3,000 kg/hr. The BPK spray nozzle uses the principle of conserving the

rotational velocity of the liquid in the vortex chamber. But instead of back flow, here provision is made for movement of a piston, which either decreases or increases the length of the vortex chamber with the change in the fuel flow rate (with its constant diameter).

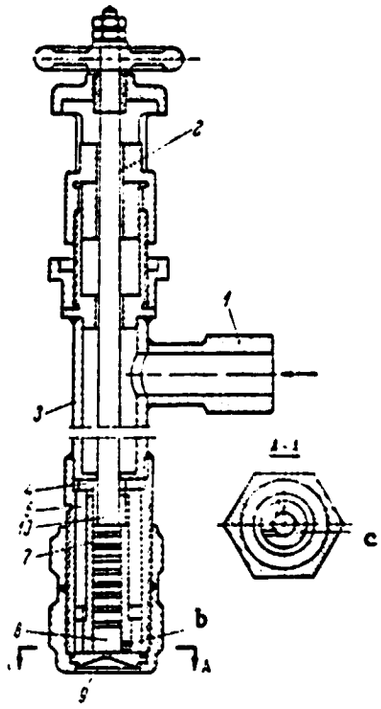

Fig. 6-6. Overall view of the BPK (Kalachev) spray nozzle.

/123

Figure 6-6 shows the overall view of the spray nozzle [6-11]. Pressurized fuel proceeds through connection 1 to the circular space between the spindle stem 2 and outside tube 3. Subsequently, the fuel runs through apertures 4 in the spray nozzle head to circular chamber 5, from which it runs via tangential apertures 6 in cylinder 7 into vortex chamber 8. The fuel acquires a vortical motion due to tangential apertures and is thence discharged to the outside via nozzle 9. Tangential aperture 6 in cylinder 7 are arranged in three rows height-wise, and depending on load, can be covered by piston 10 with its sealing rings. This piston is connected to spindle 2, and can carry out a reciprocating motion with the aid of the flywheel.

Thus, during the operation of the spray nozzle, the diameter of outlet nozzle 9 remains constant, while the cross-sectional area of the tangential apertures 6 in cylinder 7 changes depending on the fuel flow rate. The tangential channels are arranged along a threaded line for evenness of change in the passage cross-section. In some similar structures, tangential slots cut along the entire height of the chamber are employed instead of apertures. This ensures an approximately constant rate of rotation of the fluid during its different flow rates.

Thanks to such spray nozzle design, the spray nozzle satisfactorily functions in ranges of the fuel flow rate change of from 25 to 100% and is easily subject to automatic regulation. Pressure in the spray nozzle should be about 20 atm and, in any case, should not be below 15 atm. The spray nozzle requires using a fine filter. Some of its parts (the sprayer nozzle,

the cylinder with tangential channels, the regulating piston with gaskets) should be worked with high precision.

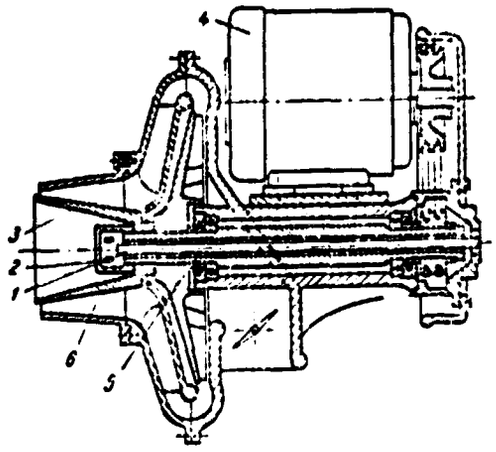

Fig. 6-7. Rotary spray nozzle.

/124

The results of testing the low capacity BPK spray nozzle with an outlet nozzle diameter of 2.5 mm are interesting. The fuel flow rate ranged from 50 to 230 kg/hr, while pressure, respectively, ranged from 16.4 to 19.5 atm. The nozzle length is 0.675 m with the minimum load and 1.86 m with the maximum load. The air excess ranged from 1.5 to 1.22. Combustion was stable and the fuel completely burned under all loads. With 15 atm pressure and a 7 mm outlet nozzle diameter, the spray nozzle ensures a fuel flow rate of 2,000 kg/hr. The angle of taper is 85 - 100°.

The rotary spray nozzle. In foreign practice [6-21], the rotary spray nozzle (Fig. 6-7) has become widely used. At low pressure (0.2 kg/cm^2), the liquid fuel is fed to hollow shaft 1, rotating at a velocity of (6-7)·10^3 rpm. Thence, the fuel proceeds via distributor 2 into glass tube 3, which widens on the furnace chamber side. The fuel is discharged into the furnace chamber in the atomized form from the sharp edge of the glass tube, which rotates together with the shaft. An electric motor 4, or an air turbine serves as the drive; in the case of the turbine, air is supplied from a compressor with a pressure head of about 5,000 mm on the water column. Air blown by fan 5, which is built into the spray nozzle or separately installed, carries out slight additional atomization of the large drops which are carried by centrifugal force to the periphery. The primary air is fed via circular aperture 6 at the edge of the glass.

/125

The spray nozzle is easily regulated within extremely broad limits (8 - 100%) without a deterioration in the quality of combustion. The maximum fuel flow rate is 3,000 kg/hr. The secondary air enters the furnace chamber separately.

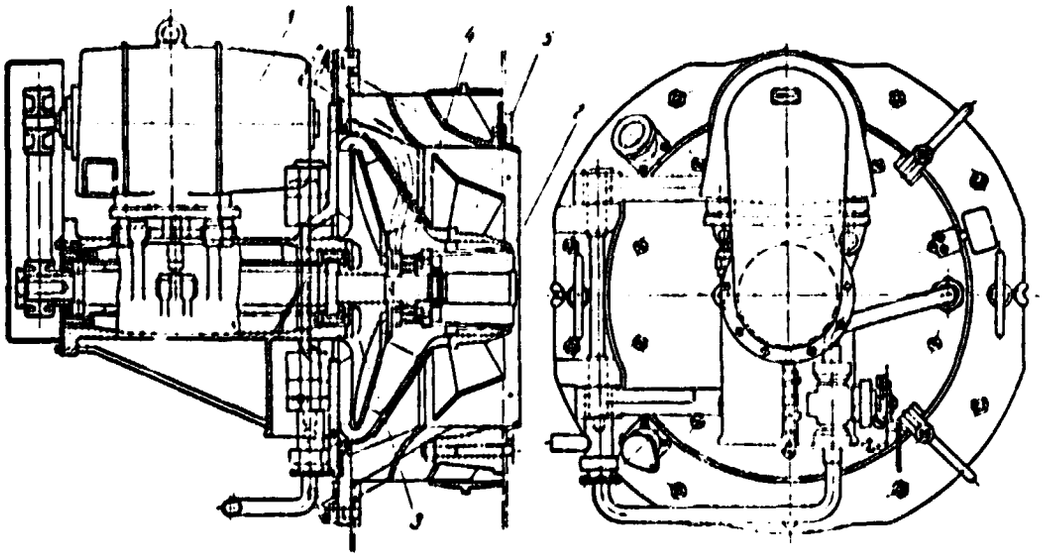

Fig. 6-8. Rotary spray nozzle with supply of secondary air via burner.

Figure 6-8 shows a rotary spray nozzle in which not only the primary air but also the secondary air is fed via a combustion device in organized fashion. Electric motor 1 serves as the drive. The liquid fuel is fed via rotating glass tube 2, at whose outlet the atomized fuel encounters the primary air supplied by the built-in fan via aperture 4. All air necessary for combustion (secondary) proceeds via circular aperture 5 in the spray nozzle head. Resistance of secondary air in this case comprises 40 mm on the water column, while that of primary air is 300 mm water column, and the pressure of the liquid fuel is recommended to be 0.5 kg/cm^2. The capacity of this spray nozzle, like that described above, reaches 3,000 kg/hr.

Both of the rotary spray nozzles shown in Figs. 6-7 and 6-8 are distinguished by a high degree of dispersion and produce a short fuel spray.

The participation of air in fragmentation of part of the drops gives basis to classify the rotary spray nozzles among the air-mechanical types as well.

A mechanical spray nozzle installed in the "Metro-Vikkers" energy trains. A mechanical spray nozzle with a capacity ranging from 170 to 600 kg/hr

(Fig. 6-9) is installed on the "Metro-Vikkers" energy trains. The basic part of the spray nozzle is the end piece, which consists of the atomizing washer 1, the turbulizing sprayer 2, and the coupling nut 3. Fuel proceeds along the internal channel 4 to housing 5, to the vortical sprayer, proceeds through the apertures 6 drilled into the vortical sprayer housing, to chamber 7, and via nozzle 8 to the spray washer 1 is discharged into the furnace chamber.

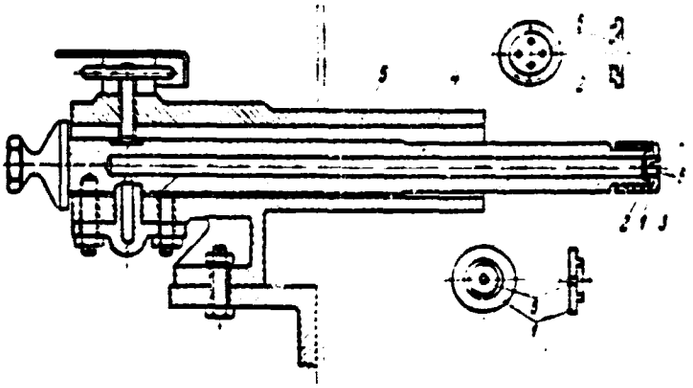

Fig. 6-9. Mechanical spray nozzle installed aboard "Metro-Vikkers" trains.

The capacity of the spray nozzle is determined by the number of coiled, vortical apertures (2, 3 or 4) and by their diameter. Although the spray nozzle can operate at pressures ranging from 7 to 12 atm according to the manufacture data, good atomization is only ensured at pressures of from 10 to 12 atm.

The capacity of the individual spray nozzle of any particular size is regulated by the change in fuel pressure but within extremely limited limits. The corresponding data for spray nozzles which have four apertues in the turbulence nozzle are given in Table 6-2. /127

One can slightly increase regulation by increasing pressure still more. It is not recommended to reduce pressure below 10 atm, as was already stated, inasmuch as this sharply worsens the quality of atomization.

The regulatable TsKTI spray nozzle. Having set the goal of constructing a spray nozzle with the maximum possible change in the angle of taper of the atomized jet, the inventors of the spray nozzle employed the principle of regulating the width of the channel which serves for the tangential supply of fuel. The regulatable spray nozzle [6-4] created by the inventors on the basis of this principle is shown in Fig. 6-10. The liquid fuel proceeds to the vortex chamber 1 via window 2, which is square and whose side is equalled to the diameter of the supply channel 3. This channel is closed by a piston 4,

TABLE 6-2

FLOW RATE OF FUEL OF THE MECHANICAL SPRAY NOZZLE INSTALLED ON "METRO-VIKKERS" ENERGY TRAINS, kg/hr.

Diameter of turbulizing apertures, mm	Pressure, atm		Diameter of turbulizing apertures, mm	Pressure, atm	
	10.5	12.3		10.5	12.3
1.98	206	224	2.57	387	422
2.17	254	274	2.78	494	530
2.37	326	350	3.00	550	590

which is brought into reciprocal motion by a flywheel 5. By rotating the flywheel, one can either totally close the supply channel or partially or fully open it. The flow of liquid is removed from the vortical chamber 1 via nozzle 6. The angle of taper in this spray nozzle can range from 3 to 100°. Experiments were performed at pressures ranging from 2 to 15 atm and with a diameter of the outlet nozzle 2; 3.5 and 5 mm.

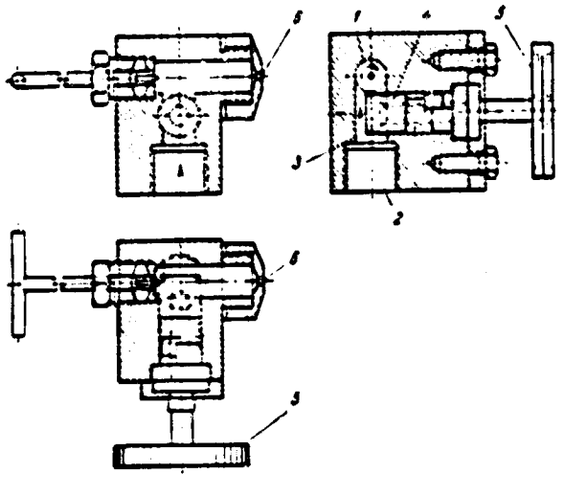

/128

Fig. 6-10. The TsKTI regulatable spray nozzle.

Depending on the degree of opening of the supply channel with diameter of the outlet nozzle of 3.5 mm and a pressure of 2.5 atm, the change in the angle of taper is shown in Fig. 6-11.

The spray nozzle has been tested at capacity of up to 700 kg/hr. Although it was in fact designed for technological needs, it can also be used for burning fuel under conditions when a frequently changing atomization angle is necessary. However, one should bear in mind that the decrease in the angle of taper achieved by reducing the flow twist leads to deterioration of atomization quality.

The spray nozzle has been tested at capacity of up to 700 kg/hr. Although it was in fact designed for technological needs, it can also be used for burning fuel under condition when a frequently changing atomization angle is necessary. However, one should bear in mind that the decrease in the angle of taper achieved by reducing the flow twist leads to deterioration of atomization quality.

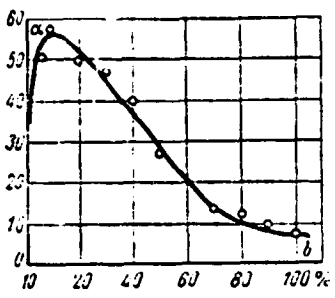

Fig. 6-11. Relationship between the angle of taper a of the atomized stream and the degree of opening b of the guide channel, %.

/129

With pressure on the order of 10 atm and an angle of taper of 150°, the average diameter of a drop comprises about 300 μ. In this case, the atomized jet in the cold state strikes approximately 10 m.

Spray nozzles for gas turbine combustion chambers. The specifics of burning fuel in gas turbine combustion chambers consists of the fact that high pressures of both volume and cross-section are created in them. These pressures exceed those achievable in steam boiler furnaces by tens of times. In connection with this, the dimensions of combustion chambers are extremely limited, both with respect to diameter and length. In the meantime, one cannot permit mechanical under-combustion in the gas turbine combustion chambers, for even a small amount of unburned liquid fuel which has struck the chamber sides leads to the formation of coke. Bits of this coke, having separated from the sides and fallen into the flow part, can cause damage and can even totally destroy the gas turbine vanes. In order to avoid this, special measures are taken which ensure the complete combustion of fuel within the chamber itself. Specifically, very fine atomization of the liquid fuel is achieved. This ensures its rapid evaporation and accelerates the occurrence of the remaining stages to the point of total combustion.

Predominantly mechanical spray nozzles of the centrifugal type are used for liquid fuel atomization and gas turbine installations. As a rule, the fuel pressure in these greatly exceeds pressure in mechanical spray nozzles of steam boiler furnaces. Quite good atomization of fuel is ensured with a short fuel

spray length. In certain combustion chambers, even air spray nozzles are installed. Combined, so-called air mechanical spray nozzles, have also begun to be used recently.

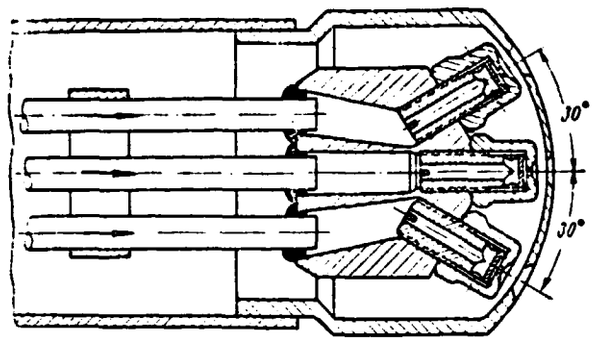

Fig. 6-12. NZL design group sprayer.

In discussing the means which ensure the reliable operation of combustion chambers, one should also mention regulation within very broad limits. Thus, for example, it is necessary to have the possibility of changing the load of single shaft aggregates from 40 to 100% and of double shaft aggregates from 10 to 100% without a noticeable deterioration in the quality of atomization. When changing pressure, it is difficult to ensure good quality of atomization within broad limits of the load change, inasmuch as in the given case it would be necessary to create a pressure head of several hundreds and even a thousand atm. Complicated devices have been created for expanding the range of load regulations, or group sprayers have been employed.

As an example, Fig. 6-12 shows the cross-section of a group sprayer consisting of five spray nozzles designed by the V. I. Lenin Nevskiy machine-building plant [6-12]. The flow rate of fuel of each of the spray nozzles, except for the operating spray nozzle, is regulated by throttling the pressure of fuel in the inlet fuel oil supply. When load decreases, the spray nozzles successively cut off, with the exception of the central spray nozzle. This latter spray nozzle is the operating one -- it maintains the dry run of the aggregate with a reduced number of rpm's and only shuts off when the assembly stops. During the operation of the group sprayer via the shut-off spray nozzles, either air or steam is run in, which protects them from clogging with sintered fuel and from extreme overheating due to the operation of the other spray nozzles. In this case, the pressure of the air or steam run through the non-working spray nozzle exceeds the pressure of the medium in the combustion chamber by 3-4 atm. /130

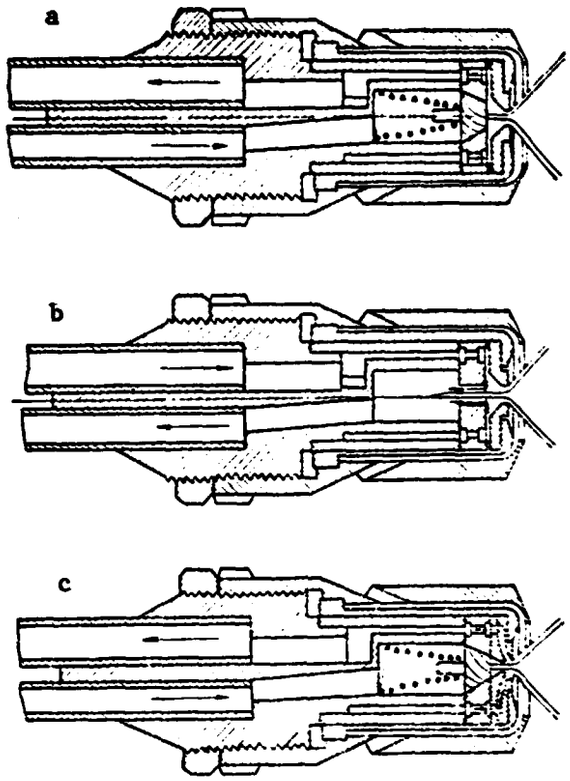

Fig. 6-13. Centrifugal spray nozzles with fuel backfeed:
a - supply of fuel from the periphery of the vortex chamber;
b - backfeed of fuel from the center of the vortex chamber;
c - backfeed of fuel from the spray nozzle.

In a design record, most spray nozzles for gas turbine combustion chambers principally differ little from spray nozzles designed for steam boiler furnaces. Thus, back fuel flow spray nozzles employed in gas turbine construction are similar to the spray nozzles of this type, described above. Figure 6-13 shows three versions of the centrifugal spray nozzle with back fuel flow [6-13]. The shortcomings of such spray nozzles were also mentioned above. One should also recall that the return of fuel oil to the tank can increase the temperature of fuel in the tank to an undesirable value, and can also hinder the operation of fuel pumps, particularly at low capacity of the spray nozzle, when the back flow sharply increases. /131

Spray nozzles with a variable area of opening of slots or apertures in the vertical combustion chamber, as was shown in Fig. 6-6, are also used, in

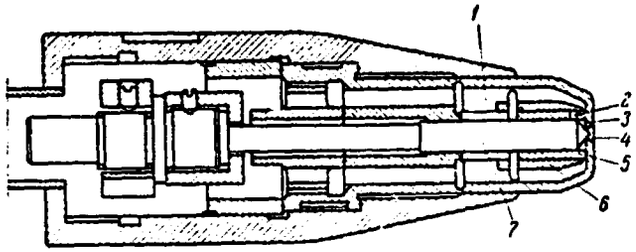

Fig. 6-14. Spray nozzle with internal regulation.

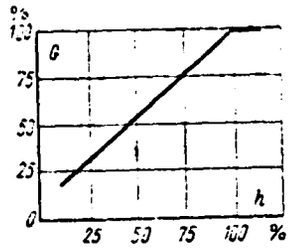

Fig. 6-15. Relationship between the fuel flow rate G and the riser height of slide valve h.

addition to the conventional centrifugal sprayers.

The internally regulated spray nozzle. A spray nozzle operating according to the already mentioned principle of changing the area of slots or apertures in the vortex chamber, but somewhat different in its design from the earlier described spray nozzle (Fig. 6-6), is shown in Fig. 6-14. In this spray nozzle, which is successfully used in combustion chambers of steam generators, the fuel /132 proceeds to a circular chamber 1 and thence via tangential apertures 2 to the vortex chamber 3. From the vortex chamber, the fuel proceeds via a nozzle 4 to the combustion chamber. The tangential apertures 2 are arranged on two helical lines apart 5. An opening in the apertures is made by slide valve 6 with the aid of rod 7.

Another characteristic of this spray nozzle is also the fact that the diameters of aperture 2 are different and are chosen such that when the slide valve moves, their total opening area increases approximately on a straight line. Such an arrangement and difference of diameters ensure a practically linear relationship between the flow rate of fuel and the value of movement of rod 7.

Figure 6-15 gives an approximate graph of the relationship between the flow rate of fuel and the riser height of the slide valve. It is evident from this graph, plotted on the basis of experimental data obtained at a constant pressure, that the flow rate of fuel changes quite linearly prior to complete opening of all tangential apertures, after which it becomes constant.

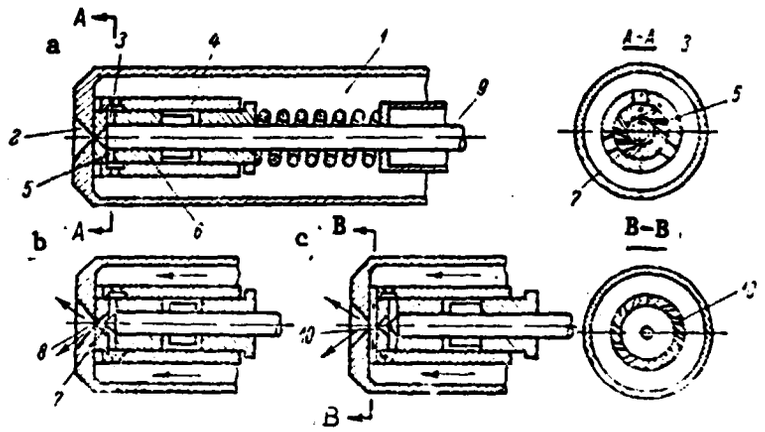

Fig. 6-16. TsKTI two-step spray nozzle.

Diagrams a, b and c correspond to equal positions of arrow 9.

Such a character of flow rate change facilitates regulation.

The diameter of the outlet nozzle aperture is 3.5 mm in a spray nozzle of the described design with the capacity of 1,000 kg/hr. The number of tangential apertures is 10 (5 per row) and their diameter ranges from 0.85 to 1.9 mm. The path of the slide valve with rod is 11 mm. Fuel pressure is approximately 25 atm. The angle of taper of the atomized jet decreases somewhat with the rise of the rod with the slide valve and, consequently, with the increase in capacity (with the constant pressure). /133

If the principle of conserving a constant flow rate of the liquid fuel in the vortex chamber by means of changing the area of opening of its inlet aperture is the basis of operation of this kind of spray nozzle, then in other spray nozzles the possibility of an additional step-wise change of the outlet aperture diameter is also provided. This is achieved in the so-called two-step spray nozzles.

The TsKTI two-step spray nozzle. In this spray nozzle (Fig. 6-16,a) [6-7], fuel from a volume 1 is supplied to a nozzle 2 by two pathways. At low fuel rates, fuel proceeds via apertures 3 into glass 4 and channels 5 to glass 6, and proceeds in glass 6 and via nozzle 2 is discharged into the combustion chamber. Fuel flow rate regulation is accomplished by needle 9.

At the first stage, with low fuel flow rates, the movement of the needle leads to an increase in the area of apertures of the tangential slots (Fig. 6-16,b). Then, when the needle reaches a certain position, its movement entails the movement of glass 6, as the result of which an additional amount of fuel proceeds via tangential channels 10 to nozzle 2 (Fig. 6-16,c). Further movement of the needle upward produces a gradual increase in the area of opening of the tangential channel 10 up to ensuring the maximum fuel flow rate. Channels 5 and 10 are arranged in checkerboard order in order to ensure a uniform regulation of fuel flow rate. Good quality of atomization by this spray nozzle is ensured when varying the fuel flow rate from 300 to 2,000 kg/hr. The operating run of the needle with action of the first stage is 3 mm and its total run is 9 mm long.

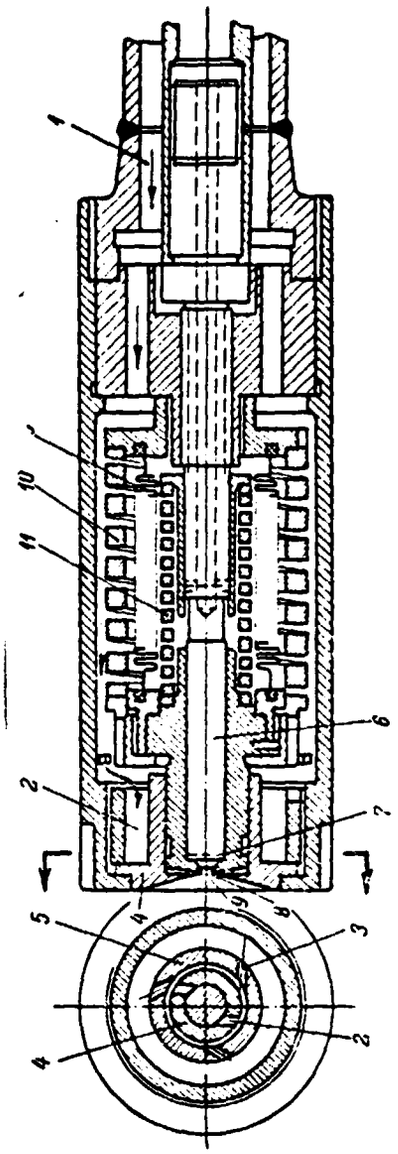

Fig. 6-17. Double atomization spray nozzle.

/134

The double atomization spray nozzle of the "Veloks" boiler combustion chamber. Fuel is supplied in this spray nozzle (Fig. 6-17) from circular channel 1 to channels 2 and 3, arranged tangentially with respect to the spray nozzle axis. Channels 2 are arranged in sleeve 4, while channels 3 are arranged in component 5. Channels 2 and 3 have identical cross-sections. Around the circumference of sleeve 4 are two channels, while three channels lie around the circumference of component 5. When the successively rising shaft 6 opens, the first row of the tangential channels and the outlet aperture 7 open. Proportional to the increase in the fuel flow rate, rod 6 rises. At a certain height of this rod, inset 4 rises and channels 3 and outlet nozzle 8 open. Membrane 9, spring 10 and 11 are associated with the regulation devices.

/135

TABLE 6-3

CAPACITY OF THE TWO-STEP SPRAY NOZZLE AND THE ANGLE OF TAPER OF THE SPRAY NOZZLE AT DIFFERENT ROD ELEVATION HEIGHTS

Elevation or rod, mm	Fuel flow rate, kg/hr.	Angle of taper, degree	Elevation of rod, mm	Fuel flow rate, kg/hr	Angle of taper, degree
0.5	300	118	7.0	3120	—
1.0	570	112	8.0	3560	118
2.0	990	112	9.0	4220	—
3.0	1370	107	10.0	4790	—
4.0	1860	100	11.0	5240	—
4.4	2120	92	12.0	5820	138
5.0	2250	—	13.0	6420	—
6.0	2750	118	14.0	6520	89

The spray nozzle operates at a pressure of 32 atm. The design ensures quite uniform regulation. The data of the firm which tested the spray nozzle at a pressure of 25 atm are given in Table 6-3.

The examined spray nozzles for gas turbine installations require particularly careful cleaning of the liquid fuel from suspended particles. The two-step spray nozzles, in all probability, will be used in furnaces of super powerful boilers.

Spray nozzles for industrial furnaces. In certain aggregates, for example, in rotating cement furnaces , flexible regulation of length of the fuel jet within wide limits is required. With the steady regime, one needs a fuel jet of long extent and with a small angle of taper. Naturally, in this case, the drops of the atomized fuel should have a relatively large size and should be supplied to the burner at a comparatively high rate. The thermal conditions in the rotating furnaces whose length sometimes exceeds 150 m ensure sufficiently complete combustion of the large drops.

The spray nozzle developed by the "Bol'shevik" cement plant and meeting /136 these requirements is shown in Fig. 6-18. The fuel oil proceeds from tube 1 to the spray nozzle and is separated into two flows. One of these flows is supplied to the internal, circular channel 2 via helical atomizer slots to 4 where it encounters the second flow. The latter proceeds along channel 5 through slots located at an angle in sprayer 6, and after encountering the first

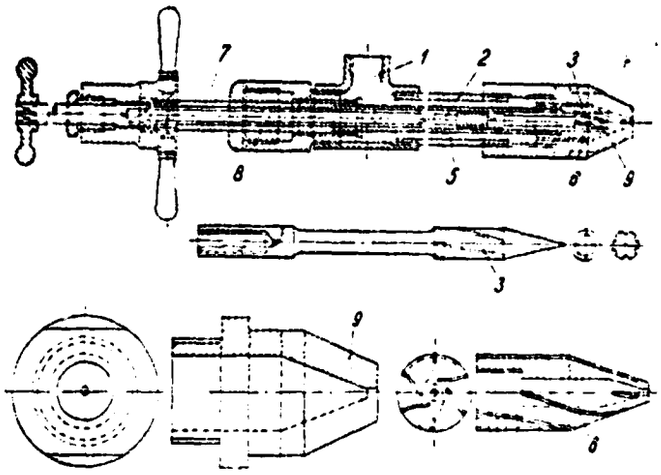

Fig. 6-18. Fuel oil spray nozzle for rotating furnaces of the "Bol'shevik" cement plant.

flow, is discharged into the furnace. Sprayers 3 and 6 are mounted on rods 7 and 8, and can be moved along the axis by their aid.

The angle of taper and the striking range of the jet are regulated by movement of the sprayers. Sprayers 3 and 6 are moveable components; they are made with a different angle of inclination of the vortex slots. The nozzle 9 is also variable. Its capacity depends upon the angle of the nozzle, and the angle of taper depends upon the length of the straight section of the nozzle.

According to Ye. I. Khodorov's data [6-18], when pressure is p = 5 atm and the diameter of the outlet nozzle is 3.5 mm, the angle of taper ranges approximately 25 to 60°, while the flow rate of fuel ranges approximately from 425 to 750 kg/hr.

Another type of spray nozzle employed in rotary furnaces was developed /137
by the "Giprotsement" Institute by A. S. Zakrytnyy) and is shown in Fig. 6-19. In this spray nozzle, fuel oil proceeds via tube 1 to channel 2, thence via turbulizing tangential slots 3 and nozzle 4, and is discharged into the furnace. The area of the slots is regulated by movement of piston 5. The angle of taper, which changes within limits of approximately from 15 to 60°, increases with the decrease in the height of the slot opening. The flow rate of fuel is about

720 kg/hr at a pressure of 5 atm and an outlet nozzle diameter of 3.5 mm.

The spray nozzle designed by "Giprotsement" Institute, shown in Fig. 6-20, has turbulizing channels 1, located on stem 2. Movement of the latter regulates the flow rate of fuel up to complete closure. The spray nozzle is designed for a fuel flow rate of 4500 kg/hr with a fuel oil pressure of 22-23 atm and a temperature of 80 - 100° C. The spray steam length reaches 35 m.

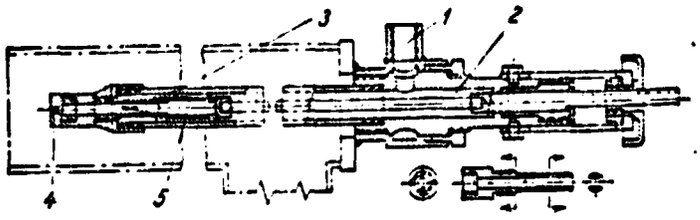

Fig. 6-19. Fuel oil spray nozzle 4 rotary furnaces (design of "Giprotsement" institute).

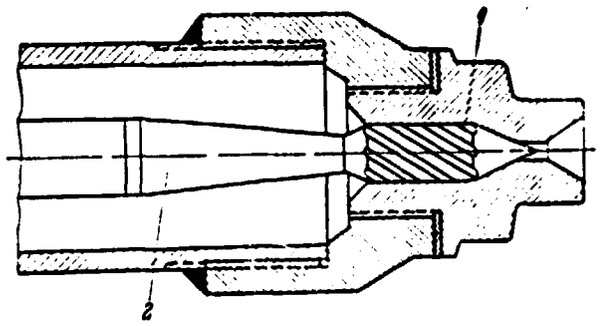

Fig. 6-20. Fuel oil spray nozzle with helical atomizer (sprayer) (design of "Giprotsement" institute. /138

6.2. Pneumatic (or steam) high pressure atomization spray nozzles

The centrifugal type pneumatic (or steam) spray nozzle. In this spray nozzle (Fig. 6-21, fuel proceeds via a valve 1 into internal tube 2, from which it proceeds through insertion 3 to turbulizing washer 4, where it encounters air. The latter proceeds via valve 5 to ring channel 6, then, through openings of insertion 3, proceeds to the turbulizing washer 4, and thence, together with the fuel, is discharged into the furnace chamber via nozzle 7.

This spray nozzle was investigated in detail under dry run conditions during water atomization [6-6]. It was mounted vertically on a special stand, facing downward, which created the axis of symmetry of the nozzle and made it easier to make tests. The flow rate of water ranged from 200 to 800 kg/hr; air pressure reached up to 5 atm, and the air flow rate ranged from 0.5 to 1.7 kg/kg. The spray nozzle demonstrated satisfactory operation throughout practic-

ally the entire range of the liquid flow rate. Section 5-1 gave data on calculating the average size of a drop for this spray nozzle.

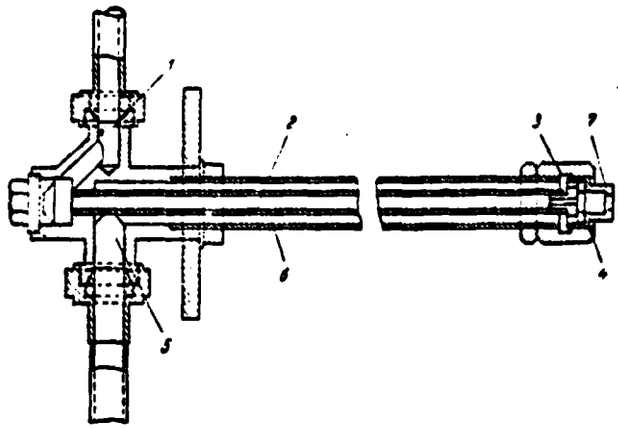

Fig. 6-21. Pneumatic (or steam) centrifugal type spray nozzle.

In order to determine the effect of the configuration of individual details which form a part of the liquid supply line, the following were tested: the conventional insertion, the insertion with skirting, suggested by Professor G. F. Knorre (Fig. 6-22,a), and the insertion with water jet turbulization (Fig. 6-22,b). The experiments showed that liquid turbulization does not have any effect in air high pressure spray nozzles. The fact of the matter is that in spray nozzles of this type, usually employed in boiler and furnace operation, the flow rate of the liquid is so small in comparison with the velocity of the air stream that it cannot have any significant effect on atomization quality. Together with this, the use of the turbulizing insertion forces one to increase the water line pressure head. The presence of the skirting also does not improve atomization, but then one notes a decrease in the required water pressure. This is because deflection of the jet with the presence of the skirting creates a certain ejection. /139

One of the most interesting characteristics of spray nozzles of the air (or steam) atomization type is G_B/G, i.e., the ratio of the flow rate of air (or steam) G_B, kg/hr, to the flow rate of the liquid G, kg/hr. The increase in this ratio improves the quality of atomization, which is indicated by the results of experiments shown in Fig. 6-23, where the diameters of drops d_i are plotted along the axis of the abscissa, while R_1 is plotted along the axis of the ordinate, i.e., the entire drop (in percentages) with a diameter greater than d_i. The improvement in atomization quality is not only expressed in a decrease in drop size, but also in greater drop homogeneity. The operationally suitable G_B/G ratio for the given spray nozzle is approximately 1. In the case of atomization by superheated steam, it is sufficient to have a G_B/G ratio of

0.4. A test of the spray nozzle under hot conditions showed that when the fuel flow rate was about 600 kg/hr, the fuel stream length was 3.5 - 4 m and the angle of taper was approximately 90°.

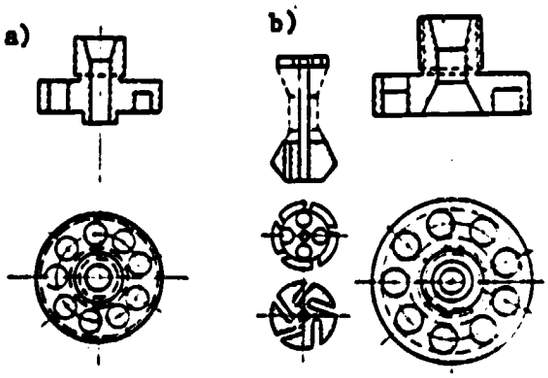

Fig. 6-22. Insertions to the spray nozzle, depicted in Fig. 6-21.

/140

Supplying steam under pressure of up to 20 atm as an atomizing agent significantly increases the capacity of the spray nozzle (up to 1250 kg/hr). One should bear in mind that the fuel oil pressure head should be about 3 atm in such a spray nozzle.

The fact that the quality of atomization of the liquid fuel by this spray nozzle noticeably improves (Fig. 6-24) when secondary air is supplied (the total air needed for combustion) via a damper with turbulizing vanes attracts attention. This is due to stream turbulization, in which the heavier drops are flung to the periphery under the effect of centrifugal forces, where they are subject to the additional effect of the secondary air, which destroys their inertial forces. The secondary air has still not lost its relative velocity. Such a phenomenon is characteristic for all centrifugal spray nozzles.

Running ahead slightly, we note that tests of the ejection type, non-centrifugal spray nozzle (Fig. 6-25) did not detect an effect of secondary air on atomization quality.

The pneumatic (or steam) ejection type spray nozzle. Figure 6-25 shows this spray nozzle. The fuel transits connection 1 into a circular chamber, from which it enters diffusor 3 through nozzle 2. The air (or steam) proceeds via connection 4 to internal tube 5, and from it through nozzle 2 and diffusor 3 is discharged into the furnace chamber. Dry run tests of the ejection spray nozzle [6-6] during the atomization of water with a flow rate change of from 200 to 800 kg/hr showed quite satisfactory dispersion with an air flow of from 0.5 kg/kg and higher. In this case, air pressure was 6 atm. The following

/141

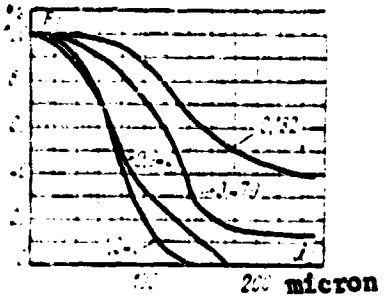

Fig. 6-23. Liquid distribution curves according to size with different G_B/G ratios. Figures on the curved lines -- G_B/G.

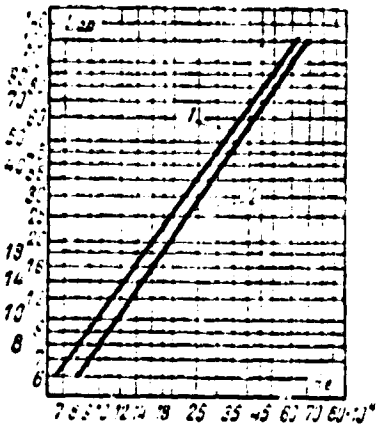

Fig. 6-24. Effect of secondary air on atomization of the centrifugal spray nozzle.

1 - atomization solely by primary air; 2 - atomization with the participation of secondary air.

rates are recommended for spray nozzles of this type: 0.8 kg/kg for air, 0.3 kg/kg for superheated steam.

As measurements showed, air pressure upon the contact of the air with the fuel, i.e., at the point of atomization, was about 1 atm. Thanks to the ejection capability, such a spray nozzle requires a low pressure head along the fuel line: pressures of 0.5 kg/cm^2 are sufficient in order to ensure the necessary fuel flow rate. Ejection spray nozzles are recommended for a capacity of from 275 to 1800 kg/hr. The fuel flow rate depends on the dimensions of the nozzle and the diffusor and on pressure of the atomizing agent. A pressure of from 8 atm (for the lowest flow rates) to 25 atm (for the highest flow rates) is recommended for superheated steam with the given nozzle and diffusor. /142

The spray nozzle depicted in Fig. 6-25 gives a comparatively long fuel spray. A special nozzle is employed to shorten it (Fig. 6-26).

The Danilin spray nozzle. In the Danilin spray nozzle (Fig. 6-27), steam is supplied to a central tube 2, via a connecting sleeve 1, and emerges via nozzle 3 at a high velocity, creating a rarefaction in circular channel 4. Fuel oil proceeds along channel 4 and is atomized upon encountering the steam

in volume 5. The uptake of air into the spray nozzle from the surrounding atmosphere takes place via aperture 6. The described spray nozzle has a high ejection capacity, thanks to which the liquid fuel need not be supplied under pressure. Practically speaking, in order to ensure reliable operation, it is sufficient to have a 2-3 m head in the fuel tank. The spray nozzle requires comparatively low pressure steam, which is evident from the data of Table 6-4 [6-10].

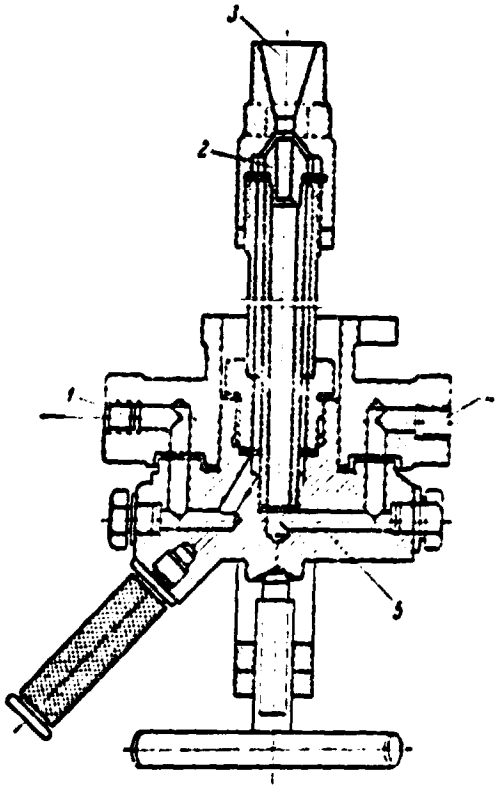

Fig. 6-25. Pneumatic (or steam) ejection type spray nozzle.

It is also evident from the table that the flow rate of steam for atomization is 0.48 - 0.41 kg/kg with a 50 kg/hr capacity, and 0.3 - 0.25 kg/kg with a 150 kg/hr capacity. The fuel spray length changes from 2.5 m at low flow rates (80 kg/hr) to 4.4 m at higher loads. The angle of taper at the spray nozzle mouth is approximately 75°.

Danilin spray nozzles usually operate with a flow rate of up to 200 kg/hr in stationary practice. These spray nozzles have become widespread in railway transport, where they are successfully used with a capacity of up to 700 kg/hr. According to Tsygankov's data [6-19], 0.15 - 0.30 kg/kg of steam under pressure ranging from 3 to 10 atm is expended on atomization.

A positive aspect of the Danilin spray nozzle is the fact that it is less noisy than other steam (air) atomization spray nozzles during operation. One should only recall that aperture 6, which joins channel 4 with the atmosphere, should always be open, inasmuch as the spray nozzle will begin to pulse strongly otherwise. In connection with this, aperture 6 should be oriented so as to prevent leakage of liquid fuel. With the aid of the valves installed in the tubes

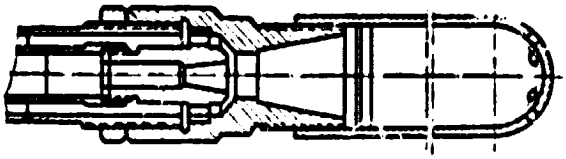

Fig. 6-26. Head of the ejection spray nozzle with nozzle.

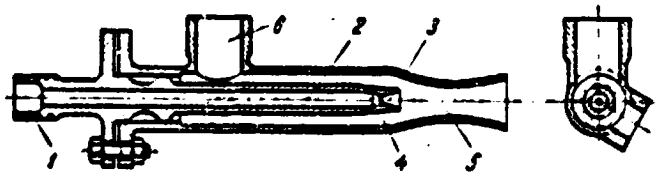

Fig. 6-27. Danilin spray nozzle.

which guide the fuel and steam to the Danilin spray nozzle, one can regulate the nominal load within limits of from 50 to 100%. One cannot fail to note the simple nature of the spray nozzle, as compared to other ejection sprayers, relative to the fuel quality. The very rare clogging of the spray nozzles is due to the extensive inter-tube cross-section for the fuel passage.

The Shukhov spray nozzle. The simplicity and operating reliability of this high pressure spray nozzle (Fig. 6-28) have ensured its extensive use in energy and at industrial enterprises already for several decades.

Fuel proceeds via tube 1 into internal tube 2 to outlet nozzle 3. Steam (or air) proceeds via connecting sleeve 4 to the space between the internal 2 and the outside 5 tubes, and via circular aperture 6 proceeds to the nozzle 3 where, meeting the fuel, it atomizes it; thence the aerosol mixture is carried into the furnace chamber. The cross-section of tube 2 remains constant and the entry of fuel is regulated by a valve on the flow line. The dimensions of circular aperture 6 altered with the aid of a flywheel, which ensures movement of tube 2. Both the flow rate and the velocity of the atomizing agent are changed by increasing or decreasing the height of the aperture. One can use a valve from the main which conducts the steam (or air) to the spray nozzle for these same purposes. However, the latter regulation method is less desirable, inasmuch as a change in the pressure of the atomizing agent occurs in the process. The spray nozzle is manufactured in ten sizes for capacities ranging from 3 to 400 kg/hr (Table 6-5. /144

It is evident from the table that an increase in the flow rate and pressure of the atomizing agent creates an ever-increasing pressure head along the

TABLE 6-4

CHARACTERISTICS OF THE DANILIN SPRAY NOZZLE

Indicator	Capacity, kg/hr.				
	50	75	100	125	150
Steam pressure before spray nozzle (p,atm) when air excess $\alpha = 1.1$.	4.2	5.7	7.7	10.0	12.7
Steam atomization flow rate (kg/kg):					
when $\alpha = 1.1$	0.48	0.40	0.35	0.32	0.30
when $\alpha = 1.3$	0.41	0.34	0.30	0.27	0.25

liquid fuel main; the corresponding increase in pressure in the fuel oil line is due to the necessity of ensuring the required fuel flow rate.

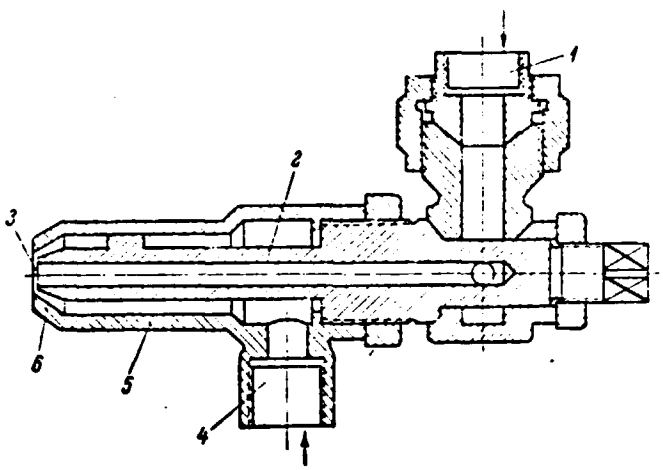

Fig. 6-28. Shukhov spray nozzle.

The F. E. Dzerzhodnskiy All-Union Thermotechnical Institute carried out detailed investigation of the Shukhov spray nozzle. Experiments established [6-10] that the aperture height should be at least 1 mm to avoid clogging. A large aperture dimension is also not recommended, inasmuch as the flow rate of steam increases in this case and atomization quality does not improve. The authors [6-16] judged the quality of atomization according to transparency of the fuel spray (the observations were made through goggles), and according to analysis of gases (completeness of fuel combustion was established). A steam flow rate in the amount of 0.3 - 0.4 kg/kg and an air flow rate in the amount of 0.5 - 0.8 nm^3/kg are recommended. In order to prevent skewing and not to permit deterioration of atomization, it is not recommended that one change aperture height during operation. The spray nozzle gives a long and narrow fuel spray. The length of the fuel spray is 2.5 - 4 m for small spray nozzles and 6 - 7 m for large spray

TABLE 6-5

CHARACTERISTICS OF THE SHUKHOV SPRAY NOZZLE

Nozzle number	Aperture diameter, mm		Capacity, kg/hr.		
	For fuel oil	For steam (or air)	With fuel oil pressure head of up to 0.5m water column	For fuel oil pressure head of 6-10 m on water column and steam pressure (or air pressure) of 3-5 atm.	For fuel oil pressure head 20 - 25 mm on water column and steam pressure (or air pressure greater than 5 atm
1	2	4.5	3	7	10
2	3	5.5	6	20	30
3	4	7	12	40	60
4	5	8	19	60	90
5	6	9	27	80	120
6	7	10	38	100	150
7	8	11	50	130	180
8	10	13	70	180	240
9	13	16	125	250	320
10	16	20	200	350	400

nozzles. Consequently, the spray nozzle is not suitable for furnace chambers with poorly developed height. According to VTI data, increasing fuel viscosity from 2 to 23° E does not alter the operating character of the spray nozzle. Tests of the Shukhov 9 spray nozzle showed that the angle of taper of the jet was about 75°.

The Best system spray nozzle. Industrial fuel combustion practice knows a whole series of so-called flat (or slot) spray nozzles (Bersenev, Kaufman, etc.). These produce a broad and short fuel spray and are simple and convenient in use.

The Best system spray nozzle is the most prevalent of these (Fig. 6-29). /146
The spray nozzle chamber is divided into two cavities -- the upper 1 and the lower 2. Fuel oil is fed along the lower cavity via aperture 3 to flat vane 4, from which it is blown by steam supplied from a chamber 1 via upper aperture 5. The height of the steam aperture 5 is 1 - 1.5 mm and does not change during operation. The dimensions of aperture 3 for the liquid fuel can be changed with the aid of a special device. The Best spray nozzle, like other flat spray

nozzles, requires very careful horizontal installation. With even a slight inclination, fuel will run from one side of the aperture, which leads to a sharp deterioration in atomization and, consequently, in combustion.

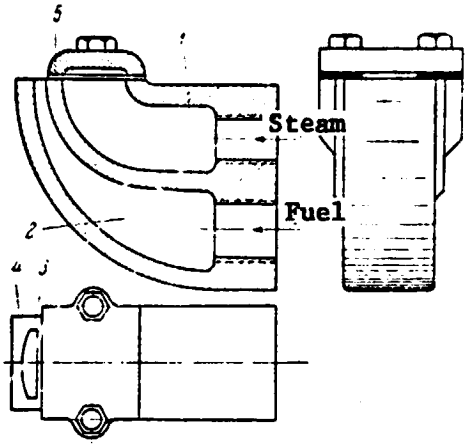

Fig. 6-29. Best spray nozzle.

Best system spray nozzles cannot operate at very low flow rates (less than 100 kg/hr); they are usually used for a capacity of 200 - 250 kg/hr (with respect to fuel). They also successfully operate at flow rates of up to 400 kg/hr. There are also reports of their satisfactory operation at still higher flow rates -- from 800 to 1,000 kg/hr.

Best system spray nozzles have many advantages. We have already mentioned the simplicity of design; we shall also recall that the Best system spray nozzle practically does not clog and, when necessary, is easily cleaned. To the same point, it requires a low steam (or air) flow rate for atomization. According to the data of tests performed by VTI [6-10], with a fuel flow rate of 200 kg/hr and steam pressure of 4.3 atm, the flow rate of steam for atomization was 0.27 - 0.24 kg/kg; combustion was totally satisfactory. It is interesting to note /147 that the excess of air a ranged from 1.1 to 1.3, while the tension of the furnace chamber volume reached 860.10^3 kcal/m^3.hr.

The positive properties of the Best spray nozzle should also include the fact that it does not practically require a fuel main pressure head. The steam jet creates a suction which draws the liquid fuel. It is sufficient to have a pressure head of 2 - 3 m on the water column in order to ensure the interrupted operation of the spray nozzle. The flat jet emerging from the spray nozzle soon also flows out and at a certain distance becomes circular. The angle of the fuel spray at the nozzle outlet comprises about 100°. The fuel spray created by these nozzles is 1.5 - 3 m long. The capacity of the spray nozzle is regulated by valves on the supply mains (fuel and steam). It is recommended that the capacity of the Best spray nozzle be changed within limits of no more than 50%. One should bear in mind that operation of the spray nozzle at the highest

flow rates gives the best results.

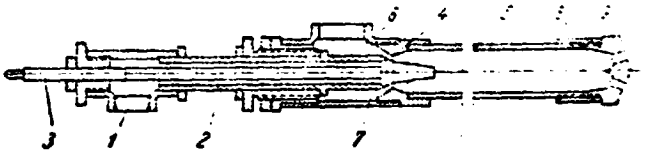

Fig. 6-30. Kaplan and Makarov multijet spray nozzle.

The Kaplan and Makarov spray nozzle. The design of the Kaplan and Makarov [6-3] multijet spray nozzle shown in Fig. 6-30 is of interest. Here the liquid fuel proceeds via a tube 1 to a ring-shaped space formed by tube 2 and rod 3, and thence proceeds via nozzle aperture 4 to a volume 5. Air also proceeds to volume 5 via connecting sleeve 6 and ring-shaped channel 7, where it atomizes the liquid fuel. Volume 5 is bounded by a valve 8 with apertures 9 on the end. The mixture of air and atomized fuel is discharged into the combustion chamber through these apertures.

Such a spray nozzle was tested during warming of heating wells at a metallurgical plant. The results of the test showed that the maximum fuel oil flow rate was 500 kg/hr. In this case, the excess air was 1.0 - 1.05, and from 0.7 - 0.8 kg of air was expended per 1 kg of fuel oil. The fuel oil spray was 2 - 2.5 meters long.

A longer fuel spray is frequently needed under industrial conditions. /148 Specifically, at certain stages of smelting in open-hearth furnaces, a long, flat fuel spray is necessary which seemingly lies on the surface of the melted metal. Such a task is most successfully solved when the liquid fuel is atomized by air (or steam) high pressure spray nozzles. Sprayers of this type include the Dobrokhotov and Kazantsev, "Stal'proyekt" spray nozzles, and those of the "Serp i molot" plant, Berman, Kaplan and Makarov spray nozzles, and others.

The Dnepropetroyskiy metallurgical institute's spray nozzle (the Dobrokhotov and Kazantsev system). The DMI spray nozzle of the Dobrokhotov and Kazantsev system (Fig. 6-31) has become widely used in open-hearth furnaces. The liquid fuel in this spray nozzle is supplied along a central tube 1, while the steam (or air) is supplied along a ring-shaped channel 2, which changes into converging tube reducer 3, and terminates in expanding nozzle 4. The fuel oil conducting tube runs for a certain distance at the mouth of the nozzle and at this encounters

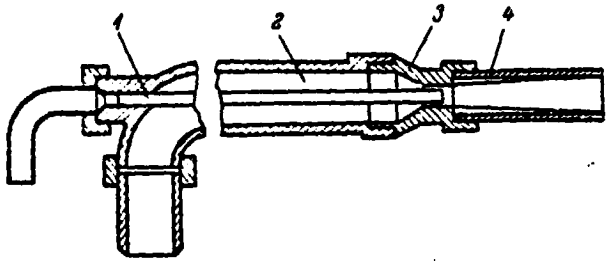

Fig. 6-31. Dnepropetrovskiy metallurgical institute spray nozzle (Dobrokhotov and Kazantsev system).

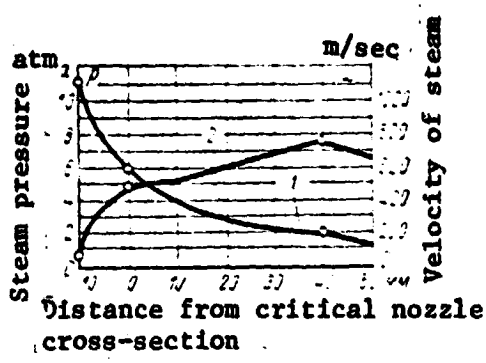

Fig. 6-32. Change of pressure (1) and velocity (2) of steam along the length of the expansion nozzle.

the atomizing medium. Thanks to the great length of the nozzle, the steam-liquid emulsion produces a powerful long-range stream at the outlet from the spray nozzle.

It is evident from Fig. 6-31 that a Laval nozzle has been used in the Dobrokhotov and Kazantsev spray nozzle as in the ejection spray nozzle as well. The spray nozzle works best of all with superheated steam at a pressure of about 11 atm. The use of saturated steam at a pressure below 10 atm greatly worsens the quality of atomization, which is due to strong cooling of the stream upon meeting the fuel with steam in the expansion nozzle. The use of low pressure compressed air as an atomizing agent in this spray nozzle rather than steam has also not produced good results up to now. Attempts of this kind have been made /149 in open-hearth furnaces, where, as a rule, air under pressure up to 6 atm exists. This proved to be insufficient for the good operation of this spray nozzle.

A. I. Karabin [6-5] gives a graph plotted by I. I. Kazantsev and which characterizes the change in the velocity and pressure of steam along the length of the expansion nozzle. It is evident from this graph (Fig. 6-32) that the pressure of superheated steam, which initially comprised 11 atm, falls to 2 atm at the point of encountering the fuel, and velocity increases to 750 m/sec. The fact that the spray nozzle has an ejection capability makes it possible to get by with lower pressure along the main fuel line.

Dobrokhotov and Kazantsev spray nozzles are employed for a capacity ranging from 250 to 2500 kg/hr. Certain data which characterize them are given in Table 6-6.

TABLE 6-6

CHARACTERISTICS OF DOBROKHOTOV AND KAZANTSEV SPRAY NOZZLE

Spray nozzle number	Capacity, kg/hr	Flow rate of atomizing agent, kg/hr		Spray nozzle number	Capacity, kg/hr.	Flow rate of atomizing agent, kg/hr.	
		Steam	Air			Steam	Air
1 & 2	250	125	188	13 & 14	1000	500	750
3 & 4	300	150	225	15 & 16	1250	625	938
5 & 6	400	200	300	17 & 18	1600	800	1200
7 & 8	500	250	375	19 & 20	2000	1000	1500
9 & 10	650	325	490	21 & 22	2500	1250	1875
11 & 12	800	400	600				

It is evident from the table that this spray nozzle uses about one and a half times more air than steam. Shortened Laval nozzles are used during compressed air operation.

The Dobrokhotov and Kazantsev spray nozzle is simple, design-wise, and is convenient in operation. However, it has a number of disadvantages, the chief of which are the following: /150

a) The spray nozzle does not produce a short fuel spray necessary at individual stages of smelting; this shortcoming is particularly perceptible for low and medium capacity furnaces.

b) Too great a nozzle length sometimes leads to the piping of part of the liquid fuel.

c) A decrease in the steam (or air) pressure leads to a shock wave; this disrupts the operating regime of the spray nozzle and hinders regulation.

The Shukhov spray nozzle for open-hearth furnaces. The modified Shukhov spray nozzle (Fig. 6-33) with lengthened end, which reduces the angle of taper and increases the length of the fuel spray, is frequently used for low capacity open-hearth furnaces. Such a spray nozzle works well at a capacity of up to

500 kg/hr; increasing the flow rate leads to a sharp deterioration of atomization. But sometimes these spray nozzles can also be seen in medium tonnage furnaces; in this case, two spray nozzles are installed. The Shukhov spray nozzle is very simple, design-wise, does not make high demands on the purity of the fuel oil, and operates satisfactorily at low pressure of the atomizing agent (3 - 4 atm). The fuel oil flow rate can be regulated within wide limits, but regulation of the fuel spray length is almost impossible, inasmuch as this operation can only be carried out by decreasing or increasing the flow rate of steam, which most frequently gives bad results. The steam (or air) slit should correspondingly be regulated in advance. It is not recommended that slit height be changed during operation. /151

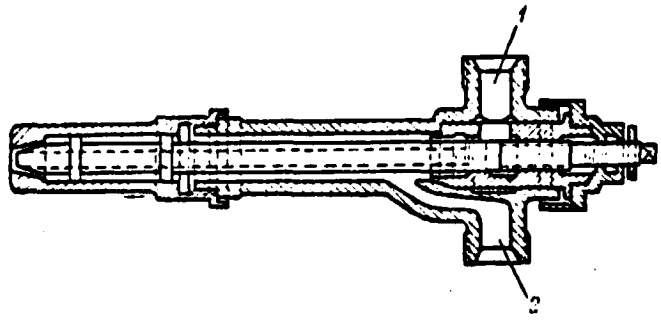

Fig. 6-33. Shukhov spray nozzle for open-hearth furnaces.
1 - fuel intake; 2 - steam intake.

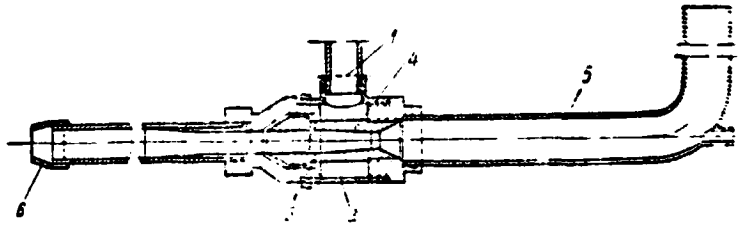

Fig. 6-34. UPI spray nozzle (Kokarev system).

The Kokarev system UPI high pressure spray nozzle. Liquid fuel is supplied along a ring-shaped channel 2 and thence via aperture 3 and nozzle 4 through connection sleeve 1 in this spray nozzle (Fig. 6-34). Air proceeds to nozzle 4 along tube 5. At the end of nozzle 4, the air meets the fuel and atomizes it. Via nozzle 6, the gas-liquid emulsion is discharged into the furnace. Regulation of the fuel and air flow rates takes place by fans installed in the fuel and air mains.

The conducted tests showed [6-8] that satisfactory operation of the Kokarev spray nozzle is ensured with sprayer (air) pressure of 3 - 5 atm. In this case, the flow rate of air comprised 0.5 kg/kg of fuel. A spray nozzle of this type provides a fuel flow rate of from 600 - 1300 to 1300 - 2500 kg/hr.

The Kokarev spray nozzle is simple in design and does not have moving parts. But the fine apertures for passing the fuel suggested by the inventor, and which are also the distinguishing feature of the spray nozzle, are subject to partial clogging. It is difficult to clean the clogged apertures during operation, which forces one to resort to stopping the spray nozzle and to disassemble it. One can only avoid this, having employed fuel oil which was extremely carefully purified in preparation.

According to Karaban [6-5], effective operation of the Kokarev spray nozzle requires steam under pressure of at least 8 - 10 atm and a temperature of 350 - 380° C, air under pressure of 6 - 7 atm and at a temperature of 250 - 300° C, and fuel oil under pressure of 4.2 - 5.5 atm.

As was already indicated, the length of the fuel spray is hard to regulate during operation in the spray nozzles examined above. Thus, during charging and smelting one needs a sharp fuel spray and the period of rimming itself needs a "soft" flame. Designs of the so-called two-step spray nozzles were created to solve this problem. /152

The Berman two-step steam (or air) spray nozzle. In the two-step Berman spray nozzle (Fig. 6-35), liquid fuel is supplied along a tube 1 and through a conical aperture 2 enters mizer 3. Primary air (or steam) proceeds into ring-shaped channel 5 via connection sleeve 4 where, in mixer 3, having encountered the fuel, atomizes it. The fuel and steam mixture (or fuel and air mixture) runs along tube 7 with an end piece 8. Secondary air is supplied along the circular section of tube 10 via connecting sleeve 9. At the outlet from tube 10, the secondary air accomplishes additional fuel atomization. All of the formed mixture is discharged into the furnace via defuser 11. The flow rate of liquid fuel is regulated with the aid of rod 12; the aperture for supplying primary air is regulated by moving nozzle 13; the decrease and increase in the flow rate of secondary air is achieved by changing the height of aperture 14. One can regulate the flow rate of fuel, primary and secondary air during operation. Table 6-7 gives data on the change of fuel flow rate depending on pressure [6-1].

TABLE 6-7

CHARACTERISTICS OF BERMAN SPRAY NOZZLE

Nozzle number	Capacity (kg/hr) with air pressure head before spray nozzle, atm:								
	4	4.5	5	5.5	6	6.5	7	7.5	8
1	136	153	170	187	204	221	238	255	272
2	215	242	269	296	323	350	377	404	430
3	392	441	490	539	588	637	686	735	784
4	632	711	790	869	948	1027	1107	1186	1265
5	1107	1245	1385	1522	1660	1800	1937	2078	2215
6	1457	1640	1820	2000	2190	2370	2550	2730	2920

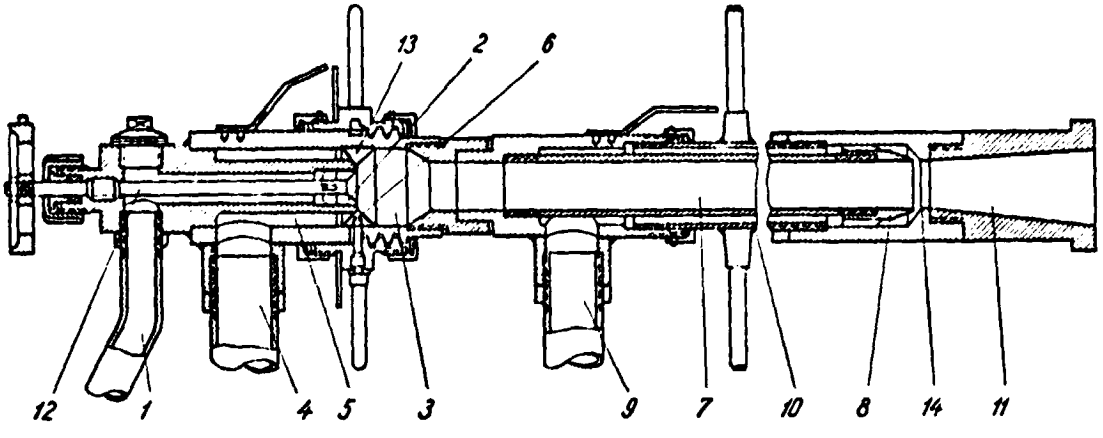

Fig. 6-35. Berman spray nozzle

It is desirable to keep liquid fuel pressure equal to air pressure, and in any case at least 75% of it. The main advantage of the two-step air supply is seen by the spray nozzle's inventor to be the fact that the primary atomizing agent imparts long range to the flame and makes it flat, while the secondary one in fact reduces the length of the fuel spray, makes it sharp and "cutting." By /154 regulating the intake of the secondary atomizing agent, one can alter the fuel spray length within wide limits. A spray nozzle of the examined design can also operate according to a combination system, according to which steam is supplied along the primary line and compressed air -- along the secondary one -- which is especially advantageous when burning highly viscous fuel oils.

Despite a number of advantages, the Berman spray nozzle has not become

widely used, which is primarily due to the complexity of its design.

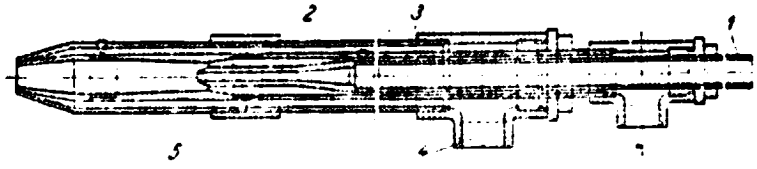

Fig. 6-36. "Stal'proyekt" and "Serp i molot" plant spray nozzle.

The "Stal'proyekt" and "Serp i molot" plant spray nozzle. The two-step atomization principle is also used in the "Stal'proyekt" and "Serp i molot" plant spray nozzle (Fig. 6-36). In this spray nozzle, liquid fuel is supplied along a tube 1, terminating in a constricted nozzle 2. Primary air runs along ring-shaped channel 3 and upon encountering the fuel carries out primary atomization. Additional droplet fragmentation is accomplished by the secondary air, supplied through connecting sleeve 4 and the circular section 5 to the mouth of the nozzle. Detailed data about the operation of this spray nozzle are not available. As A. I. Karabin [6-5] indicates, this spray nozzle, in which the length of the fuel spray is extensively regulated, is being used successfully in large open-hearth furnaces.

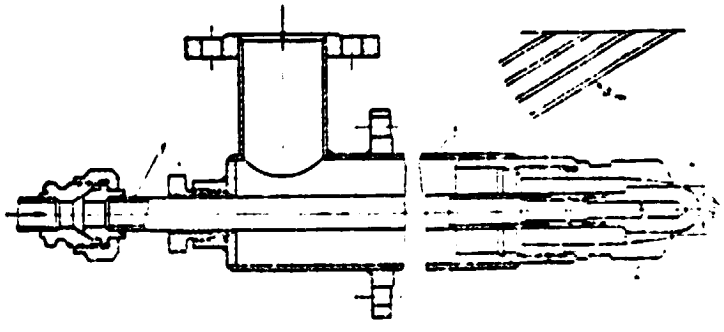

Fig. 6-37. Air atomization spray nozzle designed by NZL.

An air spray nozzle for the combustion chambers of gas turbine installations. The design of an air spray nozzle for the combustion chambers of gas turbine installations (Fig. 6-37) has been designed at the V. I. Lenin Neva machine-building plant. Here fuel proceeds along central tube 1 and via aperture 2 strikes tangential slots 3, arranged on the surface of the cone of sprayer 4. Air proceeds to slots 3 along tube 5, where it mixes with the fuel. The formed emulsion is discharged into the combustion chamber. The angle of taper can be changed within quite wide limits by means of installing sprayers with different angles of elevation α of the sprayer thread. /155

Section 6-3. Mixed air-mechanical spray nozzles

In addition to mechanical atomization spray nozzles (see Sec. 6-1), mixed air-mechanical atomization spray nozzles (Fig. 6-38) are also used in the combustion chambers of gas turbines. Here the fuel proceeds via tube 1 to circular section 2 and thence via tangential apertures 3 enters the vortex chamber 4, from which it is discharged into the combustion chamber via circular aperture 5. Air is supplied to volume 7 via tube 6, captures the escaping fuel and atomizes it. The spray nozzle is used in sectional combustion chambers; its capacity is about 400 kg/hr. Air is supplied to the spray nozzle by a specially mounted centrifugal compressor, which receives air from the main axial compressor of the gas turbine installation. The flow rate of air for atomization at nominal load is 4% of that theoretically needed for combustion. This spray nozzle is essentially an air-mechanical one, inasmuch as the pressure of liquid fuel is about 30 atm and fragmentation of the stream doubtlessly occurs to a significant extent as the result of mechanical atomization.

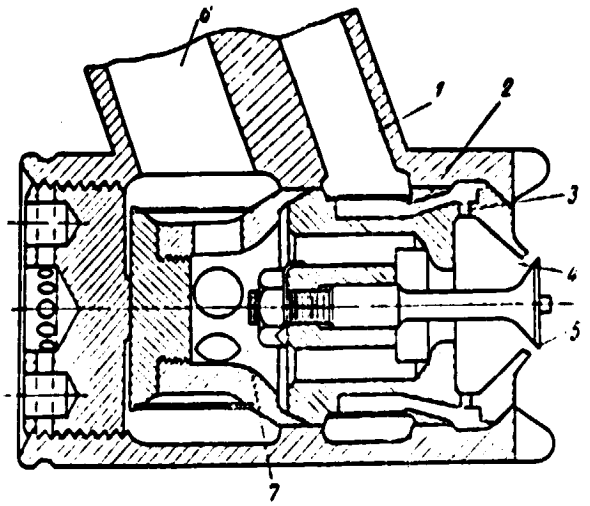

Fig. 6-38. Air-mechanical spray nozzle.

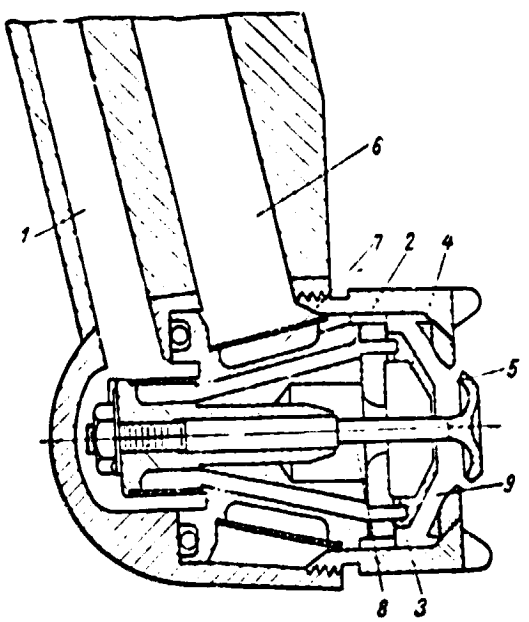

Fig. 6-39. Air-mechanical spray nozzle with double air atomization.

Figure 6-39 shows a spray nozzle of this same type. In this spray nozzle, the fuel proceeds from tube 1 along circular channel 2 and thence via aperture 3 into vortex chamber 4. Thence the fuel is discharged into the combustion

chamber via ring-shaped nozzle section 5. Air is supplied to tube 6 and thence to volume 7. Proceeding further, the air is divided into two streams. The first transits circular cross-section 8 to vortex chamber 4, at whose outlet primary fuel fragmentation occurs. The second stream is supplied along channel 9 to the mouth of nozzle 5, where it meets the gas-liquid emulsion and where the fuel is additionally atomized. A characteristic of this spray nozzle is the fact that two-step atomization of liquid fuel is ensured in it: from both the inside and outside of the fuel stream flowing from the nozzle.

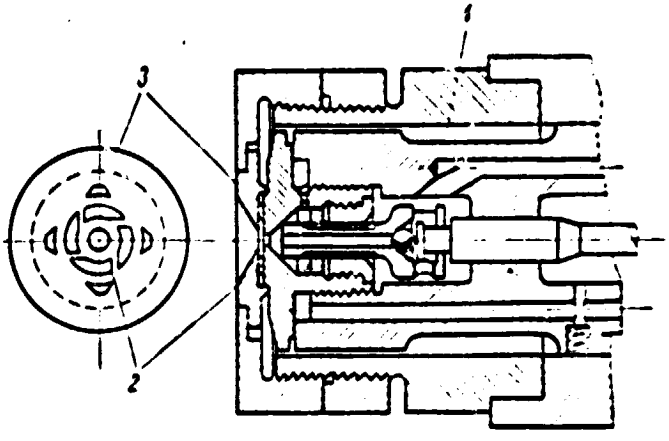

Fig. 6-40. Air-mechanical spray nozzle with encountering, turbulized streams of fuel and air.

/157

The spray nozzle shown in Fig. 6-40 is also among the air-mechanical sprayers. Its central part is a conventional type centrifugal spray nozzle. To it is added a component which ensures additional air atomization. Air proceeding to circular 1 passes through vortex channels 2 of inset 3. Along the outlet from the channels, the air meets the stream atomized by the mechanical part of the spray nozzle and additional fragmentation takes place. In this spray nozzle, the rotational direction of the air which passes through the tangential inset channels is opposite the rotational direction of the fuel stream. According to test data, the flow rate of the atomizing air comprises about 2% of that theoretically necessary for combustion. The pressure of the atomizing air exceeds pressure in the combustion chamber by about 0.5 atm. A spray nozzle of this type can be regulated within broad limits (with a change in the fuel flow rate of from 100 to 10%) without a noticeable deterioration in atomization quality. It also operates satisfactorily at still lower loads.

/158

Recently, air-mechanical and steam-mechanical spray nozzles have also come to be widely used in boiler operation. As A. A. Dmitriyev and K. F. Roddatis indicate (see "Kotel'nyye ustanovki FRG" (Boilers of the Federal Reupblic of Germany), Gosenergoizdat, 1961), the "Babcock" firm has developed a steam-

mechanical spray nozzle with a capacity of up to 3500 kg/hr.

Section 6-4. Low pressure, pneumatic spray nozzles.

As was already stated, low pressure spray nozzles are basically employed in furnaces. Their use is favored by two factors: first, the possibility of getting by with a low air pressure head for blowing and, second, reliability of operation at low flow rates, which not only cannot be ensured in any way by mechanical atomization spray nozzles, but cannot either by the air (or steam) high pressure spray nozzles. The fact of the matter is that the rate of discharge of the liquid fuel in mechanical spray nozzles and of air (or steam) in the high pressure spray nozzles should be great even with low capacity of these devices. Therefore, designers of such spray nozzles must achieve a decrease in the flow rate of fuel by reducing the cross-section of the outlet apertures of the nozzles. But with the usually consumed types of fuel oil, very small cross-sections of the nozzles completely and adjacently clog, as the result of which the operation of the spray nozzles becomes unstable.

In the low pressure spray nozzles themselves, the possibility of operating at low flow rates is ensured not only by decreasing the cross-section of outlet nozzle aperture, but also by reducing the velocity of the air stream. To the same point, either all air needed for combustion, or a significant part of it (from 40% and more), is used in these spray nozzles as the atomizing agent. It should be noted that low pressure air atomization spray nozzles are distinguished by a comparatively short fuel spray, which is extremely important when burning liquid fuel in industrial furnaces.

The STS-FOB ("Romo") spray nozzle. This spray nozzle (Fig. 6-41) consists of a housing 1 and a tube 2 centrally placed in it, through which the fuel runs. Air is supplied via tube 3 and circular aperture 4, formed by inset 5 and probe 6. Aperture cross-section is regulated by moving the cone of inset 5 with the aid /159 of wheel 7. The "Romo" spray nozzle is simple in design and is convenient in use, but has one disadvantage: during regulation of flow rate by wheel 7, the uniformity of circular section 4 is sometimes disrupted, which leads to air flow downwash.

Four sizes of the STS-FOB spray nozzle with capacities ranging from 2 to 55 kg/hr are used in industry.

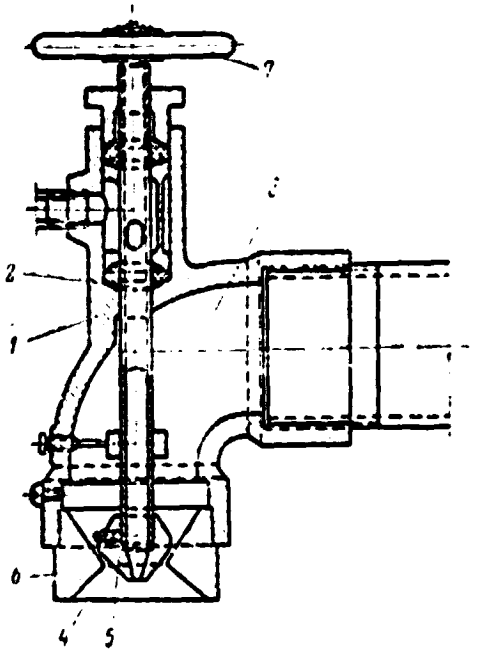

Fig. 6-41. STS-FOB spray nozzle.

According to M. M. Efros [6-20], the "Romo" spray nozzle operates well when the air pressure head for blowing is 200 mm on the water column at a minimum, and 700 mm on the water column with the maximum fuel flow rate. The lowest flow rate of fuel oil in the investigated spray nozzle was 4 kg/hr. while the highest was about 8 kg/hr. (according to the shipping specifications document -- about 9.5 kg/hr.). The flow rate of air on atomization at a pressure of 700 mm on the water column was about 47% of the air theoretically necessary for combustion.

When burning liquid fuel in furnaces, in order to increase the fuel flow rate without reducing the quality of combustion, sometimes one resorts to the so-called ejection of secondary air. This method is applied to spray nozzles where no more than 60% of the air needed for combustion is expended on atomization. In order to pass the rest of the air which participates in combustion, a special register is created which ensures the ejection of the atomized stream and significantly increases the limits of capacity of the spray nozzle. Thus, the investigated "Romo" spray nozzle can change its fuel flow rate from 7.2 to 17 kg/hr with ejection [6-20]. /160

Detailed dry-run tests of one of the "Romo" spray nozzle models were made on a special stand. The quality of atomization was investigated depending on a number of design and regime factors [6-2]. Water was employed as the atomized liquid. The detailed results which characterize the fineness of atomization and certain other parameters were given by the authors in Section 5-1.

Investigating the effect of the configuration of insets and probes on atomization quality is of interest. For this purpose, three insets and five probes

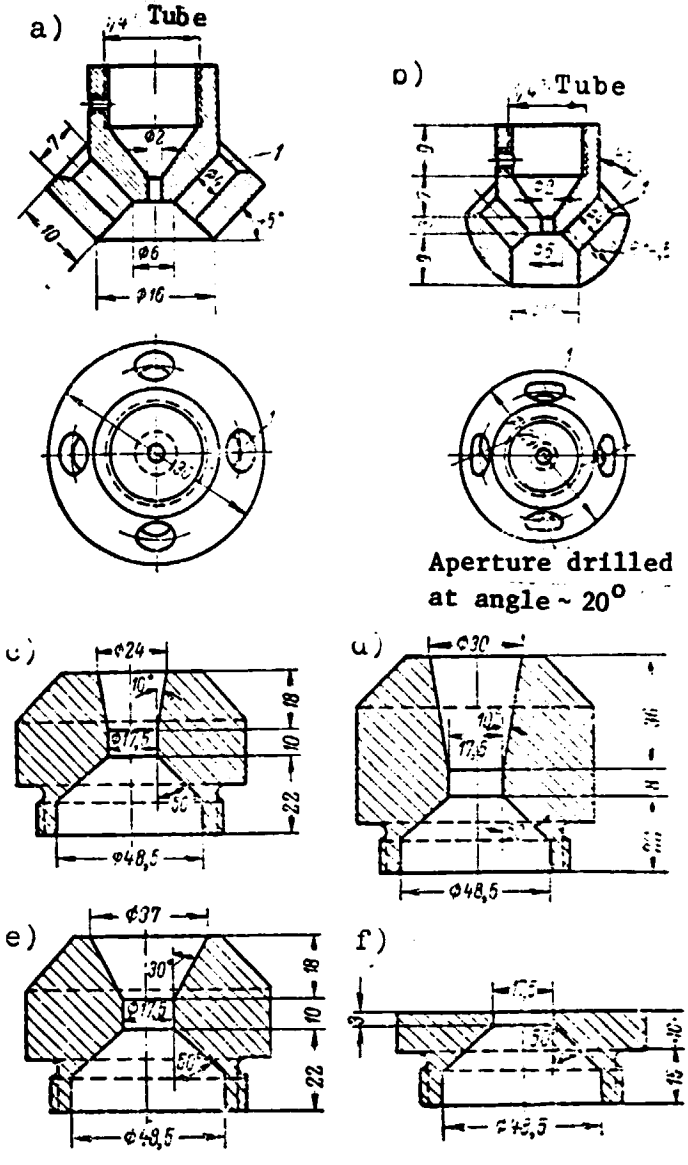

Fig. 6-42. Insertions and probes for the STS-FOB spray nozzle.

were tested in different combinations. The inset shown in Fig. 6-42,a differed from the inset shown in Fig. 6-41 in that four openings 1 were drilled in it to supply a certain amount of air to the root of the fuel stream. The inset shown in Fig. 6-42,b did not fundamentally differ from the inset just described, but apertures 1 had a tangential direction at an angle of 20°, which facilitated the turbulization of air at the root of the fuel stream. Moreover, the inside surface of the insertion was given a spherical shape. The probes shown in Fig.

6-42,c-e, differed from the probe shown in Fig. 6-41 by the presence of a small, straight sector changing into a cone. These probes differed from each other both by the length and angle of tape, as well as the length of the straight part. The probe shown in Fig. 6-42,f did not have a straight part and differed from the probe shown in Fig. 6-41 by a significantly smaller angle of taper.

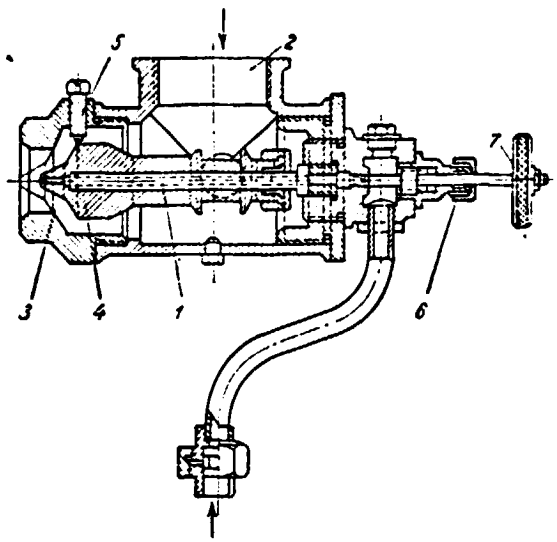

Fig. 6-43. The "Stal'proyekt" spray nozzle.

The first experiments already showed that the probes in Figs. 6-42,c and d, used in combination with the insertions according to Fig. 6-42,a and b, operate unsatisfactorily, inasmuch as a fuel film forms on the sides of the probes, which periodically breaks away and is carried into the stream. The combination of probes according to Figs. 6-41 and 6-42,f, with the insertion according to Fig. 6-42,a, requires an increased air pressure ahead of the spray nozzle in comparison with the other versions. The best results were /162
obtained during operation of the insertion shown in Fig. 6-41, with the probes made according to Figs. 6-41 and 6-42,c and d. With the combination of the same insertion with the probe according to Fig. 6-42,d, the necessary air pressure was 16% less than in the base version (Fig. 6-41).

During the use of the insertion shown in Fig. 6-41, and various probes, the angle of the jet atomized by the "Romo" spray nozzle was: 30° for the probe according to Fig. 6-41, 32° for the probe according to Fig. 6-42,c, and 34° for the probe according to Fig. 6-42,d.

One should note that the quality of atomization (the average diameter of the drop, the distribution of liquid through the cross-section) was approximately identical in all three versions just examined.

It follows from the above that changing the insertions and the probes does not noticeably improve atomization quality. The spray nozzle produces a compara-

tively short fuel spray. With optimum load, it is 1 - 1.5 m long. Increasing the air aperture leads to a deterioration in atomization and elongation of the fuel spray.

The "Stal'proyekt" spray nozzle. In the spray nozzle (Fig. 6-43), fuel oil is supplied to the inner tube 1 and air proceeds to the housing of the spray nozzle via a tube 2 and via the circular section of the air nozzle 3 enters the mouth of the fuel nozzle 4. Adjusting bolts 5 fixed the position of the fuel nozzle. The flow rate of fuel is regulated with the aid of needle 6 with wheel 7 on its outside end. One can alter the flow rate of air by the successive movement of fuel nozzle 4. For this purpose, a special lever has been fitted. A dial has been attached to the nozzle which indicates the degree of opening of the air nozzle 3. /163

The "Stal'proyekt" spray nozzle is widely used when burning liquid fuel in industrial furnaces and is manufactured for a large range of capacities (Table 6-8).

TABLE 6-8

CHARACTERISTICS OF THE "STAL'PROYEKT" SPRAY NOZZLE

Spray nozzle number	Fuel nozzle run, mm	Flow rate of fuel (kg/hr) with air pressure head, mm water column		Nozzle diameter, mm	
		300	700	For fuel	For air
$1\frac{1}{2}$	6	3,5	8	2,5	21
$2\frac{1}{2}$	13	11	24	3	[illegible]
4	21,6	32	57	4	60
5	25	54	82	5	75
6	32	80	120	5	95
8	42	135	205	6	135

It is evident from the table that when the air pressure head changes from 300 to 700 mm on the water column, the fuel flow rate changes approximately two-fold in low capacity spray nozzles, and about 1.5 times in high capacity spray nozzles. In order that the spray nozzle operate reliably, a fuel oil pressure is recommended to be kept within limits of 1 - 1.5 atm.

Conducted tests of spray nozzle No. 2-1/2 showed [6-20] that the minimum fuel oil flow rate with an air pressure head of 300 mm on the water column and a = 1.2 comprises 6.5 kg/hr without ejection and 11.8 kg/hr with ejection, and the maximum flow rate (with a pressure of 700 mm on the water column) is, respectively, 15.2 and 27.3 kg/hr.

The shortcomings of the "Stal'proyekt" spray nozzle should include the poor solution of centering the moveable nozzle of the spray nozzle with the aid of the setting screws. One cannot fail to note another, still more significant shortcoming as well, related to the fact that changing the diameter of the air nozzle aperture is carried out by moving the fuel oil nozzle. During this process, the point of meeting of the air and fuel is displaced, which cannot fail to /164
have an effect on the quality of fuel atomization. It is sufficient to indicate that freedom of movement of spray nozzle 5 is 25 mm, and that of spray nozzle No. 8 — 42 mm. Many investigations show the great significance of the point of meeting of the fuel with the atomizing air stream. If small movement has little effect on the atomization process, then a significant displacement produces a sharp deterioration.

This judgment is also valid relative to the FOB spray nozzle. It is necessary to use maximum relative velocities for best fuel atomization. Therefore, it is recommended that one set the width of the air aperture before beginning operation and regulate the flow rate only by changing air pressure. If this is insufficient, one should change the spray nozzle model. It is not recommended that one regulate the air aperture during operation.

The designs of low pressure atomizers described above are classified among the so-called single atomization spray nozzles. Double atomization spray nozzles have been extensively developed. Their operating principle is based on the fact that the obtained emulsion of the atomized fuel in a mixture with air encounters still another air stream within the spray nozzle, which carries out additional dispersion.

The STS-FDB spray nozzle. The STS-FOB spray nozzle operates according to the double atomization principle (Fig. 6-44). All air needed for combustion

proceeds via tube 1 and is distributed into two streams -- the primary and the secondary. Primary air is supplied via a constant cross-sectional channel 2 to meet the fuel jet, which proceeds via branch 3 to tube 4. The gas-liquid mixture proceeds to expansion insertion 5, and at a certain distance and nearly at a right angle, encounters the secondary air, whose amount is regulated by the variable cross-section of the ring-shaped channel 6. Valve 7 regulates the total flow rate of air. Satisfactory atomization quality of STS-FDB spray nozzles is ensured upon increasing capacity within limits of up to 100% of the nominal flow rate. When it is necessary to change capacity within wide limits, spray nozzles of the same type are used, but with components and assemblies of other design dimensions. Table 6-9 gives characteristics of the FDB spray nozzle developed by "Soyuzteplostroy."

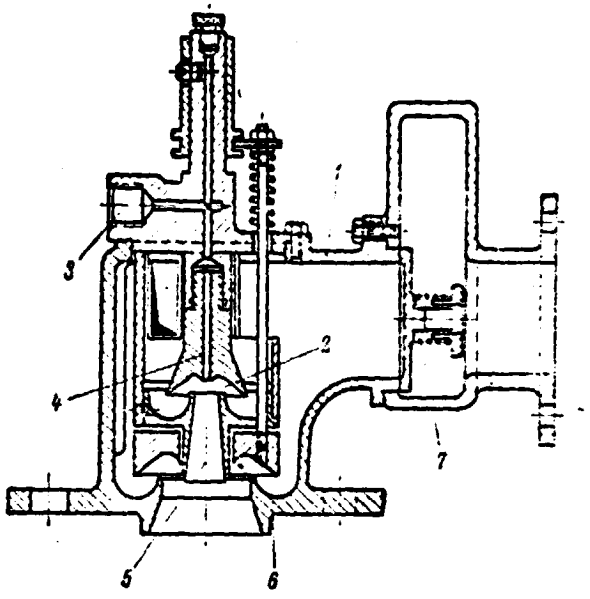

Fig. 6-44. STS-FDB spray nozzle.

The flow rate of fuel changed within limits of from 7.7 to 18 kg/hr in tests conducted with the lowest capacity spray nozzle (FDB-1). During ejection, the minimum fuel flow rate of the FDB-1 spray nozzle increased to 14.2 kg/hr, and the maximum increased to 37 kg/hr. The flow rate of atomization air was 50% of that theoretically needed for combustion. /165

The STS-FDB spray nozzle gives good atomization quality. However, it is somewhat more complicated in design than the other low pressure spray nozzles. One should bear in mind that with reduced pressure, the spray nozzle operation sharply deteriorates, in connection with which it is not recommended that it be employed at a pressure head below 400 mm on the water column. According to shipping list data, the STS-FDB spray nozzle requires a fuel line pressure head of 1.5 atm. Experiments have shown [6-20] that with heated fuel oil and situation of the fuel tank close to the spray nozzle, a pressure head of 0.15 atm is /166

TABLE 6-9

CHARACTERISTICS OF FDB SPRAY NOZZLES

Type of spray nozzle	Minimun fuel oil flow rate, kg/hr.	Air pressure, mm water column			
		450	550	600	700
		Maximum flow rates of air (in the numerator, m^3/hr) and fuel oil (in denominator, kg/hr)			
FDB-1	5	180 20	200 22	220 24	230 25
FDB-2	8,5	280 30	310 34	340 37	360 40
FDB-3	18,5	430 48	480 52	520 56	550 60
FDB-4	20	730 76	750 82	810 89	860 95

sufficient to ensure its complete capacity.

Data on the fineness of atomization by the STS-FDB spray nozzle, obtained during dry run tests with water, are given in Sec. 5-1. The angle of taper of its jet is about 28°. A short fuel spray about 1 m long is obtained.

The Berman spray nozzle. This spray nozzle (Fig. 6-45) also has double atomization. Fuel is supplied through a circular section formed by tube 1 and rod 2, to nozzle 3, and thence to volume 4. Air enters the spray nozzle via tube 5 and is divided into two streams. One of these, the so-called primary stream, proceeds via circular section 6 to volume 4, where it atomizes the fuel coming out of nozzle 3. The other stream (the secondary one) is supplied to the mouth of probe 8 via section 7, where, meeting the fuel-air emulsion, it additionally atomizes it. Regulation of the flow rate of air is carried out by moving rod 2 with the aid of wheel 9. The width of the aperture for supplying primary air /167 can be changed during installation of the spray nozzle. For this purpose, one has screws 10. The aperture for secondary air is regulated by turning control wheel 11, which moves probe 8.

Spray nozzle tests showed that the flow rate of fuel ranges from 16 to 30 kg/hr when the air pressure head changes from 200 to 700 mm on the water column. With ejection, the flow rate correspondingly increases and comprises 25 kg/hr at minimum pressure. About 60% of the air theoretically necessary for combustion is spent on atomization.

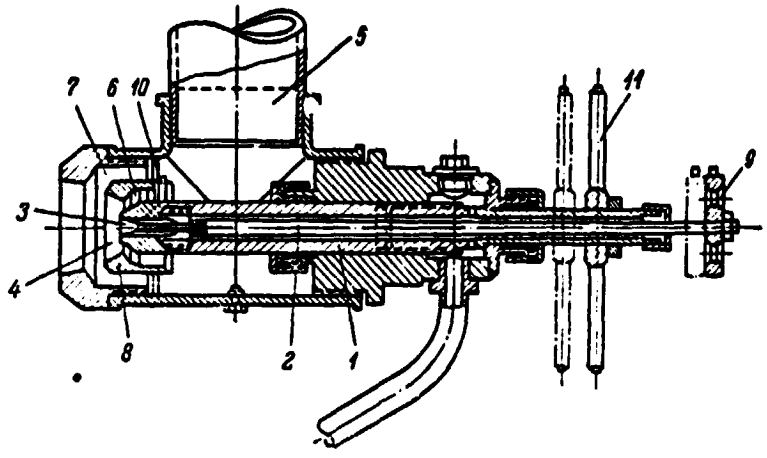

Fig. 6-45. Berman spray nozzle.

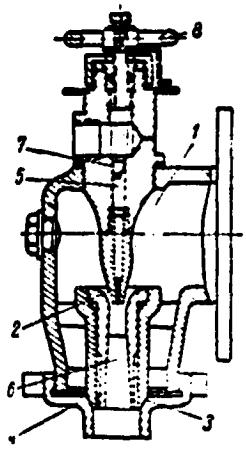

Fig. 6-46. FDM spray nozzle ("Kel'man system).

The Berman spray nozzle requires a comparatively high pressure head in the fuel line. The inventor recommends pressure of 2 atm [6-1].

The Kel'man system FDM spray nozzle. The FDM double atomization spray nozzle is adapted for very low flow rates of fuel (from 1.5 kg/hr). In this spray nozzle (Fig. 6-46), air proceeds to the fuel jet by two pathways via tube 1: the primary -- through the circular, unregulated section 2 to the root of the outflowing jet of fuel, and the secondary -- via circular aperture 3, which is regulated with the aid of probe 4. Fuel runs through the central tube 5, and together with the primary air, passes through nozzle 6 to encounter the secondary air. The flow rate of fuel is regulated by needle valve 7 with the aid of control wheel 8.

FDM spray nozzles are manufactured in two sizes. Their characteristics with an air pressure head ahead of the spray nozzle of 300 - 500 mm on the water column are given in Table 6-10.

A test consisting in atomizing water [6-2] showed the entirely satisfactory operation of the spray nozzle when the fuel flow rate changed from 1.5 to 9 kg/hr. Hot tests confirmed this conclusion: operation of the spray nozzle proved to be stable and reliable within precisely the same limits of change in the fuel flow rate. The flow rate of air in the FDM spray nozzle proved to be

/168

TABLE 6-10

CHARACTERISTICS OF FDM SPRAY NOZZLES

Type of spray nozzle	Flow rate of fuel oil, kg/hr.	Flow rate of air, mm^3/hr.
FDM-1	1.5 - 4	18 - 50
FDM-2	3 - 8	36 - 100

stable and reliable within precisely the same limits of change in the fuel flow rate. The flow rate of air in the FDM spray nozzle is 100% of the air necessary for fuel combustion. The spray nozzle is very simple and is easily regulated. It requires a comparatively low pressure head in the fuel line (in any case, no more than 0.5 atm). The spray nozzle produces a narrow fuel spray whose angle of taper is 22°. The formula for calculating fineness of atomization of fuel by the FDM spray nozzle is given in Sec. 5-1.

Double atomization spray nozzle with air stream twisting. At certain enterprises, double atomization spray nozzles with air-stream twisting are found. One of these is shown in Fig. 6-47. Fuel is supplied to the spray nozzle along central tube 1 to volume 2. Air proceeds through snail intake 3 and is divided into two streams: the primary and the secondary. The primary stream proceeds to the mouth of fuel nozzle 5 via tangential slots 4 and atomizes the fuel in volume 2. Secondary air runs along circular section 6 and carries out additional atomization, encountering the gas-liquid emulsion at the outlet from nozzle 7.

In this spray nozzle, only the primary air is turbulized, but there are also spray nozzles in which the secondary air is also turbulized. Double atomization spray nozzles with air-stream twisting give good atomization. The only significant shortcoming is the narrow regulation limit, inasmuch as the flow rate of air can be changed by a set screw on the supply line (outside the confines of the spray nozzle), but with a decrease in the flow rate of air, the velocity decreases at the point of atomization, which sharply worsens dispersion. /169

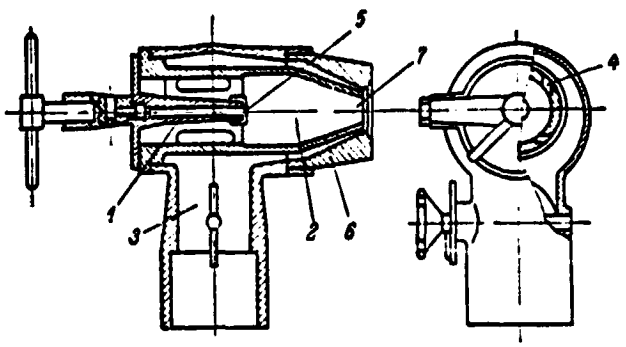

Fig. 6-47. Double atomization spray nozzle with air-stream twisting.

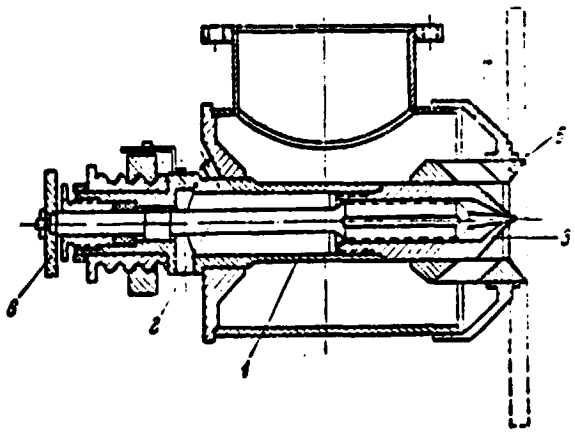

Fig. 6-48. Karabin FK-VII spray nozzle.

The Karabin FK-VII spray nozzle. A. I. Karabin has developed a spray nozzle in which both the air and the fuel at the mouth of the spray nozzle itself are regulated. In the Karabin FK-VII spray nozzle (Fig. 6-48), fuel proceeds along a tube 1, within which is a needle 2, regulating the flow rate of fuel. Air supplied to the mouth of fuel nozzle 3 via tangential windows 4 encounters fuel particles at an angle of 75 - 90°. Regulation of the air flow rate is accomplished by movement of the air nozzle 5, for which purpose handles and rods are fitted. The movement of needle 2 is accomplished by rotating it in its threads with the aid of control wheel 6.

The inventor of this spray nozzle particularly notes [6-5] that the problem of burning coal resin in small furnaces has been solved with its aid. Other spray nozzles (FDB and "Stal'proyekt") tested at one of the Ural plants during the combustion of coal resin frequently clogged, causing noticeable heavy smoking, while the Karabin system spray nozzle produced an even, short fuel spray. The observed small coking near the nose of the spray nozzle was easily eliminated by a turn of the needle without stopping spray nozzle operation.

Several standard size spray nozzles (Table 6-11) have been developed for different flow rates. /170

As is evident from the table, the air pressure head in the FK-VII spray nozzle fluctuates from 300 to 800 mm on the water column. All air needed for combustion is supplied via the spray nozzle. This spray nozzle requires signifi-

TABLE 6-11

CHARACTERISTICS OF KARABIN SPRAY NOZZLES

Size	Number	Flow rate of fuel (kg/hr) with air pressure head, mm water column					
		300	400	500	600	700	800
A	1	6.2	7.2	8	8.8	9.4	10
	2	11.7	13.5	15	16.5	18	19
	3	19	22	24	26	28	30
B	4	20	23	26	27	30	32
	5	28	32	36	40	42	45
	6	39	45	50	55	59	63
C	7	47	54	60	66	71	75
	8	62	72	80	88	95	100
	9	93	108	120	132	140	150
D	10	117	135	150	165	180	190
	11	156	180	200	220	240	250
	12	195	225	250	275	295	310

cant pressure along the fuel line -- at least 1 atm. In order that the fuel oil not adhere to the sides of furnaces, "Teploproyekt" recommends making windows in which Karabin spray nozzles are installed with expansion within the furnace at an angle 85°.

The Glushakov spray nozzle. A Glushakov system spray nozzle has been successfully operated at one of the plants. In this spray nozzle (Fig. 6-49), fuel proceeds via tube 1 to tube 2. The cross-section of nozzle 3 at the fuel outlet is regulated by a needle 4. The latter moves along a screw thread with the aid of control wheel 5. Air is supplied via tube 6 to cavity 7, and with the initial opening of the slits in conical component 8 of tube 2 proceeds to the mouth of the spray nozzle. Upon turning control wheel 9, the extending sides of tube 2 capture screws 10 and raise bushing 11, through whose slits the additional air enters. The spray nozzle provides for the possibility of burning the gas which is supplied via tube 12 to apertures 13. Ring 14 is designed to regulate air taken up through apertures 15. /171

The Glushakov spray nozzle was dry-tested and the fuel flow rate ranged from 7 to 15 kg/hr [6-2]. Within these limits, the spray nozzle produced a quite fine atomized spray. The formula for calculating the average diameter of a drop is given in Sec. 5-1. The flow rate of air in the experiments ranged from 38 to 144 nm^3/hr. Air pressure, respectively, was from 250 to 380 mm on the water column. The angle of taper with all flow rates was 25°.

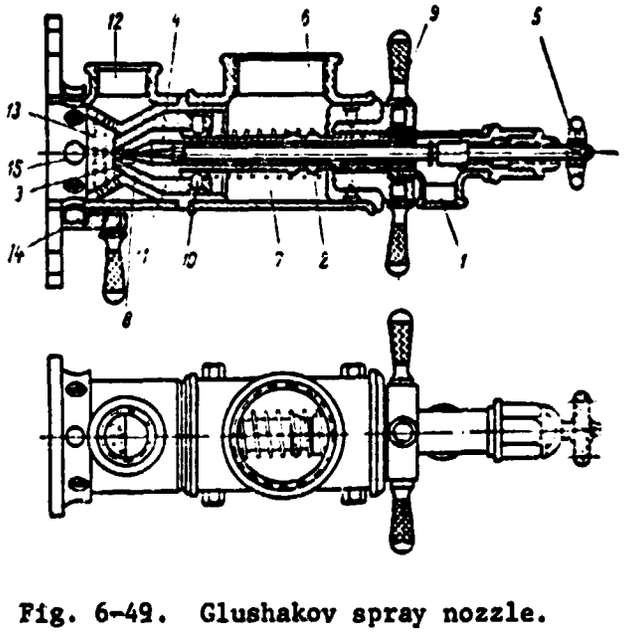

Fig. 6-49. Glushakov spray nozzle.

It is necessary to pay attention to the unsuccessful method of moving the needle which regulates the fuel flow rate. When the needle is rotated with the aid of the screw thread, as a rule, a certain eccentricity of the end of the needle relative to the outlet section of the nozzle appears, which leads to fuel spray downwash. This pertains to all spray nozzles in which the fuel flow rate of fuel is similarly regulated. It is better to employ advancing motion of the needle in its place.

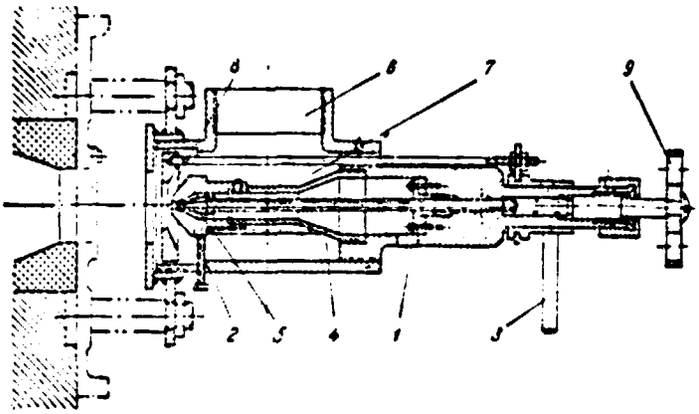

Fig. 6-50. Steam-air spray nozzle.

The steam-air spray nozzle. In industrial furnaces, fuel-air spray nozzles are being used. The design of one of these is shown in Fig. 6-50. Fuel proceeds /172 via tube 1 to the mouth of nozzle 2. The water vapor is conducted along tubes 3 and 4 to the mouth of nozzle 5, where it atomizes the fuel out of nozzle 2. Air is supplied via tube 6, volume 7, and circular section 8 to the mouth of nozzle 5,

where it mixes with the steam-liquid emulsion and carries out additional fuel atomization. Supply of the atomizing air is regulated by a moveable head and control wheel 9. Tests [6-20] showed that the spray nozzle operates well at a capacity of from 12 to 21.5 kg/hr without ejection, and from 22 to 40.5 kg/hr with ejection. The air pressure head before the spray nozzle was, respectively, 200 and 700 mm on the water column. The amount of air for atomization comprises 53% of that theoretically necessary for combustion. The spray nozzle can also operate on one air blower. The flow rate of steam is about 7% of the total amount of fuel.

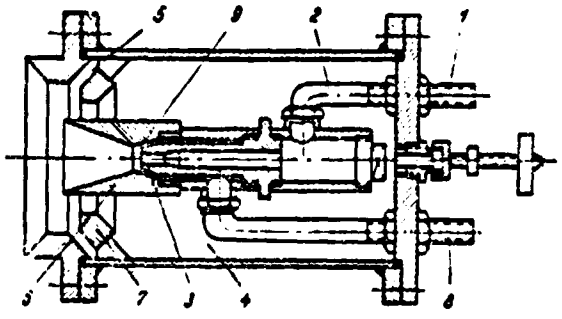

Fig. 6-51. "Orgenergoneft" spray nozzle.

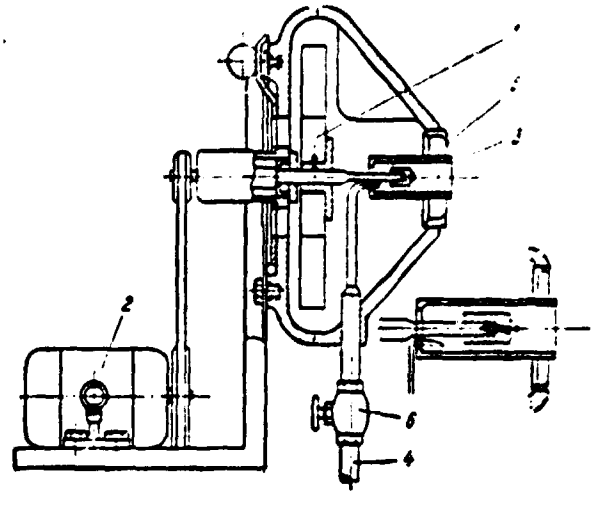

Fig. 6-52. Ktrdzhan spray nozzle.

The "Orgenergoneft" spray nozzle. Figure 6-51 shows the "Orgenergoneft'" spray nozzle. Fuel is supplied via tube 1 and tube 2 to nozzle 3. Air enters volume 4, passes through circular aperture 5, at whose outlet the fuel flowing from defuser 6 is atomized. Regulation of air flow rate takes place by movement of ring 7 with the aid of a special device. Fuel atomization can also be accomplished by water vapor. The vapor is supplied along tube 8 and circular section 9 to the mouth of nozzle 3. The supply of vapor in the "Orgenergoneft'" spray nozzle is provided for as a reserve for a case of cessation of the air supply for any technical reason.

According to I. P. Lyubimov [6-14], the "Orgenergoneft'" spray nozzle operates satisfactorily with an air pressure head of about 150 mm on the water column and a fuel oil pressure of 0.3 atm. /173

The Ktrdzhan spray nozzle. The spray nozzle of original design shown in Fig. 6-52 is equipped with a fan 1 with electric motor 2. The electric motor drives the fan and, together with it, probe 3. The air driven by the fan runs partially through the probe and partially from its circular aperture 5. The Ktrdzhan spray nozzle was tested at the Yerevan machine tool building plant /174
[6-15] and produced good results. The fuel spray was very short and atomization was sufficiently fine, which ensured the complete combustion of fuel with a small excess of air. The flow rate of fuel is regulated by fan 6 on the fuel supply line, while the flow rate of air is regulated by changing the area of the fan tube intake. The power rating of the electric motor ranges from 0.25 to 0.6 kw with a fuel flow rate of up to 20 kg/hr. The spray nozzle is certainly complex, but then it is suitable for automatic operation, when the production area has neither compressed air nor steam.

Section 6-5. Examples of calculating spray nozzles

A. Calculating centrifugal type mechanical spray nozzles.

Example. To design a mechanical, centrifugal type spray nozzle with the following data. Fuel (fuel oil) flow rate G = 500 kg/hr, volumetric weight of fuel $\gamma = 950$ kg/m^3, coefficient of surface tension $\sigma = 0.003$ kg/m, coefficient of kinematic viscosity $\nu = 2 \cdot 10^{-5}$ m^2/sec. Fuel oil temperature $t = 90^\circ$. Fuel is supplied to the spray nozzle under pressure p = 40 atm.

We shall assign values $D_к/d_0 = 7,5$; $l_{вх}/l_0 = 1,5$

We determine the value of A:

$$A = \frac{D_к l_0}{d_0 l_{вх}} = \frac{7,5}{1,5} = 5.$$

We determine the flow velocity of the fuel oil v:

$$v = \varphi \sqrt{2g \frac{p}{\gamma}} = 0,97 \sqrt{19,6 \frac{4 \cdot 10^4}{95}} = 88 \text{ m/sec.}$$

Here, ϕ is the velocity coefficient.

The flow rate coefficient when A = 5: $\xi = 0.15$ (Fig. 4-3). Consequently, the equivalent velocity $v_э$:

$$v_э = \xi v = 0{,}15 \cdot 88 = 13{,}2 \quad \text{m/sec.}$$

We determine the diameter of the outlet nozzle d_0:

$$d_0 = \sqrt{\frac{4G}{\pi v_э \gamma}} = \sqrt{\frac{4 \cdot 0{,}147}{950\pi \cdot 13{,}2}} = 3{,}87 \cdot 10^{-3}\ м = 3{,}87\ мм.$$

We determine:

$$Re_э = \frac{v_э d_0}{\nu} = \frac{13{,}2 \cdot 3{,}87 \cdot 10^{-3}}{2 \cdot 10^{-5}} = 2550.$$

We calculate the flow rate coefficient of the real liquid according to the formula (4-29): /175

$$\xi = 12{,}9 \left(\frac{D_к}{d_0}\right)^{0{,}5} Re_э^{-1/6} \xi_0 = 12{,}9\,(7{,}5)^{0{,}5} \cdot 255[illegible] \cdot 0{,}15 =$$

$$= \frac{5{,}31}{13{,}63} = 0{,}39.$$

We carry out the second calculation (in the first approximation):

$$v_э = 0{,}39 \cdot 88 = 34{,}3\ \text{m/sec};$$

$$f_0 = \frac{0{,}139}{34{,}3 \cdot 950} = 4{,}27 \cdot 10^{-6}\ м^2;$$

$$d_0 = \sqrt{\frac{f_0}{0{,}785}} = 2{,}33 \cdot 10^{-3}\ м = 2{,}33\ мм;$$

$$Re_э = \frac{34{,}3 \cdot 2{,}33}{2 \cdot 10^{-5}} = 4000;$$

$$\xi = 5{,}31 \frac{1}{4000^{1/6}} = 0{,}335.$$

Calculation in the second approximation:

$$v_э = 0{,}335 \cdot 88 = 29{,}4 \text{ m/sec}$$

$$f_0 = \frac{0{,}139}{29{,}4 \cdot 950} = 4{,}98 \cdot 10^{-6} \text{ м}^2;$$

$$d_0 = 2{,}52 \text{ мм};$$

$$Re_э = 3700; \quad \xi = 0{,}342.$$

Calculation in the third approximation gives:

$$v_э = 30 \text{ m/sec} \quad d_0 = 2{,}5 \text{ мм}; \quad f_0 = 4{,}9 \text{ мм}^2; \quad Re_э = 3740; \quad \xi = 0{,}342.$$

We determine the area of the tangential apertures:

$$f_{вх} = 1{,}5 f_0 = 1{,}5 \cdot 4{,}9 = 7{,}35 \text{ мм}^2.$$

We accept the number of apertures n = 2.

Then the diameter of the tangential apertures:

$$d_{вх} = \sqrt{\frac{4 f_{вх}}{n\pi}} \approx 2{,}2 \text{ мм}.$$

The diameter of the vortex chamber:

$$D_к = 7{,}5 \cdot d_0 \approx 19 \text{ мм}.$$

The average drop diameter is determined according to formula (4-36): /176

$$\frac{d}{d_0} = \frac{47{,}8}{A^{0{,}6} \cdot Re^{0{,}7} \Pi_1^{0{,}1}}$$

Here:

$$A^{0{,}6} = 5^{0{,}6} = 2{,}63;$$

$$Re^{0{,}7} = 3740^{0{,}7} = 316;$$

$$\Pi_1 = \frac{\gamma v^2}{g \sigma d_0} = \frac{950 \cdot 4 \cdot 10^{-10}}{9{,}8 \cdot 3 \cdot 10^{-3} \cdot 2{,}5 \cdot 10^{-3}} = 5{,}2 \cdot 10^{-3};$$

$$\Pi_1^{0{,}1} = (5{,}2 \cdot 10^{-3})^{0{,}1} = 0{,}5$$

Then:

$$\frac{d}{d_0} = \frac{47,8}{2,63 \cdot 316 \cdot 0,59} = 0,0975.$$

The average drop diameter is:

$$d = 0,0975 \cdot 2,5 \cdot 10^{-3} = 243 \text{ microns}$$

The angle of taper of the jet according to Fig. 4-3: $\phi \approx 115^{\circ}$

B. Designing the air (or steam) atomization spray nozzle.

Air (or steam) atomization spray nozzles, as a rule, are straight-jet spray nozzles. Design primarily necessitates determining the outlet cross-sections of both the fuel itself and the atomizing agent. In this case, it is important to have in mind the desirable length of the fuel spray, the angle of taper, the average drop diameter of the atomized liquid, and the cross-sectional distribution of the atomized liquid.

The length of the fuel spray and the angle of taper are given above for most examined spray nozzles. With respect to the fineness of atomization, then for a number of the investigated spray nozzles, formulas are given with the corresponding calculation coefficients.

Designing low pressure air atomization spray nozzles

For low pressure spray nozzles, the average drop diameter is determined from equation (5-3'):

$$\frac{d}{d_0} = A \left(\frac{\rho_r v^2 d_0}{\sigma} \right)^{-0,45},$$

where d -- average drop diameter, m;

d_0 -- diameter of liquid nozzle, m;

ρ_r -- gas density, $\cdot \text{sec}^2/\text{m}^4$;

$v = v_1 - v_2$ -- relative velocity at nozzle outlet, m/sec (v_1 -- velocity

of gas, v_2 -- velocity of liquid);

σ -- coefficient of surface tension, kg/m;

A -- experimental coefficient.

Inasmuch as the liquid fuel, as a rule, is preliminarily heated and its viscosity drops sharply, then coefficient A for a low-viscosity liquid can be assumed to be 1.2 for the STS-FDB spray nozzles; 0.9 for the STS-FOB spray nozzles; 0.78 for the STS-FDM spray nozzles; 0.75 for the Glushakov spray nozzle and 0.61 for the two-step spray nozzle. For the remaining spray nozzles that operate under low pressure, one can assume that A ≈ 0.9 until the accumulation of experimental data. /177

The flow rate of air is determined according to the assigned capacity of spray nozzles. This relates to the air used for atomization which, depending on design, ranges from approximately 40 to 100% of the air theoretically needed for combustion for low pressure spray nozzles. In order to determine the outlet cross-section of the fuel nozzle in low pressure spray nozzles, the velocity of the liquid fuel v_2 is assumed to be no more than 4 m/sec. However, the diameter of the nozzle for liquid should not be less than 2 - 3 mm in order to avoid clogging. The velocity of the gas (steam) v_1 is assigned so as to obtain the necessary number of drops. In this case, one should bear in mind the requirements made on the range and angle of taper of the jet.

We shall cite several examples of designing spray nozzles.

Example 1. Determining the average drop diameter according to the assigned capacity of the spray nozzle and the velocity of the air flow for the STS-FOB-2 spray nozzle (Fig. 6-41).

The spray nozzle capacity G = 8 kg/hr; velocity of the air stream in the constricted cross-section v_1 = 60 m/sec; air temperature t = 20° C; flow rate of air theoretically necessary for combustion L_o = 11 nm^3/kg; 50% of the air theoretically needed for combustion is expended on atomization; volumetric weight of the liquid fuel γ = 950 kg/m^3, coefficient of surface tension $\sigma = 3 \cdot 10^{-3}$ kg/m.

The flow rate of air is determined according to the formula:

$$L = L_0 \frac{273 + t}{273} G \cdot 0{,}5 = 11 \cdot \frac{293}{273} \cdot 8 \cdot 0{,}5 = 47{,}3 \text{ m}^3/\text{hr}$$

The area of the live cross-section of the air stream at the point of atomization is:

$$F = \frac{L}{3600 v_1} = \frac{47{,}3}{3600 \cdot 60} = 2{,}18 \cdot 10^{-4} \text{ м}^2.$$

The inside diameter of the fuel nozzle is d_0 = 2 mm. From the design concepts, the outside diameter of the nozzle (least), within limits of the assumption, is $d_{н.о} = 8 \text{ мм} = 8 \cdot 10^{-3} \text{ м}$. Then the diameter of the air nozzle:

$$D = \sqrt{\frac{F}{0{,}785} + d_{н.о}^2} = \sqrt{\frac{2{,}18 \cdot 10^{-4}}{0{,}785} + 8^2 \cdot 10^{-6}} =$$
$$= 1{,}85 \cdot 10^{-2} \text{ м} = 18{,}5 \text{ мм}.$$

The velocity of the liquid fuel is:

$$v_2 = \frac{G}{\gamma \cdot 3600 \cdot 0{,}785 \cdot d_0^2} = \frac{8}{950 \cdot 3600 \cdot 0{,}785 \cdot 4 \cdot 10^{-6}} = 0{,}75 \text{ m/sec}$$

Then the relative velocity in the constricted cross-section:

$$v = v_1 - v_2 = 60 - 0{,}75 \approx 59{,}2 \text{ m/sec}.$$

The average drop diameter is determined according to the formula:

$$d = A \left(\frac{\varrho_г v^2 d_0}{\sigma} \right)^{-0{,}45} \cdot d_0 =$$
$$= 0{,}9 \left(\frac{0{,}12 \cdot 59{,}2^2 \cdot 2 \cdot 10^{-3}}{3 \cdot 10^{-3}} \right)^{-0{,}45} \cdot 2 \cdot 10^{-3} = 143 \cdot 10^{-6} \text{ м} = 143 \text{ microns}$$

Example 2. Determination of the flow rate of air and dimensions of the air nozzle according to the assigned capacity of the spray nozzle and average drop diameter. /178

The fuel flow rate in the "Stal'proyekt" spray nozzle (Fig. 6-43) is G = 205 kg/hr; the average drop diameter d = 250 micron = $2.5 \cdot 10^{-4}$ m; the volumetric fuel weight γ = 950 kg/m^3; the coefficient of surface tension $\sigma = 3 \cdot 10^{-3}$ kG/m;

temperature of the atomizing air t = 200° C.

A 75% flow rate of air theoretically necessary for combustion is required for atomizing fuel in the "Stal'proyekt" spray nozzle. This comprises:

$$L = 205 \cdot 11 \cdot 0{,}75 \cdot \frac{200 + 273}{273} = 2910 \text{ m}^3/\text{hr}$$

The velocity of the liquid fuel v_2 is assumed to be 2 m/sec. Then the nozzle diameter for the liquid fuel will be:

$$d_0 = \sqrt{\frac{G}{3600 \cdot 0{,}785 \gamma v_2}} =$$

$$= \sqrt{\frac{2{,}5}{3600 \cdot 0{,}785 \cdot 950 \cdot 2}} = 6{,}15 \cdot 10^{-3} \text{ м} \approx 6 \text{ мм}.$$

We determine the relative velocity from the formula (5-3') with a coefficient value A = 0.9:

$$\lg v = \frac{1}{0{,}9}\left(\lg \frac{A d_0}{d} - 0{,}45 \lg \frac{\varrho_r d_0}{\sigma}\right) =$$

$$= \frac{1}{0{,}9}\left(\lg \frac{0{,}9 \cdot 6 \cdot 10^{-3}}{2{,}5 \cdot 10^{-4}} - 0{,}45 \lg \frac{0{,}12 \cdot 6 \cdot 10^{-3}}{3 \cdot 10^{-3}}\right) = 1{,}8,$$

thence v = 63 m/sec.

The velocity of the air stream will be:

$$v_1 = v + v_2 = 63 + 2 = 65 \text{ m/sec}.$$

The cross-sectional area for the passage of air in the atomization point is:

$$F = \frac{L}{3600 v_1} = \frac{2910}{3600 \cdot 65} = 12{,}5 \cdot 10^{-3} \text{ м}^2.$$

Assuming the least outside diameter of the liquid nozzle $d_{н.о} = 25$ мм $= 2{,}5 \cdot 10^{-3}$ м, we obtain the diameter of the air nozzle:

$$D = \sqrt{\frac{F}{0{,}785} + d_{н.0}^2} = \sqrt{\frac{125 \cdot 10^{-4}}{0{,}785} + 6{,}2 \cdot 10^{-4}} = 132 \cdot 10^{-3} \approx 135 \text{ мм}.$$

During the design of double atomization spray nozzles, for example, the FDM (Kel'man system), relative velocity is determined according to the formula:

$$v = \sqrt{\frac{v_{1.0}^2 G_в' + v_{2.0}^2 G_в''}{G_в' + G_в''}}.$$

where $v_{1.0}$ -- initial relative velocity between primary air and the fuel jet; /179

$v_{2.0}$ -- relative velocity of the gas-liquid stream upon encountering secondary air;

$G_в'$ -- flow rate of primary air;

$G_в''$ -- flow rate of secondary air.

Here primary and secondary air are defined as the amount of air coming into the spray nozzle itself in two streams.

Having assigned the general flow rate of air used for atomization, one can determine the amount of primary and secondary air proportional to the areas of the outlet cross-sections by ignoring local resistances.

Designing air (or steam) high pressure atomization spray nozzles

When designing air (or steam) high pressure atomization spray nozzles, extremely high velocities are usually employed. For a number of designs, velocity at the point of atomization reaches the critical velocity and even exceeds it. During the design of the outlet cross-sections for gas (steam), one can assume that the process is an adiabatic one within the spray nozzle. Then, for the escape of gases and steam via the cylindrical and convergent nozzles, with a pressure ratio greater than the so-called critical one

$$\varepsilon = \frac{p_2}{p_1} > \left(\frac{2}{k+1}\right)^{\frac{k}{k-1}}$$

theoretical velocity of the nozzle mouth is:

$$v = \sqrt{2g\frac{k}{k-1}\left[1-\left(\frac{p_2}{p_1}\right)^{\frac{k-1}{k}}\right]\cdot p_1 V_1}\,.$$

where p_1 -- absolute pressure in the medium from which the outflow takes place, kG/m^2;

p_2 -- absolute pressure in the medium to which outflow occurs, kG/m^2;

V_1 -- specific gas volume in the medium from which outflow occurs, m^3/kg;

k -- adiabatic index, which is 1.4 for air; 1.135 for dry saturated steam; 1.3 for superheated steam;

g -- gravity acceleration, m/sec^2.

The theoretical gas flow rate is:

$$G = F\sqrt{2g\frac{k}{k-1}\left[\left(\frac{p_2}{p_1}\right)^{\frac{2}{k-1}}-\left(\frac{p_2}{p_1}\right)^{\frac{k+1}{k}}\right]\frac{p_1}{V_1}} \quad [kg/sec]$$

If the pressure ratio is critical or below critical, then outflow occurs at a certain (critical) velocity, i.e., when

$$\varepsilon = \frac{p_2}{p_1} \leqslant \left(\frac{2}{k+1}\right)^{\frac{k}{k-1}} \qquad v_{kp} = \sqrt{2g\frac{k}{k+1}p_1 V_1} \quad [m/sec]$$

The theoretical flow rate of gas in this case will be: /180

$$G = f\sqrt{2g\frac{k}{k-1}\left(\frac{2}{k+1}\right)^{\frac{2}{k-1}}\cdot\frac{p_1}{V_1}} \quad [kg/sec]$$

The critical ratio ε is 0.528 for air; 0.546 for superheated steam; 0.577 for dry saturated steam.

In practical calculations, it is convenient to use the caloric equations of the gas (steam) state. In this case, for an adiabatic process (S = const), the expressions for the outflow velocity are transformed to the type:

$$v = 91{,}53\sqrt{i_1 - i_2} \text{ [m/sec]}$$

where i_1 and i_2 -- gas (steam) enthalpy, respectively, in the initial and terminal states, determined according to the i - S diagram according to the assigned initial pressure and temperature and terminal pressure.

In this case, one determines the specific volume V, the temperature t, and the steam dryness x in the terminal state according to the diagram.

An example is given below for calculating one of the spray nozzles (ejection type) which is widely used in boiler operations. The average number of drops for this spray nozzle is determined according to the equation (5-1):

$$\frac{r\varrho_r v^2}{\sigma} = A\left(\frac{vd_0}{\nu_r}\right)^n,$$

where d_o -- characteristic size;
r -- average drop radius;
ϱ_r -- air density;
ν_r -- coefficient of kinematic gas viscosity (steam viscosity);
v -- relative velocity;
A -- $9.04 \cdot 10^{-10}$)
n -- 1.97) -- experimental coefficients.

Example. Design and ejection type spray nozzle (Fig. 6-25) with the following specifications:

Fuel flow rate G = 1500 kg/hr = 0.417 kg/sec; volumetric rate of fuel γ = 950 kg/m^3; coefficient of surface tension σ = 0.003 kG/m; atomization is carried out with steam; initial pressure of superheated steam p_1 = 15 atm, temperature t_1 = 300° C, specific flow rate of steam g_n = 0.3 kg/kg.

We determine the steam flow rate:

$$G_n = g_n G = 0{,}3 \cdot 1500 = 450 \text{ kg/hr} = 0.125 \text{ kg/sec}.$$

Pressure at the outlet from the Laval nozzle can also be somewhat below atmospheric pressure, inasmuch as there is a diffusor after the mixer. However, to maintain a certain reserve, as well as to avoid a shock wave during operation of the spray nozzle at reduced pressures, pressure is set at the nozzle outlet: p_2 = 1 atm.

In this case the pressure ratio:

$$\varepsilon = \frac{p_2}{p_1} = \frac{1}{15} < \varepsilon_{кр}.$$

Consequently, in a narrow nozzle cross-section, a critical velocity is established. /181

Pressure in the critical cross-section is:

$$p_{кр} = 0{,}546 p_1 = 0{,}546 \cdot 15 = 8.2 \text{ atm.}$$

Temperature in the critical cross-section is the following, according to the i - S diagram for steam:

$$t_{кр} = 230^\circ \text{ C.}$$

Velocity in the critical cross-section:

$$w_{кр} = 91{,}53\sqrt{i_1 - i_{кр}} = 91{,}53\sqrt{725{,}4 - 692{,}7} = 91{,}53\sqrt{32{,}7} = 524 \text{ m/sec}$$

The specific volume in the critical cross-section:

$$V_{кр} = 0{,}28 \text{ m}^2/\text{kg}$$

The area of the critical cross-section:

$$F_{кр} = G_п \frac{V_{кр}}{w_{кр}} = 0{,}125 \cdot \frac{0{,}28}{524} = 0{,}0000669 \text{ м}^2 = 0{,}669 \text{ см}^2.$$

Nozzle diameter in the critical cross-section:

$$d_{кр} = \sqrt{\frac{4F_{кр}}{\pi}} = \sqrt{\frac{4 \cdot 0{,}669}{\pi}} = 0{,}92 \text{ см} \approx 9 \text{ мм}$$

Velocity of the nozzle outlet:

$$v = 91{,}5 \sqrt{i_1 - i_2} = 91{,}5 \sqrt{125} = 1020 \text{ m/sec}$$

We determine cross-sectional area at the nozzle outlet:

$$F_2 = G_п \frac{V_2}{v}.$$

According to the i - S diagram for steam, when p_2 = 1 atm, t_2 = 100° C and x = 0.93, we have:

$$V = 1.67 \text{ m}^3/\text{kg}$$

Thence:

$$V_2 = xV = 0{,}93 \cdot 1{,}67 = 1{,}55 \text{ m}^3/\text{kg}$$

$$F_2 = 0{,}125 \cdot \frac{1{,}55}{1020} = 1{,}9 \cdot 10^{-4} \text{ м}^2 = 1{,}9 \text{ см}^2.$$

Nozzle diameter:

$$d_2 = \sqrt{\frac{4F_2}{\pi}} = \sqrt{\frac{4 \cdot 1{,}9}{\pi}} = 1{,}55 \text{ см} \approx 16 \text{ мм}.$$

The external diameter of the steam nozzle with wall thickness at the outlet $\delta_{ст}$ = 2 mm will be:

$$d_2' = d_2 + 2\delta_{ст} = 16 + 4 = 20 \text{ мм}.$$

We accept the angle of taper of the diffusor part of the nozzle to be: /182

$$2\alpha = 8°.$$

The length of the diffusor part of the nozzle is:

$$l = \frac{d_2 - d_{кр}}{2 \operatorname{tg} \alpha} = \frac{16 - 9}{2 \cdot 0{,}07} = \frac{7}{2 \cdot 0{,}07} = 50 \text{ мм}.$$

We determine the area of the outlet cross-section for a liquid fuel, assuming velocity at the intake to the mixing zone to be $v_2 = 2$ m/sec:

$$F_ж = \frac{G}{\gamma_ж v_2} = \frac{0{,}417}{950 \cdot 2} = 2{,}2 \cdot 10^{-4} \text{ м}^2 = 2{,}2 \text{ см}^2.$$

We calculate the aperture width for supplying the liquid fuel:

$$l_ж = \frac{F_ж}{\pi d_2} = \frac{2{,}2}{\pi \cdot 2} = 0{,}35 \text{ см} = 3{,}5 \text{ мм}.$$

We assume that at a distance $l_2 / d_2 = 3$ equalization of the velocities of the liquid and the steam occurs. Velocity after mixing $v_{см}$ is determined from the condition of constancy of the amount of motion. The presence of certain losses is taken into account by introducing the coefficient $\phi = 0.95$.

$$v_{см} = \frac{\varphi v g_п}{1 + g_п} = \frac{0{,}95 \cdot 1020 \cdot 0{,}3}{1{,}3} = 224 \text{ m/sec}$$

As the result of braking during impact, steam temperature is:

$$t = t_1 - \frac{A v_{см}^2}{2 g c_p} = 300 - \frac{224^2}{427 \cdot 19{,}6 \cdot 0{,}468} = 300 - 13 = 287 \text{ °C}.$$

By ignoring heat exchange with the fuel, we consider that this temperature is established after mixing in the mixer. The cross-sectional area at this point (which is the outlet cross-section of the nozzle) will be:

$$F_{см} = \frac{G_п v'}{v_{см}} = 0{,}125 \cdot \frac{2{,}5}{224} = 14 \cdot 10^{-4} \text{ м}^2 = 14 \text{ см}^2.$$

According to the i - S diagram, $V' = 2.5$ kg/m^3, whence diameter will be:

$$d_{см} = \sqrt{\frac{4 \cdot 14}{\pi}} = 4{,}22 \text{ см} \approx 42 \text{ мм}.$$

We determine the angle of taper of the diffusor part of the mixer:

$$\alpha_1 = \operatorname{arc\,tg}\frac{d_{см} - d_2}{2l_{см}} = \operatorname{arc\,tg}\frac{42-20}{2\cdot 60} \approx 10{,}5°.$$

The solid angle $2\alpha_1 = 2\cdot 10{,}5 = 21°$.

We determine the average drop radius according to the following formula:

$$\text{Lap} = 9{,}04\cdot 10^{-10}\cdot \text{Re}^{1{,}97}.$$

Here the diameger at the outlet from the nozzle $d_0 = d_2 = 16$ mm is the determinative dimension. We have: /183

$$\frac{r\varrho_r v^2}{\sigma} = 9{,}04\cdot 10^{-10}\frac{v^{1{,}97}d_0^{1{,}97}}{\nu_r^{1{,}97}};$$

$$\varrho_r = \frac{1}{\nu g} = \frac{1}{1{,}67\cdot 9{,}8} = 0{,}061 \text{ kg}\cdot\text{sec}^2/\text{m}^4$$

$$\nu_r = \frac{\mu_r}{\varrho_r} = \frac{1{,}22\cdot 10^{-4}}{0{,}061} = 2\cdot 10^{-3} \text{ m}^2/\text{sec}$$

The average drop radius is:

$$r = \frac{\sigma\cdot 9{,}04\cdot 10^{-10}\cdot d_0^{1{,}97}}{\varrho_r v^{0{,}03}\cdot \nu_r^{1{,}97}} = \frac{3\cdot 10^{-3}\cdot 9{,}04\cdot 10^{-10}(16\cdot 10^{-3})^{1{,}97}}{6{,}1\cdot 10^{-2}(1020)^{0{,}03}\cdot(2\cdot 10^{-3})^{1{,}97}} \approx 19 \text{ microns}$$

We determine the average diameter of drops:

$$d = 2r = 2\cdot 19 = 38 \text{ microns}$$

CHAPTER SEVEN

APPARATUS WITH PRELIMINARY LIQUID FUEL GASIFICATION

Having gas fuel, industry has been able successfully to adopt in production both the slow, so-called diffusion combustion with the extended flame, and the fast, so-called flameless combustion. This has been favored by the comparative simplicity of the process of buring a purely gas fuel spray -- the success of matters here practically depends chiefly on the intensity of mixing of two gas streams -- the fuel and the co-combustant; the rate of the reaction itself in the gas fuel spray does not limit the process as a whole.

A somewhat different situation is created when burning a liquid, hydrocarbon fuel, which fuel oil primarily is. Fuel oil in recent years has become widely used in boiler operation. The combustion of fuel oil in the suspended state in an air stream requires the successive occurrence of a number of stages: evaporation, pyrogenic decomposition, occurring in the central parts of the fuel spray with the copious liberation of soot-forming coke (if a special primary air supply has not been provided), mixing with air, and combustion itself.

According to modern concepts, the combustion process only occurs on the /184
peripheral zone of the fuel spray, representing, as it were, the flame, comparatively thin envelope in which the process proceeds according to the laws of uniform combustion. This "surface of combustion" is characterized, as in the gas fuel spray, by the theoretical excess of air ($\alpha \approx 1$) and the maximum temperature throughout the entire gas field $T_{max} = \mu T_{theor}$, where $\mu < 1$ -- the emission coefficient of the fuel spray.

Thus, the resultant rate of the combustion process depends to a known degree on the rate of occurrence of the preliminary stages: evaporation and pyrogenic decomposition. The evaporation process, besides the thermal conditions, depends to a significant degree on the degree of dispersion (atomization) of the fuel oil. This question has been examined by many investigators and was presented in detail in Chapters 8 and 9. One must still state that even today the sprayers employed in combustion technology are not equipped with devices of

sufficiently precise regulation, as the result of which the evaporation process of fuel oil in the fuel spray takes place at random. Precisely the same thing can also be said about another extremely important preliminary stage -- pyrogenic decomposition: and up to now it also remains practically uncontrolled.

Without even mentioning that the thermal conditions created at the base of the fuel spray as the result of back radiation of the flame are usually arbitrarily established, few attempts have been made to utilize such physicochemical factors as introducing air or steam, whose effect on the course of the process could significantly increase the possibility of regulating fuel spray operation. The employed air or steam blow stream, as the result of specific organization of the process, has little effect on pyrogenetics at the initial stage of the liquid fuel decomposition process.

If one takes into account the special technical goals which sometimes force one to accept the severe operating conditions of the fuel oil spray (close, strongly cooled volumes of furnace chambers, characterized by high values of the ratio of screened surfaces to the volume of the combustion chamber, significant limits of fluctuations of the specific load, etc.), then the possibility of operating regulation of this usually extended part of the process is of great technical interest.

In order to determine the course of pyrolysis at the initial stage of burning the liquid fuel, and the effect of temperature and oxidation factors on it, investigations were performed on a special stand [7-1]. The installation was a /185
hermetically sealed vertical chamber whose temperature was brought up to 550 - 700° C by electric heaters.

The experiments were carried out with kerosene, solar oil and fuel oil. The fuel was preliminarily heated in a coil to 250 - 300° C and was atomized with the aid of a spray nozzle in the gasification chamber. The chamber was supplied from 3 to 11% of the air theoretically required for combustion. The vapor-gas mixture proceeded from the gasification chamber to normal and deep cooling refrigerators. The obtained liquid and gaseous produces were analyzed in detail.

The primary data on fuel oil gasification in the temperature range of 450 - 700° C are given in Fig. 7-1. These data showed the relationship between the composition of the gas at the end of the gasification chamber and the temperature regime. One can note an increase in the yield of CH_4 (recalculation of the terminal C_nH_{2n+2} hydrocarbons to "arbitrary" methane) and hydrogen H_2 with the increase in temperature.

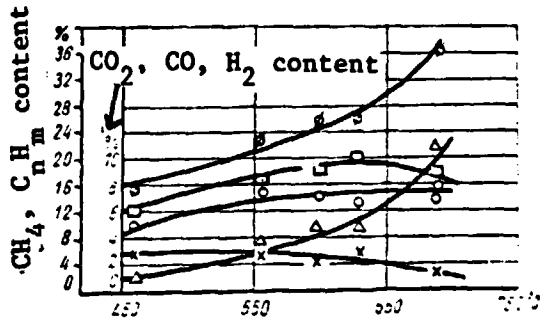

Fig. 7-1. Relationship of composition of gas at the end of the gasification chamber with temperature.

ø — CH_4; □ — C_nH_m; × — CO_2; ○ — CO; △ — H_2.

A noticeable acceleration in the hydrogen increase was only observed after chamber temperature rose to 600° C. A stable C_nH_m maximum is also characteristic (the group of unsaturated hydrocarbons) in the 550 - 650° C range. A decrease in the CO_2 content and a slowing of the CO increase, beginning with a certain temperature, evidently occurs as the result of formation of acids and spirits.

One can obtain a certain concept of the operation of the gasification chamber and its role in the subsequent process of combustion of the gasified liquid fuel from the gas analysis data, according to which the coefficient β is calculated for the gas and the condensed vapors, depending on gas temperature in the gasification chamber (Fig. 7-2). The linear character of the relationship between coefficient β and temperature attracts attention. The addition of air in the amount of 8 - 11% of that theoretically necessary for combustion had the greatest effect on pyrolysis. /186

The prospectives which are provided by preliminary gasification of fuel oil and the advantages associated with burning fuel with a practically, extremely small excess of air, the possibility of sharply increasing the thermal intensity of the volume and cross-section of the combustion chambers -- all of these things have led to the realization of the preliminary gasification of liquid fuel by various technical and design methods. In this case, technology has aimed its efforts at two basic methods of gasification. According to one of these, preliminary gasification takes place in special vessels, so-called gasifiers, with

C-3

the output of ready gas to the furnace volumes of the combustion chamber and furnace. The other method is technically the most interesting one for energy production, and consists in an organization of the gasification process in which the fuel devices are mounted in the combustion chambers and furnaces, comprising a single unit with them.

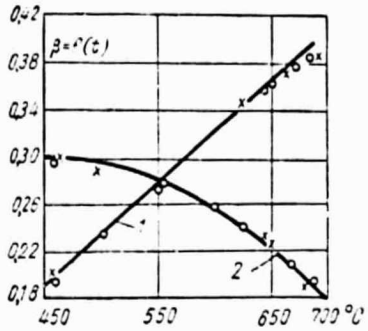

Temperature of gas in gasification chamber

Fig. 7-2. Relationship between coefficient β and decomposition temperature.

1 - gas; 2 - condensate: the relationship between the gravimetric flow rates of air and the liquid fuel was: O - 0.4 - 0.8; X - 1.3.

In the recent foreign literature, problems of obtaining and burning gas obtained from petroleum are extensively illuminated. To a known degree, these questions were discussed at the IV International Petroleum Conference held in Rome in 1955 [7-4]. In the USA, periodically acting installations have come to be used for obtaining a high caloric gas from liquid fuel [7-3].

The gasification of fuel oil according to the method of the French association of engineers attracts attention. This method has not only become widely used in France, but also in the Federal Republic of Germany, England, Italy and Sweden. The essence of the method [7-5] is that the fuel oil is initially /187
gasified in a chamber (gasifier) with the supply of primary air in the amount of about 30% of that theoretically needed for combustion. The gasifier is a small vertical ceramic tube whose lower part contains tangentially mounted nozzles for primary air: the fuel oil is also supplied here.

As a result, one obtains a gas of approximately the following composition: 4% CO_2, 16% CO, 14% H_2, 4% CH_4 and 62% N_2. The heat-producing capacity of this gas is 1900 kcal/nm^3; its temperature is about 1200°C. The obtained gas mixes with the secondary air and proceeds to the furnace chamber via a burner which is linked with the gasifier by design. The capacity of the presently employed gasifiers is 300 - 1200 kg/hr. Combustion of the gasified fuel oil takes place with an extremely small excess of air, with a range of fuel flow rate of from 100 to 25%.

The Ural Polytechnical Institute has built a device for the preliminary gasification of fuel oil with its subsequent combustion in a furnace [7-3]. During gasification, gas was obtained containing 6% CO_2, 0.4% C_nH_m, 13% CO, 3% CH_4, 14% H_2, and 65% N_2. This gas proceeds to a furnace at temperature of 1150 - 1200° C. The known disadvantages are the necessity of periodically cleaning the gasification chamber of the formed coke.

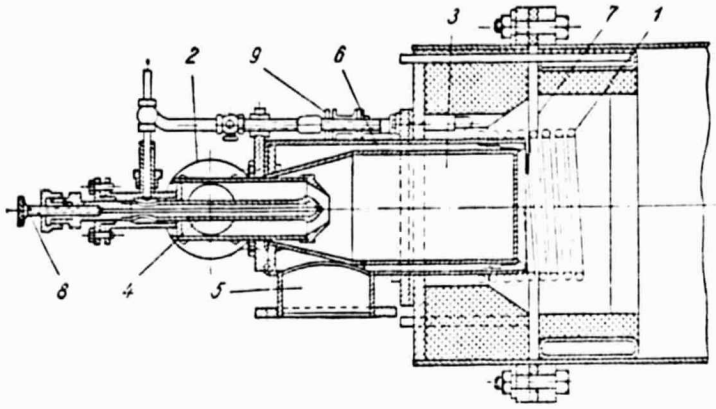

Fig. 7-3. TsKTI spray nozzle with liquid fuel preliminary gasification.

Figure 7-3 shows a TsKTI spray nozzle with the preliminary B. D. Katsnel'son gasification system [7-1]. Fuel proceeds through the fuel line to coil 1, heated by furnace chamber radiation heat. The vapor-fuel mixture proceeds from the coil to the coarse atomization spray nozzle 2, from which it enters the gasification chamber 3. Primary air in the amount of 3 to 10% of that theoretically needed for combustion, proceeding via tube 5 along circular channel 6, and is turbulized at the output by vanes 7. The regulation of fuel flow rate is accomplished by needle 8.

The temperature of preliminary fuel heating is regulated by increasing or decreasing the coil surface. This is accomplished with the aid of a special mechanism 9, which makes it possible to move the coil forward for complete radiation reception, to leave it in the partial radiation reception regime, and finally, fully to place it in the niche. The radiation coil which receives the radiation heat of the fuel spray ensures necessary heating of the fuel, although it does have a small surface. /188

In order to avoid coking of the coil, the velocity of the liquid fuel in it should be at least 0.5 m/sec. The selection of the particular material for the coil also plays an important role in combating coke deposition. Chrome-plated copper is most suitable in this case. It is also permissible to make the

coil out of chrome-nickel or chrome-molybdenum steel. Known limitations are also made on the heating temperature, which should be about 300° C.

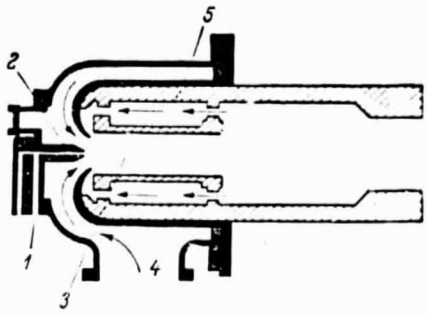

Fig. 7-4. Spray nozzle with recirculation of gas in the preliminary gasification chamber.

Pyrogenic decomposition of liquid fuel occurs in the gasification chamber. Experiments have established that temperature at the end of the gasification chamber reaches about 600 - 700° C. In this case, a significant content of CO, CH_4 and C_nH_m is detected in the gases. The capacity of the spray nozzle ranged within limits of G = 15 - 60 kg/hr. The air excess was α = 1.03 - 1.07, the thermal stress of the combustion chamber volume GQ/V was up to $17.5 \cdot 10^6$ kcal/m^3·hr (G -- flow rate of fuel; Q -- thermal capacity of fuel; V -- volume of combustion chamber). The fuel spray was very short.

The radiation heater comes into action immediately after ignition of the /189
spray nozzle and ensures a uniform increase in fuel temperature. Spray nozzle ignition and its regulation are extremely simple. Precisely the same positive result was obtained on a 200 kg/hr capacity spray nozzle. One should note that movement of the coil in the described structure was due to the necessity of comparatively widely altering load. With reduced requirements on regulation (from 100 to 50%), the need for the moveable mechanism does not exist. Such a change in design was made by "Soyuzteplostroy."

Several types of spray nozzles have been created in the USA [7-6], which are principally similar to the TsKTI spray nozzle, the only difference being that the metal walls of the gasification chamber are replaced by ceramic ones, while heating and gasification of the liquid fuel are primarily ensured by convective heat, for which purpose an insertion is employed which creates recirculation of gases. Figure 7-4 gives an overall view of such a spray nozzle.

Atomized, preliminarily heated liquid fuel is supplied along tube 1 via spray nozzle 2. This fuel enters a gasification chamber 3. Air proceeds along

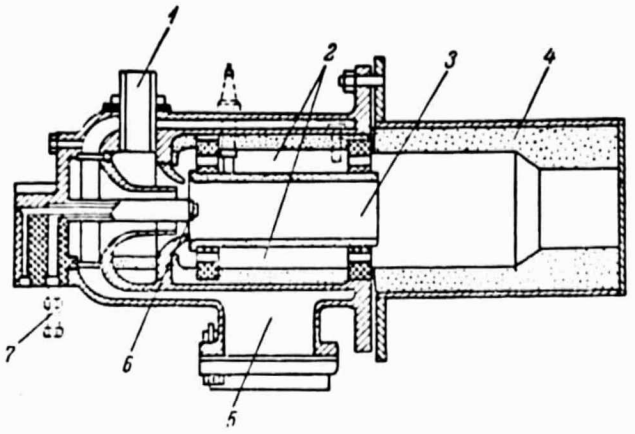

Fig. 7-5. Spray nozzle with preliminary gasification adapted for the combined combustion of gasified liquid fuel and natural gas.

1 - tube for gas supply; 2 - circular channel for recirculation of hot gases; 3 - liquid fuel preliminary gasification chamber; 4 - ceramic tube; 5 - tube for air supply; 6 - spray nozzle; 7 - tube for liquid fuel supply.

channel 4. In circular 5, the hot exhaust gases recirculate, which facilitates stabilization of the flame and of fuel oil gasification. A spray nozzle of this type with a capacity of 250 kg/hr is successfully operating at a number of enterprises. It produces a very short fuel spray, operates with a low air excess, and is regulated within limits of up to 25% without altering operating quality. Combustion practically ends at a short distance, and the intensity of the GQ/V volume reaches $80 \cdot 10^6$ kcal/$m^3 \cdot$hr. The velocity of gas at the output from the gasification chamber is about 120 m/sec. The use of a spray nozzle with preliminary gasification in the metallurgical industry has made it possible noticeably to improve the quality of heating materials, having simultaneously reduced the time spent upon it.

At present, work is being carried out in the USA to create spray nozzles /190
with preliminary gasification of both high (up to 1500 kg/hr) and low (up to 25 kg/hr) power. Having somewhat modified such spray nozzles, they can be successfully used for the combined combustion of a liquid fuel and a gas. Figure 7-5 shows this kind of spray nozzle for the combined combustion of fuel oil and natural gas.

An original design of a spray nozzle with preliminary gasification (Fig. 7-6) was suggested and tested by G. F. Knorre [7-2]. It is an open type burner whose gasification protector 1 is turned by its mouth to meet a stream of air moving at a velocity of from 100 to 150 m/sec. The total cross-section of the small side slots 2 is equal to the mouth cross-section 3. The burner end 4 is a spray nozzle with a spiral channel for fuel heating. This spiral channel heats

the fuel supplied to the gasification chamber along tube 5 to meet the stream of air. The sides of the chamber are fireproof, and the mouth of its head is given a streamlined shape.

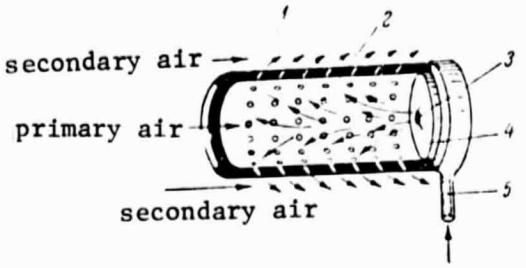

Fig. 7-6. Spray nozzle with preliminary gasification of the G. F. Knorre system.

After a brief period of heating such a chamber, the external flame disappears and burning on the surface becomes flameless. As the result of the sintered sides and the primary air which penetrates beneath the pressure head stream and penetrates into the cavities of the chamber, evaporation and the entire gasification process succeeded in terminating in this cavity throughout the entire range of tested loads. The burner operates in an open stream the better (according to brightness of flameless luminosity), the higher the velocity of the flow-around air.

CHAPTER EIGHT /191

COMBUSTION OF A UNIT DROP

Section 8-1. Diffusion theory

The combustion process for a flame of liquid fuel is greatly determined by the combustion conditions and the evaporation of unit drops comprising the flame. The combustion of unit drops of liquid fuel has been studied in many reports, domestically and abroad.

Of great importance, in particular, is the study by G. A. Varshavskiy on the diffusion theory of combustion published in 1945 [8-3]. It must be noted that more recent works of foreign researchers [8-2, 4, 5, 12 and 18], repeating the procedures and computational method of G. A. Varshavskiy, give rougher estimates in some sections. Some of these works do not consider such facts as the dependence of the heat conductivity coefficient on temperature, the Stefanov stream, etc.

The following premises lie at the basis of the diffusion theory.

1. The process is considered to be quasistationary. This means that no consideration is given to the change in the temperature of the gas medium or the concentration of its individual components caused by a change in the mode due to a decrease in the drop dimensions. It may be shown that, due to the relatively small capacity of the boundary layer (with respect to amount of heat and gases), this assumption does not lead to great errors. The problem of considering the /192 heating of the drop itself will be studied in greater detail below.

2. The temperature and concentration fields are symmetrical. The transport of heat and gases takes place by heat conductivity and by diffusion through concentric "reduced" films. The transport by the Stefanov stream is also considered. In actuality, the assumption regarding the symmetry and the proposed transport scheme would only be valid for small Re and Gr numbers. However, to a great extent, the error is compensated by introducing a thickness of the reduced film

which, in the case of molecular transport, would provide the same heat transfer conditions (or mass exchange) as exist under given conditions of flow by a gas stream around a drop.

For a drop around which air or flue gases pass, we may assume the following at $\mathrm{Re} < 80-100$

$$\mathrm{Nu} = 2\,[1 + c\mathrm{Re}^{m}\,\mathrm{Pr}^{1/3}],$$

where c = 0.3; m = 0.5; Pr -- Prandtl number. For large Re numbers, we may assume the following according to Vyrubov:

$$\mathrm{Nu} = 0{,}54\mathrm{Re}^{0{,}5}.$$

The following is recommended in [8-20]:

$$\mathrm{Nu} = 2 + 2{,}56\cdot 10^{3}\left(\mathrm{Re}\,\mathrm{Sc}\,\frac{gl}{\bar{c}^{2}}\right)^{0{,}6}\frac{\lambda_{r}}{\lambda_{n}},$$

where Sc -- Schmidt number equal to ν/D;

g -- acceleration of gravity;

$l/\bar{c}^{2}$ -- ratio of average molecular mean free path to the mean square velocities;

ν -- kinematic viscosity;

λ_{r}, λ_{n} -- heat conductivity of gas and vapor;

D -- diffusion coefficient.

The Nu number and the diameter of the external surface of the reduced film $d_{пл}$ are related by the following relationship:

$$\frac{d_{пл}}{d_{к}} = \frac{1}{1-\frac{2}{\mathrm{Nu}}},$$

where d_k is the drop diameter.

It must be noted that in calculating the Nu number, the results of experiments on heat exchange without mass transport or with a small influence of this

transport are used. Therefore, we may use the Nu number to determine the reduced film, and further on both the molecular exchange through the latter and the Stefanov stream are taken into account. Naturally such a calculation is arbitrary to a certain extent, since the transverse convective stream must have a certain influence upon the hydrodynamic conditions of the process and upon the Nu number.

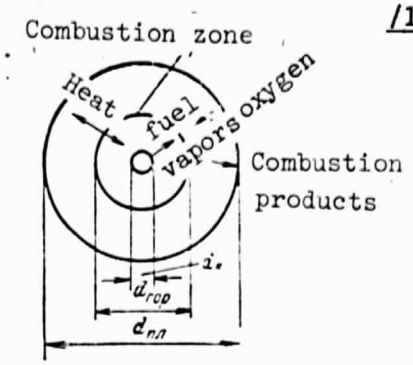

Fig. 8-1. Diagram of diffusion combustion of drop.

3. It is assumed that the kinetic resistance to combustion is negligible as compared with the diffusion resistance. The scheme for this process is shown in Fig. 8-1.

There is a combustion zone on a spherical surface with the diameter d_{rop} located between the drop and the reduced film. Since the kinetic resistance is negligible, the combustion occurs in a very thin layer, almost on the surface. The composition of the mixture on this surface must correspond to stoichiometry. For a purely diffusion process, the concentrations of the oxygen and the fuel vapors must be zero. Actually, oxygen and the fuel cannot exist at the same time unless the reaction takes place. Since the concentration field must be continuous, in the volume between the combustion zone and the drop, there must be only fuel vapors and combustion products, and in the external film -- only oxygen and the combustion products.

All of the reaction heat is given off on the combustion surface and propagated partially within, being used for the evaporation of the fuel and heating of the vapor up to the combustion temperature, and in the direction to the surface of the reduced film, through which the basic reaction heat is supplied (since the heat of evaporation and overheating are returned with the vapors to the combustion surface).

It is not considered in the diffusion theory that when fuel vapors are heated, a certain portion of them are decomposed and produce soot, which burns

outside of the combustion chamber according to laws governing the combustion of carbon particles. This fact could be considered if the decomposition conditions were known.

The calculation of the process using the diffusion theory is reduced to solving the equations for the propagation of heat and transport of matter for each of two zones -- internal (between the drop surface and the combustion surface) and external (before the external surface of the reduced film). /194

A. Transport of heat in the internal film:

$$4\pi r^2\lambda\frac{dT}{dr} = Gq_{исп} + Gc_{пп}(T - T_к). \qquad (8\text{-}1)$$

where r - radius;

$c_{пп}$ - heat capacitance of vapor;

λ - heat conductivity;

T and T_k - temperature and temperature of drop surface;

G - amount of vapor evaporated from a drop per unit time (it is more advantageous to perform the calculation in moles);

$q_{исп}$ - heat of evaporation at the temperature T_k.

If heating of the liquid takes place in the drop along with combustion, then the corresponding amount of heat would have to be added to the heat of evaporation. It is very difficult to introduce an accurate correction. However, if the average drop temperature at the beginning of combustion $T_{нач}$ is known,[1)] then we may approximately assume that the correction for the liquid heating equals:

$$\Delta = c_ж(T_к - T_{нач}).$$

where $c_ж$ -- liquid heat capacitance.

[1)] The problem of correction for preliminary heating will be examined below.

The boundary conditions for equation (8-1):

$$\text{at} \quad r = r_к \quad T = T_к;$$
$$\text{at} \quad r = r_{rop} \quad T = T_{rop}.$$

The following quantities are still unknown: the amount of evaporated heat G, temperature of the drop T_k, temperature of the combustion surface T_{rop}, and radius of the combustion zone r_{rop}.

B. Diffusion of fuel vapors:

$$-4\pi r^2 \frac{DP}{RT} \cdot \frac{dc_т}{dr} + Gc_т = G, \tag{8-2}$$

where D -- diffusion coefficient; /195

P -- atmospheric pressure at which evaporation occurs;

c_T -- portion of fuel vapors in moles per mole of mixture.

The second term in the left side determines the vapor transport by a Stefanov stream. It may be readily shown that the Stefanov stream (see, for example, [8-14]) equals, in volume, the amount of evaporated liquid vapors.

The boundary conditions are:

$$\text{at} \quad r = r_{rop} \quad c = 0;$$
$$\text{at} \quad r = r_к \quad c = c_{тк}.$$

The value of $c_{тк}$ is unequivocally connected with T_k as the pressure of the saturated fuel vapor at this temperature:

$$c_{тк} = f(T_к).$$

C. The propagation of fuel on the external layer between the combustion surface and the surface of the reduced film:

$$-4\pi r^2\lambda\frac{dT}{dr}=Gq_{\text{гор}}-Gc_{pr}T, \qquad (8\text{-}3)$$

where $q_{\text{гор}}$ -- combustion heat of 1 mole of fuel (or 1 kg of fuel, if the calculation is performed by weight).

The boundary conditions:

$$\text{at} \quad r=r_{\text{пл}} \quad T=T_{\text{ср}};$$
$$\text{at} \quad r=r_{\text{гор}} \quad T=T_{\text{гор}}.$$

The temperature of the medium $T_{\text{ср}}$ is assumed to be known.

The second term on the right side of equation (8-3) determines the heat content removed by the Stefanov stream of gases. It is assumed that during the fuel combustion, the number of moles does not change and equals the sum of the moles of air and fuel. Then the Stefanov stream in the external film, just as in the internal film, equals G.

The equation could be written for any other assumption regarding the ratio of the combustion products volume to the reagent volume. It must be noted that even a large area in determining the Stefanov stream in this case cannot greatly influence the final results, since the first term in the right side of (8-3) must always be greater than the second.

D. Diffusion of oxygen: /196

$$4\pi r^2\frac{DP}{RT}\cdot\frac{dc_{\text{к}}}{dr}-Gc_{\text{к}}=\beta G, \qquad (8\text{-}4)$$

where β -- ratio of oxygen and fuel flow rates during combustion. Since the molecular weight of liquid fuels is much greater than the molecular weight of oxygen, β is much greater than $c_{\text{к}}$. Therefore, in the diffusion equation of an external film, we may disregard the Stefanov stream without any great error.

Excluding G from equations (8-1) and (8-2), we may obtain:

$$\frac{\lambda \frac{dT}{dr}}{q_{исп} - c_{pп}(T - T_к)} = -\frac{DP}{RT(1-c_г)} \cdot \frac{dc_г}{dr},$$

or, integrating from the drop surface to the combustion zone (where $c_г = 0$):

$$-\int_{T_к}^{T_{гор}} \frac{\lambda RT}{DP[q_{исп} - c_{pп}(T - T_к)]}\, dT = \ln(1 - c_{гк}). \tag{8-5}$$

If it is assumed that the values of λ and D do not depend on the gas composition, then all of the quantities under the integral sign are functions of only the temperature.[1)] The criterion

$$\frac{a}{D} = \frac{\lambda}{c_{pг}\rho D} = \mathrm{Le} = \frac{\lambda RT}{Dc_{pг}}$$

is close to unity and barely depends on temperature.

Here $c_{pг}$ -- heat capacitance of the gas mixture.

Therefore, equation (8-5) may be rewritten in the form

$$-\mathrm{Le}\int_{T_к}^{T_г} \frac{c_{pг}}{q_{исп} - c_{pп}(T - T_к)}\, dT =$$

$$= -\mathrm{Le}\int_0^{T_г/T_к} \frac{d\frac{T}{T_к}}{\frac{q_{исп}}{c_{pг}T_к} - \frac{c_{pп}}{c_{pг}}\left(\frac{T}{T_к} - 1\right)} = \ln(1 - c_{гк}).$$

---

1)It was shown in [8-19] that close to the drop surface the influence of the fuel vapors on the physical constants is always great. However, even at a relatively short distance from the surface, the gas phase consists mainly of two- and three-atom gases with a small content of hydrocarbon.

Since the ratio $c_{p\,n}/c_{p\,r}$ cannot greatly depend on temperature, integration gives: /197

$$\frac{1}{1+\frac{c_{p\,n}}{c_{p\,r}}\left(\frac{T_{rop}}{T_K}-1\right)}=(1-c_{TK})^{\frac{c_{p\,n}}{c_{p\,r}}Le}. \qquad (8\text{-}6)$$

The partial pressure of fuel vapors on the drop surface may be assumed to equal the pressure of the saturated vapor at the temperature T_K. It may be found from the corresponding curves or tables or may be approximately determined using the formula:

$$pc_{TK}=p_0e^{-\frac{q_{исп}}{R}\left(\frac{1}{T}-\frac{1}{T_0}\right)}, \qquad (8\text{-}7)$$

where P_o is the saturated vapor pressure at the temperature T_o.

From equation (8-6) we may find the drop temperature and the corresponding temperature for different values of T_{rop}. With an increase in the value of T_{rop}, the relative vapor content in the mixture strives to $c_{TK}=1$, and the temperature -- to the saturation temperature. Since the vapor pressure rapidly increases with temperature, for values of T_{rop}, which are usually encountered in practice, the drop temperature differs little from the liquid boiling temperature at the pressure in the chamber. If the calculation is performed using heat exchange, at ordinary drops of the temperature T_{rop} — T_K, which comprise around 1000° C and greater, the inaccuracy in determining T_K at 20 - 30°C and even somewhat higher cannot lead to any great errors. Therefore, for the calculations using heat exchange, we may, in general, use the solution of equation (8-6) and assume that the drop temperature equals the boiling temperature. When determining the partial pressure of the fuel vapors, if it is necessary to introduce a diffusion calculation, only for very high temperatures T, we may assume that $c_{TK}=1$.

In the majority of cases, we may assume that the temperature on the drop surface equals the boiling temperature. Then the system of equations is closed without the diffusion equation (8-2) for the internal layer, and the unknowns T, r, G are determined from equations (8-1), (8-3), (8-4).

The amount of evaporated liquid is determined from the equation (8-1):

$$G\left[\frac{1}{r_к}-\frac{1}{r_{\text{гор}}}\right]=4\pi\int_{T_к}^{T_{\text{гор}}}\lambda\frac{dT}{q_{\text{исп}}-c_{p\,\text{п}}(T-T_к)}.$$

Changing to the dimensionless quantities and assuming that /198

$$\frac{\lambda}{\lambda_к}=\left(\frac{T}{T_к}\right)^n=\vartheta^n,$$

we obtain:

$$\frac{Gc_{p\,\text{п}}^{n+1}}{\lambda_к r_к}\left(1-\frac{1}{R}\right)=4\pi\int_1^{\vartheta_{\text{гор}}}\frac{(c_{p\,\text{п}}\vartheta)^n c_{p\,\text{п}}d\vartheta}{\frac{q_{\text{исп}}}{T_к}+c_{p\,\text{п}}(\vartheta-1)}. \qquad (8\text{-}8)$$

Here

$$R=\frac{r_\text{г}}{r_к};\ \vartheta=\frac{T}{T_к} \qquad \text{and} \qquad c_{p\,\text{п}}=\text{const}.$$

If n is known, then the integral may be calculated for different values of $\vartheta_{\text{гор}}$. The value of n changes from 0.5 - 0.75 and on the average may be assumed to equal 0.6.

For simplification on the order of the first approximation, we may ssume that n = 0.5. Then it follows from equation (8-8) that at

$$\frac{q_{\text{исп}}}{T_к}>c_{p\,\text{п}}$$

$$\frac{Gc_{p\,\text{п}}^{n+1}}{r_к\lambda_к}\left(1-\frac{1}{R}\right)=8\pi\left\{\sqrt{c_{p\,\text{п}}\vartheta_{\text{гор}}}-\sqrt{c_{p\,\text{п}}}-\right.$$

$$\left.-\sqrt{\frac{q_{\text{исп}}}{T_к}-c_{p\,\text{п}}}\left[\operatorname{arctg}\sqrt{\frac{c_{p\,\text{п}}\vartheta_{\text{гор}}}{\frac{q_{\text{исп}}}{T_к}-c_{p\,\text{п}}}}-\operatorname{arctg}\sqrt{\frac{c_{p\,\text{п}}}{\frac{q_{\text{исп}}}{T_к}-c_{p\,\text{п}}}}\right]\right\}.$$

If it is assumed that $\frac{q_{\text{исп}}}{T_к}<c_{p\,\text{п}}$, then we have the following from equation (8-8):

$$\frac{Gc_{p\,n}^{n+1}}{r_к\lambda_к}\left(1-\frac{1}{R}\right)=8\pi\left\{1\overline{c_{p\,n}\vartheta_{гор}}-1\overline{c_{p\,n}}-\frac{1\overline{\frac{q_{исп}}{T_к}-c_{p\,n}}}{2i}\times\right.$$

$$\times\ln\left[\frac{\frac{q_{исп}}{T_к}-c_{p\,n}-c_{p\,n}\vartheta_{гор}+2i\sqrt{c_{p\,n}\vartheta_{гор}\left(\frac{q_{исп}}{T_к}-c_{p\,n}\right)}}{\frac{q_{исп}}{T_к}-2c_{p\,n}+2i\sqrt{c_{p\,n}\left(\frac{q_{исп}}{T_к}-c_{p\,n}\right)}}\times\right.$$

$$\left.\left.\times\frac{1}{1+c_{p\,n}(\vartheta-1)\frac{T_к}{q_{исп}}}\right]\right\}.$$

Here $i=1\overline{-1}$.

To determine the combustion zone radius and the temperature in this zone, /199
we must use the equation for heat transport and matter transport on the external film.

The problem is solved in a somewhat simpler way if we disregard the Stefanov flow. Excluding the quantity G from (8-3) and (8-4):

$$\mathrm{Le}\frac{dT}{q_{гор}c_{p\,г}}=-\frac{dc_к}{\beta}.$$

After integration, we have:

$$\mathrm{Le}\,(T_{гор}-T_{ср})=\frac{q_{гор}}{c_{p\,г}}\cdot\frac{c_{к\,ср}}{\beta}. \qquad (8\text{-}9)$$

It is apparent that:

$$\frac{q_{гор}c_{к\,ср}}{\beta c_{p\,г}}=T_{теор}-T_{ср},$$

where $T_{теор}$ -- theoretical combustion temperature with an air excess temperature of $\alpha = 1$ and for a given temperature of the medium.

Thus, the design temperature of the combustion zone equals:

$$T_{гор}=T_{ср}+\frac{T_{теор}-T_{ср}}{\mathrm{Le}}. \qquad (8\text{-}9')$$

at Le = 1:

$$T_{\text{гор}} = T_{\text{гсор}}. \qquad (8\text{-}9'')$$

Determining $T_{\text{гор}}$ using equation (8-5), we may calculate the value of $r_{\text{гор}}$.

When calculating the drop evaporation rate, we may approximately assume that $r_{\text{гор}} \approx r_{\text{п.п}}$.

Actually, the amount of heat proportional to the heating value of the fuel is discharged over the external film, and over the internal film -- only the heat of evaporation and the fuel vapor overheating, and the overheating heat does not reach the drop surface, but is expended as the temperature increases over the film volume.

The ratio of these flow rates of the fuel is on the order of:

$$\frac{q_{\text{т}}}{q_{\text{исп}} + \frac{c_{p\,\text{п}}(T_{\text{гор}} - T_{\text{к}})}{2}} \approx 20 - 40,$$

i.e.,

$$\frac{d_{\text{п.п}}}{d_{\text{гор}}} \ll \frac{d_{\text{гор}}}{d_{\text{к}}} \qquad \text{and} \qquad d_{\text{гор}} \approx d_{\text{п.п}}.$$

For Nu numbers which are close to 2, i.e., for very large diameters of the reduced film, as compared with the drop diameter, it must be remembered that the surface for the heat transition is much greater in the external film than in the internal film. This partially compensates for the difference in the heat flow rates through these films. /200

At $r_{\text{т}} \approx r_{\text{п.п}}$, the evaporation rate of the drop may be calculated very simply. At first, using equation (8-9'), we determine the temperature of the combustion zone and the quantity $T_{\text{гор}}/T_{\text{к}} = \vartheta_{\text{гор}}$. Then, assuming

$$\frac{r_{\text{гор}}}{r_{\text{к}}} \approx \frac{d_{\text{п.п}}}{d_{\text{к}}} = \frac{1}{1 - \frac{2}{\text{Nu}}},$$

we obtain the following from equation (8-8):

$$\frac{4G}{d_к \mathrm{Nu}} = \frac{4\pi\lambda_к}{c_{p\,п}^{n+1}} \int_1^{\vartheta_{гор}} \frac{(c_{p\,п}\vartheta)^n d(c_{p\,п}\vartheta)}{\frac{q_{исп}}{T_к} + c_{p\,п}(\vartheta - 1)} = F(T_к, \vartheta_к). \qquad (8\text{-}10)$$

or

$$-\frac{dd_к^2}{d\tau} = \frac{4}{\gamma_к} \cdot \frac{\mathrm{Nu}\,\lambda_к}{c_{p\,п}^{n+1}} \int_1^{\vartheta_{гор}} \frac{(c_{p\,п}\vartheta)^n d(c_{p\,п}\vartheta)}{\frac{q_{исп}}{T_к} + c_{p\,п}(\vartheta - 1)} =$$

$$= \frac{\mathrm{Nu}\,\Phi}{\gamma_к}(T_к, \vartheta_{гор}). \qquad (8\text{-}10')$$

For one and the same fuel, with an identical condition of the surrounding medium, the rate at which the drop area decreases (square of the diameter) remains constant in time, if the value of Nu does not change. The latter condition holds for small Nu numbers (i.e., for small drops and small relative stream velocities), when the Nu number is close to two.

A linear dependence of the square of the drop diameter on the evaporation time is called the Sreznevskiy law -- the name of the researcher who first published this law. Designating the right side of equation (8-10') by Ψ, we may write the Sreznevskiy law in the form of the dependence:

$$d_к^2 = d_{0к}^2 - \psi\tau. \qquad (8\text{-}10'')$$

Figures 8-2, 8-3 and 8-4 give experimental curves which confirm the correctness of this law [8-17] in the case of combustion of unit drops. The curves were obtained by measuring the dimensions of incident drops of n-heptane, isooctane and kerosene at a freeze temperature of about 860° C. /201

There are numerous studies in the literature investigating the evaporation rate of drops of different fuels suspended on wires and freely falling. These studies give a great many experimental data showing that the square of the drop diameter actually decreases following a linear dependence on time.

Figure 8-5 shows curves for the change in the square of the drop diameter for different drops of solar oil [8-11]. The small change in the diameter at

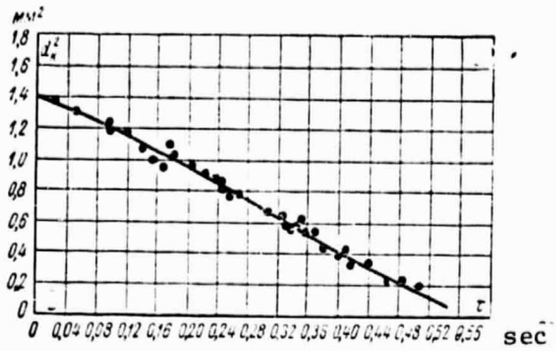

Fig. 8-2. Burning of n-pentane in air at 860° C.

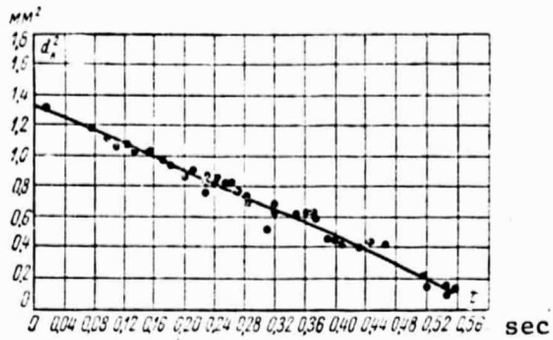

Fig. 8-3. Burning of ethyl octane in air at 860° C.

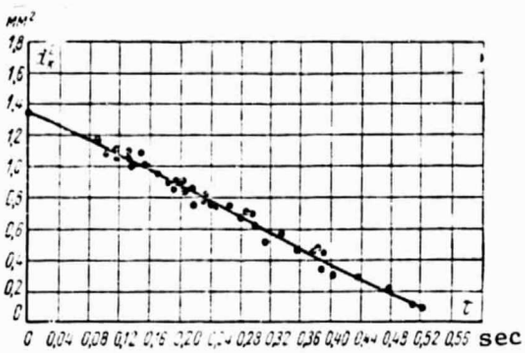

Fig. 8-4. Burning of kerosene in air at 860° C.

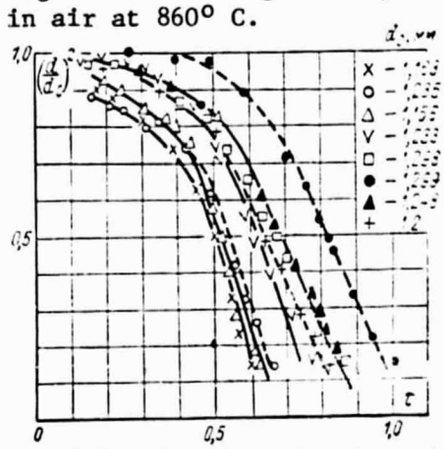

Fig. 8-5. Burning of solar oil with differing initial diameter.

the beginning corresponds to the heating period. However, for large initial drop diameters or for large relative velocities, the value of the Nu number may change very greatly during the evaporation process. Therefore, when the relative velocity is great or when the drops have relatively large dimensions, i.e., when the Nu criterion decreases as the drop evaporates, the curve is smoother than that corresponding to formula (8-10"). It must be noted that natural convection occurs around the large drops at a flame temperature which greatly exceeds the medium temperature, and the Nu number becomes a function of the criterion:

$$\mathrm{Gr} = \frac{gd^3}{\nu^2}\beta\Delta T,$$

where g -- acceleration of gravity, and β -- volumetric expansion coefficient of the gas.

Under the conditions of industrial combustion of fuels, this fact is not of great importance, but may be significant in a laboratory study of the combustion rate of a unit suspended drop. The influence of the Gr number on the combustion rate was examined in [8-16].

Under real conditions at the beginning of the process the drop has a lower temperature and a smaller vapor pressure on the surface than under the corresponding conditions for quasistatic diffusion.

Therefore, a certain amount of time is required for heating the drop to a temperature of T_k, and at the same time evaporation takes place with the heating. As a result, combustion also may occur until the drop surface temperature reaches the value of T_k.

It is very difficult to make a precise calculation with allowance for all /203
these factors. Therefore, a simplified method is usually used to determine the time of preliminary heating, based on the fact that the fuel vapor pressure sharply increases with temperature. Thus, it is assumed that until the temperature T_k is reached on the surface, neither evaporation nor combustion occurs. Then the heating time may be readily determined from the well-known graphs of nonstationary heating of a sphere [8-5, 10].

First, the time is determined which is necessary to reach the temperature T_k on the surface. Using this time, on two other graphs we may find the corresponding temperature of the sphere center and the average sphere temperature (the graphs give the value of the heat received by the sphere which is proportional to the latter). The heating time thus found will be somewhat smaller as compared with the actual time, since evaporation occurs in parallel with the heating, on which a certain amount of heat is expended. In further calculations, this error was partially compensated by the fact that the combustion time in the case of the quasistatic process is somewhat increased, since the calculation is performed for the total weight of the drop.

It is assumed in the calculation that the drop temperature does not change and equals T_k, and the combustion begins when the temperature T is reached on the

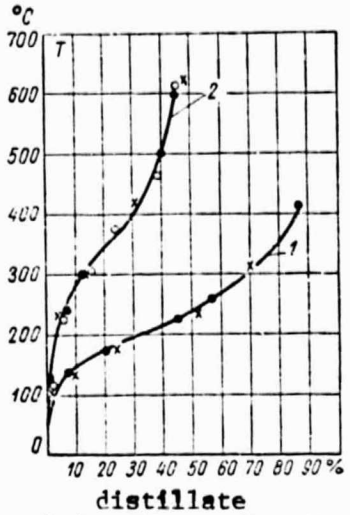

Fig. 8-6. Curves for distillation of solar oil (1) and mazut (2) before combustion (●) and during burning by 7% (O) and by 17% (X).

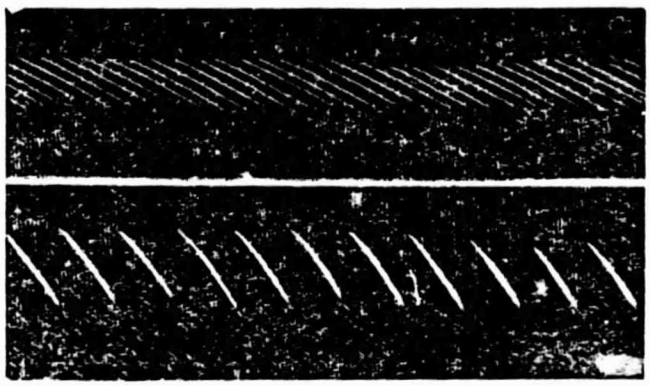

Fig. 8-7. Photograph of tracks of falling hot drops on a film moving horizontally.

surface of the drop. On the average, the drop has a certain temperature $T_{исп}$. This fact may be taken into account by the fact that the calculated heat of evaporation is assumed to be larger than the real one, by the quantity $c_{ж}(T_к - T_{исп})$, where $c_{ж}$ is the liquid heat capacitance.

The fuel is usually not a homogeneous liquid, but consists of many fractions. In the case of slow distillation of the fuel, individual fractions may be distinguished. In the case of rapid evaporation of the fuel drops, two processes /204 occur. On the one hand, evaporation from the surface occurs; on the other hand -- within the drop, diffusion processes occur with which the lightest fuel fractions are added to the surface of the drop. If the diffusion transport within the drop took place much more rapidly than the evaporation process, there would be fractional distillation of the drop. In the opposite case, the internal redistribution has no great influence, and evaporation of a drop of any average composition takes place. The criterion determining the condition for this process must be similar to the Bi criterion in heat exchange and may be described in the form:

$$\mathrm{Bi} = \frac{G}{D_{ж} d_к \gamma_{ж}} = \frac{\pi}{D} \cdot \frac{d d_к^2}{d\tau},$$

where $D_{ж}$ and $\gamma_{ж}$ -- diffusion coefficient and specific weight of the liquid.

At evaporation rates which are characteristic for modes of drop combustion, the values of Bi_r are apparently very high. This is demonstrated in Fig. 8-6, which gives the curves for the distillation of solar oil and mazut before combustion and in the case of burning by 7 and 15% [8-11].

The distillation isobars remain practically unchanged with combustion. It is probable that at the end of combustion a coke residue may accumulate on the drop of such a heavy fuel as mazut. The drop temperature then increases, since the heat exchange surface is larger than the evaporation surface. It may be even be found that within the drop a vapor pressure is produced which is large as compared with the surrounding medium, and the drops disintegrate. These phenomena were observed in certain studies, for example, in [8-11] in experiments of the Laboratory of Thermophysics of the Leningrad Polytechnic Institute. Very frequently, swelling and rupture are observed when large drops of highly viscous mazut undergo combustion. The smaller the drop, the smaller /205
the coke residue and the greater its influence upon the evaporation process.

There are a great number of studies to verify the conclusions of the diffusion combustion theory. A large number of these studies determined the rate of decrease in the dimensions of a drop suspended on a wire. The initial drop dimension could not be smaller than 1.4 - 2 mm.

In other studies, a falling drop undergoing self-ignition in a furnace or burned by a foreign source (spark, small flame), was investigated. The initial dimension of the drop was known. In addition, the initial drop dimension at a certain distance from the point where it was introduced into the furnace was determined, or a study was made of the existence time of a drop of a given initial dimension. For this purpose, the drop was photographed on a film moving horizontally at a given rate. It was possible to determine the drop flight velocity on a kimogram along the drop track. Figure 8-7 gives two kimograms of the flight of burning drops with initial dimension of 300 microns (upper) and 900 microns (lower). Each line on the kimogram represents the track of hot drops entering the chamber in practically identical time intervals. The photographs were taken in natural light.

The data for measuring the evaporation rate (or the existence time of the drop) satisfactorily coincide with the results of calculations using the diffusion theory, if only combustion occurs. In individual cases, in order to make experiment and calculation agree, it is also necessary to take into account such conditions as the heat transfer over the sample, the emission of the medium, the influence of rising flows, the loss by emission into the surrounding medium, etc. A photograph of the flame of a rising drop shows that in actuality the flame around the drop is not completely symmetrical and that the rising forces greatly influence the flame configuration and the temperature zone around the drop. Figure 8-8 shows a photograph of a flame and Schlieren photograph[1] in the case of the combustion of drops of n-heptane and ethyl. The photographs were made in a furnace falling at different velocities in experiments of S. Kumagai and G. Isoda [8-21].

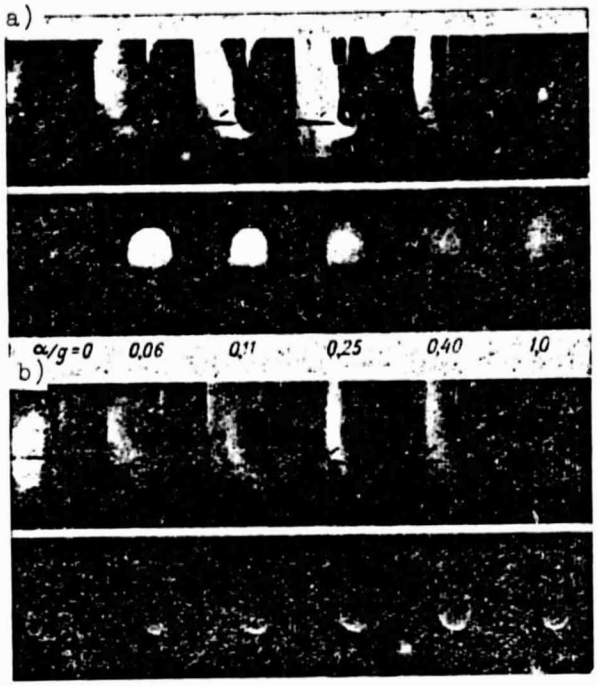

Fig. 8-8. Photographs of drops of n-heptane (a) and ethyl (b), moving with a different α/g ratio.

/206

With a change in the rate of the descending furnace, conditions may be produced when the lifting forces are equalized and the relative velocity between the flow and the drops equals zero. This corresponds to the case $\alpha/g = 0$, where α is the acceleration with respect to the furnace. For a fixed furnace $\alpha/g = 1$.

/207

It may be seen from the photographs that at $\alpha/g = 0$ there is complete symmetry, which is disturbed with an increase in the α/g ratio.

---

[1] The contours of the stream of hot air (or gas) may be seen in the photographs.

For small drops which are customary in furnaces, the influence of the lifting forces is very small.

These experiments are of interest for verifying the agreement between experiment and theory. It is found that at $\alpha/g = 0$, the evaporation rate constant is approximately two times smaller than the theoretical value, and at $\alpha/g = 1$ (in a fixed furnace), the evaporation rate approximately coincides with that determined according to a theoretical scheme for its spherical symmetry.

However, it was found in experiments of other authors [8-13, 14], particularly in experiments with small drops [8-8], that the agreement with theory was better and the calculation gave a smaller evaporation rate than the experiment.

In experiments to determine the combustion zone diameter [8-14], the measured dimension was much less than that calculated according to the diffusion theory.

In individual studies, the flame temperature for the drop was determined. Without discussing the method of the experiments, we must note that the measured temperature was much less than the calculated value.[1)]

Using the diffusion theory, it is necessary to determine whether self-ignition of the vapor-gas mixture for the drop occurs, or whether the drop which is lighted by a foreign source burns, or the flame goes out when the source is removed.

For practical problems, the question of the existence of the drop combustion process is extremely important, as we may see from the following example.

[1)] When determining the value of T_{rop}, the dissociation phenomenon was not taken into account for the calculation. In the opposite case (i.e., with a reduction of the calculated temperature T_{rop}), it was found, as a rule, that the numbers were too low for the drop evaporation rate.

The use of 1% oxygen of the air increases the temperature by approximately 120°C (if there are no heat losses). If, other conditions being equal, the drop is in a medium with an air temperature of about 720°C and an oxygen content of about 15%, and the oxygen content is about 10% in a medium with $t \approx 1300°C$ then according to the kinetic theory the combustion must take place at approximately the same rate, since in both cases the theoretical combustion temperatures are approximately the same. This actually occurs if combustion takes place around the drop. However, experience has shown that in the first case a drop with a diameter of 1.5 - 1.7 mm, even when lighted by a foreign source, is extinguished at a relative flow velocity of about 3 m/sec, whereas at 1300° C the same drop undergoes self-ignition. Thus, the diffusion theory incorrectly determines the combustion rate in the first case, since in actuality the drop evaporation will occur for a given medium temperature. /208

The diffusion theory does not consider the influence of kinetic conditions upon the process. Allowance for the latter is extremely important for determining the possibility of stable drop combustion and for solving the problem of the self-ignition limits. In addition, only with consideration of the kinetic resistance can we solve the problem of whether complete combustion of the fuel vapors occurs within the limits of the reduced film, as is assumed by the diffusion theory, or whether a significant portion of the vapors leaves the film and burns in a furnace area following the laws of gas-mixture combustion.

Section 8-2. Allowance for kinetic conditions of the process

The combustion theory, which takes into account the kinetics of combustion, has been developed by several authors [8-1, 19, 22]. Even with a differing formulation of the problem and differing methods of solution, all of these authors introduce almost the same assumptions for the phenomenon and assume almost identical conditions of the process. One exception is the scheme of Hottel, which will be discussed later.

A consideration of the kinetic resistance to combustion greatly complicates an analysis of the process. Therefore, the following simplifications are

introduced for solving the problem.

The following scheme is assumed:

a) Just as with the diffusion problem, spherical symmetry is assumed and an arbitrary dimension of the boundary film is introduced;

b) Although the reduced film is an arbitrary quantity, and not a real surface which limits the volume within which heat and mass transport occurs, it is assumed that in this arbitrary volume, combustion occurs following the laws of the kinetics of the reaction. A reaction of second order with respect to the concentration of oxygen and fuel is usually assumed; /209

c) The amount of fuel (or oxygen) which undergoes combustion per unit volume per unit time is determined by the equation:

$$N = k_0 c^{-\frac{E}{RT}} \frac{p^2}{R^2T^2} c_{O_2} c_T,$$

where c_{O_2} and c_T are the molar portions (in moles per mole of the mixture) of oxygen and fuel vapors; the quantity k_0 for this fuel changes in accordance with the stoichiometric relationship in a calculation of the oxygen or fuel flow rate;

d) It is assumed that Le = α/D = 1. As will be seen below, this greatly simplifies the calculation;

e) The heat conductivity is selected according to the average value of the temperature and the composition, and is assumed to be constant.

The equation for the heat and oxygen balance for an elementary spherical layer may be written in the following form.

For heat:

$$\frac{d}{dr}\left[4\pi r^2 \lambda \frac{dT}{dr}\right] + 4\pi r^2 N q_{O_2} - \frac{d}{dr}(Gc_{cp}T) = 0. \qquad (8\text{-}11)$$

The first term corresponds to the amount of heat which remains in the layer examined as a result of the heat transferred by heat conductivity. The second determines the input of heat from combustion (q_{O_2} -- heating value referred to oxygen); the third -- heat consumption for heating a convective (Stefanovski) flow D.

For oxygen:

$$\frac{d}{dr}\left[4\pi r^2 \frac{DP}{RT}\cdot\frac{dc_{O_2}}{dr}\right]-\frac{d}{dr}(Gc_{O_2})-4\pi r^2 N=0, \qquad (8\text{-}12)$$

where G, as previously, is the amount of vapor liberated from the drop per unit time (in moles).

Let us use the drop temperature as the beginning for calculating the temperature. The complete enthalpy of a mole of the mixture will be calculated from the sum of the heat content and the heating value of oxygen in the mixture:

$$b = c_p(T - T_k) + c_{O_2}q_{O_2}. \qquad (8\text{-}13)$$

Multiplying equation (8-12) by q_{O_2} and adding with (8-11), we obtain (keeping in mind that $P/RT = \gamma$): /210

$$\frac{d}{dr}\left[\frac{4\pi r^2\lambda}{c_p}\cdot\frac{db}{dr}\right]-\frac{d}{dr}Gb=0. \qquad (8\text{-}14)$$

Since the temperature and oxygen content are known for the medium, then the value of $b = b_\infty$ is known at $r = r_{пл}$. Designating the quantity b_{rk} as the unknown at $r = r_k$, we obtain

$$\frac{b-b_{rk}}{b_\infty-b_{rk}} = 1-\frac{1-e^{-F\left(\frac{1}{r}-\frac{1}{r_{пл}}\right)}}{1-e^{-F\left(\frac{1}{r_k}-\frac{1}{r_{пл}}\right)}}. \qquad (8\text{-}15)$$

where $F = Gc_p/4\Pi\lambda$.

In equation (8-15), the quantities G (or F) and $D_{rк}$ are unknown. Since

$$G = \frac{4\pi r_к^2 \lambda}{q_{исп}} \left(\frac{dT}{dr}\right)_{r=r_к},$$

we may write:

$$G = \frac{4\pi r_к^2}{q_{исп}} \cdot \frac{\lambda}{c_p} \left[\frac{db}{dr} - q_{O_2} \frac{dc_{O_2}}{dr}\right]_{r=r_к}. \qquad (8\text{-}16)$$

Due to the low temperatures close to the drop surface, there is no combustion. The drop surface cannot be penetrated by oxygen (just as for the combustion products) from which it follows that:

$$-4\pi r_к^2 \frac{DP}{RT} \left(\frac{dc_{O_2}}{dr}\right) + Gc_{O_2} = 0. \qquad (8\text{-}17)$$

Replacing DP/RT by λ/c_p, after substituting r = r_k into (8-16), we obtain:

$$G = \frac{4\pi r_к^2}{q_{исп}} \cdot \frac{\lambda}{c_p} \left(\frac{db}{dr}\right) - (q_{O_2} G c_{O_2})_{r=r_к}. \qquad (8\text{-}18)$$

Taking into account equation (8-15), we have:

$$G = \frac{4\pi r_к^2}{q_{исп}} \cdot \frac{\lambda}{c_p} \cdot \frac{(b_\infty - b_{rк}) \frac{F}{r_к^2} e^{-F\left(\frac{1}{r_к} - \frac{1}{r_п}\right)}}{1 - e^{-F\left(\frac{1}{r_к} - \frac{1}{r_п}\right)}} - \frac{(q_{O_2} G c_{O_2})_{r=r_к}}{q_{исп}} \qquad (8\text{-}19)$$

or after the simplest transformation: /211

$$\frac{b_\infty - b_{r\,к}}{q_{исп}\left[e^{\frac{Gc_p}{4\pi\lambda}\left(\frac{1}{r_к} - \frac{1}{r_п}\right)} - 1\right]} - \frac{(q_{O_2} c_{O_2})_{r=r_к}}{q_{исп}} = 1. \qquad (8\text{-}19')$$

Taking into account the fact that the drop temperature (which differs little from the boiling temperature) is used as the beginning of the calculation, i.e., $b_{r\,к} = c_{O_2(r=r_к)} q_{O_2}$, we obtain:

$$G = \frac{4\pi\lambda}{c_p\left[\frac{1}{r_к} - \frac{1}{r_п}\right]} \ln \frac{q_{исп} + b_\infty}{q_{исп} + q_{O_2} c_{O_2 (r=r_к)}}. \qquad (8\text{-}20)$$

Hottel and others in the study mentioned above [8-19] assumed that $c_{O_2 (r=r_к)} = 0$.

Then

$$G = \frac{4\pi\lambda}{c_p\left(\frac{1}{r_к} - \frac{1}{r_п}\right)} \ln\left(1 + \frac{b_\infty}{q_{исп}}\right). \qquad (8\text{-}20')$$

It must be noted that the amount of evaporated liquid does not depend on the combustion kinetics and will be the same as in the case of the diffusion combustion.

More complete calculations confirm this conclusion. However, it is only valid if combustion occurs in the boundary layer independently of whether the combustion occurs completely in the narrow combustion zone, appoximating the purely diffusion case, or whether it occurs in a more or less large section of the reduced film, and the fuel vapors are not completely burned within the limits of this film and are carried away into the furnace.

However, the conditions change sharply if the combustion of the fuel vapors in the reduced film does not occur (the drop is extinguished or does not burn). Then regular evaporation of the fuel drop occurs into the surrounding medium at the temperature of this medium, and not at the combustion temperature.

The complete calculation is much more complex, since it is necessary to solve the problem by a very cumbersome computational calculation. This calculation may be done as follows. The value of the oxygen concentration on the drop surface $c_{O_2 (r=r_к)}$ is first given (with the subsequent correction). We must keep in mind that usually this concentration is either very close to zero (combustion occurs) or differs very little from the case of regular evaporation (no combustion). /212

For the latter case:

$$G = \frac{4\pi\lambda}{c_p\left(\frac{1}{r_к} - \frac{1}{r_п}\right)} \ln \frac{c_p T_{ср} + q_{исп}}{q_{исп}}.^{1} \qquad (8\text{-}20'')$$

After determining G, we calculate the value $b = c_p T + c_{O_2} q_{O_2}$ for all points of the film; however, the values of T and c_{O_2} are known individually only for the drop surface and for the film radius.

For further calculations, we must integrate (8-11) and (8-12), for which it is necessary to determine N. The concurrent solution of the complex nonlinear equations (8-11) and (8-12) and of the equation for the fuel vapors entails great difficulty. It is necessary to use an approximate method, for example, the method of finite differences. We must first give the value of the oxygen concentration on the drop surface $c_{O_2(r=r_к)}$, and determine the evaporation rate. Then we must know the amount of fuel vapors for the surface. The calculation of this quantity may be given from the following considerations.

The medium for the drop surface consists of oxygen, nitrogen, which corresponds to residual oxygen (in the case of combustion in air, this residual nitrogen equals $c_{N_2} = \frac{79}{21} c_{O_2}$), the combustion products c_r, which also contain nitrogen corresponding to the previous reaction, and the fuel vapors $c_т$. We may write (the letter "k" means that the composition is taken for the drop surface):

$$c_{тк} + c_{O_2 к} + c_{N_2 к} + c_{rк} = 1. \qquad (8\text{-}21)$$

Assigning the oxygen concentration, we may determine the nitrogen concentration. To determine the unknown quantities $c_{rк}$ and $c_{тк}$, in addition to equation (8-19), we must have the equation for the material balance for the combustion product; it may be written in the form:

$$\frac{d}{dr}\left[4\pi r^2 \frac{DP}{RT} \cdot \frac{dc_r}{dr}\right] - \frac{d}{dr}(Gc_r) + 4\pi r^2 NS = 0, \qquad (8\text{-}22)$$

---

1) Everywhere the temperature is calculated from the drop temperature, i.e., approximately from the boiling temperature.

where S is the amount of flue gases received from one mole of burning oxygen (together with the nitrogen of this oxygen). Dividing all terms of the equation by S and adding with equation (8-12), as the result of integration we obtain (keeping in mind that close to the drop N = 0 due to the low temperature): /213

$$4\pi r_к^2 \frac{DP}{RT} \cdot \frac{d}{dr}\left(c_{O_2} + \frac{c_г}{S}\right) - G\left(c_{O_2} - \frac{c_г}{S}\right) = B = 0. \tag{8-23}$$

The integration constant B must equal zero due to the nonpermeability of the drop surface for gases.

Further integration of equation (8-23) to $r = r_{пр}$ gives (taking into account that $c_{г\,п.т} = 0$ in the medium):

$$\ln \frac{c_{O_2\,п.т}}{c_{O_2} + \frac{c_г}{S}} = \frac{Gc_p}{4\pi\lambda}\left(\frac{1}{r} - \frac{1}{r_{п.т}}\right). \tag{8-24}$$

Thus, the concentration of the combustion products for the drop surface equals:

$$\frac{c_{г\,к}}{S} = c_{O_2\,п.т} e^{-\frac{Gc_p}{4\pi\lambda}\left(\frac{1}{r_к} - \frac{1}{r_п}\right)} - c_{O_2\,к}. \tag{8-25}$$

Thus, the composition of the gases (for an amount of oxygen known beforehand) is known for the drop surface.

For the fuel vapor, the equation of balance is the same as equation (8-12) and (8-22):

$$\frac{d}{dr}\left[4\pi r^2 \frac{DP}{RT} \cdot \frac{dc_г}{dr}\right] - \frac{d}{dr}(Gc_г) - 4\pi r^2 N\beta = 0. \tag{8-26}$$

where β is the fuel flow rate per one mole of oxygen.

We may use the method of finite differences (dividing all the reduced film by several small layers and beginning from the film surface) to calculate the change of temperature and concentration of the reagent. If in the last analysis

a given medium temperature is not obtained on the film surface, then the assumption regarding the quantity $c_{O_2 K}$ is incorrect and the calculation must be repeated. Figure 8-9 shows schematically the possible distribution obtained as a result of the calculation. It gives the curves for the dimensionless temperatures $\theta = \frac{T - T_K}{T_\infty - T_K}$, the dimensionless concentrations of oxygen $z_{O_2} = \frac{c_{O_2}}{c_{O_2 \infty}}$ and fuel $z_T = c_T / c_{TK}$ as a function of the dimensionless constants r/r_k. In general, two quasistationary solutions are possible. The first is when there is intense combustion within the limits of the reduced film, and the second is when there is no combustion. At low temperatures of the surrounding medium, low concentrations of oxygen, and small drop dimensions, only one solution is possible -- without combustion of the drop (curves with the index 1). In the other extreme case (curves with the index 2), there is only one solution -- the drop undergoes self-ignition. The presence of two equally possible solutions means that the drop does not undergo self-ignition, but in the case of ignition from a foreign source the combustion becomes stable.

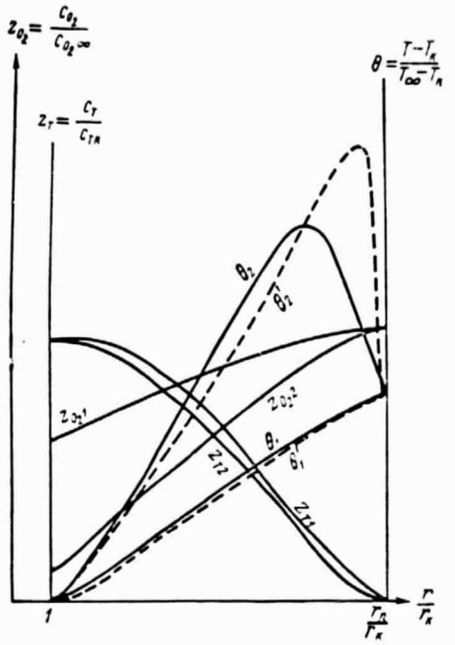

Fig. 8-9. Diagram of the distribution of temperature and concentration of oxygen and fuel in a film around the drop.

/214

The dotted line on the graph shows the temperature curves for pure evaporation θ_1' and diffusion combustion θ_2'. The former almost coincides with θ_1 over the entire range, and the second is close to the curve θ_2 close to the drop. This means that the evaporation rates, calculated with allowance for the kinetic resistance and without considering it -- practically coincide. This explains the fact that using the evaporation rate, the diffusion theory gives results which satisfactorily coincide with experiment, if only combustion occurs.

It must be noted that although kinetic characteristics of the burning mixtures are necessary for several other calculations, particularly for the combus-

tion stabilization, and they are included in many theoretical studies, there are very few data on them in the literature.

The report by Longwell and Wise [8-9] investigated two fuels -- a solvent of naphtha close in composition to heptane, and isooctane. The combustion conditions for both fuels were the same. Their compositions correspond to the formula C_8H_{18}. If we start with the second order of the reaction, as was assumed in previous calculations,[1)] then the value of $E \approx 40{,}000$ is obtained for the activation energy. An approximate value of $8.5 \cdot 10^{13}$ $m^3/sec \cdot mole$ is obtained in the system assumed here when calculating for oxygen combustion. If it is assumed that the reaction for the fuel combustion takes place with the same order, then $k_0' = k_0\beta$, where β is the number of moles of fuel burned per one mole of oxygen. /215

It must be noted that the values of E and k_o, given by different authors, greatly diverge. The values of E given in the literature [8-13] for hydrocarbon are between $26 \cdot 10^3$ and $40 \cdot 10^3$. However, since large values are recommended for k_o for large values of E, the divergence in the calculation is not very great.

As may be seen, the calculation of the kinetic conditions for the process is very complex and contains several simplifying assumptions. The results obtained, correctly reflecting general rules, do not pretend to have sufficient quantitative accuracy. Therefore, approximate themes are of interest which make it possible to consider the influence of the most important factors. Using the experimental data, we may obtain more or less reliable numerical characteristics for the process.

Spaulding [8-12] started with the following concepts. With an increase in the flow rate, the amount of evaporated liquid increases, and for the vapor combustion, a thicker reaction zone is necessary. The following dependence (at $Pr \approx 1$)

---

1) It was shown in this study that somewhat better results may be obtained by assuming the order of the reaction is 1.8, which, however, is less suitable for all the calculations.

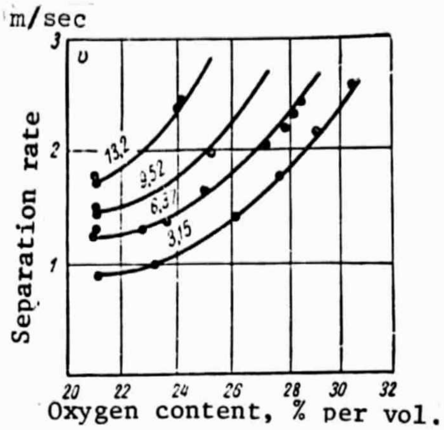

Fig. 8-10. Separation rate v as a function of sphere diameter d and oxygen content in stream at room temperature.

Numbers on the curves -- d, mm

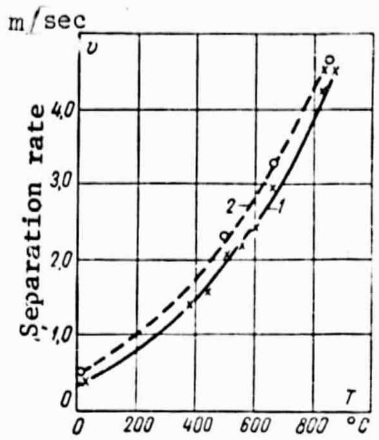

Fig. 8-11. Separation rate for large (1.5-1.7 mm) drops of kerosene (1) and benzene (2) as a function of the medium temperature.

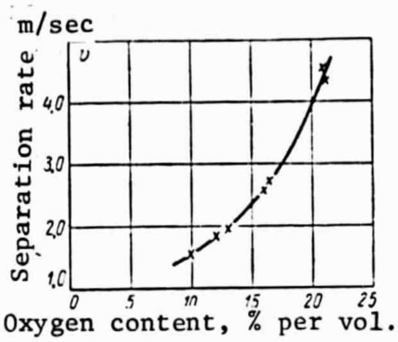

Fig. 8-12. Separation rate for large (1.5-1.7 mm) drops of kerosene at t = 870° C as a function of oxygen concentration in stream.

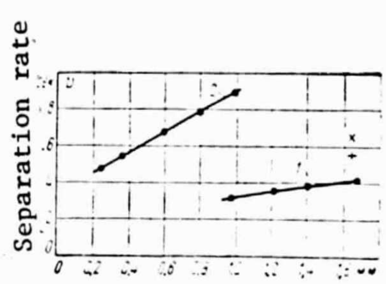

Fig. 8-13. Influence of drop diameter on combustion separation rate at $t \approx 870°$ C.

is assumed for the evaporation rate from a unit of surface:

$$\frac{G}{F}=\frac{\mu}{d_{\kappa}}0{,}53L^{[illegible]}\cdot \mathrm{Re}^{0{,}5}, \quad (8\text{-}27)$$

where L is a quantity depending on other evaporation conditions, particularly the fuel consumptions for vapor heating and liquid evaporation. Equating the flame propagation rate in a laminar flow $S_{л}$ to the flow velocity of the vapor, Spaulding obtained for the separation:

$$S_{л}\varrho\beta<\frac{G}{F}=\frac{\mu}{d_{\kappa}}0{,}53L^{[illegible]}\cdot \mathrm{Re}^{0{,}5}. \quad (8\text{-}28)$$

Here $\rho\beta$ determines the amount of vapor per unit volume of mixture. For a given fuel and given composition of the medium and its temperature, the left side of (8-28) changes very little and the right side is approximately proportional to $\sqrt{v/d}$. Thus, the separation characteristics must have the form: v/d = const. According to the Spaulding experiments, this assumption is confirmed to a great extent: /216

Diameter of porous sphere moistened with fuel, d, mm.	Value of separation characteristic v/d in the case of flame separation, 1/sec.	Diameter of porous sphere moistened with fuel, d, mm	Value of separation v/d in the case of flame separation, 1/sec.
26.0	90	10.1	98
19.7	91	7.0	101
12.8	97		

It must be noted that the experiments of certain authors do not confirm this dependence. In particular, Ageston and others [8-15] give a separation dependence with the form $v/\sqrt{d}$ = const, and the computed values of v/d are greater than those of Spaulding by a factor of 1.5 - 2.5.

Figure 8-10 gives the curves for the dependence of the separation rate on the sphere diameter and the oxygen content in the medium at room temperature.

Below we give certain materials obtained at the LPI by F. A. Agafonov and M. A. Burevich. /217

Figure 8-11 gives the dependence of the separation rates for large drops of benzene and kerosene upon the medium temperature (air). Figure 8-12 gives the dependence of the separation rate for large drops of kerosene on the oxygen content at a medium temperature of about 870° C. Figure 8-13 gives the curves for the dependence of the separation rate on the drop diameter at a flow temperature of about 870° C. Curve 1 refers to the large drop suspended on a quartz wire; Curve 2 -- to a freely falling small drop.

It must be noted that in the first case, the drop is located on the initial section of the gas stream discharged in the laboratory. The surrounding medium and the enclosure are at room temperature. In the second case, a study was made of a drop moving in the furnace, whose walls have a higher temperature than the stream. In the first case, the conditions favor separation of the flame more than in the second case. When measures were taken to reduce the drop heat exchange by installing a heated tube, the separation rate greatly increased (to experimental point noted by the sign "+" for a tube temperature of 400° C and the sign "X" for a tube temperature of 700°C. It may be assumed that with an increase in the enclosure temperature, the curves converge better. Thus, the heat exchange by emission with the walls influences the flow separation rate. This may be important for large drops suspended on a wire, i.e., under conditions which occur for many researchers.

CHAPTER NINE /218

COMBUSTION OF ATOMIZED LIQUID FUEL IN A FLAME

Section 9-1. General Assumptions

In examining the problem of the combustion of a unit drop, we have assumed that the temperature of the surrounding medium and its composition are given. Although the combustion in the flame is reduced in the last analysis to the evaporation of individual drops and the combustion of the vapors produced, the solution of this problem is much more difficult. In the general case, we would have to examine the following processes:

a) The motion of individual fractions of atomized fuel in a gas flow;

b) Evaporation of drops of different dimension;

c) The distribution in the gas flow of the liquid phase and the hot gases.

As was indicated above, not all the vapors of each drop burned completely in the gas phase of the boundary layer, as is assumed by diffusion.

For many smaller drops, there is no combustion, even at high temperatures of the medium. For other drops, only partial combustion of the vapors occurs in the combustion zone. The remaining vapor is propagated by turbulent diffusion in the medium and burns according to the same laws as a gas fuel. The distribution of the liquid and vapors in the gas flow determines the condition for the formation of the hot mixture.

In the case of pneumatic atomization, together with fuel, air is supplied to the spray nozzle which is necessary for the combustion. In the case of mechanical atomization, and even in the case of vapor atomization, the air is supplied individually. Thus, only in rare cases (as, for example, in Martensite furnaces) the air is so heated that the mixture ignites by itself, without any special measures.

In the majority of cases, combustion stabilization is achieved by adding combustion products to the root of the flame from the furnace at room temperature. Due to this, a portion of the mixture exists under temperature conditions which provide for its ignition. Further propagation of the flame occurs as the result of turbulent exchange in the stream, similar to the propagation of the flame in the case of the gas fuel, although it is more complex due to the nonhomogeneity of the hot mixture.

The return of the combustion products to the flame root is partially done /219
by injection of the entering stream. In many cases, the reverse stream is achieved by twisting the entering air with a blade register or tangential input. Rarefaction is produced in the center of the twisted stream, causing inverse currents. In certain furnace devices, special stabilizers are used in the form of poorly stream-lined bodies placed on the flow path. In the stern zone of such bodies,

there is always a recirculation zone which provides for combustion stabilization.

In the general case, the solution of the problem entails insurmountable difficulties, not only due to purely mathematical complexities. For certain phenomena which comprise the process, it is difficult to formulate the physical problems specifically in a closed form. For example, it is sufficient to note that at present there is not a unified point of view with respect to the simpler problem of the mechanism of turbulent flame propagation in a flow of hot gases which is first mixed. Therefore, an experimental study of furnace devices with different purposes is of great importance, as well as the accumulation of material on existing devices.

On the basis of this material, structural forms of furnace devices for different purposes were developed, and norms were stipulated for determining their dimensions. Thus, for example, the dimensions for the furnace of steam boilers are presently selected based on the stresses per unit volume of the furnace. For the combustion chamber of gas turbines, one usually starts with the stress per unit area of the transverse section of the furnace as applied to 1 atm pressure. It is considered that the residence time in the chamber and the stress are proportional to the pressure. Calculated norms reflect not only the combustion process, but also factors such as the permissible head losses, the required cooling of the gases in the furnace part of the boiler, purely technological requirements, etc.

Along with that, in order to analyze the experimental data and to generalize them, a theoretical examination of individual problems of the combustion of a liquid fuel flame is extremely important even in their simplest formulation. In almost all calculations it is assumed that the drop volumetric concentration in the furnace is usually so small that the indirect mutual influence of the drop during combustion may be disregarded. There are several experimental studies /220 which, in general, confirm the correctness of this assumption. These experiments were performed with large drops suspended on wires during their combustion in relatively cold air. It may be expected that for small drops which are characteristic for furnace devices and at high temperatures of the medium, the influence of the

drops will be smaller.

We may point out the study by Rex, Fuhs, Penner [9-13] with respect to this problem. This study showed that for a system of drops, such as for a unit drop, there is a linear dependence between the square of the drop diameter and time:

$$-\frac{dd_k^2}{d\tau} = \sigma.$$

However, the value of σ has a maximum at a certain distance between the drops. This is explained by the opposite influence of two factors. The convergence of the drops, on the one hand, decreases the heat losses, and on the other hand worsens the approach of the oxygen to the surfaces which are very close together.

Section 9-2. Combustion stabilization

Atomized liquid fuel and air enter the furnace from the spray nozzle (and in the case of mechanical atomization, from the spray nozzle and air register or another device). Only in exceptionally rare cases (for example, in a Martensite furnace), the air is heated so much that it causes evaporation and ignition of the fuel without additional heating. Usually, ignition requires evaporation of a certain part of the fuel and heating of the mixture of fuel vapors with air to a temperature at which the combustion would liberate more heat than is necessary for evaporating the remaining fuel and covering the losses to flame cooling. Then the mixture temperature will increase without input of heat from the outside, ignition occurs, and further combustion will be determined to a significant extent by the fact that the aerodynamic conditions provide the necessary supply of oxidant to the fuel, whatever the evaporation rate of individual drops.

For combustion stabilization, certain, frequently very bounded, volumes may be removed in the furnace devices. Simple calculations of the possible heat exchange by emission between the furnace volume and the ignition zone show that, due to this emission, only a small part of the heat required may be supplied due to this emission. Usually, it can be disregarded. In the overwhelming majority of cases, the mixture is prepared by mixing the combustion products of the flame

/221

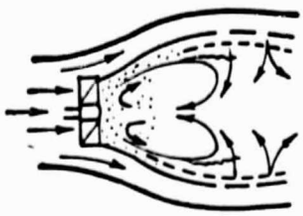

Fig. 9-1. Diagram of register combustion chamber of gas turbine.

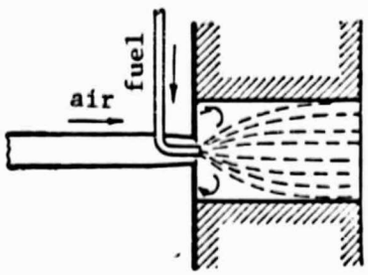

Fig. 9-2. Simplest furnace device for burning liquid fuel.

with it. For this purpose, an inverse flow of hot gases is produced toward the flame root due to injection, organization of the reduced pressure at the root of the incoming stream, etc.

Figure 9-1 shows a diagram of the register combustion chamber of a gas turbine. When the primary air is twisted, a zone of reduced pressure is formed in the center. This causes the occurrence of inverse streams consisting of combustion products at a high temperature. Figure 9-2 shows the simplest furnace for liquid fuel: the stream emanating from the spray nozzle injects hot combustion products from the furnace volume.

Introducing certain assumptions which simplify the formulation of the problem and its solution, we may clarify the combustion stabilization conditions under certain other conditions.

Examining a similar problem regarding ignition of a coal dust flame, G. F. Knorr [9-3] determined the amount of recirculating hot gases based on the requirement that the mixing with them would provide the heating of the fuel and primary air to 700 - 800° C. It is very apparent that the less the primary air which is supplied, i.e., air supplied together with the atomized fuel, the more readily does ignition take place. However, the mixture formation at further stages of the process is complicated.

The study [9-1] examines the ignition of a poly-fraction of liquid fuel, under conditions described below. Drops of fuel and air at a given ratio $1/\alpha_1 L_{теор}$ /222

enter the furnace, where α_1 is the excess of the primary air as opposed to the theoretically required quantity $L_{теор}$ (frequently $\alpha < 1$). Combustion products with oxygen content of $c_{O_2 п}$ and at a given temperature are added to this mixture. The process is studied for different ratios of the consumption of the fresh mixture and the hot combustion products. It is assumed that within the limits of each transverse cross-section of the flow, the mixing is complete and the composition and temperature are identical. It is assumed that the liquid and gas have identical rates. In this case, the Nu number would equal 2 for all the drops. In order to introduce the correction for a certain relative motion, we may assume that the value of Nu is somewhat greater than 2 (for example, Nu = 2.5), but identical for all the drops. Under these conditions, the degree of fuel evaporation is determined in a given time (or in a given volume) and the possibility of ignition is established. For a constant Nu value, for all of the drops the rate at which the square of the radius decreases is the same, and depends only on the value assumed for the Nu number, the type of liquid and the temperature of the gas stream and the drop, i.e.,

$$-dr_к^2 = \frac{Nu}{\gamma_к}\Phi(T_{ср}, T_к)\,d\tau, \qquad (9\text{-}1)$$

where, as follows from the equation (8-10') given above,

$$\Phi = \int_{T_к}^{T_{ср}} \frac{\lambda\,dT}{q_{исп} + c_p(T - T_к) + c_ж(T_к - T_{нач})}.$$

For any two initial radii of the drops $r_{к\,i0}$ and $r_{к\,j0}$, for one and the same moment of time $\Delta\tau$, we must have :

$$r_{к\,i0}^2 - r_{кi}^2 = r_{к\,j0}^2 - r_{к\,j}^2, \qquad (9\text{-}2)$$

if only one of these drops does not evaporate completely earlier than the time $\Delta\tau$.

It is convenient to perform the calculation for the largest drop, whose initial radius may be designated as $r_{к10}$, and whose current radius -- by $r_{к1}$. Let us set:

$$\frac{r_{\kappa i}}{r_{\kappa i0}} = x \text{ and } \frac{r_{\kappa i0}}{r_{\kappa i0}} = y < 1.$$

Let us follow the liquid evaporation process. If at a certain moment of time τ a drop has completely evaporated with the initial radius $(r_{\kappa j0})_\tau$, then from each drop greater than $(r_{\kappa j0})_\tau$ a portion of the initial weight remains equaling $(r_{\kappa i}/r_{\kappa i0})^3$. The relative weight of a drop with a dimension greater than $r_{\kappa j0}$ is R_{i0} in the initial atomization flame. /223

At the examined moment of time, a portion of the initial fuel remains in liquid form, which equals:

$$M = \int_{r_{\kappa j0\tau}}^{r_{\kappa i0}} \frac{dR_{i0}}{dr_{\kappa i0}} \left(\frac{r_{\kappa i}}{r_{\kappa i0}}\right)^3 dr_{\kappa i0}. \tag{9-3}$$

The fractional composition in initial atomization is determined either by the condition:

$$R_{i0} = e^{-bd_{\kappa i0}^m}, \tag{9-4}$$

where b and m are constants characterizing the spray nozzle and assumed to be known, and $d_{\kappa i0} = 2r_{\kappa i0}$ -- initial drop diameter, or by the condition:

$$R_{i0} = e^{n y^m}. \tag{9-5}$$

The quantity $d_{\kappa i0}$ may be selected only arbitrarily. We may select the maximum calculated dimension, for example, as that corresponding to a certain small, arbitrarily selected residue R_{10}, equaling 1%, 0.5%, etc.

When solving the problem of stabilization, it is important to follow the evaporation of a comparatively small portion of the fuel. We may show that even with evaporation up to 80-90% of the fuel weight, the calculation gives practically identical results when R_{10} is selected in very wide limits. If we assume R_{10} = 1%, then n = 4.6.[1] Formula (9-3) gives the following with

[1] For other R_{10}, the value of n changes, but the value of y changes so that the results of further calculations practically coincide.

allowance for (9-2) and (9-5):

$$M = mn \int_{1-x^2}^{1} \frac{e^{-ny^m}}{(1-x^2)^{1/2}} [y^2 - (1-x^2)]^{1/2} dy. \qquad (9\text{-}6)$$

Thus, if the quantity m is known, then for a given value of x -- the current relative dimension of the maximum drop -- we may determine what portion of each kilogram of initial fuel weight does not evaporate.

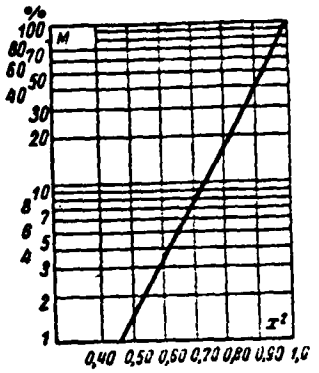

Fig. 9-3. Dependence between percent of nonevaporated fuel M and relative dimension x^2 of the largest drop. /224

Figure 9-3 gives the relation between x^2 and M according to formula (9-6) for m = 2.5 and n = 4.6. We must then determine the process of the evaporation of a drop with maximum dimensions.

The conclusions reached above refer to the case when all the drops are preliminarily heated to their surface temperature which is close to the boiling point (more correctly, the temperature of the "wet thermometer").

Therefore, we should establish the time of preliminary drop heating before their evaporation. This may be done for drops of each dimension, using the well-known graph on heating in a nonstationary mode, as was indicated when examining the combustion of a unit drop.

However, a determination of the drop heating time for each of the dimensions would greatly complicate the calculations, since the heating time changes with diameter, and consequently, for a precise calculation using equation (9-6), we would have to start not with the initial flame distribution in terms of the fractional composition, but with the atomization which will occur at the beginning of the evaporation of the largest drops. Individually, we would have to determine the preliminary evaporation of drops of different dimensions.

Since the heating time is relatively small, even a comparatively large inaccuracy in the calculation of the process during this period has no great influence on the result of the entire calculation. In this connection, we may

perform the calculation not for the real distribution of drops by dimensions, but by the average dimension, assuming a monofractional composition for the zone of preliminary heating. Thus, we may comparatively simply determine both the time of preliminary heating, and the change in the gas stream temperature due to the consumption of heat for the drop heating.

In addition, we may determine the average temperature of the fuel at the beginning of evaporation, when the drop surface is heated to the temperature of the "wet thermometer." This is necessary for introducing a correction for the evaporation heat into the evaporation calculation. The calculated evaporation heat is assumed to equal: /225

$$q_{\text{р. исп}} = q_{\text{исп}} + c_{\text{т}}(t_{\text{м}} - t_{\text{н}}),$$

where $q_{\text{исп}}$ -- actual evaporation heat; $c_{\text{т}}$ -- heat capacitance of liquid fuel; $t_{\text{м}}$ and $t_{\text{н}}$ -- the temperature of the "wet thermometer" (close to the boiling point) and the average liquid temperature at the end of preliminary heating -- usually in the case of high temperature furnaces, this differs little from the initial temperature of the atomized fuel.

The calculation of the basic zone is carried out for the evaporation of a drop of maximum dimensions using equation (9-1), just as when calculating the combustion of a unit drop.

The temperature $T_{\text{ср}}$ is determined from the heat balance for a gas stream. It is necessary to establish the mixing of air entering with the fuel and the returning gases drawn in with the stream.[1)] We must also consider the heat consumption for fuel evaporation, the liberation of heat from combustion, and the heat losses to heat exchange with the surrounding volume. For the section Δz, to which the time $\Delta\tau = \Delta z/v$ corresponds (where v -- average stream velocity in

---

[1)] As has already been indicated, it is assumed that the composition and temperature are equal in each cross-section, i.e., the mixing occurs simultaneously and uniformly with respect to each cross-section.

the given section) the heat balance is determined by the condition:

$$Gc_pT_{ср} + \frac{\Delta G}{\Delta z}\Delta z c_p T_п + \\ + k_0 e^{-\frac{E}{RT}} \overline{T_{ср}} c_т^m c_к^n q_т F \Delta z = \left(G + \frac{\Delta G}{\Delta z}\Delta z\right) \times \\ \times (T_{ср} + \Delta T_{ср}) - B\frac{\Delta M}{\Delta z}\Delta z \times \\ \times [q_{исп} + c_п(T_{ср} - T_{кип}) + c_т(T_{кип} - T_{нач})] + Q_{потерь}, \quad (9\text{-}7)$$

where G -- gas consumption;

ΔG -- change of this consumption in the segment Δz;

$T_{ср}$ -- temperature of the medium carrying the fuel;

$T_п$ -- temperature of the gas supplied to this medium;

B -- liquid consumption;

ΔM -- amount of liquid evaporated in the section examined per unit consumption;

$Q_{потерь}$ -- heat losses in the section Δz.

Some terms of the balance may be so small that they cannot be taken into account. Thus, frequently the heat consumption for fuel evaporation and vapor heating is of no importance. In the case of forced processes, we may disregard the heat consumption for cooling. /226

Dividing the volume studied of the furnace space into individual small sections, we may perform an approximate consecutive calculation for sections. We first determine $\Delta x^2 = \Delta r_{к1}^2 / r_{к10}^2$, assuming that the temperature of the medium in (9-1) equals the final temperature of the previous section. When selecting the temperature, we may take into account the mixing of the gases in the basic stream, which must give a more accurate result. We then determine ΔM using the equation (9-6) and calculate the concentration of the fuel vapors and oxygen vapors at the end of the section examined. In addition, using equation (9-7) we find the temperature at the end of this section. Using this method, we calculate the process along the stream for the volume examined and determine whether there is ignition which is characterized by a sharp increase in temperature due to a relatively large value of heat liberation from the fuel vapor combustion, i.e., the quantity:

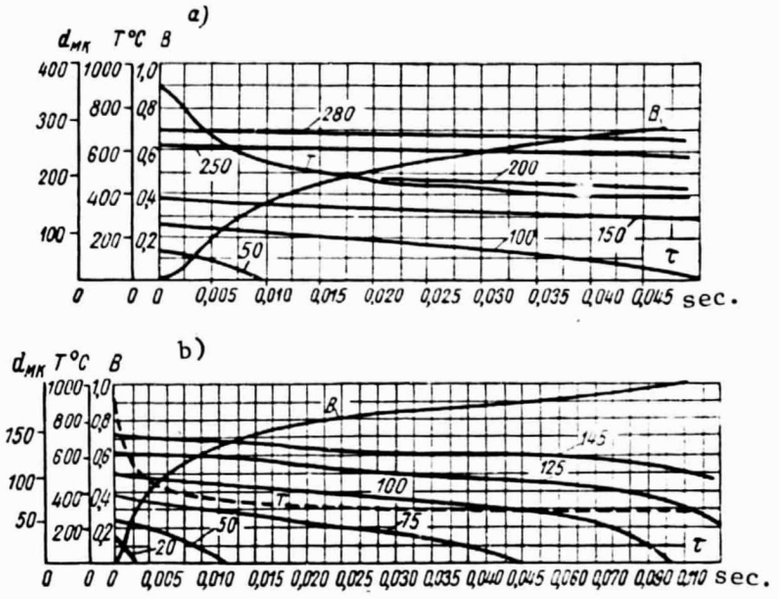

Fig. 9-4. Calculated dependences of the temperature T, of the relative amount of evaporated liquid B = 1 —M and drop diameter d on time: a — $d_{ср.\,об}$ = 96.5 micron; b - $d_{ср.\,об}$ = 50 micron.

Numbers on the curves -- d, micron

$$k_0 e^{-\frac{E}{RT}} \sqrt{T_{ср} c_1 c_к q_г}.$$

We may refine the calculation, repeating it over the sections with allowance for the change in temperature and concentration of fuel and oxygen on the basis of the first calculation. However, the basic assumptions contain simplifying statements which by themselves give a calculation scheme with large deviations from the actual process conditions. Thus, it is not really valid to describe the calculation itself, because it is in the nature of a tentative determination of the ignition conditions. Calculations of this type may be particularly useful for obtaining comparative indices regarding the influence of individual parameters upon the process, such as the excess of primary air, the amount of recirculating gases, the dimensions of the ignition zone, type of fuel, etc.

Figure 9-4 shows the results of calculations on the evaporation of drops of solar oil in an aerosol machine whose purpose is to completely evaporate the liquid in the shortest time possible without causing ignition. The calculations were performed under the following conditions: The exponent m for the spray nozzle equals /227

2.5; the initial gas temperature T_r = 920° C; the gases were obtained from combustion of liquid fuel at an air excess of α = 2.65; 1.15 kg gases were consumed per 1 kg of solar oil supplied by the spray nozzle. There is no ignition for an average volumetric initial diameter of the drop of $d_{cp.o6}$ = 96.5 microns (Fig. 9-4,a), or at $d_{cp.o6}$ = 50 microns (Fig. 9-4,b). The evaporation occurs more intensely in the case of a finer atomization. Correspondingly, the stream temperature decreases more rapidly. The calculations show that it would be necessary to raise the gas temperature to approximately 1150° C for ignition. Although the calculation is arbitrary and based on rather rough assumptions, the experiment shows a fairly good agreement between the calculated and actual ignition modes.

Section 9.3. Calculation of combustion for certain simplified schemes /228

Several simplifying assumptions are sometimes used to facilitate the calculation. Below we examine such assumptions.

Evaporation of monofractional flame. Let us consider the case of liquid fuel combustion in the case of its monofractional atomization [9-15]. We select the drop diameter so that for a given number of drops, their surfaces coincide with the actual surface of the poly-fractional atomization:

$$d_{cp}^2 = \frac{\sum n_i d_i^2}{\sum n_i}.$$

We assume that combustion takes place at a constant temperature. For the initial combustion stage, this assumption must greatly diverge from actual conditions. For the basic section of the combustion zone, this procedure is permissible, although it is impossible to give a valid method for selecting the calculated average temperature. We also assume that the velocity of the drop and the stream are identical. In actuality, as already indicated, a portion of the vapors immediately burns in the flame of an individual drop, and a portion -- in the medium following the laws of homogeneous gas consumption. For simplification, we shall now assume that all of the combustion occurs in the gas phase, whose composition is identical within the limits of each transverse cross-section of the stream,

i.e., we assume that the liberated fuel vapor is instantaneously and uniformly distributed over the stream cross-section.

Thus, we may individually examine the evaporation of drops and the combustion of the vapor produced. The rate of vapor liberation must be calculated according to the laws of simple evaporation at low medium temperatures and according to the laws of diffusion combustion at high medium temperatures, when combustion occurs in the zone of individual drops.

It was shown in Section 8-2 that the calculation according to the diffusion combustion scheme rather correctly determines the drop evaporation rate, if combustion actually occurs in its boundary layer, but incorrectly reflects other aspects of the process.

In spite of these simplifications, the problem remains very complex, and new assumptions are necessary to solve it, which will be introduced as needed.

A change in the square of the drop diameter $dd^2/d\tau$ must be constant both in the case of regular evaporation and in the case of diffusion combustion, if only the Nu number remains constant: /229

$$-\frac{dd^2}{d\tau} = \sigma = \frac{\mathrm{Nu}\lambda\Delta T}{q_\tau(q_{\text{исп}} + c_n\Delta T)}. \tag{9-8}$$

Here ΔT is the temperature drop between the drop and the surface of reduced film, which depends on the temperature of the medium and on whether combustion occurs in the boundary layer of the drops.

At α = const:

$$d_0^2 - d^2 = \sigma\tau \tag{9-9}$$

and

$$f = \frac{d^2}{d_0^2} = 1 - \frac{\sigma\tau}{d_0^2}. \tag{9-10}$$

The relative portion of evaporated fuel equals:

$$1-\left(\frac{d}{d_0}\right)^2=1-f^{2/3}. \qquad (9\text{-}11)$$

If a certain portion w of all of the fuel burns in the vapor-formation phase, then the relative amount of fuel remaining in the vapor-formation phase equals:

$$W=1-f^{2/3}-w. \qquad (9\text{-}12)$$

In the majority of cases, when examining the kinetics of fuel combustion in the gas phase, we may write the conditions in the form:

$$\frac{dq}{d\tau}=kc_{\text{т}}^{m_1}c_{\text{к}}^{m_2}. \qquad (9\text{-}13)$$

The content of vapors of fuel and oxygen is calculated separately. In certain cases it is convenient to regard all of the fuel as a single-component mixture. We may then write this dependence in the form:

$$\frac{dq}{d\tau}=k_1c_{\text{т}}^{m}, \qquad (9\text{-}13')$$

where

$$m=m_1+m_2;\ k_1=k\left(\frac{c_{\text{т}}}{c_{\text{т}}}\right)^{m_1}\left(\frac{c_{\text{к}}}{c_{\text{т}}}\right)^{m_2}.$$

Sometimes it is more convenient to assume that the fuel vapor concentration is determinant. Then: /230

$$\frac{dq}{d\tau}=k_{\text{т}}c_{\text{т}}^{n}; \qquad (9\text{-}13'')$$

Thus:

$$n=m_1+m_2 \text{ и } k_{\text{т}}=\left(\frac{c_{\text{к}}}{c_{\text{т}}}\right)^{m_2}k.$$

In the regions of the flame where the amount of oxygen is rather large (this occurs for large excesses of air in the furnance, for example, in the combustion chambers of gas turbines and in the initial sections of the flame), in general we may assume that the combustion rate is only determined by the fuel concentration.

An expression of the type (9-13") will be used below. In the general case, $c_к/c_г$ may change over the length of the furnace. We shall use the average value of $c_к/c_г$, assuming $k_г$ is constant at a constant temperature.

Then the combustion rate may be written in the form:

$$\frac{d\omega}{d\tau} = K(1 - f^{3/2} - \omega)^n, \tag{9-14}$$

where $K = k(c_{г0})^{n-1}$;

$c_г$ -- initial fuel concentration.

Very frequently we assume n = 1, and then k = K. Replacing $d\tau$ in equation (9-10) by $\frac{d_0^2}{\sigma} df$, instead of equation (9-14), we may write:

$$\frac{d\omega}{df} = \frac{Kd_0^2}{\sigma}(\omega - 1 + f^{3/2}) = b(\omega - 1 + f^{3/2}), \tag{9-15}$$

where the criterion $b = Kd_0^2/\sigma$ characterizes the ratio of the fuel evaporation time to the fuel vapor combustion time in the case of simultaneous evaporation of drops in the gas phase [with the factor n -1)]. At n = 1 the solution of equation (9-15) has the form:

$$\omega = 1 - f^{3/2} + \frac{3}{2b}(e^{-b(1-f)} - \sqrt{f}) -$$

$$- \frac{3\sqrt{\pi}}{4b^{3/2}} e^{bf} \frac{2}{\sqrt{\pi}} \left[\int_0^{\sqrt{b}} e^{-x^2} dx - \int_0^{\sqrt{bf}} e^{-x^2} dx \right]. \tag{9-16}$$

The value $2/\sqrt{\pi}\int_0^a e^{-x^2}dx$ of the integrals of the errors may be found in the handbooks of mathematical tables. /231

Equation (9-16) gives the relationship between the quantity f characterizing the evaporation of the liquid phase, and the quantity w, determining the degree of combustion of all the fuel as a function of the parameter b. At b = 0, i.e., in the case of instantaneous evaporation of the liquid, f = 0, and equation (9-14) gives the following for the first order of the reaction:

$$\frac{d\omega}{d\tau} = K(1 - \omega). \tag{9-14'}$$

If we assume that the stream moves over the length of the furnace at a constant velocity v_z, the time which the gases remain in the furnace with the length L equals $\tau_{np} = L/v_z$ and $d\tau = dz/v_z$, then equation (9-14') changes into the form:

$$\frac{d\omega}{d\left(\frac{z}{L}\right)} = \frac{LK}{v_z}(1-\omega) = a(1-\omega). \tag{9-17}$$

where a characterizes the relationship between the gas residence time in the furnace and the combustion time.

We may introduce the following relationship, in accordance with equation (9-10), into (9-16) instead of f:

$$f = 1 - \frac{\sigma L}{d_0^2 v_z}\left(\frac{z}{L}\right) = 1 - c\left(\frac{z}{L}\right).$$

where c characterizes the ratio between the residence time of drops in the furnace to the time of their evaporation; c is not a new independent criterion, since c = a/b.

Figure 9-5 gives curves of flame combustion for different values of a and b.

Evaporation of poly-fractional flame. Probert [9-12] examined the problem of evaporation of a poly-fractional flame with a drop distribution by dimensions following the Rozin formula:

$$R_i = e^{-\left(\frac{d_i}{d_0}\right)^m}.$$

where R_i -- "residue on a screen" with the diameter i;
d_0 -- average initial dimension of the drop;
d_i -- certain initial dimension;
m -- constant determining the atomization uniformity. At m = ∞, the atomization is uniform.

Just as in the previous case, it is assumed that the evaporation constant /232
σ is a constant quantity. The combustion process was not considered in this

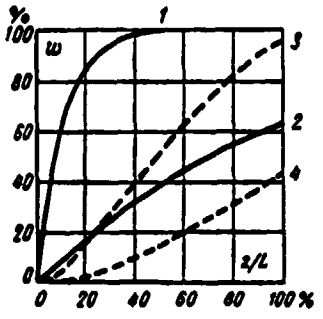

No. of Curve	Value	
	a	b
1	10	0
2	1	0
3	10	10
4	10	1

Fig. 9-5. Combustion procedure over the flame length.

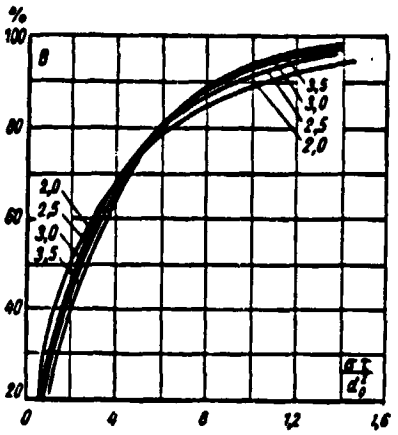

Fig. 9-6. Curves of drop evaporation in flame.

Numbers on the curves - values of the distribution constant m.

study. Only the portion of evaporated fuel was determined. It is assumed that the combustion in the gas phase occurs so intensely that it does not limit the process intensity.

Figure 9-6 gives the results of a very complex mathematical calculation. The abscissa axis shows the value of $\sigma\tau/d_0^2$; the ordinate axis -- B (percent of evaporating fuel). The distribution constant m is the parameter. It must be noted that allowance for the poly-fractionation of the flame introduces a comparatively small correction, and in particular after that the combustion percent amounts to 30-40. The influence of m is stronger in the initial stage. Here the degree of evaporation greatly increases, other conditions being equal, with a decrease of m. This means that for one and the same average diameter d_0, the portion of evaporated fuel in a given time is larger due to the presence of small drops. On the other hand, after evaporation of approximately half of the fuel, at small m the rate of the process slows down due to the influence of large fractions. Thus, in spray nozzles giving a less uniform atomization, the evaporation process, other conditions being equal, is accelerated in the initial stage, which /233 facilitates ignition. The problem of ignition is not considered either in the study of Probert or in the calculations carried out before this. In both cases, it is assumed that the stream temperature and evaporation rate coefficient σ are unchanged.

The verification of the theoretical solution requires, first of all, an experimental determination of the degree of fuel combustion in the chamber, which entails great difficulties. There are certain studies of this type. They may be used both for comparing the calculated results with the experimental data, and for selecting the empirical design formulas. For example, we may mention the study of Flederman and Hansh [9-5] which studied the evaporation rate of a hexane flame by placing the samples at different distances from the nozzle. There was no good agreement obtained with the experimental calculation according to Probert. It was found that the relative velocity of the drop and the stream plays a significant role, which was not taken into account in the theory of Probert. In addition, the influence of the stream turbulence was calculated.

The experiments of Zaks [9-5] on the evaporation of kerosene showed that the theoretical calculation according to Probert gives (at least for the initial stages) much larger values than does an experiment. The portion of evaporated fuel equals 0.2 - 0.3, whereas calculation gives the degree of evaporation as 50%. Nevertheless, the theoretical calculation correctly predicts the direction of the process and the relative role of individual factors. Therefore, it is very important for analyzing the effect which would be expected from a certain measure which changes the dimensions of the drop, the temperature in the furnace, etc. Due to the complexity of the experiment, there are very few studies on the evaporation of drops in the furnace. In many of them, the authors confine themselves to investigating the evaporation of atomized liquid without combustion.

Ingebo [9-9] studied the evaporation of isooctane in air at temperatures close to room temperature. The fuel was supplied through a cylindrical nozzle against the gas stream. The air velocity was 45-60 m/sec. High-speed photography at different distances from the nozzle was used to determine the current dimensions of the drop and their velocity with respect to the flow. The processing of the materials and their comparison with theoretical calculations led to the following important conclusions:

1. The calculation based on the drop diameter which is average over the /234
surface, under the assumption of multifractional composition of the atomization

flame, gives results which closely coincide with the actual one. This greatly facilitates the calculations.

2. We may simplify the calculation of the drop motion by assuming a law of hydraulic resistance which is similar to the Stokes law up to the numbers $Re \approx 200$. The formula for the resistance coefficient may be represented in the form $c = 8.4/Re$ instead of the regular one $c = 24/Re$.

Here c, as is usual, is the coefficient in the quadratic resistance formula:

$$F = c \frac{\pi d^2}{4} \varrho_r \frac{u^2}{2},$$

where F -- force acting on a particle;

u -- its relative velocity to the flow.

The linear dependence between the resistance and the relative velocity makes it possible, when calculating the drop motion, to consider separately, independently from each other, the equation of motion with respect to each of the coordinates.

Actually, if we write the equation of drop motion in general form in the direction of the coordinate i, then it has the form:

$$\frac{1}{6} \pi d^3 \varrho_m \frac{dw_i}{d\tau} = c \frac{\pi d^2}{4} \cdot \frac{u u_i}{2} + \frac{1}{6} \pi d^3 \varrho_m g_i. \qquad (9\text{-}18)$$

Here, w is the absolute drop velocity and u is its relative velocity which equals:

$$u = \sqrt{(v_x - w_x)^2 + (v_y - w_y)^2 + (v_z - w_z)^2},$$

where v -- stream velocity;

g_i -- projection of the acceleration of gravity on the i axis.

Equation (9-18) includes the velocity components for the stream and the drop for all directions, and only in the case of resistance according to a linear law,

when c ~ 1/u, the quantity u is excluded, and the equations of motion may be examined separately with respect to each coordinate.

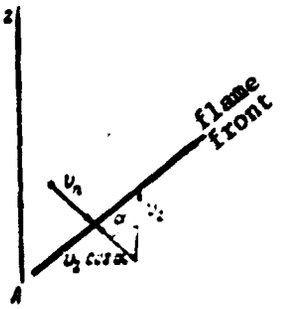

Fig. 9-7. Flame propagation in a gas mixture moving uniformly.

/235

The study [9-9] gives the results of investigating the evaporation of ethyl octane input to a stream opposite its direction from a nozzle with the diameter 0.6 - 1 mm. The fuel supply pressure changes between 1.7 - 6 atm. The absolute pressure in the experimental tube with a diameter of about 200 mm is 0.66 - 1 atm. The air velocity is between 3[illegible] - 120 m/sec at temperatures from room temperature to approximately 200° C. The results of the experiments are given in the form of the empirical power relationship:

$$\frac{\varepsilon}{1-\varepsilon} = 6{,}3\left[\left(\frac{T_a}{100}\right)^{4{,}4}\left(\frac{v_z}{10}\right)^{0{,}8} p_a^{-1{,}2}\Delta p_n^{0{,}42} z^{0{,}84}\right], \qquad (9\text{-}19)$$

where ε is the portion of evaporated fuel.

The very great influence of temperature is explained by the fact that the experiments were performed in the comparatively low temperature region, where even a small increase in the medium temperature leads to a great increase in the psychrometric difference. With an increase in the medium temperature, the exponent must decrease.

The following two characteristics of the process are of great importance when examining the combustion condition of a hot gas mixture which is mixed beforehand: the flame propagation rate and the combustion time. The first quantity determines the configuration of the flame front; the second -- the width of the combustion zone.

Figure 9-7 shows the simplest case of transition through the flame front of a gas mixture moving uniformly and laminarly with the ignition source at the point A. The angle α (between the velocity direction v_z of the stream up to the flame front and the normal to this front) and the flame propagation rate v_n

are related by the following relationship first shown by Michelson:

$$v_n = v_2 \cos \alpha. \qquad (9\text{-}20)$$

In a mixed stream moving laminarly, the combustion time is very large; therefore, the width of the combustion zone may be disregarded as compared with other linear dimensions, for example, the length L of the front, and it is assumed that in essence the combustion occurs on the flame front surface. Here the same assumption as in the diffusion theory with respect to the combustion zone of an individual drop is used. /236

For a laminar flow, the flame propagation rate and the combustion time are quantities which depend only on the properties of the mixture. Thus, the flame propagational rate is proportional to the square root of the thermal conductivity of the mixture and inversely proportional to the square root of the combustion time. The combustion time is determined by kinetic characteristics of the mixture.

The conditions are much more complex in turbulent flow. It is convenient here to use the concept of the flame propagation rate and the combustion time. However, these quantities are not determined only by the physical properties of the mixture, but depend on the flow hydrodynamic conditions up to the flame front, and on the hydrodynamic situation which is produced behind the flame front.

There is still no unified viewpoint on the mechanism for the flame turbulent propagation. However, is is presently believed that the intensity of the incoming mixture turbulence and the change in the turbulent intensity when passing through the flame front are of great importance.

The case is much more complex of the combustion of a two-phase gas mixture with a liquid fuel atomized in it. However, convenient concepts are frequently introduced regarding the flame propagation rate and the combustion time, although naturally these quantities are very complex and depend on many factors. Thus,

for example, when designing a register combustion chamber for light liquid fuel, it is sometimes assumed that the flame propagation rate is about 8-10 m/sec. [9-4]. Thus, not only the flame propagation rate, but also the flow rate is arbitrary, since they are not distributed uniformly over the chamber cross-section.

V. G. Tikhomirov [9-7] studied the combustion of a two-phase mixture. Figure 9-8 shows a diagram of the equipment. The fuel was atomized by a centrifugal spray nozzle 1 up to a drop with a diameter of 50 - 110 microns in an air stream with $t \approx 300^{\circ}$ C and a velocity range of between 20 - 85 m/sec. The air excess coefficient changed from 0.65 to 1.85. The flame was maintained using a circular stabilizer 2, which could be moved at different distances from the spray nozzle cross-section. Thus, the degree of preliminary evaporation of the fuel changed from 18 - 70%. Separation of the drops by dimensions occurred in the /237 stream. Therefore, by moving the stabilizer in a normal direction to the spray nozzle axis, it was possible to change the drop dimensions in the stream, retaining the multifractional atomization composition approximately in each experiment. The flame propagation rate was studied on photographs of the internal 3 and the external 4 cones of the flame using the Michelson method. The combustion time was determined from the combustion zone width on the flame axis from the point where combustion began to the point where it could be assumed that the combustion had ended based on the measurements of temperature and gas analysis.

Based on these experiments, the author of this study reached the conclusion that the turbulence intensity is of basic importance for the flame propagation rate. The influence of the air excess is much less pronounced. The influence of the remaining conditions could not be determined.

Figure 9-9 gives the results of the experiments. The abscissa axis plots the air excess; the ordinate axis -- the ratio of the flame propagation rate to the stream pulsation velocity. For purposes of comparison, this graph also gives the combustion propagation rate in a homogeneous mixture of air with vapors of the same fuel. As may be seen from the graph, if the air excess α is greater than 1.3 and less than 0.6, the flame propagation rate in a two-phase

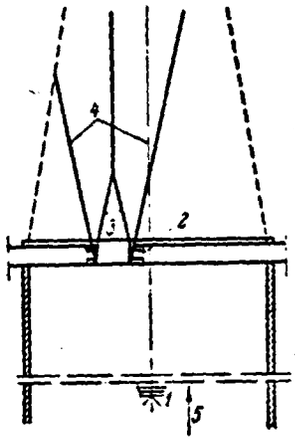

Fig. 9-8. Diagram of experimental device for studying combustion of atomized liquid fuel.

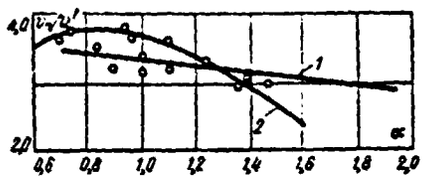

Fig. 9.9. Influence of turbulizer on completeness of fuel combustion.

1 - two-phase mixture;
2 - uniform gas mixture.

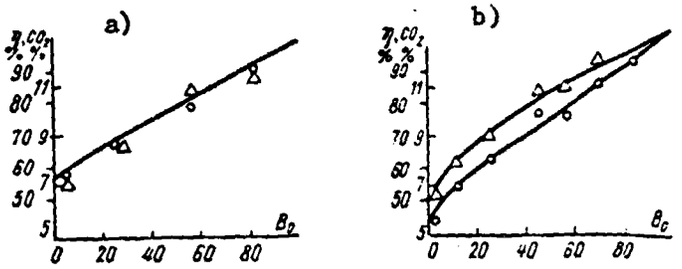

Fig. 9-10. Combustion of drops η for differing degree of preliminary fuel evaporation B_o with the presence (Δ) and absence (0) of a turbulization grid.

Drop dimension: a - 90 microns; b - 290 microns

mixture is greater than in a homogeneous mixture. A maximum is not observed at $\alpha = 0.8 - 0.9$.

The combustion time for a two-phase mixture is greater than for a homogeneous mixture. It greatly depends on the drop dimensions; however, not to the same extent as indicated by diffusion theory. Thus, /238 for a stream velocity of about 40 m/sec and a turbulence intensity which is approximately 3.5%, the combustion time of a drop with a dimension of 55 microns is two times less than the combustion time of a drop with a diameter of 110 microns. Based on the diffusion theory, the combustion time must be proportional to the square of the diameter. The divergence may be caused by temperature conditions of the process, a certain lag of the drop from the stream when the stream is accelerated after passing through the flame front, and also the influence of the kinetics, which is stronger, the smaller the drop.

It must be noted that based on these materials, the turbulent pulsation rates of the incoming stream greatly influence the mixture combustion time. This is in

contrast to certain other studies, which detected a great influence of turbulence at the input upon the heat and the mass exchange between the stream and the suspended particles.

It must be noted that the author evidently did not carry out special studies to directly determine the influence of the turbulent pulsation velocity upon the combustion time or the flame velocity. With a change in the stream velocity, the pulsation changed, since the turbulent intensity remained constant (about 3.5%). The effect produced with a change in the stream velocity is attributed only to a change in the pulsation rate. This statement is not adequately verified. In generaly, it must be considered that in a natural flame, the drop dimensions are different, and therefore the combustion conditions will differ from those which were observed in this study.

In another study [9-2], a special investigation was made of the influence of the stream turbulence at the input to the combustion zone upon the degree to which the fuel was heated η for different degrees of preliminary fuel evaporation. The grid was set up so as to increase the degree of turbulization at the input to the combustion chamber from 4-6 to 11-16%, i.e., by a factor of 2.7. Figure 9-10 gives the values of the degree of the fuel combustion B_o (and the content of carbon dioxide in the gases) at an arbitrary distance of 750 mm from the stabilizer for different amounts of the preliminarily evaporated fuel B_o.

With one and the same excess ($\alpha = 1$) and an identical fuel consumption, the experiments were performed for two initial average diameters of the drop, 90 and 290 microns. It was found in the experiment that with a drop diameter of 90 microns, there was no influence of turbulence. In a rough atomizer -- with an initial drop diameter of 290 microns -- the turbulence had a great influence in /239
the case of a slight preliminary evaporation. It may be assumed that this was caused by an increase of the heat transfer coefficients due to a large relative velocity between the gas stream and the drop. A rough drop was not carried by turbulent pulsations, and this improved the heat and mass exchange between it and the stream.

In this study, as well as certain studies examined above, it was found that the combustion time in the flame of a drop with different dimensions increases with an increase in the dimensions much more slowly than according to a square dependence, as follows from diffusion theory. One of the reasons for this is the influence of turbulence. Along with this, the kinetic conditions are apparently important, and also the fact that with an increase in the stream velocity the larger drops remain as a result of combustion, and the longer they are therefore retained in the combustion zone.

CHAPTER TEN

CERTAIN PROBLEMS OF SPRAYER TEST METHODS

Following are the determinant quantities in an experimental study of the atomization of a liquid by spray nozzles: the spray nozzle flow rate coefficient, the distribution of the dispersed liquid over the stream cross-section, the stream angle of taper, the drop dimension distribution, and the average drop diameter. /240

It is advantageous to carry out a study of atomization in a cold state, when there is no combustion. For spray nozzles to be used for engineering purposes, this state completely corresponds to the working conditions. With respect to spray nozzles which atomize liquid fuel, the picture obtained in the cold state will correspond to the conditions of a stream immediately when it leaves the sprayer. Atomization of the working liquid is most desirable, i.e., the liquid which is used under given conditions and in different equipment. However, for convenience in performing the experiment another liquid is frequently used (usually water which is lighter and can be studied more easily). Using relationships presented in the previous chapters, we may transfer the results obtained to the conditions corresponding to physical properties of the working liquid.

The tests of spray nozzles are usually carried out on special stands. When the spray nozzle is placed vertically upward, this produces an axis of symmetry, and the conditions for carrying out the experiment are facilitated. One of the scans for studying atomization by laboratory pneumatic spray nozzles is shown in Fig. 10-1 [10-2]. The working liquid is removed by air pressure from the measuring burette 1, which serves as a fuel tank, and passes through tube 2 into the spray nozzle of the air sprayer 3. The air stream from compressor 4, passing the equalizing tank 5, branches out: through the branch 6 and the cavity 7, it enters the spray nozzle opening for atomization, and through branch 8 -- into the fuel tank 1 for liquid transport. The air consumption is measured by the rheometer 9, and its pressure -- by the manometers 10, 11 and 12.

The liquid flow rate is determined by the graduated burette 1, whose capacity is 200 cm^3. The computational accuracy is within the limits of 2 cm^3.

The liquid distribution over the cross-section of the atomized stream is determined by the measuring glasses 13 placed on the frame 14, which moves upward along the support 15 and is fastened at a certain level by the clamps 16. This makes it possible to obtain the fuel distribution over the stream cross-section at different heights, i.e., at a different distance from the spray nozzle opening. The amount of liquid in the measuring glasses is determined by weighing or by the volumetric content. To determine the sprinkling density of the flame, the measurements were performed at different distances along the stream length. Figure 10-2 shows the arrangement of the measuring glasses over the stream cross-section. /242

The volumetric liquid consumption is determined by the formula:

$$V_o = \frac{V}{t} \ [cm^3/sec], \qquad (10\text{-}1)$$

where V -- volume of atomized liquid per 1 cm^3 measured by the burette 1;

t -- experiment time, sec.

In addition, the weight flow rate of the liquid is determined:

$$G = 3{,}6\, V_o \gamma \ [kg/hr], \qquad (10\text{-}2)$$

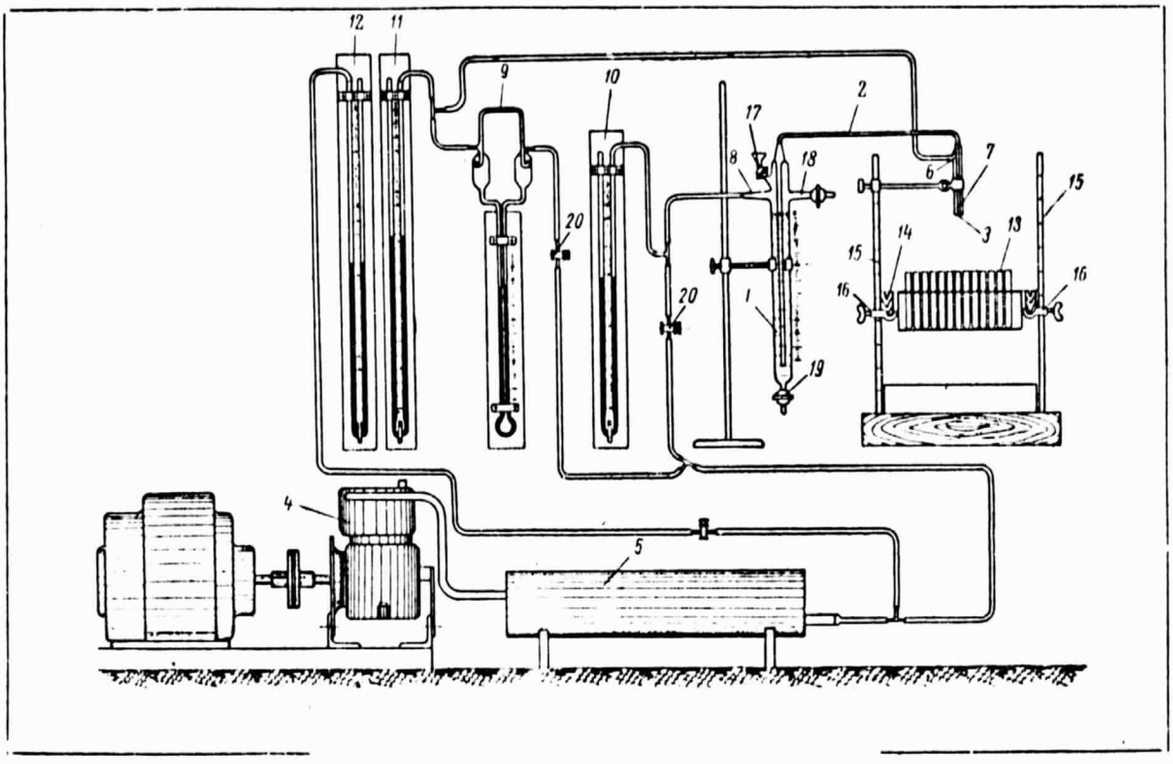

Fig. 10-1. Diagram of equipment of the laboratory type.

where γ is the volumetric weight of the liquid, g/cm^3.

The spray nozzle flow rate coefficient may be calculated with the formula:

$$\xi = \frac{\dot{V}_o}{\omega \sqrt{2gH}}, \qquad (10\text{-}3)$$

where ω -- transverse section area of the liquid nozzle, cm^2; g = 981 cm/sec;

H -- liquid head before the spray nozzle, cm;

$$H = \frac{p_o}{\gamma} + \Delta h;$$

$p_o\gamma$ -- manometric pressure measured by the manometer, cm water column;

Δh -- difference in the liquid levels in the burette and the nozzle opening, cm.

The weighing data are used to determine the sprinkling density q_i -- the weight of liquid passing per unit time through a unit area of the plane located at a given distance from the spray nozzle opening:

$$q_i = \frac{g_i}{f_i t} \text{ [g/cm}^2\text{·sec]}, \qquad (10\text{-}4)$$

where g_i is the weight of the liquid in the i-th measuring glass;

f_i -- area of the transverse cross-section of the i-th measuring glass.

/243

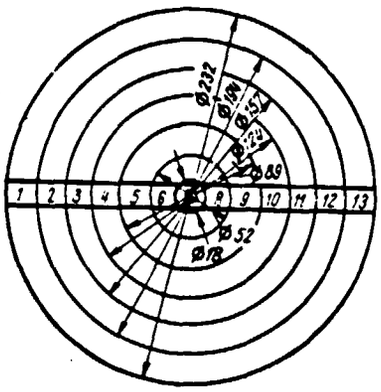

Fig. 10-2. Distribution of measuring glasses in slides over the stream cross-section.

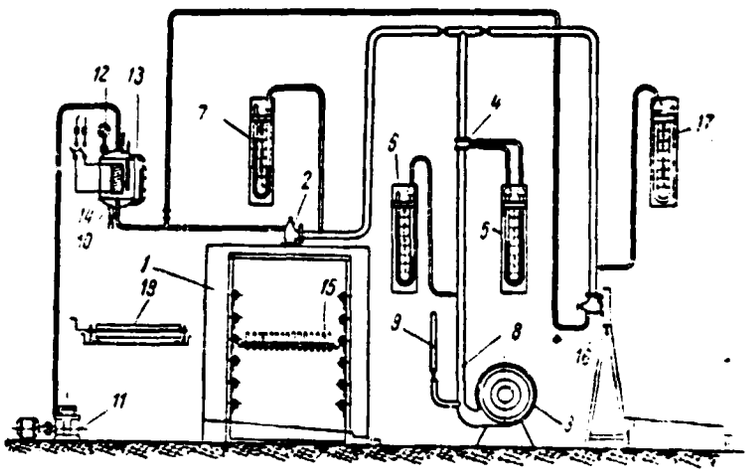

Fig. 10-3. Diagram of equipment for spray nozzle tests.

In order to compare the sprinkling density for different flow rates, the quantity q_i is expressed in percents of the total flow rate:

$$q_{i\%} = \frac{q_i 100}{V_0 \gamma} [\%]. \qquad (10\text{-}4')$$

The formulation of the curve for the relation

$$q_i = f(r_i) \qquad (10\text{-}5)$$

makes it possible to determine the width of the flame R_o at different distances from the sprayer opening h and, on the basis of this, to calculate the stream angle of taper:

$$\operatorname{tg}\varphi = \frac{R_o}{h}. \qquad (10\text{-}6)$$

When the liquid distribution over the cross-section is determined by the volumetric method (the volumes V_i of the liquid are measured in the measuring glasses), the sprinkling density is calculated from the relation:

$$q_{i\%} = \frac{V_i 100}{\sum_i V_0} [\%]. \qquad (10\text{-}4'')$$

One of the stands for testing low-head pneumatic spray nozzles [10-2] is shown in Fig. 10-3. The central part of the stand represents a wood chamber 1, above which the spray nozzles 2 to be tested are placed in a vertical position. The bottom of the chamber is attached to the collection of liquid to be tested. The air is supplied by the centrifugal fan 3 and its flow rate is measured by the washer 4 and the manometer 5. The air pressure is measured by manometers 6 and 7, and the temperature — by thermometer 8. The branch 9 serves for more convenient control of the air flow rate, and in addition prevents overheating of the fan at low flow rates. The fuel from the tank 10 enters spray nozzle 2 at the pressure produced by compressor 11. Below the tank there is a branch for liquid overflow, and above -- a funnel for filling, a manometer 12, and a pocket with the thermometer 13. A heater 14 is supplied for use with highly viscous liquids. The fuel flow rate is measured using a measuring glass. Within wood chamber 1 there is a frame with lateral guides, on which there is a plate with measuring glasses 15 over the stream center to study the flame density over the stream diameter. Six guides fastened on the frame in the upward direction determine the position of the measuring glasses with respect to the spray nozzle opening. The first guide is located at a distance of 450 mm from the spray nozzle. The remaining guides are placed every 200 mm from each other. The method and processing of the experiments coincide with that described above. /244

This procedure may also be used to test spray nozzles in the horizontal position. In this case, the fuel from the pressure tank 10 enters the spray nozzle 16. The air pressure is measured by manometers 6 and 17.

The central part of the stand may frequently be used for testing centrifugal spray nozzles [10-1]. In this case the air line is disconnected. A high pressure pump is used to supply the liquid, but it may be done by a measurement tank under

a pressure produced by a tank of compressed air.

In some experiments, the atomized liquid is placed in sector vessels which are divided into parts by cylindrical, concentrically located partitions, as shown in Fig. 10-4 [10-6]. The stream angle of taper may also be determined by photographing *

In order to determine the stream degree of dispersion, all drops in the stream are divided into several groups based on dimensions. Thus, the average drop diameter d_i in each group is calculated as the arithmetic mean. Thus, d_i = 12.5 microns for drops from 0 to 25 microns; 37.5 microns for drops from 25 to 50 microns; 62.5 microns for drops from 50 to 74 microns, etc. The number of drops in the group are determined experimentally, after which the average drop diameter is calculated using formulas (1-2) - (1-8) and formulas (1-9) and (1-10) are used to determine their distribution based on dimensions. /245

Several methods exist for determining the number and dimensions of drops in a flame. Following are the most widely used:

a) trapping drops;

b) prints;

c) use of the molten material with a low melting point, with subsequent consolidation of the drops in flight;

d) photographing the drops in flight.

When the method of trapping the drops is used, microscopes are covered with a layer of viscous liquid, in which the drops of atomized liquid do not dissolve. The thickness of the covering layer must be greater than the diameter of the largest drops, and the density and viscosity must be such that the drops sink, without adhering to each other and without losing their spherical form. In the atomization of water, the liquid used for trapping the drops may be a mixture of vaseline with transformer oil in a ratio of 1:3. This mixture has the property that it can retain the drops in it for a long period of time, without letting them merge and evaporate. Castor oil may be used for this purpose, but in this case it is necessary that the trapped drops are kept in a

*) Illegible in foreign text.

saturated atmosphere at a certain temperature before they are measured.

Fig. 10-4. Sector vessels for recovering atomized stream.

To trap the drops, special equipment is necessary with a gate to cut off the drops. For example, a device may be recommended (18 in Fig. 10-3) which represents a cylinder with a slot which rotates around a fixed axis. This axis holds slides covered with a trapping compound. In order to arrange the slides, it is necessary that measuring glasses be placed on the upper edge layer so that the amount and location where they are installed correspond to the amount and location of the measuring glasses. When a cylinder containing the slot is located, it passes over the slides at a high velocity, making it possible to count the individual drops. The device is placed on frame guides, instead of a plate with measuring glasses. /246

The slides with the trapped drops are placed under a microscope with a measuring grid, whose divisions determine the range of drop dimensions in the group. Either a direct calculation of the number of drops in the group is made, or they are microphotographed [10-2] with subsequent calculation of the number of drops. One disadvantage of this method is its difficulty, since in order to obtain a correct picture of the drop distribution based on dimension, the number of drops must be very large (no less than several hundreds).

Recently many researchers have determined the number and dimensions of drops using automatic calculators of different systems.

In the method of trapping on slides, it is impossible to discover the smallest drops in the gas stream, since they are deflected together with the gas. However, the magnitude of the error is very small, since the total volume of these drops is insignificant.

The discrete drop diameters obtained for each section characterize the atomized mass which is determined by the sprinkling density and the area of the

corresponding semi-circular section. The mean mass diameter is found by summing the mass of the liquid distributed in terms of drops in the corresponding section:

$$d = \frac{1}{G}\sum_{k} q_k f_k \frac{\sum n_{i\,k} d_i^4}{\sum n_{i\,k} d_i^3}.$$

For purposes of control, the material balance is formulated in the following form based on the results of calculating the drops and direct sprinkling density measurements: /247

$$q_{k\ \text{расч}} = \frac{\gamma}{f}\sum_{i=1}^{m} n_i \frac{\pi d_i^3}{6} = q_{k\ \text{замер}}. \qquad (10\text{-}7)$$

where f -- area of the microscope field of view;

n_i -- number of drops of average diameter d_i in the group;

i -- number of group; changes from 1 to m;

k -- number of circular cross-sections;

q_k -- sprinkling density at the distance r_k from the stream axis;

f_k -- area of circular cross-section;

r_k -- average radius of circular cross-section;

G -- liquid flow rate.

The method of prints is frequently used to trap drops in the case of atomization of hydrocarbon liquids and mineral oils.

The method described above is used to calculate the number of drops and determine their dimensions. The difference consists of the fact that the drops are trapped on slides covered by a layer of soot, on whose surface a layer of magnesium oxide is applied. This method is not suitable for trapping drops of water and aqueous solutions, since this type of drop spreads out and loses the initial form. The dimensions of the print differ somewhat from the true dimensions of the drops.

Based on data of Stoker [10-13], the relationship between the drop diameter and its print diameter on the soot layer is determined by the formula:

$$\frac{d'}{d} = 0{,}77\,\mathrm{We}^{1.5}, \tag{10-8}$$

where d' -- print diameter;

d -- drop diameter:

$$\mathrm{We} = \frac{\rho v^2 d}{\sigma},$$

where ρ -- liquid (drop) density;

v -- drop removal velocity;

σ -- coefficient of drop surface tension with respect to the air.

This relationship was refined by Strulevich and Dityakin, who found that the value of d'/d also depends on the relative thickness of the soot layer:

$$\frac{d'}{d} = f\left(\mathrm{We}, \frac{h}{d}\right). \tag{10-9}$$

In its turn, the We number is variable and may be expressed by the equation: /248

$$\mathrm{We} = f_1\left(\frac{h}{d}, \mathrm{Re}^*\right). \tag{10-10}$$

where h -- soot layer thickness;

$$\mathrm{Re}^* = \frac{vd\varrho}{\mu};$$

μ -- soot viscosity.

The We number has a maximum at $\frac{h}{d} = \frac{\pi}{3}\mathrm{Re}^*$.

The experiments performed in [10-8] showed that when the soot layer thickness is greater than 1.5 the diameter of the drops, the print dimension practically coincides with the drop dimension (the deviation of these dimensions does not exceed 2-3%). Thus, for drop diameters of no more than 500 microns, the soot layer thickness may be 0.7 - 0.75 mm.

Recently increasing use has been made of the method employing an atomized substance with a low melting point, with subsequent consolidation of the drops

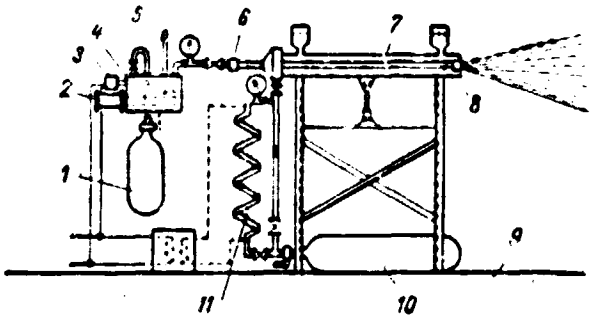

Fig. 10-5. Diagram of equipment.
1 - tank with nitrogen; 2 - heater; 3 - thermostat; 4 - tank for working substance (paraffin); 5 - thermometer; 6 - measuring washer; 7 - spray nozzle tested; 8 - water; 9 - sheets of paper under the chamber; 10 - air tank; 11 - air heater.

in flight. The consolidated drops are collected, pass through a set of grids placed in decreasing order of the hole dimensions, and then the residues are weighed on screens. This method may be implemented either by freezing the drops of the liquid being studied in a cold chamber, or by studying the fuel atomization on a model. The model may be a substance which is in a solid state at room temperature, and which melts when heating and has physical properties at a certain temperature (viscosity, density, surface tension) which are close to the properties of the fuel studied.

To provide for reliable operation, the head of the spray nozzle is heated to a temperature at which sharp cooling of the atomized liquid is excluded.

The working substance is frequently paraffin. Problems related to its atomization were studied in detail by N. N. Strulevich [see 10-5, page 184].

Figure 10-5 shows a diagram of a device used by Joyce [10-11] to perform tests for the atomization fineness of four air spray nozzles. The working liquid was paraffin with an admixture of 14% tartratene. This mixture was melted and heated to 100° C (it was somewhat overheated). Its viscosity was /249
$16 \cdot 10^{-6}$ m^2/sec. The experiments were performed at a constant flow rate — about 200 m/hr. The spray nozzles were heated with hot water with a temperature of about 100° C; the water was passed over special jackets. One of the spray nozzles which did not have a jacket was heated with hot water, which passed through the head of the spray nozzle before the beginning of the experiment. During the experiment, the drops in flight fell on the chamber floor and were collected on sheets of paper.

By the end of the experiment, the basic number of drops (about 50%) was weighed, then passed into water and in the form of a suspension was passed through a screen. The distribution curves were formulated based on the data obtained.

Fig. 10-6. Drops partially adhering in agglomerates (typical photograph).

Figure 10-6 shows drops which accumulated in agglomerates. This accumulation, in all probability, basically took place during the trapping and affected those drops in a semi-moist state at that time.

Miroshkin and Geller recommended using ceresine, brand 57, with the addition of an isobutylene polymer [10-7] as the substance simulating the atomization of highly viscous mazut by spray nozzles. The isobutylene polymer forms with ceresine a homogeneous mixture, whose melting point is below 70° C. The material first melted after atomization rapidly solidifies in the chamber and has sufficient strength to be /250 subjected to screen analysis.

As may be seen from Fig. 10-7, the mixture viscosity depends on the temperature and the percent content of isobutylene polymer. The figure shows the viscous characteristics of other materials which may be used as the working substance in spray nozzle tests. The surface tension of a mixture of ceresine, marked 57, with 30% isobutylene polymer at 70, 80 and 90° C equals 2.74, 2.71 and $2.64 \cdot 10^{-3}$ kG/m. The specific weight of this mixture at 20° C equals 830 kg/m^3. The decrease in the drop mass due to evaporation is insignificant. It must be kept in mind that when the drops solidify, they may be somewhat deformed due to the resistance of the gas medium and change their dimensions as a result of the /252 density change. Both of these phenomena may be taken into account by introducing

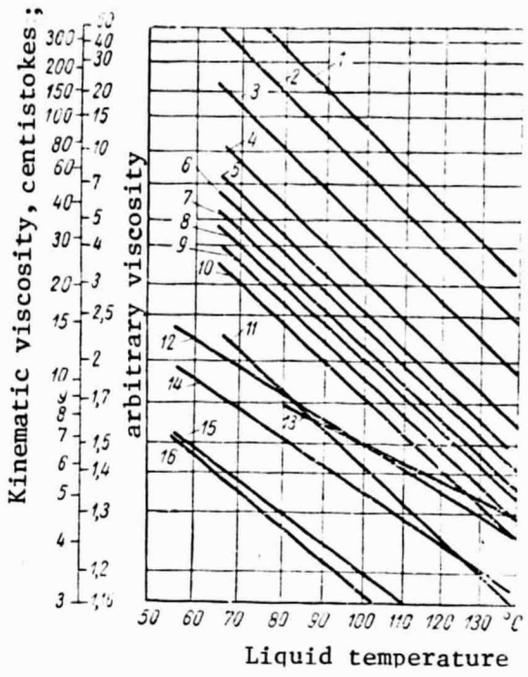

Fig. 10-7. Dependence of viscosity of model liquids on temperature.

No. of lines	Components of mixture, %		No. of lines	Components of mixture %	
	Brand 57 ceresine	Isobutylene polymer		Brand 57 ceresine	Isobutylene polymer
1	-	100	7	70	30
2	10	90	8	75	25
3	25	75	9	80	20
4	40	60	10	86	14
5	50	50	11	100	--
6	60	40			

12 - Paraffin (75%) plus isobutylene polymer (25%);
13 - Naphthalene; 14 - osocerite; 15 - exported paraffin (based on data of GrozNII; 16 - purified paraffin (based on data of GrozNII).

experimental coefficients: The simplicity and the relative ease of performing this analysis have led to great interest in its use.

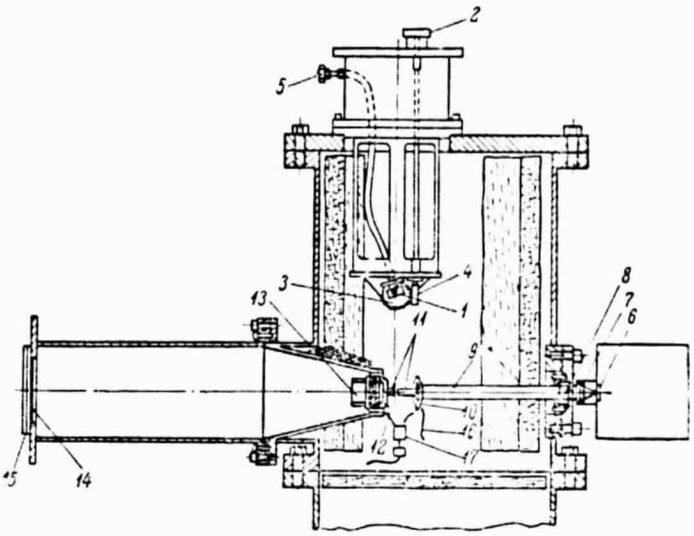

Fig. 10-8. Diagram of experimental equipment.

The photometric method makes it possible to determine the dimensions and number of drops not only atomized in the atmosphere, but also in the chamber with excess pressure or in a vacuum. In addition, the method has several disadvantages:

a) It is impossible to photograph the entire flame cross-section simultaneously;

b) It is only possible to obtain the drop distribution based on the cross-section by combining the data from photographs of different sections obtained sequentially for one and the same mode;

c) This method, just like the previous one, is very cumbersome, because it requires calculating the drops, apart from the photography;

d) There are certain difficulties involved in correctly determining the position of drops of differing dimensions in space in order to collect them for the calculation.

Figure 10-8 shows a diagram of the equipment for studying atomization at different pressures of the surrounding medium [10-9]. The working chamber /253 represents a tube with an internal diameter of 450 mm and a height between the flanges of 760 mm.

The photographic chamber, the light tube, and the light source are attached to the tube walls so that there is a common axis which is perpendicular to the

stream axis for the vertical arrangement of the spray nozzle 1. The spray nozzle is moved upward by device 2, and rotated in the vertical plane at the angle θ from 0 to 56° around the axis passing through the nozzle opening. This rotation is performed by the flywheel 3 using the worm gear 4. The fuel is supplied along line 5. The light from a source which is a plane xenon tube 6 passes through a thin opening and the condensor lens 7, the window 8, the tube 9, the gate 10, the additional tube 11, the gate 12, the equipment lens 13, the grid 14, and falls on the film 15. The lens is located in the conical part of the photographic chamber. A window made of plastic is in front of the lens and protects the photographic equipment from pressure. The lens diameter is 32 mm, and its focal distance is 89 mm. The grid 14 consists of a wire with a diameter of 0.0127 mm, and its print in the photograph makes it possible to calculate the drops.

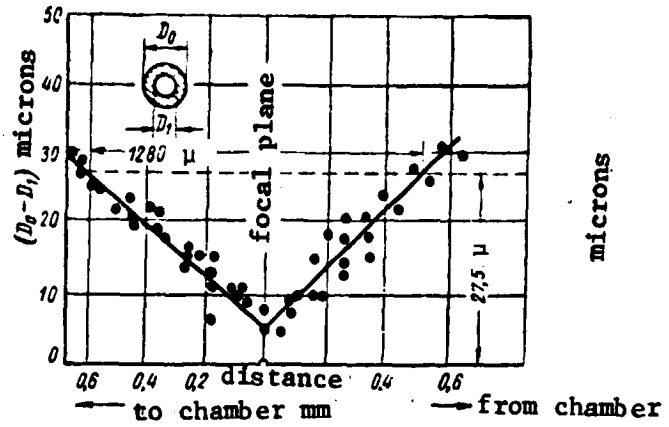

Fig. 10-9. Dependence of width of first Fresnel circle on drop position.

The system of gates 10 and 12 protects the optical surfaces from contamination by the film of liquid. The gates have a diaphragm with a diameter of about 10 mm, opened for 0.12 sec. (this makes it possible to obtain 24 photographs with an exposure time of 1/200 sec.). The gates are opened synchronously with the switching on of the light source, using the device 16; this is done by closing the electrical system line, turning on the solenoid, and supplying the gas in a cylinder with the plunger 17. When the stream density is large, additional tubes 11 are set into motion with a diameter of about 19.5 mm, between which a narrow slit is produced. In order to prevent the drops coming in contact with the surface of the tube in the slit, the tubes carry small protuberances. Screens prevent the drops from being reflected from the walls. Before the photography, a liquid barrier is made in the tube on the level of the photographic chamber axis, in order to determine the sprinkling density at a given angle θ. The photography is performed on a contrast orthofilm having a light sensitivity in the narrow range of the blue-green region of the spectrum.

The drops are calculated using a comparator with a magnification of 20. Thus, the total increase is 182 times, which makes it possible to determine dimensions in a 5 micron interval. It is very important to correctly establish the thickness of the layer of the field in which the drops of differing dimensions are calculated, due to the fact that the large drops have prints which are clearer than the small drops at the layer boundary. Manson [10-12] showed that with a change of the drop diameter from 12.5 to 500 microns, the thickness of the layer in which the drops are calculated changes from 3.7 to 8 mm. York and Stubbs [10-14], when calculating the drops, used indicators which showed the smallest brightness of the image of drops with different dimensions. The study [10-9] proposed using the phenomenon of diffraction which leads to the formation of Fresnel circles. Their width is determined by the distance from the drop to the focal plane of its image on the film which senses monochromatic light. Selecting the thickness of the layer in which the drops are calculated, using Fig. 10-9 we may establish the maximum width of the diffraction circles of the drops which are to be calculated.

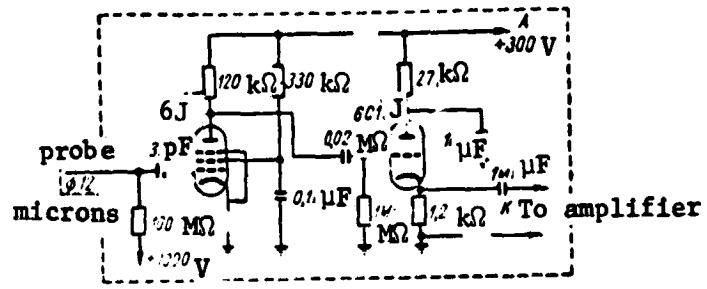

Fig. 10-10. Line diagram of output unit.

/254

There is another photographic method for determining the drop dimensions [10-10].

The original method for studying the drop dimensions in the case of atomization by spray nozzles was developed by Yu. Yu. Zhitkovskiy [10-3]. The diagram of the output block for studying drops of hydrocarbon fuels is shown in Fig. 10-10. The drop dimensions are determined from their electric capacitance, for which preliminary calibration is carried out, and the dependence of the capacitance change on the drop dimensions is established. The latter are determined by trapping the drops on plates covered with a layer of soot, on which there is an additional layer of magnesium. The probe introduced into the stream of atomized liquid senses the pulses from the falling drops.

/255

The first amplifier cascade, in the form of a cascade with a melting grid, is placed alongside the sensor. The next cascade, mounted according to the cathode follower scheme, protects the previous cascade from the shunting influence of the adjacent cable. Both of the cascades and the sensor are located in a single unit. The pulses from the output block are supplied to the amplifier, where they are amplified to a quantity determined by the discrimination level. Then they are supplied to the analyzers consisting of a level discriminator and a scaling circuit.

Apart from its complexity, a serious disadvantage of this method is the fact that it can be used, according to its author, only if the absolute velocity of the drops does not exceed 1 m/sec, and the transit density of the uniformly distributed drops is no more than 10^4 - 10^5 per 1 second every 1 cm^2.

REFERENCES

/256

Chapter Two

2-1. Kirpichev, M. V. Teoriya podobiya (Similarity theory), AN SSSR, 1953.

2-2. Kochin, N. Ye., Kibel', I. A., Roze, N. V. Teoreticheskaya gidromekhanika (Theoretical hydrodynamics). Gostekhizdat, 1948.

2-3. Kutateladze, S. S., Styrikovich, M. A. Gidravlika gazozhidkostnykh sistem (Hydraulics of gas-liquid systems), Gosenergoizdat, 1958.

2-4. Levich, V. G. Fiziko-khimicheskaya gidrodinamika (Physico-chemical hydrodynamics), Fizmatgiz, 1959.

2-5. Sedov, L. I. Metody podobiya i razmernosti v mekhanike (Methods of similarity and dimensionality), Gostekhizdat, 1954.

2-6. Eygenson, L. S. Modelirovaniya (Modeling), Sov. Nauka, 1952.

Chapter Three

3-1. Blinov, V. I., Feynberg, Ye. L. Pulsation of a stream and its decomposition into drops. AhTF, 1933, III, No. 5.

3-2. Bever, K. Decomposition of a stream of liquid. In the collection: Dvigateli vnutrennego sgoraniya (internal combustion engines), edited by S. N. Vasil'yev, ANTI NKTP SSSR, 1936.

3-3. Vereshchagin, L. F., Semerchan, A. A., Sekoyan, S. S. Problem of decomposition of a high velocity water stream, ZhTF, 1959, XXIX, No. 1.

3-4. Vitman, L. A. Atomization of a viscous liquid by spray nozzles of the centrifugal type. Collection of scientific studies of the LIMSX, S, Lenizdat, 1953.

3-5. Vitman, L. A. Calculation of the length of a solid section in the decomposition of a liquid stream. Collection: Voprosy teplootdachi i gidravliki dvufaznykh sred (Problems of heat transfer and hydraulics of two-phase media). Gosenergoizdat, 1961.

3-6. Vitman, L. A., Katsnel'son, B. D., Efros, M. M. Atomization of a liquid fuel by pneumatic spray nozzles. Collection: Voprosy aerodinamiki i teploperedachi v kotel'no-topochnykh protsessakh (Problems of aerodynamics and heat transfer in boiler-furnace processes), edited by G. F. Knorre, Gosenergoizdat, 1958.

3-7. Volynskiy, M. S. Breakup of drops in an air stream. DAN SSSR, 1948, 62, No. 3.

3-8. Genleyn, A. Decomposition of a liquid stream. Collection: Dvigitali vnutrennego sgoraniya (Internal combustion engines), edited by S. N. Vasil'yeva, ONTI NKTP SSSR, 1936.

3-9. Gol'dfel'der, O. Process of stream decomposition as a function of the nozzle form and counterpressure. Internal combustion engines, edited by S. N. Vasil'yev, ONTI NKTP SSSR, 1936.

3-10. Dement'yev, V. G. Experience in using high-speed photography to study the forms of decomposition of water streams in air. Izvestiya VNIIG imeni B. Ye. Vedeneyev, 52, Gosenergoizdat, 1954.

3-11. Dityakin, Yu. F. Stability and decomposition of a drop of a liquid stream with elliptical cross-section. Izvestiya AN SSSR, OTN, 1954, No. 10.

3-12. Knorre, G. F. Topochnyye protsessy (Furnace processes). Gosenergoizdat, 1959. /257

3-13. Levich, F. G. Fiziko-khimicheskaya gidrodinamika (Physico-chemical hydrodynamics). Fizmatgiz, 1959.

3-14. Lyshevskiy, A. S. Fractionation of a stream of non-viscous liquid from a slit spray nozzle. Tr. Novocherkasskiy Politekhnicheskogo Institute, 90, No. 1, 1958.

3-15. Lyshevskiy, A. S. Influence of the surrounding medium on the stability and decomposition of a hollow stream of viscous liquid. Tr. Novocherkasskog politekhnicheskogo instituta, 90, 1958.

3-16. Lyshevskiy, A. S. Stability and decomposition of a plane stream of viscous liquid surrounded by another viscous liquid. Tr. Novocherkasskogo politekhnicheskogo instituta, 86, 1959.

3-17. Raleigh, D. V. Theory of Sound, II, Gosenergoizdat, 1955.

3-18. Trotskiy, Ya. Problem of decomposition of a liquid stream into drops, ZhTF, 1933, III, No. 5.

3-19. Miesse, C. C. Correlation of experimental data on the disintegration of liquid jets, Ind.and Eng. Chemistry, 1955, 47, No. 9.

3-20. Probert, R. P. The influence of spray particle size and distribution in the combustion of oil droplets. Phil. Mag., 1946, 37, No. 265.

3-21. Tresch, Chemie Eng. Technik, 1954, 26, No. 6.

Chapter Four

4-1. Abramovich, G. N. Prikladnaya gazovaya dinamika (Applied gas dynamics), Gostekhizdat, 1958.

4-2. Blokh, A. G., Kichkina, Ye. S. Atomization of a liquid fuel by mechanical spray nozzles of the centrifugal type. Collection: Problems of aerodynamics and heat transfer in boiler-furnace processes. Gosenergoizdat, 1958.

4-3. Blokh, A. G., Kichkina, Ye. S. Flow rate coefficients and flame angle of taper. Teploenergetika, 1957, No. 10.

4-4. Geller, Z. I., Miroshkin, M. Ya. Hydraulic characteristics of centrifugal spray nozzles. Izvestiya vysshikh uchebnykh zavedeniy, seriya "Energetika", 1960, No. 3.

4-5. Dunskiy, V. F. Coagulation in the case of liquid atomization. ZhTF, 1956, 26, No. 6.

4-6. Zass, F. Collection: Internal combustion engines, edited by S. N. Vasil'yev, ONTI NKTP SSSR, 1936.

4-7. Knorre, G. F. Topochnyye protsessy (Furnace processes). Gosenergoizdat, 1959.

4-8. Li, D. U. Collection: Internal combustion engines, edited by S. N. Vasil'yev, ONTI NKTP SSSR, 1936.

4-9. Lyshevskiy, A. S. Tonkost' raspylivaniya zhidkogo topliva obychnymi forsunkami (Fineness of atomization of liquid fuel by regular spray nozzles). Teploenergetika, 1956, No. 10.

4-10. Bases of the combustion of hydrocarbon fuels. Izdat. inostrannoy literatury (IIL), 1960.

4-11. Talakvadze, V. V. Theory and design of centrifugal spray nozzles. Teploenergetika, 1961, No. 2.

4-12. Watson, E., Clark, J. Equipment and combustion processes. Collection: physics and chemistry of jet engine No. 3, IIL, 1949.

4-13. Binnie, A. M., Harris, D. P. The Quart. Journ. of Mech. and Applied Mathematics, 1950, 3, part 1.

4-14. DeCorso. Effect of ambient and fuel pressure on spray drop size, Journ. of Eng. for Power. Trans. ASME, Series A., 1960, 82, No. 1.

4-15. Doumas, M., Laster, R. Liquid-film properties for centrifugal spray nozzles, Chem. Eng. Progress, 1953, 49, No. 10.

4-16. Fraser, R. P. Sixth Symposium (International) on Combustion, 1957, New York, London. /258

4-17. Giffenen, E., Lamb, A. J. The effect of air density on spray atomization. The Motor Industry Research Ass., Report No. 1953/5.

4-18. Pohlhausen, K., Zeitschr. f. angew. Math. and Mech., 1921, No. 1.

4-19. Tate, R. W., Marschall, W. R. Atomization by centrifugal pressure nozzles. Chem. Eng. Progress, 1953, 49, No. 4 and 5.

4-20. Taylor, G. I. Proc. of the 7th Internat. Congress for Applied Mechanics, 1948, 2, part 1.

4-21. Taylor, G. I. The Quart. Journ. of Mech. and Appl. Mathematics, 1950, 3, part 2.

4-22. Turner, G. M.., Moulton, R. W. Drop size distribution from spray nozzles, Chem. Eng. Progress, 1953, 49, No. 4.

4-23. Woltzen, A. Fineness of fuel atomization, Darmstadt, 1925.

Chapter Five

5-1. Baum, V. A. Issledovaniye protessa turbulentnogo peremeshivaniya v potoke zhidkosti (Study of turbulent mixing process in liquid flow), 1952, Izv. AN SSSR, OTN, 2.

5-2. Vitman, L. A. Atomization of a viscous liquid by spray nozzles of the centrifugal type. Collection: Nauchnykh rabot LIMSKh, Kh (Scientific reports of LIMSKh, Kh), Linizdat, 1953.

5-3. Vitman, L. A. Study of spraying density by atomized liquid stream. Collection: Scientific reports of LIMSKh, Kh, XI, Sil'khozgiz, 1955.

5-4. Vitman, L. A. Certain rules of liquid atomization by pneumatic spray nozzles. Collection: Problems of aerodynamics and heat transfer in boiler-furnace processes. Gosenergoizdat, 1958.

5-5. Vitman, L. A., Katsnel'son, B. D., Efros, M. M. Atomization of liquid fuel by pneumatic spray nozzles. Collection: Problems of aerodynamics and heat transfer in boiler-furnace processes. Gosenergoizdat, 1958.

5-6. Katsnel'son, B. D., Shvav, V. A. Study of mazut atomization. Collection: Issledovaniye protsessov goreniya natural'nogo topliva (Study of combustion processes of natural fuel). Edited by G. F. Knorre, Gosenergoizdat, 1948.

5-7. Lebedev, P. D., Verba, M. I., Leonchik, B. I. Certain rules of superheated liquid atomization. Izvestiya vysshikh uchebnykh zabedeniy. Seriya "Energetika", 1959, No. 10.

5-8. Loytsyanskiy, L. G. Distribution of vortex stream in infinite space filled with the same liquid. Prikladnaya matematika i mekhanika, Izvestiya, AN SSSR, 1953, XVII, No. 1

5-9. Lyakhovskiy, D. N. Aerodynamics of stream and flame processes. Teploperedacha i aerodinamika, Book 12, Mashgiz, 1949.

5-10. Bases of hydrocarbon fuel combustion. IIL, 1960.

5-11. Trubchikov, B. Ya. Thermal method of measuring turbulence in wind tunnels. Izd. TsAGI, 1938, No. 372.

5-12. Conroy, E. H., Johnstone, H. F. Combustion of sulfur in a venturi spray burner, Ind. and Eng. Chem., 1949, 41, No. 12.

5-13. Golitzine, N., Sharp, C. R., Badham, L. G. Spray nozzles for simulation of cloud conditions in icing tests of jet engines, Rep. 14, Nat. Aero Est (Canada), 1951.

5-14. Heath, H., Radcliffe, A. The performance of an air blast atomisers, Rep. NR71 British NGTE, 1950.

5-15. Ingebo, R. D. Vaporization rates and drag coefficients for isooctane sprays in turbulent air stream, NACA TN 3265, 1954.

5-16. Nukiyama, S., Tanasawa, J. Experiments on the atomization of liquids in an air stream, Rep. 1 Trans. from Trans. Soc. Mech. Eng. (Japan), 1938, 4, No. 14. /259

5-17. Nukiyama, S., Tanasawa, J. Experiments on the atomization of liquids in an air stream, Rep. 2 Trans. from Trans. Soc. Mech. Eng. (Japan), 1938, 4, No. 15.

5-18. Nukiyama, S., Tanasawa, J. Experiments on the atomization of liquids in an air stream, Rep. 4 Trans. from Trans. Soc. Mech. Eng. (Japan), 1938, 5, No. 18.

5-19. Radcliffe, A., Clare, H. Rep. NR 144 British NGTE, 1953.

Chapter Six

6-1. Berman, S.S. Forsunki i mazutnoye khozyaystvo goryachikh tsekhov (Spray nozzles and mazut use in fuel plants). Gostekhizdat, 1950.

6-2. Vitman, L.A., Katsnel'son, B.D., Yefros, M.M. Atomization of liquid fuel by pneumatic spray nozzles. Collection: Problems of aerodynamics and heat transfer in boiler-furnace processes. Gosenergoizdat, 1958.

6-3. Zav'yalov, N.M. Multistream high pressure spray nozzle. Appendix by V.G. Kaplan and D.M. Makarov, TEKhSO, No. 1180/14, 1953.

6-4. Zamaziy, I.O., Syrkin, S.N. Controlled spray nozzle for liquid atomization. Kotloturbostroyeniye, No. 9, 1936.

6-5. Karabin, A.I. Szhiganiye zhidkogo topliva v promyshlennykh ustanovkakh (Combustion of liquid fuel in industrial plants). Metallurgizdat, 1957.

6-6. Katsnel'son, B.D., Shvab, V.A. Study of mazut atomization. Collection: Issledovaniye protsessov goreniya natural'nogo topliva (Use of natural fuel combustion processes). Edited by G.F. Knorre, Gosenergoizdat, 1948.

6-7. Kirillov, I.I. Gasovyye turbiny i gazoturbinnyye ustanovki (Gas turbines and gas turbine plants). Mashgiz, 1956.

6-8. Kitayev, B.I., Kokarev, N.N., Butanov, D.D., Zamotayev, S.P. Methods of finding effective mazut flames. Stal', No. 3, 1948.

6-9. Konstruktsii gorelok i forsunok dlya nagrevatel'nykh pechey (Construction of gas jets and spray nozzles for furnaces). Transzheldorizdat, 1961.

6-10. Kornitskiy, S.Ya. Comparative tests of vapor spray nozzles. Izvestiya VTI, 1931, No. 9 (68).

6-11. Kotel'nyye ustanovki (Boiler plants). Vol. 1, edited by M.V. Kirpichev, E.N. Romma, T.T. Usenko. Gosenergoizdat, 1941.

6-12. Kuznetsov, L.A. Kamery sgoraniya stationarnykh gazo-turbinnykh ustanovok (Combustion chambers of stationary gas turbine plants). Mashgiz, 1957.

6-13. Kurochkin, N.N. Kamery sgoraniya gazoturbinnykh dvigateley (Combustion chambers of gas turbine engines). Gosenergoizdat, 1955.

6-14. Lyubimov, I.P. Short-flame combustion of highly viscous mazuts to improve their combusion process. Collection: Energosnabzhenive i ikspluatatsiya energoustanovok neftyanoy promyshlennosti (Energy supply and operation of power plants for the petroleum industry). Gostoptekhizdat, 1952.

6-15. Matevosyan, L.A. Spray nozzle providing good atomization of mazut for small air pressure, N.V. Ktrdzhan, TEKhSO, No. 1653/68, 1953.

6-16. Ramzin, L.K., Kozlinskiy, G.Yu., Novi, Yu.O. Use of paraffin mazut in boiler plants. Izvestiya VTI, 1927, No. 2/25.

6-17. Khaslam, R.T., Russel', R.P. Fuel and its combustion. ONTI, NKTP SSSR, 1934.

6-18. Khodorov, Ye.I. Pechi tsementnoy promyshelnnosti (Cement industry furnaces). Promstroyizdat, 1950.

6-19. Tsygankov, A.Z. Ispytaniya forsunok i kladok dlya parovozov (Tests of spray nozzles and furnace linings for steam engines). Gosenergoizdat, 1931.

6-20. Efros, M.M. Study of low pressure spray nozzles for mazut combustion. Trudy Vsesoyuznoy nauchno-tekhnicheskoy sessii po promyshlennym pecham, Gosenergoizdat, 1949.

6-21. Kolbe, H. Der wirtschaftliche Dampfkesselbetrieb (Most economical operation of steam boilers). I, Halle, 1958.

Chapter Seven

7-1. Katsnel'son, B.D., Knorre, G.F. Combustion of mazut with preliminary gasification. Collection: Issledovaniye protsessov goreniya natural'nogo topliva (Study of processes of natural fuel combustion). Edited by G.F. Knorre, Gosenergoizdat, 1948.

7-2. Knorre, G.F. Topochnyye protsessy (Boiler processes). Gosenergoizdat, 1959.

7-3. Troyb, S.G., Nosov, G.L., et al. Industrial-economic bulletin No. 3, Sverdkovsk sovnarkhoz, Central bureau of technical information, 1957.

7-4. Fourth International Petroleum Congress. Rim, 1955, VII. Use of Petroleum products. Gostoptekhizdat, 1956.

7-5. The Engineer, 1955, June, 200, No. 5191.

7-6. Reskin, L. Application of high velocity combustion to the steel industry. Iron a Steel Industry, 1955, 32, No. 4.

Chapter Eight

8-1. Agafonova, F.A., Gurevich, M.A., Paleyev, I.I. Theory of liquid fuel combustion. ZhTF, 1957, XXVII, No. 8.

8-2. Bolt, D., Boyl', T. , Arbor, A. Combustion of liquid atomized fuel. Voprosy raketnoy tekhniki, 1957, No. 5.

8-3. Varshavskiy, G.A. Goreniye kapli zhidkogo topliva (diffuzionnaya teoriya) Combustion of drops of liquid fuel (diffusion theory). Izd. BNT NKAP, 1945.

8-4. Goldsmit, M. Experiments on combustion of individual drops of fuel. Voprosy raketnoy tekhniki, 1957, No. 4.

8-5. Goldsmit, M., Penner, S. Combustion of individual drops of fuel in an oxidized atmosphere. Voprosy raketnoy tekhniki, 1955, No. 2.

8-6. Greber. G., Erk, S., Grigull', U. Bases of studying heat exchange. IIL, 1958.

8-7. Gurevich, M.A., Shteynberg, V.B. Temperature of the flame of a single drop of liquid fuel. ZhTF, 1958, XXVIII, No. 2.

8-8. Kutateladze, S.S., Borishanskiy, V.M. Spravochnik po teploperedache (Handbook on heat transfer). Gosenergoizdat, 1959.

8-9. Longwell, I. Weiss, M. Velocity of high temperature reactions in the combustion of hydrocarbons. Voprosy taketnoy tekhniki, 1956, No. 6.

8-10. Mikheyev, M.A. Osnovy teploperedachi (Bases of heat transfer). Gosenergoizdat, 1956.

8-11. Paleyev, I.I., Agafonova, F.A. Study of combustion of drops of liquid fuel. Collection: Problems of aerodynamics and heat transfer in boiler-furnace processes. Edited by G.F. Knorre, Gosenergoizdat, 1958.

8-12. Spolding, D. Experimental study of combustion and damping of liquid fuel on a spherical surface. Voprosy raketnoy tekhniki, 1954, No. 3.

8-13. Fenn, I., Kal'kot, Kh. Energy of activation under combustion conditions at a high temperature. Voprosy raketnoy tekhniki, 1955, No. 3.

8-14. Frank-Kamenetskiy, D.A. Diffusion and heat transfer in chemical kinetics. Izd. AN SSSR, 1947.

8-15. Ageston, G.A., Wood, B.J., Wise, H. Jet propulsion, 1958, No. 3.

8-16. Arch. fuer Eisenhuettenwesen, 1951.

8-17. Bolt, J.A., Saad, M.A. Combustion rates of freely falling fuel drops in a hot atmosphere. Sixth Symposium (International) on Combustion, New York, London, 1957.

8-18. Goodsave, G.A.E. Studies of the combustion of drops in a fuel spray - the burning of single drops of fuel. Fourth Symposium (International) on Combustion, Baltimore, 1953.

8-19. Hottel, H.C., Williams, G.C., Simpson, H.C. Combustion of droplets of heavy liquid fuel. Fifth Symposium (International) on Combustion, New York, 1955.

8-20. Ingebo, R.D. Atomization, acceleration and vaporization of liquid fuels. Sixth Symposium (International) on Combustion, p. 684, New York, London, 1957.

8-21. Kumagai, S., Isoda, H. Combustion of fuel droplets in a falling chamber. Sixth Symposium (International) on Combustion, p. 727, New York, London, 1957.

8-22. Lorell, J., Wise H., Carr, R.S. Journ. of chem. Phys, 1956, No. 2.

Chapter Nine

9-1. Aref'yev, K.M., Maslichenko,P.A., Paleyev,I.I. Scientific-technical bulletin of Leningrad Polytechnic Institute, 1959, No. 8.

9-2. Basevich, V.Ya. Collection: Goreniye pri ponizhennykh davleniyakh i nekotoryye voprosy stabilizatsii plameni v odnofaznykh i dvukhfaznykh sistemakh (Combustion at low pressures and certain problems of stabilization of flames in single phase and bi-phase systems). Izd. AN SSSR, 1960, p. 71.

9-3. Knorre, G.F. Topochnyye protsessy (Furnace processes). Gosenergoizdat, 1959.

9-4. Mikhaylov, A.N., Gorbunov,G.M., Borisov, V.V., Krasnikov, L.A., Markov, N.I. Operational process and design of combustion chambers of gas turbine engines. Oborongiz, 1959.

9-5. Bases of hydrocarbon fuel combustion. IIL, 1960.

9-6. Spolding, D.B. Osnovy teorii goreniya (Bases of combustion theory). Gosenergoizdat, 1959.

9-7. Tikhomirov, V.G. Basic characteristics of the combustion of a bi-phase fuel-air mixture. Collection: goreniye dvukhfaznykh sistem (Combustion of biphase systems). Izd. AN SSSR, 1958, p. 10.

9-8. Greenhough, Lefebvre. Sixth Symposium (International) on Combustion., p. 858, New York - London, 1957.

9-9. Ingebo, R.D. Vaporization rates and drag coefficients for isooctane sprays in turbulent air stream. NACA TN 3265, 1954.

9-10. Longwell, J.P., Weiss, M.A. High temperature reaction rates in hydrocarbon combustion. Ind. a Eng. Chem., 1955,47, No. 8.

9-11. Miesse, C.C. On the Combustion of liquid spray. Sixth Symposium (International) on Combustion, p. 732, New York, London, 1957.

9-12. Probert, R.P. The influence of spray particle size and distribution in the combustion of oil droplets. Phil. Mag., 1946, 37, No. 265.

9-13. Rex, J.F., Fuhs, A.E., Penner, S.S. Jet propulsion, 1956, 26, p. 179.

9-14. Schope, F. VDI Forschungsheft, 1956, No. 456.

9-15. Startkman, E.S., Cattango, A.G., McAllister, S.H. Carbon formation in gas turbine combustion chambers, Ind. a Eng. Chem., 1951, No. 12, p. 2822.

Chapter Ten

10-1. Blokh, A.G., Kichkina, E.S. Atomization of liquid fuel by mechanical spray nozzles of the centrifugal type. Collection: Problems of aerodynamics and heat transfer in boiler-furnace processes. Gosenergoizdat, 1958.

10-2. Vitman, L.A., Katsnel'son, B.D., Efros, M.M. Atomization of liquid fuel by pneumatic spray nozzles. Collection: Problems of aerodynamics and heat transfer in boiler-furnace processes. Gosenergoizdat, 1958.

10-3. Zhitkovskiy, Yu.Yu. Electron device for studying the dispersion of atomized liquids. Inzhenerno-fizicheskiy zhurnal, 1958, No. 6.

10-4. Kler, G., Redkliff, A. Pneumatic spray nozzle for atomizing viscous fuels. Voprosy raketnoy tekhniki, 1956, No. 2.

10-5. Knorre, G.F. Topochnyye protsessy (Boiler processes). Gosenergoizdat, 1959.

10-6. Kuznetsov, N.M., Lebedev, M.A. Topochnyye ustroystva sudovykh parovykh kotlov (Boilers for ship steam boilers). Sudpromgiz, 1959.

10-7. Miroshkin, M.Ya., Geller, Z.I. Problem of selecting material for simulating the atomization of highly viscous residues. Izvestiya vysshikh uchebnykh zavedeniy, Seriya "Neft' i gaz", 1960, No. 5

10-8. Panasenkov, N.S. Influence of turbulence of a liquid stream on atomization. ZhTF, 1951, XXI, No. 2.

10-9. De Corso. Effect of ambient and fuel pressure on spray drop size. Journ. of Eng. for Power, Trans. ASME, series A, 1960, 82, No. 1.

10-10. Gebhardt, H. Die Tropfengroessen bei Drallzerstauebung (Drop sizes in the case of angular momentum atomization). Brennstoff-Waerme-Kraft, 1958, 10, No. 8, 361-366.

10-11. Joyce, J. Droplet size measurement of various steel furnace oil burners. Journ. Inst. fuel, 1953, 26, No. 153.

10-12. Manson, N., Banejea, S.K., Eddi, R. Arrangement for a microphotographic study of liquid fuel pulverization. Revue d l'Inst. Francais de Petrole, 1955, X, June.

10-13. Stoker, R.H. Journ. appl. Phys, 1946, 17, No. 4

10-14. York, J.L. Stubbs, H.E. Photographic analysis of sprays. Trans. ASME, 1952, 74, 1157-1162.